PHYSICO-CHEMICAL PROPERTIES OF TITANIFEROUS IRON-MAKING SLAGS UNDER NEUTRAL AND UNDER REDUCING CONDITIONS.

by

J.C.G.K. van der Colf

A thesis submitted to the Faculty of Engineering in fulfilment of the requirements for the degree of Doctor of Philosophy.

University of the Witwatersrand,

Johannesburg.

August, 1974.

UNDERTAKING

I hereby certify that this is my own work, and that it has not been submitted for the degree of Doctor of Philosophy at any other university.

J. van der Colf

J.C.G.K. van der Colf.

ACKNOWLEDGEMENTS

The author wishes to record his appreciation of the assistance afforded him by his supervisor Professor D.D.Howat, B.Sc. (Glas.), Ph.D., F.I.M., F.R.I.C.

Due acknowledgement is also made to the Highveld Steel and Vanadium Corporation for the research grant which enabled the project to be undertaken.

SYNOPSIS

Available data on particularly viscosities of titaniferous melts under oxidizing conditions are reviewed, and and an attempt is made to explain the high fluidity of such melts.

Selected members of the $CaO-MgO-SiO_2-Al_2O_3-TiO_2$ system were subjected to measurements of viscosity, electrical resistivity and liquidus temperature in a neutral atmosphere. A logarithmic relation appears to exist between the first two parameters for most of the slags tested. Electronic conduction is definitely significant.

The original synthetic slags were also reduced by graphite. The degree of reduction with respect to titanium oxide, the melting temperature, the viscosity and the electrical resistivity in selected instances, of the reduced derivatives, were subsequently determined. Whether the liquidus temperature of a slag is materially altered by reduction is a function of the primary crystallization product of the unreduced slag. Especially acidic slags go through an initial period of enhanced fluidity. Basic slags tend to "thicken" subsequently. This phenomenon, as well as the progressive decrease in electrical resistivity as the reduction period is extended, are explained in terms of fundamental slag structural theory and the appreciable contribution of electronic conduction.

The compositional features of initial slags that favour pronounced thickening are mainly a high basicity expressed as $(CaO + MgO)/SiO_2$ and a low CaO/MgO ratio. SiO_2 and FeO in the starting slag retard thickening by being simultaneously and preferentially reduced respectively. It was also attempted to relate the degree of reduction of the slag with respect to titanium oxide, to its physico-chemical properties.

Slag thickening, when it is severe, alters the rate determining step of the heterogeneous reduction reaction.

The possible significance of these findings on an industrial scale is illustrated and discussed.

CONTENTS

		Page
1.	INTRODUCTION	1
2.	LITERATURE REVIEW	
	2.1 Melting temperatures and phase compositions of titaniferous slags under oxidizing conditions	7
	2.2 Viscosity of titaniferous oxide systems under oxidizing and neutral conditions	
	2.2.1 Binary systems	12
	2.2.2 Ternary systems	13
	2.2.3 The quaternary system $CaO-Al_2O_3-TiO_2-SiO_2$	15
	2.2.4 The 5-component system $CaO-MgO-Al_2O_3-TiO_2-SiO_2$	20
	2.2.5 Discussion	24
	2.3 Reaction product and rate studies	
	2.3.1 The system Ti-O	30
	2.3.2 Reduction of TiO_2	33
	2.3.3 Carbonaceous reduction of TiO_2 from titaniferous slags	35
	2.3.4 Co-reduction of SiO_2 and TiO_2 from titaniferous slags	39
	2.3.5 Co-reduction of titania and iron oxide	42
	2.4 The influence of reducing conditions on viscosity and melting temperatures of titaniferous slags	
	2.4.1 The possible reasons for the difficulties experienced during the smelting of titaniferous ores	42
	2.4.2 Mikhailov and Belyakova (1939)	43
	2.4.3 Semik (1941)	44
	2.4.4 Delve, Meyer and Lander (1961)	44
	2.4.5 Ohno and Ross (1963)	45
	2.4.6 Freidenzon (1965) and Shavrin (1966)	48
	2.4.7 McRae (1968)	49
	2.4.8 Gruzdev et al (1971)	51
	2.4.9 Handfield, Charette and Lee (1972)	52
	2.4.10 Summary	54
	2.5 Electrical conductivity of titaniferous slags	
	2.5.1 The electrical conductivity of slags high in TiO_2	56
	2.5.2 The effect of reducing conditions on the conductivity of high titania slags	57
	2.5.3 Electrical conductivity of low titania slags	58

Page

2.6 The influence of variable oxidation states in analogous systems
2.6.1 Systems containing iron oxide 59
2.6.2 Other systems 61
2.6.3 Conclusion 61

3. EXPERIMENTAL WORK
3.1 Selection of slag compositions 62
3.2 Preparation of synthetic slags 63
3.3 The furnace assembly for measurements of viscosity and electrical conductivity and for reduction experiments 66
3.4 Preparation of reduced slags 68
3.5 Measurement of viscosity
3.5.1 Description of equipment 74
3.5.2 Calibration of the viscometer 76
3.5.3 Procedure of viscosity measurement 77
3.6 Measurement of electrical conductivity
3.6.1 Description of equipment 79
3.6.2 Calibration of the conductivity cell 80
3.6.3 Procedure of resistance measurement 84
3.7 Measurement of liquidus temperatures 84
3.8 Determination of primary phases 87
3.9 Determination of degree of reduction of reduced slags 88
3.10 Critical appraisal of experimental techniques 92

4. RESULTS
4.1 Unreduced slags
4.1.1 Liquidus temperatures and primary phases of unreduced slags 95
4.1.2 Viscosity of unreduced slags
4.1.2.1 The effect of basicity upon viscosity 119
4.1.2.2 The effect of mass% CaO/MgO on viscosity 121
4.1.2.3 The effect of mass% (TiO_2+Al_2O_3) content upon viscosity 122
4.1.2.4 Comparison with other results 123
4.1.3 Electrical resistivities of unreduced slags
4.1.3.1 Influence of basicity upon resistivity 126
4.1.3.2 Influence of CaO/MgO on resistivity 126
4.1.3.3 Influence of (TiO_2+Al_2O_3) on resistivity 126

Contents (continued)

Page

4.1.4 Relation between viscosity and resistivity 136

4.1.5 Comparison of physico-chemical properties of oxidized titaniferous slags with those of slags of selected other processes 141

4.2 Slags reduced by carbon

4.2.1 The influence of composition on variations in viscosity and melting temperature

4.2.1.1 Basicity 145

4.2.1.2 CaO/MgO ratio 154

4.2.1.3 (TiO_2 + Al_2O_3) content 156

4.2.1.4 Oxides of iron and vanadium 157

4.2.2 Influence of reduction temperature on variations in viscosity and melting temperature 158

4.2.3 Resistivity of reduced slags

4.2.3.1 Resistivities of reduced derivatives of slag B14 186

4.2.3.2 A consideration of the trends shown by resistivity and viscosity during reduction 189

4.2.4 X-ray analyses of selected reduced slags 191

4.2.5 Degree of reduction of reduced slags

4.2.5.1 Preliminary work 198

4.2.5.2 The effect of composition on the rate of reduction 203

4.2.5.3 General treatment of rate results 208

4.2.5.4 The rate of reduction of slag B11 211

4.2.5.5 The rate of reduction of slag B14 217

4.2.5.6 The rate of reduction of slag B17 222

5. GENERAL DISCUSSION

5.1 Reducing conditions and melting temperature 228

5.2 Reducing conditions and viscosity 235

5.3 Reducing conditions and electrical conductivity 249

6. INDUSTRIAL SIGNIFICANCE 255

7. REFERENCES 287

1. INTRODUCTION

1.1 The titaniferous magnetite ore from the Bushveld Igneous Complex

The ore that is utilized by the Highveld Steel and Vanadium Corporation for production of steel and vanadium pentoxide, has the following average chemical composition:

Fe	:	55,8 - 57,5 %
TiO_2	:	12,2 - 13,9 %
V_2O_5	:	1,4 - 1,6 %
SiO_2	:	0,9 - 1,5 %
Al_2O_3	:	2,5 - 3,5 %
CaO	:	0,1 %
MgO	:	0,24 - 1,26 %
Cr_2O_3	:	0,13 - 0,45 %

with lesser quantities of Cu, Ni, P and S.

The approximately oval shaped B.I.C. is marked out by Lydenburg, Zeerust, Potgietersrus and Pretoria. The Basic Intrusive Phase is the main source of the mineral wealth associated with the Complex. In this Phase, the Critical zone overlies the Marginal Norite zone, followed by the Main and Upper zones. In the Upper zone, the main Magnetite seam of maximum thickness about 8,5 feet, generally outcrops and can be followed for more than 200 miles along the exposed strike. It separates the iron-rich Upper zone from the Main zone. Magnetite seams also occur in the Main zone as well as lower down, but the Main Magnetite seam is particularly important as far as pyrometallurgical extraction of iron and vanadium is concerned.

Ilmenite as such is present in the ore mainly as small granules, constituting only a minor percentage of the overall titanium content. Titanium further occurs as ulvospinel (Fe_2TiO_4) and as intergrowths of ilmenite with particularly magnetite, but also with other ore constituents. Vanadium is present mainly through isomorphous replacement of iron in the iron oxide containing minerals.

1.2 Production of vanadium bearing pig iron

1.2.1 Preliminary treatment and handling

The ore is prereduced in rotary kilns to a degree between 25 and 35 %. The charge to the kilns consists of ore, coal, dolomite and quartz in the ratio 1,000 : 0,415 : 0,205 : 0,035. Pulverized coal is used as a fuel. It is aimed at maintaining the kiln temperature at approximately 1000°C.

The hot kiln discharge material is transferred to bunkers above the electric furnace, each with a capacity of ± 30 tons of prereduced burden.

1.2.2 The submerged arc electric furnace

The four 33 MVA furnaces have shell diameters of 14 m. Current is supplied to the furnace through three 1,6 m diameter Soederberg type electrodes from a three-phase transformer which is connected in delta.

The secondary windings of the regulating transformer are provided with motor operated sliding tap changers. Capacitors for power factor correction are installed between the secondary of the regulating transformer and the primary of the furnace transformer.

The electrode position is either current or impedance controlled. Electrode slipping is done by means of wisdom brakes. Under normal operating conditions the electrode to bath voltage and the furnace current are approximately 110 V and 90 KA respectively. At a furnace resistance of 1 m ohm, the smelting load is approximately 24,3 MW.

The kiln discharge material enters the furnace at ± 800°C. Three bunkers charge in front of the electrodes, while each of the remaining three delivers its charge between two adjacent electrodes. Each electrode is also supplied with two ports for charging correcting materials, and two explosion doors are located in the furnace roof. These, as well as the contact shoes and mantles, are water cooled. Each furnace is provided with two venturi scrubbers and a continuous gas analyzer.

Tapping is performed through two tapholes with independent launder systems.

It is normally done after 55 to 60 MW hours and the tap to tap time varies between 3½ and 4 hours. Fifty to sixty tons of pig iron are produced per tap and the slag to metal ratio is 0,75 to 0,80 / 1,00.

Ranges of slag and metal compositions are:

Mass per cent composition

Slag	CaO	MgO	SiO_2	Al_2O_3	TiO_2	V_2O_5	FeO
	14,4-19,6	10,4-15,6	16,2-20,9	12,5-15,4	28,5-33,0	0,8-1,4	2,5-6,5

Metal	C	Si	S	P	V
	2,70-3,70	0,10-0,35	0,06-0,11	0,04-0,08	0,90-1,35

The hot metal is oxygen blown in a shaking ladle for the removal of vanadium oxide, before being transferred to the B.O.F steel plant.

1.3 Difficulties experienced in the operation of the submerged arc furnaces

More detailed comments on such difficulties and remedial action as performed on the plant, will be listed in chapter 6. Salient features of earlier research work, both on laboratory and on plant scale, specifically connected with Highveld practice, will also be summarized in the same chapter.

Difficult operation is often reflected in low metal temperatures ($\pm$1370°C) and invariably in poor metal chemistry. (low C and Si)

During periods of rough operation, the furnaces are difficult to tap and no-slag taps are not uncommon. These are manifestations of several possible trouble sources in the furnace. Electrode breakages occur relatively frequently and the effect of pieces of electrode drifting on the slag is an obvious one. The formation of solid bridging crusts in the furnace giving rise, in extreme cases, to slag confining craters round the electrodes, is another possible cause for a no-slag tap. Such problems are often asso-

ciated with short electrodes and a cold furnace. Even during periods of more normal operation the slag in the launder appears to be insufficiently superheated. Successive no-slag taps are only remedied by blanking off the furnace and smelting down its contents.

A so-called boiling slag represents a very troublesome condition. In the extreme case, when the phenomenon is accompanied by severe crusting, violent gas eruptions may occur. Apart from the obvious consequences, a boiling slag also causes rapid electrode erosion. A sudden flare-up may be the result of consecutive no-slag taps. It seems to be promoted by high power input especially when the electrodes are short.

A tendency for the electrodes to ride high, is promoted by such factors as short electrodes, an overcarboned burden and high power input. Many of the correcting materials are aimed at increasing the resistivity of the burden. A low resistivity leading to a high electrode position is closely interwoven with the phenomena of boiling slag and crust formation. It seems to be accepted as normal that the electrodes start losing resistivity approximately 1 - 1½ hours before tapping.

1.4 The motivation for the present work

The research work described in the following chapters was undertaken in the light of the operational complexities underlying the brief outline of practical difficulties that was given in section 1.3. A more complete assessment of the value of the parameters that were determined, will be given in chapter 6.

The melting temperature of the slag formed during a metal and slag producing process is important mainly due to the requirement of satisfactory metal superheat. Completely molten slag that drains away from the reaction zone at the liquidus temperature of the alloy to join the slag layer, cannot provide the underlying metal bath with the required degree of superheat. Operational phenomena such as difficult tapping, crust formation and even a boiling slag appear to be intimately connected with slag liquidus temperature.

The true significance of slag viscosity is a function of the particular

process. If the reduction of metal oxides from a slag phase either by carbon dissolved in the metal or by solid reductant is important, then viscosity may become a rate limiting factor for such a reduction reaction. A similar argument applies when the rate of dissolution of oxides in a liquid slag influences the rate of the overall reaction.

The rate at which metal droplets that are produced in the reaction zone settle through a slag layer, is also a function of the slag viscosity.

The time consumed by tapping of the furnace is "dead time" from a production point of view. For constant production, a more viscous slag means a direct increase in tapping time.

While an optimum final slag-metal temperature difference can be stipulated for a desired metal temperature, the required final slag temperature is not a function of its liquidus temperature only. If even the initial slag is a very fluid one, a composition of higher liquidus temperature may be better suited to effect the same degree of metal superheat.

Finally, a slag that becomes labelled as a boiling slag does not necessarily owe its properties to locally intensified gas evolution. It may alternatively be due to normal or or near-normal gas evolution in a locally thickened slag.

There is no absolute guide regarding the relative importance of resistance heating in submerged arc furnaces. The resistance of the burden as a whole does influence the electrode position, but while slag resistivity is becoming a more prominent factor in more recent approaches to the subject of power dissipation, its relative contribution to furnace resistance is ill-defined. Once again, the existence of such a contribution cannot be discounted, even if it has to be vaguely regarded as the final integrated manifestation of many step-wise processes.

Measurements of electrical resistivity conducted as part of this research work, were consequently aimed at gaining some understanding of the operational phenomena that can be summarized in the term "low electrode resistivity".

Literature data indicated that the properties of titaniferous slags:

melting temperature, viscosity and electrical conductivity, were all likely to be influenced by the degree of reduction of the slags, with respect to titanium oxide. An exploration of these indications formed the core of this work. This approach was further based on the facts that:

(a) the slags are known to be very attractive under oxidizing conditions, judging mainly from their liquidus temperatures and viscosities and

(b) reducing conditions appeared to adversely affect all these properties.

2. LITERATURE REVIEW

2.1 Melting temperatures and phase compositions of titaniferous slags under oxidizing conditions.

Very extensive research work has been done into the melting and primary crystallization properties of the quaternary system $CaO-Al_2O_3-TiO_2-SiO_2$ and the various ternary and binary systems constituting the quaternary. Much of this work, notably that of Agamawi and White on the systems $Al_2O_3-TiO_2-SiO_2$[1], Calcium metasilicate - sphene - silica and Calcium metasilicate - anorthite - sphene - silica[2] were inspired by the need for understanding the high temperature behaviour of silcrete refractory components. However, the research of Ohno and Ross[3] was directed specifically at gaining a wider knowledge of problems arising when titaniferous iron ores are smelted in the blast furnace.

Ohno and Ross, while also assessing the effect of alumina addition to the ternary $CaO-TiO_2-SiO_2$, extended the composition range by inclusion of higher levels of titania than previously reported by eg. DeVries, Roy and Osborn[4], working in the less than 10% titania range. Ohno and Ross[3] found that 10% and 20% additions of alumina extended the range of the low temperature trough where the primary phase is sphene, on the equilibrium diagram for $CaO-TiO_2-SiO_2$.

The need for studies of the five-component $CaO-MgO-Al_2O_3-SiO_2-TiO_2$ system arises from the fact that MgO is normally present in the vast deposits of titaniferous magnetite ores. It assumes greater importance as a variable in the slags from smelting such ores when limestone is partially or completely replaced by dolomite as a flux. In the latter case, the CaO/MgO ratio may further be varied by addition of either limestone or serpentine.

A very comprehensive study of the liquidus temperatures of slags belonging to the five-component system was made by Holmes, Banning and Brown.[5] These authors worked at selected mass % ratios of TiO_2/Al_2O_3 ranging from 0,35 to 4, with limited variation of $(\%TiO_2 + \%Al_2O_3)$ at each ratio, the main variables being silica, lime and magnesia contents. A total of 345 mixtures were tested. Liquidus temperatures varied from 1217°C to 1667°C. In general the lowest liquidus temperature for a particular $(\%TiO_2 + \%Al_2O_3)$ occurred when the condition $(\%CaO + \%MgO) - \%SiO_2 \leq 12\%$ was met. At

At constant CaO and MgO contents, substitution of SiO_2 for $TiO_2+Al_2O_3$ normally lowered the melting temperature of the slags. Substitution of either CaO for SiO_2 or MgO for CaO resulted in a change of the liquidus temperature of base slags from -93°C to +251°C.

Zhilo and co-workers[6] studied the influence of titania additions (6 to 15 %) on the fusibility of synthetic slags of the system CaO-MgO-SiO_2-Al_2O_3. The slag basicity, expressed as mass per cent ratios CaO/SiO_2, was varied from 0,7 to 1,2. They found the fusibility temperature to decrease on addition of TiO_2 up to a certain critical limit, depending on the basicity. Beyond this critical limit of TiO_2 content, the fusibility temperature of the slag was raised. The relevant experimental values are given in table 1.

Table 1 Critical titania contents with corresponding basicities in the system CaO-MgO-SiO_2-Al_2O_3-TiO_2.[6]

Critical TiO_2 content (mass %)	Basicity (%CaO/%SiO_2)
10	0,91
9,85	0,97
9,75	1,06
8,9	1,17

The initial decrease in fusibility temperature was ascribed to an increase in the amount of augite and a change in the melelite composition of the base slag. The eventual increase was attributed to the formation of spinel and perovskite and the decreasing amounts of diopside.

Handfield et al[7] also found that additions of TiO_2 up to 10 mass % to an industrial blast furnace slag sample caused a decrease in the fusibility temperature, while the latter tended to rise upon further titania additions.

Pilot plant operations conducted prior to commisioning the Highveld Steel and Vanadium Corporation iron plant, showed that slags containing about 35 % TiO_2 would be produced. Consequently, all earlier laboratory test work were concentrated on slags of higher titania contents than those

presently encountered on the plant. (approximately 30 %)

The equilibrium phase studies conducted by Jochens, Sommer and Howat[8] were aimed at clarifying the influence of both mass % ratio CaO/MgO and mass % total basicity (CaO + MgO), while keeping the (TiO_2 + Al_2O_3) content and the TiO_2/Al_2O_3 ratio constant. Their results are shown in figures 1 and 2.

Figure 1 shows the phase equilibrium diagram for the system 19,69 % SiO_2, 13,12 % Al_2O_3, 37,19 % TiO_2, 30 % (CaO + MgO) with CaO varying from 0 % to 30 % while MgO varies from 30 % to 0 %. Increase of the MgO content from 0 % to 12 % by mass, lowered the liquidus temperature from 1520°C to 1340°C. Further replacement of CaO by MgO caused a gradual rise in the liquidus temperature, which reached 1505°C at 0 % CaO. Based purely on this result of experiments over a limited composition range, conducted under oxidizing conditions, the use of dolomite as a flux resulting in a slag CaO/MgO ratio of 16/14, appears desirable.

Figure 2 shows the effect of variation of MgO content at three different levels of (%CaO + %MgO). In general, the liquidus temperature minimum shifted towards lower MgO contents with a decrease in overall basicity. The absolute value of the minimum was reduced at the same time. However the rise in liquidus temperature with increasing MgO content after passing through the minimum, was more drastic in the case of the lowest level of (CaO + MgO). It should further be noted that changes of basicity had much more pronounced effects on liquidus temperature for slags of low CaO/MgO ratio.

There is also a change of primary phase, from perovskite ($CaO.TiO_2$) at MgO contents lower than that corresponding to the liquidus temperature minimum, to magnesium aluminium titanate ($Mg_4Al_2Ti_9O_{25}$) as the MgO is increased further. The repeated occurrence of the latter phase, which is a member of the solid solution series with the two pseudobrookite end members $MgO.2TiO_2$ and $Al_2O_3.TiO_2$, both as a primary phase and in subsequent crystallization, is a peculiar feature of the system which will be discussed more fully in section 4.1.2.

While the present work was in progress , Hejja[9] determined the liquidus

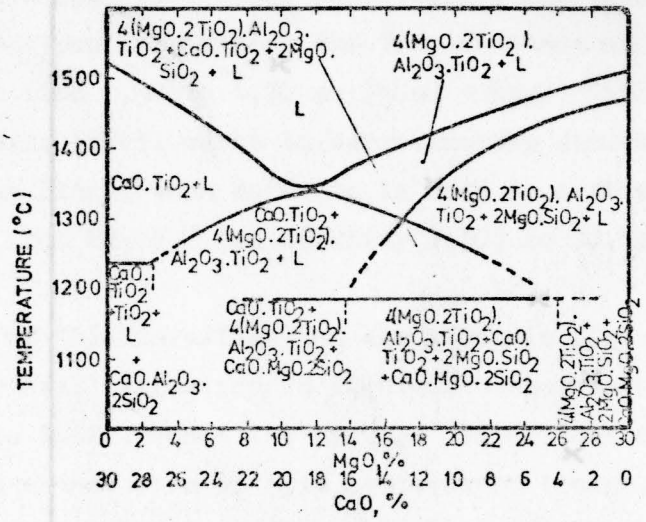


Figure 1 The effect of CaO/MgO ratio on liquidus temperature at constant TiO_2, Al_2O_3, SiO_2 and (CaO + MgO) (8)

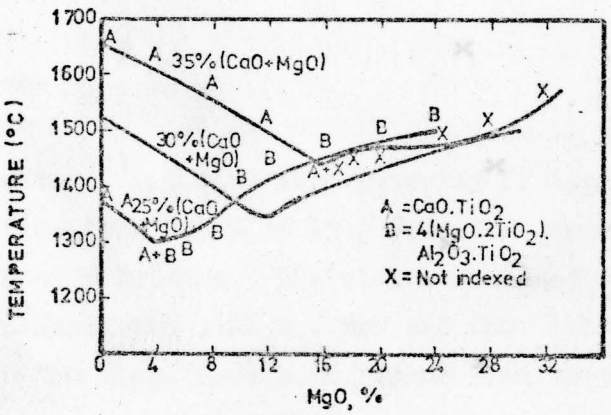


Figure 2 The effect of CaO/MgO ratio on liquidus temperature at various (CaO + MgO) contents. (8)

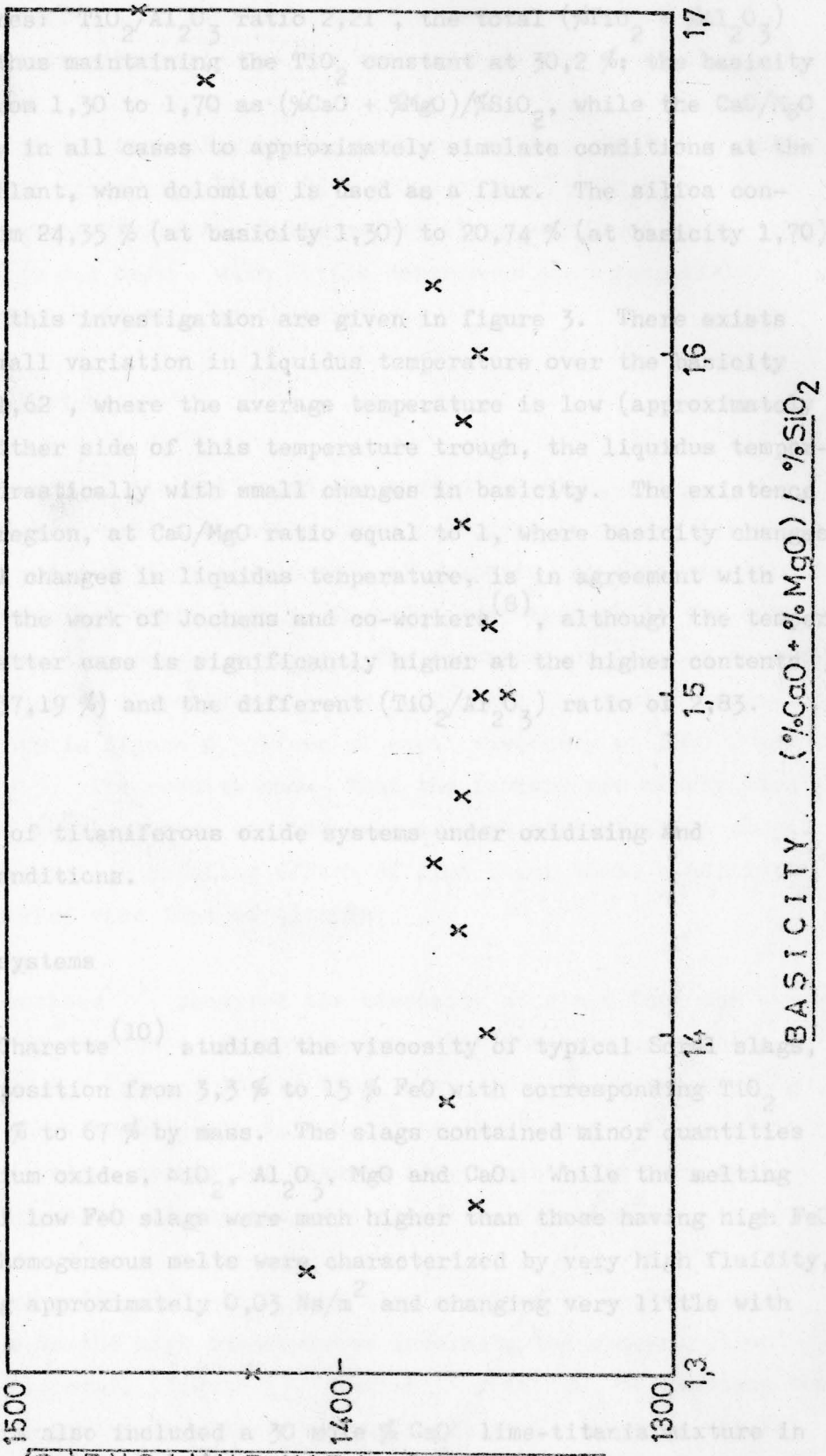


Figure 3 Variation of liquidus temperature with basicity[9]

temperatures of a series of slags whose compositions fell within the range investigated by the author. This series had the following compositional features: TiO_2/Al_2O_3 ratio 2,21 , the total ($\%TiO_2 + \%Al_2O_3$) content 44 %, thus maintaining the TiO_2 constant at 30,2 %; the basicity being varied from 1,30 to 1,70 as ($\%CaO + \%MgO)/\%SiO_2$, while the CaO/MgO ratio was unity in all cases to approximately simulate conditions at the Highveld Iron Plant, when dolomite is used as a flux. The silica content varied from 24,35 % (at basicity 1,30) to 20,74 % (at basicity 1,70).

The results of this investigation are given in figure 3. There exists surprisingly small variation in liquidus temperature over the basicity range 1,35 to 1,62 , where the average temperature is low (approximately 1360°C). On either side of this temperature trough, the liquidus temperature changes drastically with small changes in basicity. The existence of a basicity region, at CaO/MgO ratio equal to 1, where basicity changes result in small changes in liquidus temperature, is in agreement with the results of the work of Jochens and co-workers[8], although the temperature in the latter case is significantly higher at the higher contents of TiO_2 used (37,19 %) and the different (TiO_2/Al_2O_3) ratio of 2,83.

2.2 Viscosity of titaniferous oxide systems under oxidizing and neutral conditions.

2.2.1 Binary systems

Handfield and Charette[10] studied the viscosity of typical Sorel slags, ranging in composition from 3,3 % to 15 % FeO with corresponding TiO_2 contents of 80 % to 67 % by mass. The slags contained minor quantities of lower titanium oxides, SiO_2, Al_2O_3, MgO and CaO. While the melting temperatures of low FeO slags were much higher than those having high FeO contents, all homogeneous melts were characterized by very high fluidity, viscosity being approximately 0,03 Ns/m^2 and changing very little with temperature.

The same authors also included a 30 mole % CaO lime-titania mixture in their investigation. The viscosity of the homogeneous melt in this instance was only 0,02 Ns/m^2, this value also being virtually independent

of temperature.

The rise of viscosity upon cooling below the freezing temperature was found to be an extremely rapid one for both systems investigated.

Tuset[11] studied the viscosity of the titanium oxide - magnesium oxide system, the melts containing 58 to 85 % TiO_2, 8 to 33 % Ti_2O_3 and 3 to 21 % MgO. The viscosity of the fully molten slags was found to lie in the range 0,05 to 0,1 Ns/m^2, with little dependence upon composition within the range considered, or temperature.

2.2.2 Ternary systems

Frohberg and Weber[12] investigated the system $CaO-Al_2O_3-TiO_2$. Although these workers used a rotating inner cylinder viscometer for which both inner and outer cylinders were made of graphite, so that conditions were in fact reducing, their work is included here because of the comprehensive composition ranges covered. The research was limited to mixtures having liquidus temperatures below 1600°C and the tested compositions are shown in figure 4. Lines of equal viscosity at 1600°C are given in figure 5. The results show that the isokoms are nearly parallel to the lines of equal alumina content over a large concentration range. Moreover, the viscosity reducing effect of lime under these conditions is much more marked than that of titania.

Pliner and co-workers[13] measured the viscosity of slags from the aluminothermic production of ferrotitanium. For a sample containing 60,6 % Al_2O_3, 12,8 % CaO and 10,1 % TiO_2, with minor percentages of MgO, FeO and SiO_2, the viscosity was 0,18 Ns/m^2 at 1760°C and 0,15 Ns/m^2 at 1830°C, the activation energy for viscous flow again being very small. The melting temperature of the slag was approximately 1750°C.

The ternary system $SiO_2-TiO_2-Al_2O_3$ was also examined by Frohberg and Weber[12]. Due to the high temperatures involved, the concentration range tested, was small (figure 6). The ability of TiO_2 to increase the fluidity in this system is clearly shown in figure 7. However, it is noteworthy that the difference in effect upon viscosity existing between

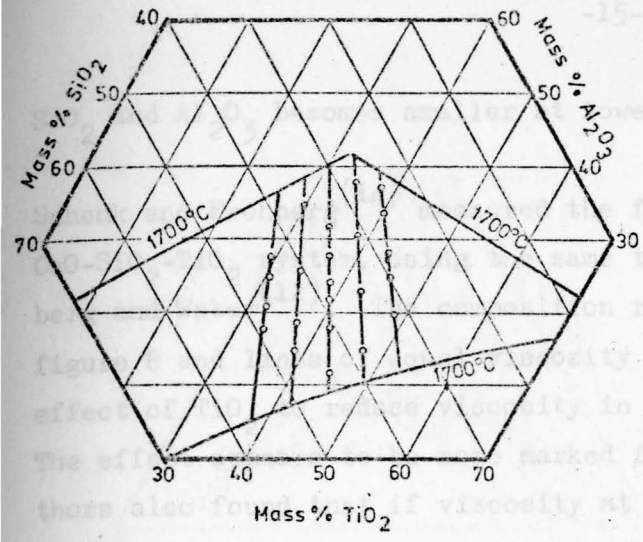


Figure 6 Concentration range of melts investigated in the system SiO_2-TiO_2-Al_2O_3 (12)

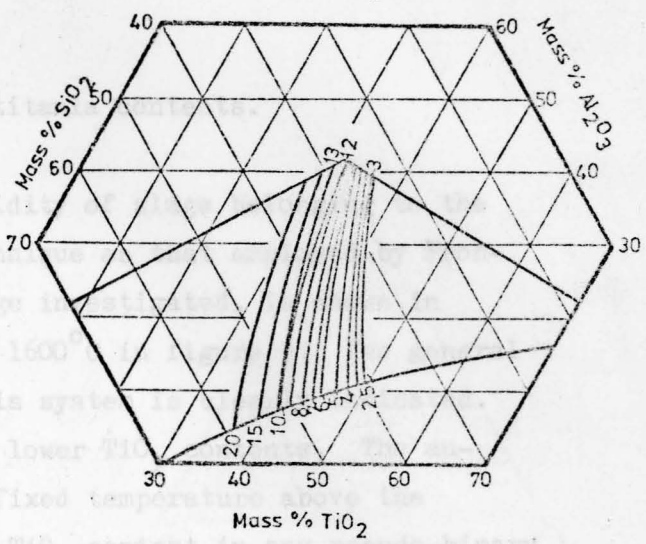


Figure 7 Lines of equal viscosity at 1700°C for the system SiO_2-TiO_2-Al_2O_3 (12)

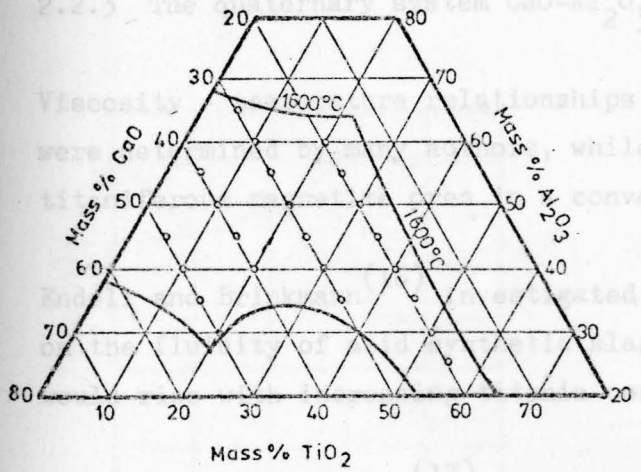


Figure 4 Composition range investigated in the system CaO-Al_2O_3-TiO_2 (12)

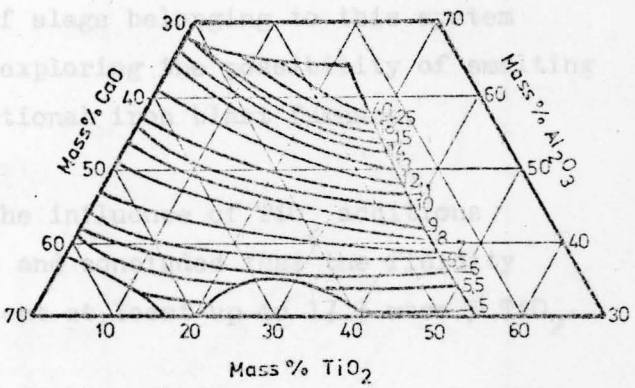


Figure 5 Lines of equal viscosity (poise) in the system CaO-Al_2O_3-TiO_2 at 1600°C (12)

SiO_2 and Al_2O_3 becomes smaller at lower titania contents.

Schenk and Frohberg[14] measured the fluidity of slags belonging to the $CaO-SiO_2-TiO_2$ system, using the same technique as that employed by Frohberg and Weber[12]. The composition range investigated, is shown in figure 8 and lines of equal viscosity at 1600°C in figure 9. The general effect of TiO_2 to reduce viscosity in this system is clearly indicated. The effect appears to be more marked for lower TiO_2 contents. The authors also found that if viscosity at a fixed temperature above the liquidus temperature was plotted against TiO_2 content in any pseudo-binary section along which % TiO_2 increases, the resulting curve tends to follow the one for liquidus temperature itself. (figure 10)

Thakur[15] showed that for the series of sodium silicate glasses $Na_2O.\ xRO_2.(3-x)SiO_2$, where $RO_2 + SiO_2 = 75$ mol % and R = Ti, the partial replacement of SiO_2 by TiO_2 causes an increase in the low temperature viscosity of the glass, as indicated in figure 11. Solid lines represent $\log \eta = 12$ and broken lines $\log \eta = 9$, where viscosity (η) is given in poise.

2.2.3 The quaternary system $CaO-Al_2O_3-TiO_2-SiO_2$

Viscosity - temperature relationships of slags belonging to this system were determined by many authors, while exploring the possibility of smelting titaniferous magnetite ores in a conventional iron blast furnace.

Endell and Brinkmann[16] investigated the influence of TiO_2 additions on the fluidity of acid synthetic slags and concluded that the fluidity would rise with increasing titania content at least up to 17,3 mass % TiO_2.

Mikhailov and Belyakova[17], using both acid and basic slags with titania levels varying from 0 to approximately 25 mass %, found that the addition of TiO_2 lowered the viscosity of acid slags, while the viscosity of basic slags was increased.

Using graphite viscometer components, Frohberg and Weber[12] selected base slags from the system $CaO-SiO_2-TiO_2$ according to a scheme similar to that used by Schenk and Frohberg.[14] To these ternary melts, additions

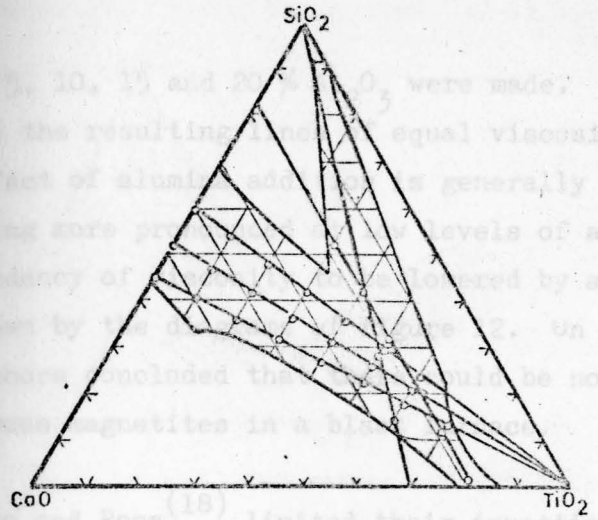


Figure 8 Composition range of melts in the system $CaO-SiO_2-TiO_2$ (1600°) (14)

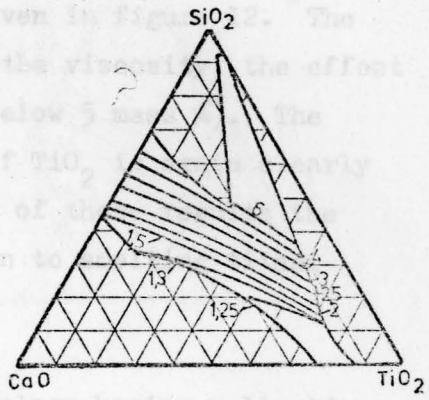


Figure 9 Isokoms in the system $CaO-SiO_2-TiO_2$ at 1600°C (14)

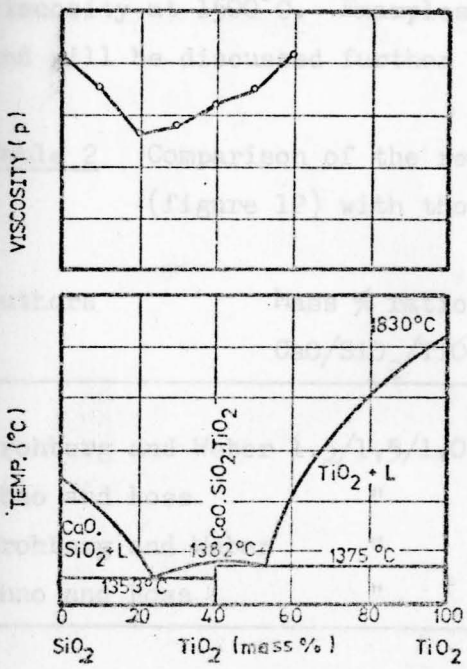


Figure 10 Liquidus temperature and viscosity at 100°C above liquidus for $CaO.SiO_2-TiO_2$ (14)

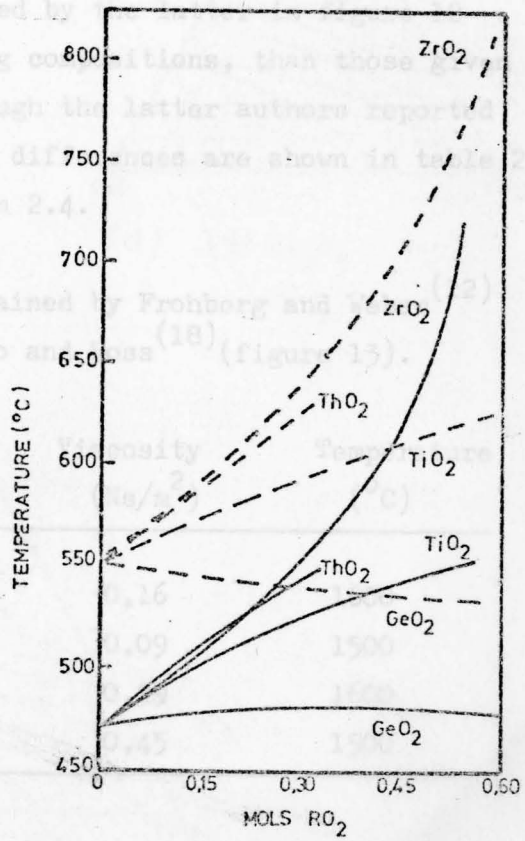


Figure 11 Isokoms for the series of glasses $Na_2O.xRO_2.(3-x)SiO_2$ (15)

of 5, 10, 15 and 20 % Al_2O_3 were made. Viscosity was measured at 1600°C and the resulting lines of equal viscosity are given in figure 12. The effect of alumina addition is generally to raise the viscosity, the effect being more pronounced at low levels of alumina (below 5 mass %). The tendency of viscosity to be lowered by addition of TiO_2 is again clearly shown by the diagrams of figure 12. On the basis of these results the authors concluded that there could be no objection to smelting titaniferous magnetites in a blast furnace.

Ohno and Ross[18] limited their investigation to slags having a liquidus temperature below 1450°C. Viscometer components were made of molybdenum and measurements carried out in a neutral atmosphere. Equal viscosity lines at 1500°C are shown in figure 13.

The salient features emerging from an investigation of these diagrams are the viscosity raising influence of Al_2O_3 and the property of both CaO and TiO_2 to reduce the viscosity.

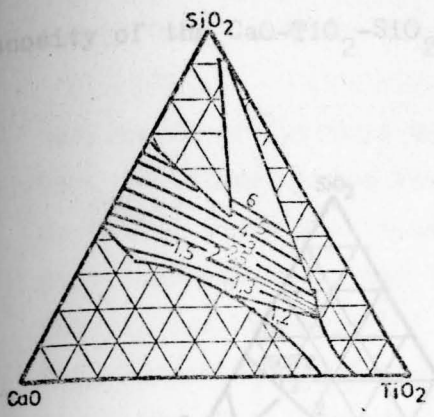
The general findings differ from those of Frohberg and Weber[12] mainly in the fact that the viscosities reported by the latter in figure 12 are considerably higher for similar slag compositions, than those given in figure 13 by Ohno and Ross, even though the latter authors reported viscosity at 1500°C. Examples of these differences are shown in table 2 and will be discussed further in section 2.4.

Table 2 Comparison of the results obtained by Frohberg and Weber[12] (figure 12) with those of Ohno and Ross[18] (figure 13).

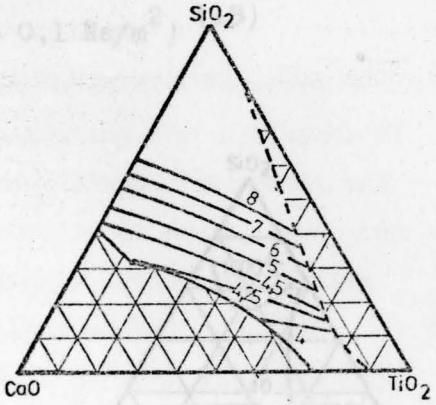
Authors	Mass % ratio $CaO/SiO_2/TiO_2$	Mass % Al_2O_3	Viscosity (Ns/m^2)	Temperature (°C)
Frohberg and Weber	1,5/1,5/1,0	0	0,16	1600
Ohno and Ross	"	0	0,09	1500
Frohberg and Weber	"	20	0,99	1600
Ohno and Ross	"	20	0,45	1500

Figure 12

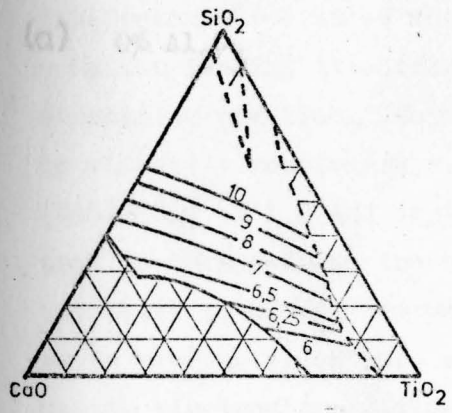
sokoms at 1600°C for the system $CaO-Al_2O_3-TiO_2-SiO_2$ (viscosity in poise) (12)



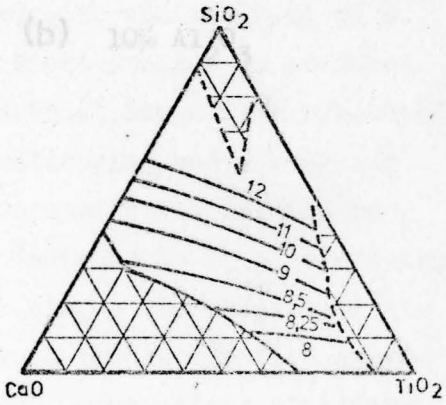
(a) 0% Al_2O_3



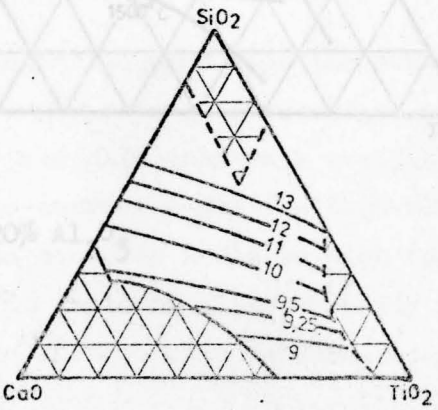
(b) 5% Al_2O_3



(c) 10% Al_2O_3



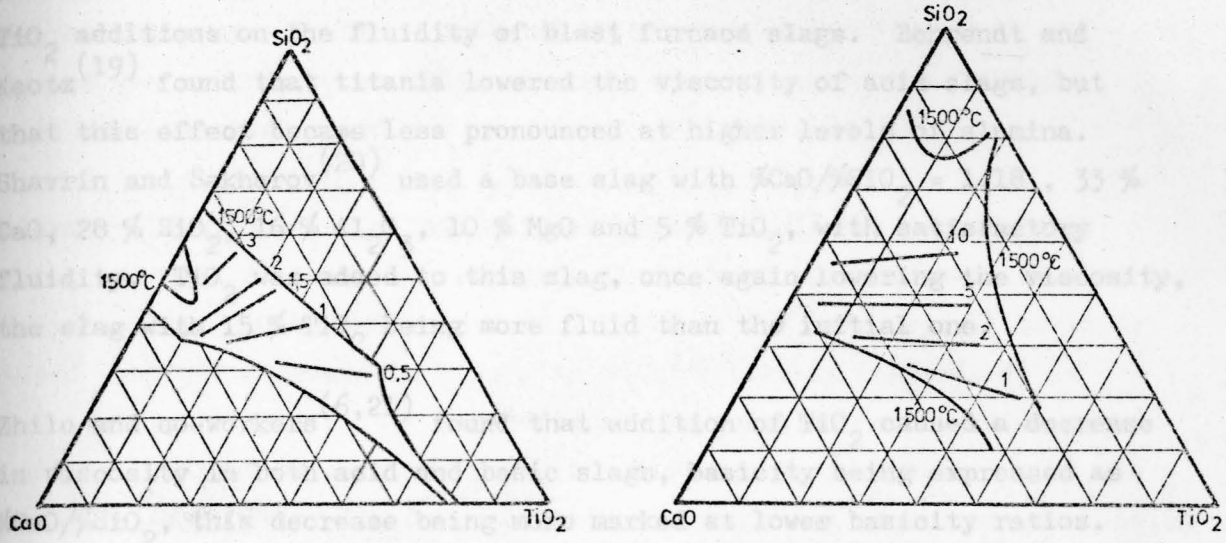
(d) 15% Al_2O_3



(e) 20% Al_2O_3

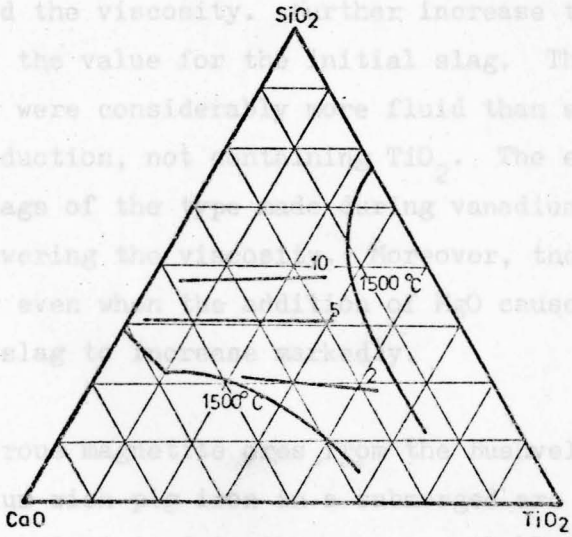
Figure 13

scosity of the $CaO-TiO_2-SiO_2-Al_2O_3$ system ($1p = 0{,}1\ Ns/m^2$) (18)



(a) 0% Al_2O_3

(b) 10% Al_2O_3



(c) 20% Al_2O_3

2.2.4 The 5-component system $CaO-MgO-Al_2O_3-TiO_2-SiO_2$

Earlier investigations were all aimed at determining the influence of TiO_2 additions on the fluidity of blast furnace slags. Behrendt and Kootz[19] found that titania lowered the viscosity of acid slags, but that this effect became less pronounced at higher levels of alumina. Shavrin and Sakharov[20] used a base slag with $\%CaO/\%SiO_2$ = 1,18 , 33 % CaO, 28 % SiO_2, 16 % Al_2O_3, 10 % MgO and 5 % TiO_2, with satisfactory fluidity. TiO_2 was added to this slag, once again lowering the viscosity, the slag with 15 % TiO_2 being more fluid than the initial one.

Zhilo and co-workers[6,21] found that addition of TiO_2 caused a decrease in viscosity in both acid and basic slags, basicity being expressed as $\%CaO/\%SiO_2$, this decrease being more marked at lower basicity ratios.

Freidenzon[22] studied the problems associated with the smelting of a vanadium bearing titaniferous magnetite in a blast furnace to produce a vanadium pig iron. Both synthetic and industrial slags were subjected to viscosity measurements. The initial synthetic slag had a basicity (CaO/SiO_2) of 1,2 and contained 5 % TiO_2. Increasing the titania content to 10 % reduced the viscosity. Further increase to 15 % raised the viscosity to almost the value for the initial slag. The industrial titania bearing slags were considerably more fluid than slags from steel making pig iron production, not containing TiO_2. The effect of adding MgO to synthetic slags of the type made during vanadium pig iron production, was one of lowering the viscosity. Moreover, the fluidity did not drop materially even when the addition of MgO caused the liquidus temperature of the slag to increase markedly.

The use of titaniferous magnetite ores from the Bushveld Igneous Complex to produce a vanadium rich pig iron in a submerged arc electric furnace called for more viscosimetric data than were available at the time of pilot plant investigations conducted for the Highveld Steel and Vanadium Corporation. Slag titania contents would be high (approximately 35 %). Moreover, the CaO/MgO ratio would be close to unity if dolomite, which was preferred to limestone for economic reasons, were to be used as a flux.

The research work conducted by McRae[23] involved compositions at three levels of basicity, $(CaO + MgO)/SiO_2$, of 1,18 , 1,52 , and 1,91. The total (%CaO + %MgO) had the values 25, 30 and 35. The corresponding TiO_2 contents were 39,84 , 37,19 and 34,52 , while the TiO_2/Al_2O_3 content was maintained at 2,83. At each basicity ratio the CaO/MgO ratio was also varied.

In general, an increase of basicity at approximately the same CaO/MgO ratio, caused a decrease in viscosity at constant temperature. Progressive replacement of CaO by MgO on a mass % basis at the same overall basicity caused a slight decrease in viscosity at a particular temperature as shown in figure 14. If the same data are represented as the value of viscosity at a fixed temperature above the liquidus temperature, higher viscosity is associated with lower liquidus temperature. Moreover, increasing the measuring temperature - liquidus temperature gap tends to make this effect less pronounced. These trends are clearly demonstrated in figure 15.

Values of the activation energy for viscous flow over the composition range outlined above, varied from 102 to 140 KJ/mol.

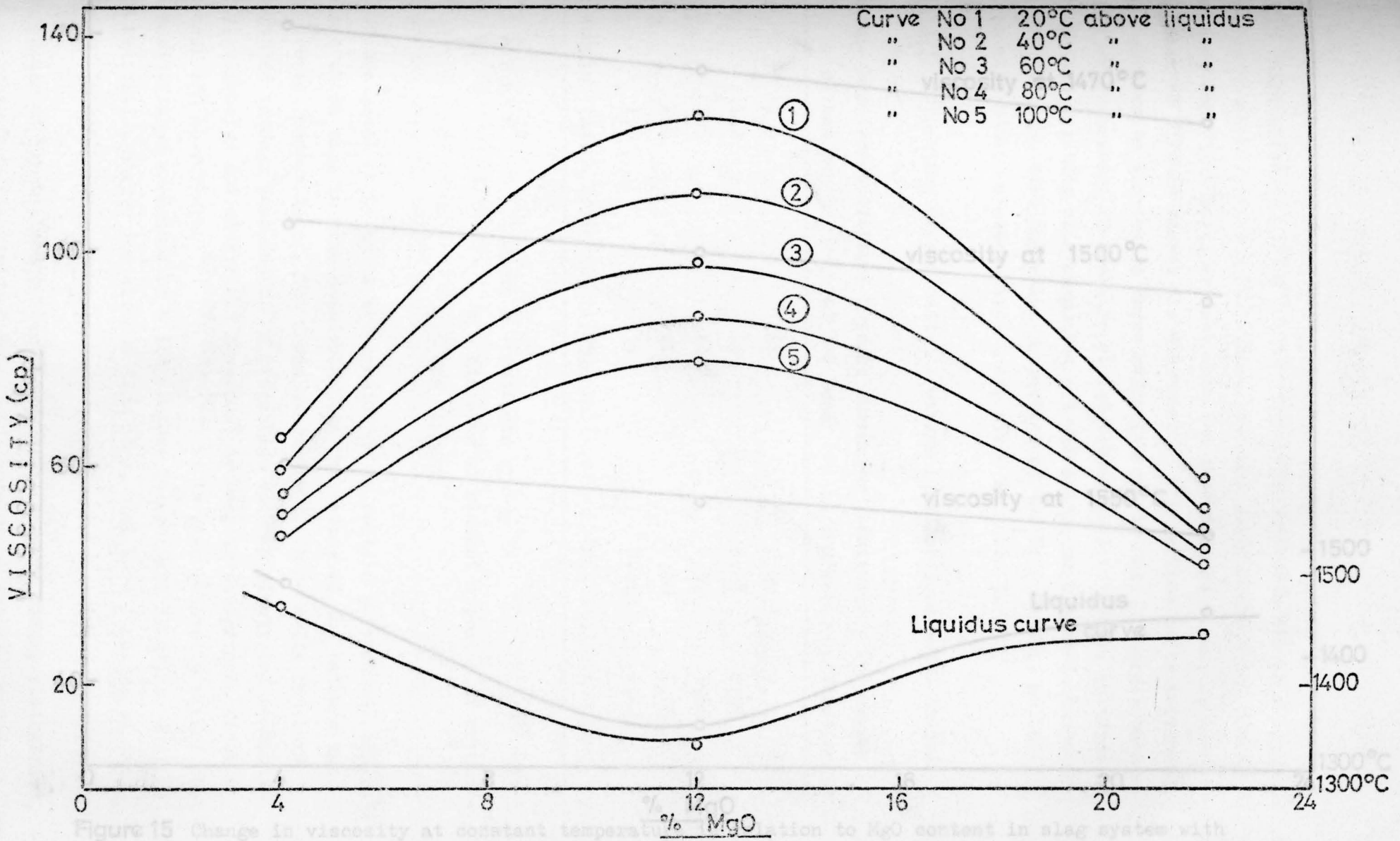


Figure 14 Change in viscosity as measured at 20°C intervals above the liquidus temperature in relation to MgO content in slag system with (CaO + MgO) = 30% (23)

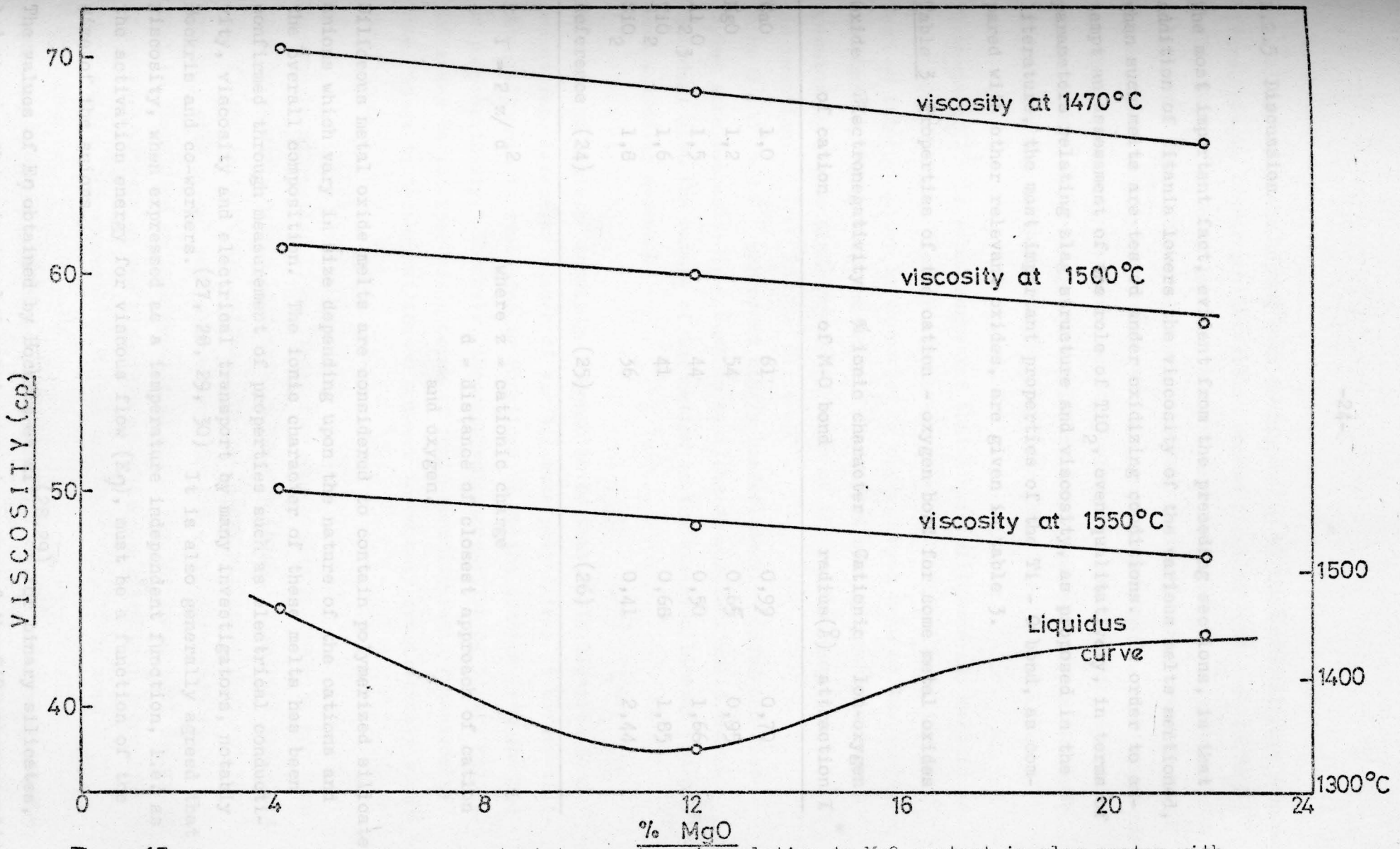


Figure 15 Change in viscosity at constant temperature in relation to MgO content in slag system with (CaO + MgO) = 30%. (23)

2.2.5 Discussion

The most important fact, evident from the preceding sections, is that addition of titania lowers the viscosity of the various melts mentioned, when such melts are tested under oxidizing conditions. In order to attempt an assessment of the role of TiO_2, even qualitatively, in terms of parameters relating slag structure and viscosity, as proposed in the literature, the most important properties of the Ti - O bond, as compared with other relevant oxides, are given in table 3.

Table 3 Properties of the cation - oxygen bond for some metal oxides

Oxide	Electronegativity of cation	% ionic character of M-O bond	Cationic radius(Å)	Ion-oxygen attraction I *
CaO	1,0	61	0,99	0,70
MgO	1,2	54	0,65	0,95
Al_2O_3	1,5	44	0,50	1,66
TiO_2	1,6	41	0,68	1,85
SiO_2	1,8	36	0,41	2,44
Reference	(24)	(25)	(26)	

* $I = 2z/d^2$ where z = cationic charge
d = distance of closest approach of cation and oxygen.

Siliceous metal oxide melts are considered to contain polymerized silicate anions which vary in size depending upon the nature of the cations and the overall composition. The ionic character of these melts has been confirmed through measurement of properties such as electrical conductivity, viscosity and electrical transport by many investigators, notably Bockris and co-workers.[27, 28, 29, 30] It is also generally agreed that viscosity, when expressed as a temperature independent function, i.e. as the activation energy for viscous flow (E_η), must be a function of the size of the anions.

The values of E_η obtained by Bockris et al[28,29] for binary silicates, led these authors to conclude that, upon increase of the SiO_2 concentration

of a binary silicate beyond that corresponding to the orthosilicate composition, simple linear polymerization occurs first to ions such as $Si_2O_7^{6-}$ and to $Si_3O_{10}^{8-}$. Ring ions of the type $Si_3O_9^{6-}$ and $Si_4O_{12}^{8-}$ appear later at 50 mol % SiO_2. Upon increasing the SiO_2 content further, the rings are believed to polymerize face to face to produce compact, almost spherical ions. However, $E\eta$ varies smoothly with SiO_2 concentration and such a relationship does not provide evidence for sudden changes in the type of discrete ion in the melt.

Richardson[31] therefore suggested that liquid silicates may contain an array of ions whose distribution is governed by chemical equilibrium. Such an interpretation is supported by experimental data on the analogous phosphate system. Toop and Samis[32] employed similar concepts in expressing the ionic distribution in terms of the equilibrium constant for the reaction: $2O^- = O^o + O^{2-}$, where O^-, O^o and O^{2-} represent singly bonded, doubly bonded and free oxygen ions respectively. Such an equilibrium constant would then be dependent upon the nature of the cation in the binary silicate. Masson[33] used a similar approach.

The present state of knowledge appears to be that ionic distributions and average molecular masses of the silicate poly-anions in binary silicate melts can be evaluated as functions of silica content with the aid of polymer theory. Moreover, thermodynamic properties of binary silicate melts may be interpreted in terms of ionic constitution. Extension of these ideas to ternary silicates appears to be only qualitatively possible.

Ion-oxygen attraction I, as listed for some oxides in table 3, has been used to separate oxides into network formers (high I), network modifiers (low I) and intermediate oxides. $E\eta$ for binary silicates does not vary smoothly with I, but the table shows that TiO_2, together with Al_2O_3, must be classified as intermediate oxides. For the purpose of comparing the effect of TiO_2 on the viscosity of siliceous melts with those of other oxides, the approach of Marboe and Weyl[15] will be used.

According to these authors an increase in the oxygen to silicon cation ratio, by addition of oxides whose cations possess lower I than Si^{4+},

to SiO_2, not only increase the number of O^{2-} ions, but also renders the O^{2-} ions better screeners of the positive Si^{4+} core. The latter effect is due to the fact that the polarizability of O^{2-} decreases with an increase in the strength of adjacent positive fields and that the screening power of an anion increases with its polarizability. Assuming Ti to be present in the structure only in 6-fold coordination, it would on a molar basis, produce twice as many "weak points" in the network as a divalent cation eg. Ca^{2+}, as suggested by Schenk and Frohberg.(14)

As viscous flow is believed to involve continuous deformation of O^{2-} ions and a gradual change in their positions with respect to the central cation, the binding forces within the polyhedra are also important. These would be governed firstly, by the charge of the central cation. In this respect Ti^{4+} would be expected to behave in a manner very similar to Si^{4+}. However, binding forces within the polyhedra are further influenced by the state of polarization of the O^{2-} ions, which should be a function of the ion-oxygen attraction of the other oxides present eg. CaO, Na_2O etc. The state of polarization of the anions will also be influenced by the polarizability of the central cation itself, polarizability being described as the ability of the cation to adjust its electron cloud in a manner to be best accommodated in its environment. A highly deformable electron cloud can screen its core even under conditions of temporarily reduced coordination with respect to oxygen, such as would arise during the process of viscous flow. Here it must be noted that Ti^{4+} is a non-noble gas type cation, compared with Si^{4+} which is of the noble gas type. This would mean that the force field of Ti^{4+} is not necessarily spherically symmetrical. Such dissymmetry would cause inherently distortable sites in a network based on tetrahedrally coordinated Ti and Si, a condition that would be enhanced by the presence of other cations of low field strength.

The semi-conducting property of non-stoichiometric rutile and the influence it must necessarily exert on the electrical conducting properties of oxide melts containing titanium oxide, will be discussed in a later section. In the present context, it is only important that rutile does lose oxygen even when heated in air, and that the effect is intensified as the partial pressure of oxygen in contact with the solid phase is lowered. This departure from stoichiometry is accompanied by a darkening in

the colour of the initially white rutile. The same property, though less pronounced, is exhibited by titaniferous oxide melts. If a melt containing both SiO_2 and TiO_2 in addition to one or more modifying oxides, is assumed to be based on a silicate network, with some replacement of Si^{4+} by Ti^{4+}, oxygen loss must give rise to vacant anion sites, associated with electrons, which may cause a permanent lowering of the valency of Ti. In the event of such an extreme electron transfer, Ti may enter into 6-fold coordination. However, if the electrons are assumed to remain associated with the vacancy, their position probability sphere being extended with increase in the temperature, the vacancy may be pictured as a mobile one, a condition dictated by the requirements of viscous flow. Moreover, the polarizing influence of a cation such as Ca^{2+} on a doubly bonded oxygen in the statistical vicinity of a vacancy will be enhanced by the "reduced" charge of the central cation Ti^{4+}.

The cationic radius of Ti^{4+} is very close to that of Mg^{2+} and considerably greater than that of Si^{4+}. If Mg^{2+} and Ti^{4+} were present in a siliceous melt, Ti^{4+} would be favoured as part of a tetrahedrally coordinated network, due to its higher charge. However, the comparable accepted ionic radii, the fact that calculation of these radii presupposes spherically symmetrical ions, the possibility that Ti possesses a radius in the melt that is slightly larger than the one quoted for Ti^{4+} and that its charge may on the average be imagined to be lower than 4, makes the differentiation less certain. Moreover, Ti^{4+} possesses high polarizability. If in the light of this, the titanium and magnesium ions may be assumed to require the same increase in coordination number due to their larger sizes, as compared with that of Si^{4+}, titanium must create at least 1,5 times, but probably closer to twice the number of distortion sites in the network that could be provided by magnesium, on a molar basis.

The findings of Thakur[15] as shown in figure 11, relate to low temperature viscosity of glasses of the system Na_2O-TiO_2-SiO_2, where SiO_2 is replaced progressively by TiO_2. The results are reported as the temperature at which a glass of particular composition reaches a certain viscosity. Marboe and Weyl explained this tendency for additions of TiO_2 to increase the temperature for a given viscosity value on the basis of Ti^{4+} being a larger ion than Si^{4+} and consequently having greater coordination requirements so that presumably, Si^{4+} is eventually forced out of the

tetrahedral network to share corners of the TiO_6^{8-} octahedra. While such a mechanism may be feasible at low temperature, there exists no evidence in the literature that octahedrally coordinated Ti may constitute the building unit of a network in high titania slags at slag forming temperatures.

On the basis of atomic properties as listed in table 3, alumina and and titania are normally classed together as intermediate oxides. The cationic radius of Al^{3+} is considerably smaller than that of Ti^{4+}, the difference in valency giving the latter the greater field strength. Furthermore the Al^{3+} ion is of the noble gas type. Aluminium oxide does not show the departure from stoichiometry that is such a well known property of TiO_2, so that a mean field strength larger than the one normally accepted is not likely in the case of Al^{3+}.

From the work of Kozakevitch[34], it is evident that addition of alumina to a $CaO-SiO_2$ melt initially increases the viscosity at a constant CaO/SiO_2 ratio. This effect is reversed upon exceeding a molar ratio of Al_2O_3/CaO of 1. This behaviour is attributed to Al_2O_3 initially entering the liquid structure in 4-fold coordination. As it can only do so with the simultaneous addition of CaO, due to the requirements of electrical neutrality, the composition requirements for complete tetrahedral coordination only becomes fulfilled at $Al_2O_3/CaO = 1$. Beyond this limit Al^{3+} can exist in the structure in octahedral coordination as well.

The work done on the analogous titaniumoxide bearing systems $TiO_2-SiO_2-Al_2O_3$ and $CaO-SiO_2-TiO_2$[12,14] although less exhaustive, reveals no trends similar to what was established for the $CaO-SiO_2-Al_2O_3$ system. From the work of Frohberg and Weber[12] on the system $SiO_2-TiO_2-Al_2O_3$, it appears as though the thickening effect of alumina is less pronounced at high TiO_2/Al_2O_3 ratios. In this respect the effect of TiO_2 is obviously not similar to that of lime and it may in fact indicate 4-fold coordination of Ti^{4+} under these conditions, with a gradual change towards higher coordination numbers at lower TiO_2/Al_2O_3 ratio. Because of the doubtful nature of these results due to the use of graphite viscometer components, such a conclusion can have little claim on absolute validity.

Even replacement of $(CaO + Al_2O_3)$ by $2TiO_2$ on a molar basis in the sys-

tem $CaO-SiO_2-Al_2O_3-TiO_2$ do not lead to similar effects, judging from the limited information available on the system.[18]

In the discussion of their results of viscosity measurements carried out on Sorel type slags, Handfield and Charette[10] discard the suggestion of Reznichenko[35] that octahedral anions of the type TiO_6^{8-} might constitute the "flow units" in these very high titania slags. Reznichenko based his hypothesis on the fact that the TiO_6 octahedron is the structural unit of solid anosovite and found support for his view in the rapid crystallization rate of these slags, as reflected also in the rapid rise of viscosity upon crystallization. A melt consisting of such non-polymerized units would be very fluid. However, Handfield and Charette concluded on the basis of the very high electrical conductivity of these melts, that such units were unlikely and that the structure of high titania slags will not be understood until a more general theory explaining the semi-conducting properties of these melts is developed.

In conclusion, it may be said that the author accepts the possibility of the following two extreme conditions in oxide melts based on TiO_2 and SiO_2, under oxidizing conditions:

(a) An essentially tetrahedral network at very low titania contents, the Ti^{4+} entering the structure in octahedral coordination, possibly with relatively strong "bridging" effects.

(b) Essentially octahedral anions based on Ti^{4+}, interlinked by Si^{4+} and other cations, at very high titania contents.

The intermediate levels of TiO_2 concentration would be characterized by mixed coordination of Ti^{4+}. As TiO_2 is only believed capable of decreasing the viscosity of such melts, regardless of its coordination, and as there can be no sharp transition between coordination states, due mainly to its property of losing oxygen, TiO_2 will increase the fluidity at increasing levels of concentration in a relatively continuous manner. Transition is vizualized as an equilibrium process, depending upon the concentrations and field strengths of other cations present, and the temperature.

2.3 Reduction product and rate studies

The high fluidity of titaniferous iron-making slags under oxidizing conditions is now generally accepted, and the difficulties experienced during the smelting of titanferous iron ores are commonly attributed to the reduction of TiO_2 to either lower oxides or to high melting titanium compounds eg. TiC or to both. Consequently, the data available on reduction of both pure TiO_2 and TiO_2 in slags are relevant to this study.

2.3.1 The system Ti - O

In 1954 DeVries and Roy[36] published a "not impossible" phase diagram for this system, based on their selection of data available in the literature at the time. This diagram is shown in figure 16.

2.3.1.1 The composition range $TiO_{0 - 0,5}$

According to Andersson et al[37] the maximum solubility of oxygen in Ti is generally accepted to correspond to $TiO_{0,5}$. Oxygen atoms are randomly arranged in the octahedral interstices of the close packed hexagonal lattice of Ti. With increased incorporation of O, the a-axis goes through a maximum at $TiO_{0,35}$, while the steady increase of the c-axis is suddenly accelerated here.

2.3.1.2 The composition range $TiO_{0,5 - 1,4}$

High temperature samples with compositions $TiO_{0,64 - 1,26}$ give powder photographs showing only the pattern of a single sodium chloride type phase. Titanium and oxygen occupancy in this range vary between the approximate limits 96 % to 77% and 61 % to 98 % respectively. Outside this composition range, additional phases - either α Ti or Ti_2O_3 - appear.

Low temperature samples (below approximately 990°C) consist of a complex mixture of phases including Ti_2O, an oxide of approximate composition $TiO_{0,65}$, TiO (a low temperature modification of the stoichiometric composition), TiO (NaCl type of very narrow homogeneity range and approximate composition $TiO_{1,2}$) and Ti_2O_3.

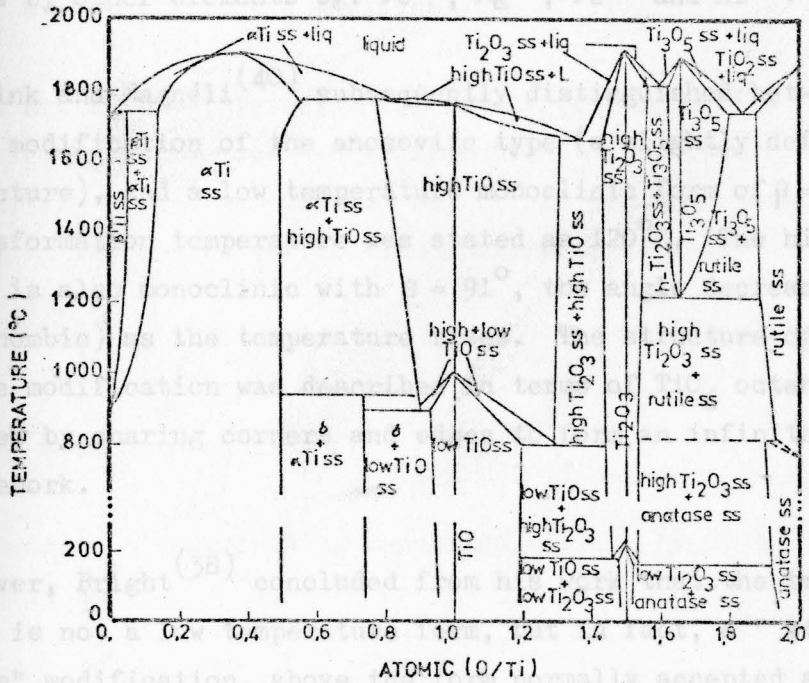


Figure 16 Phase diagram for the system Ti-TiO_2 based on literature data.[36]

2.3.1.3 The composition range $TiO_{1,4 - 1,7}$

Ti_2O_3 possesses the corundum structure and has a homogeneity range of $TiO_{1,49 - 1,51}$ according to Andersson et al.

The compound Ti_3O_5 however, is less well defined. Rusakov and Zhdanov[39] prepared a phase of this nature from the titaniferous slags produced during ilmenite smelting. They classified it as orthorhombic and attached the name anosovite to it. Doubt arises over the validity of this result, the method of preparation making possible contamination of the titanium oxide by other elements eg. Fe^{2+}, Mg^{2+}, Fe^{3+} and Al^{3+}.

Åsbrink and Magnéli[40] subsequently distinguished between a high temperture modification of the anosovite type (a slightly deformed pseudobrookite structure), and a low temperature monoclinic form of $\beta = 91,5^{\circ}$. The phase transformation temperature was stated as $120^{\circ}C$. The high temperature form is also monoclinic with $\beta = 91^{\circ}$, the angle decreasing to 90° (orthorhombic) as the temperature rises. The structure of the low temperature modification was described in terms of TiO_6 octahedra which are joined by sharing corners and edges to form an infinite three-dimensional framework.

However, Bright[38] concluded from his work that the truly monoclinic form is not a low temperature form, but in fact, a " still higher temperature" modification, above the form normally accepted as orthorhombic.

2.3.1.4 The composition range $TiO_{1,7 - 1,9}$

Andersson found that the lines for Ti_3O_5 were completely replaced by those of a new phase at $TiO_{1,75}$. Upon increasing the oxygen content, these lines remained basically the same although closer examination revealed a continual alteration between single phase and two-phase regions. The successive phases appeared to have the general formula Ti_nO_{2n-1}. Members corresponding to values of n = 4 - 10 were identified. The successive members constitute a homologous series of rutile structure.

2.3.1.5 The composition range $TiO_{1,9}$ - 2,0

There are indications that the homologous series mentioned above, exists beyond $TiO_{1,9}$, but apparently the difference between X-ray patterns for successive homologues decreases as n increases, so that the two-phase regions are not detected. However, it remains uncertain whether distinct phases of Ti_nO_{2n-1} exist right up to the two-phase region with TiO_2, or whether it terminates in a phase of variable composition. The first trace of rutile appears at $TiO_{1,95}$.

2.3.1.6 The allotropic modifications of TiO_2

These are anatase (tetragonal), rutile (tetragonal) and brookite (orthorhombic). Anatase has two modifications: a low temperature β - form, converting to the α - form at 640°C. At 915°C α changes to rutile. Brookite changes to rutile with measurable velocity at all temperatures above 650°C.

2.3.2 Reduction of TiO_2

The equations representing reduction of TiO_2 by CO and C are summarized in table 4.

Table 4 Thermodynamic data for reduction of TiO_2 by carbon and carbon monoxide

Reaction	ΔG° = f(T) (cals/mol TiO_2)	Minimum reduction temperature (°C)
$TiO_2 + \frac{1}{2}CO = Ti_2O_3 + \frac{1}{2}CO_2$	13 950 - 0,30 T	-
$TiO_2 + CO = TiO + CO_2$	24 390 - 0,28 T	-
$TiO_2 + \frac{1}{2}C = \frac{1}{2}Ti_2O_3 + \frac{1}{2}CO$	29 350 - 21,15 T	1115
$TiO_2 + C = TiO + CO$	65 190 - 42,93 T	1245
$TiO_2 + 2C = Ti + 2CO$	171 100 - 84,23 T	1784
$TiO_2 + 3C = TiC + 2CO$	126 100 - 81,44 T	1276

2.3.2.1 Reduction by CO

Assayag et al[41] studied the stoichiometric reaction for reduction of TiO_2 by CO to give TiO_{2-x} and CO_2, where TiO_{2-x} is the overall composition of the solid product, by equilibration of the oxide with known CO/CO_2 ratios, between 840°C and 1250°C. For values of $x \geq 0,6$, two solid phases were in equilibrium and X-ray studies of the product with $x = 0,11$ showed a rutile phase in addition to a phase that was not identified, but which was not Ti_2O_3.

Nishimura et al[42] reduced TiO_2 with CO over the temperature range 800°C to 1400°C for periods varying from 1 hour to 24 hours. The reduced equilibrium product corresponded to $Ti_{64,2}O_{35,8}$.

In a much earlier work, Mikhailov and Belyakova[43] reported that reduction at 1300°C only gave a 7,9 % reduction. (The corresponding figure for reduction by H_2 at the same temperature was given as 26,3 %). The product after reduction by CO was a mixture of TiO_2 and Ti_2O_3.

Ohno and Ross[44] kept TiO_2 in a CO atmosphere at 1500°C for periods up to 3 hours. X-ray analysis of the final product after reduction for 3 hours, showed the presence of a rutile phase and another unidentified phase, which could be Ti_3O_5.

3.2.2.2 Reduction of TiO_2 by carbon

Belyakova et al[45] found the product of reducing TiO_2 with charcoal at 1100°C to 1500°C to be a solid solution of TiC and TiO, the TiC content varying from 33 to 60 %.

The sequence of products after reduction either in vacuum or in a CO atmosphere, was found by Kubo and Shurniki[46] to be $TiO_2 \longrightarrow TiO_{1,8-1,7} \longrightarrow Ti_2O_3 \longrightarrow (TiC_xO_y)$. The latter phase could then further react with carbon beyond 1400°C to yield TiC. In fact, Mikhailov and Belyakova[43] stated that the reduction reaction started at 927°C and that pure TiC could be obtained by heating a mixture of TiO_2 and C for 2 hours at 1850°C to 1900°C.

Ohno and Ross[44] conducted the reduction in both argon and nitrogen atmospheres, the tests lasting for two hours at 1450°C. Oxygen was removed faster in the latter case. When the atmosphere for the experiment was argon, the product was found to be TiC. Under nitrogen, TiN was identified, but no TiC was present.

2.3.3 Carbonaceous reduction of TiO_2 from titaniferous slags.

2.3.3.1 Reduction products

The range of products formed during carbonaceous reduction of TiO_2 contained in titaniferous burdens includes the lower oxides of titanium, titanium carbides and oxy-carbides, in addition to nitrides, oxy-nitrides and carbo-nitrides, if nitrogen is present in the furnace atmosphere. Evidence exists for the formation of virtually all these products, in the form of both plant observation and laboratory investigations.

In 1921 Osann[47] reported analytical results of the copper coloured crystals on a piece of magnesite mixer lining. The product was found to be titanium carbo-nitride. Jansson[48] investigated similar crystals recovered from the interstices of the lining bricks in the hearth of a blast furnace. The composition corresponded to approximately (6TiN + TiC). The sintered ore charged to the furnace contained 0,14 % Ti.

Freidenzon et al[22] seperated the "buckshot slag" produced during blast furnace smelting of titano-magnetite ores into slag and metal fractions. The slag differed from the roughing slag in having a considerably higher carbon content. The metallic fraction differed from the tapped pig iron as shown in table 5.

Table 5 Metal analyses during vanadium pig iron production

Product	Composition (mass %)				
	Si	S	V	Ti	C
Metal from buckshot	11,84	0,400	0,40	3,00	5,20
Tapped pig iron	0,47	0,038	0,41	0,41	4,75

It is significant that the composition of the buckshot slag metallic fraction is much closer to that of the metal in the bosh and bosh parallel regions, than to the composition of the tapped pig iron.

Metallographic examination of both the metallic fraction of the buckshot slag and the vanadium pig iron, revealed abundant TiN inclusions.

Ohno and Ross [44] examined the surface films produced on slags of the system $CaO-SiO_2-Al_2O_3-TiO_2$ after reduction in a graphite crucible both in argon and in nitrogen atmospheres. Titanium nitride was identified on slags reduced in an atmosphere of nitrogen. Conclusive identification of TiC on these slags and on those that were reduced in argon was impossible due to the possible presence of other similarly coloured materials, especially graphite and lower titanium oxides. However, the authors strongly suggested that the films might be the carbide, because of their similarity to the product obtained when pure TiO_2 was reduced by carbon, a product which was identified as TiC.

Although many authors mention the limited solubility of Ti in iron melts and the precipitation of high melting phases such as carbides and nitrides, when the solubility limit is exceeded, [22,49,50] the work carried out by Delve, Meyer and Lander [51] is particularly significant, as the solubility limits were shown to be even lower than those previously accepted. These authors measured the solubility of titanium in carbon-saturated iron at 1500°C and 1600°C under neutral and nitrogen atmospheres. The precipitated phases were also examined. The results are shown in table 6:

Table 6 Solubility of Ti in carbon and carbon-nitrogen saturated iron [51]

Temp. (°C)	Atmosphere	Ti solubility (mass %)	Precipitated phase
1500 ± 10	CO and A	0,263 ±0,006	TiC
"	N_2	0,152 ±0,010	Carbo-nitride
1602 ± 10	CO and A	0,299 ±0,080	TiC
"	N_2	0,202 ±0,011	Carbo-nitride

The table shows that when iron is saturated with nitrogen in addition to carbon, titanium solubility drops even further.

There are also indications that silicon in the presence of nitrogen, decreases the solubility of titanium.

The existence of slag oxygen levels corresponding to lower oxides of titanium in titaniferous slags under reducing conditions, is implied by the end products observed in the above investigations.

2.3.3.2 The effect of slag composition on the rate of reduction of TiO_2 in titaniferous slags.

Extensive evidence exists to the effect that basicity of the slag, expressed in various ways, influences titania reduction. In 1939 Mikhailov and Belyakova[52] reported that TiC was formed more readily in basic slags than in acid slags of the system SiO_2-TiO_2-Al_2O_3-CaO. The results of Ohno and Ross,[44] obtained from reduction of acidic and basic slags at 1500°C in a nitrogen atmosphere show the same trend. These results are shown in figure 17, the slag compositions being given in table 7.

Table 7 Compositions of slags reduced in graphite crucibles at 1500°C in a nitrogen atmosphere.[44]

Slag No.	Mass % composition		
	CaO	SiO_2	TiO_2
3	27,20	42,80	30,00
4	37,63	32,37	30,00

Chukukere and Ross[53] reduced slags of the system CaO-SiO_2-FeO-Al_2O_3-TiO_2 in graphite crucibles, the slag being in contact with carbon-saturated iron. Titania reduction from the slag was followed by analysis of the metal phase. Figure 18 shows the effect of basicity, expressed as CaO/SiO_2, upon the reduction rate of TiO_2 in a slag of initial TiO_2 content 20 mass %. The slopes of the curves further indicate that titanium saturation in the metal is attained sooner with slags of higher

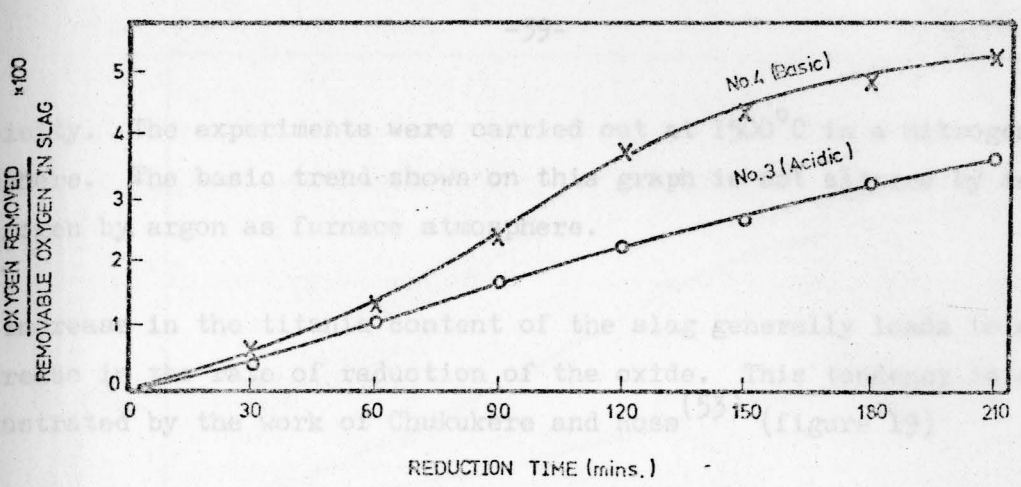


Figure 17 Effect of basicity on the reduction of acidic and basic slags by carbon in a nitrogen atmosphere at 1500°C.(44)

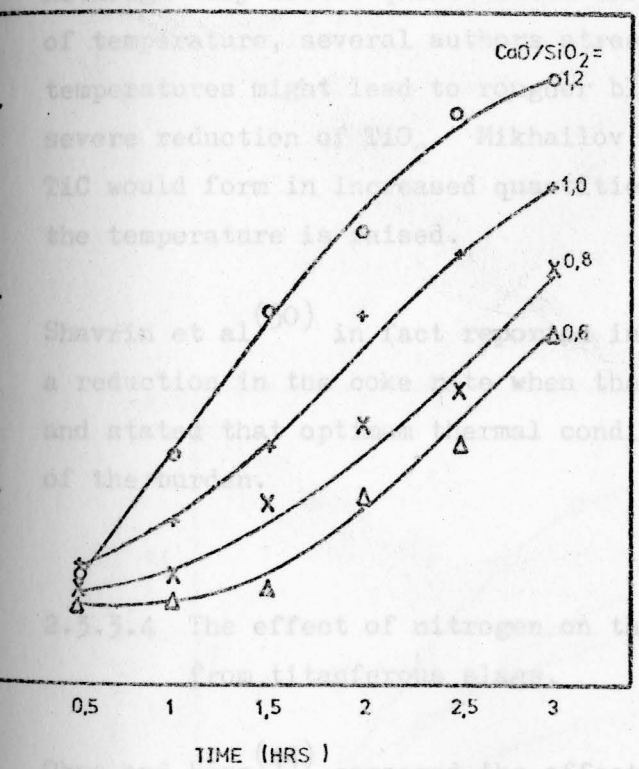


Figure 18 Titania reduction rate as a function of slag basicity.(53)

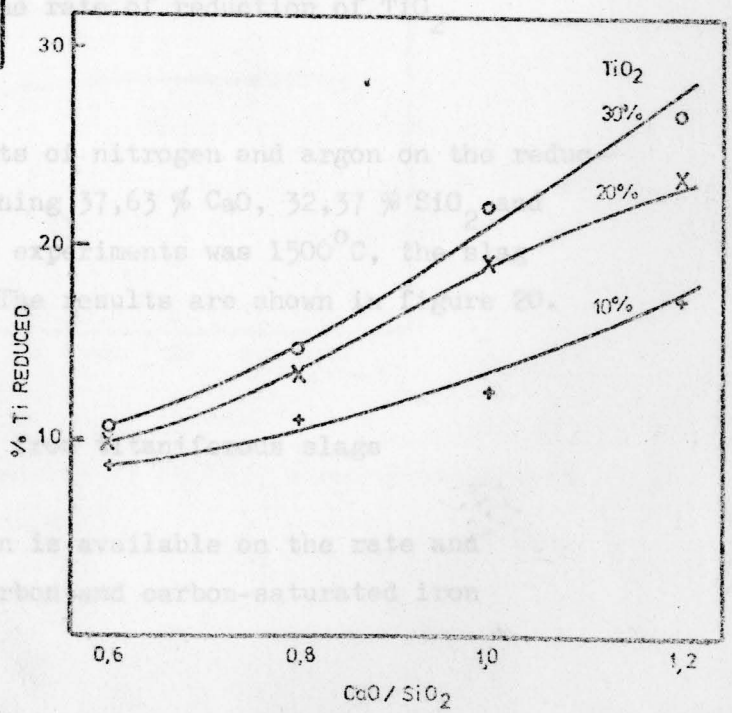


Figure 19 The influence of initial TiO_2 content on the extent of reduction after 2 hrs. at 1500°C. (53)

basicity. The experiments were carried out at 1500°C in a nitrogen atmosphere. The basic trend shown on this graph is not altered by replacing nitrogen by argon as furnace atmosphere.

An increase in the titania content of the slag generally leads to an increase in the rate of raduction of the oxide. This tendency is also illustrated by the work of Chukukere and Ross[53] (figure 19)

2.3.3.3 The effect of temperature on the rate of reduction of TiO_2 from titaniferous slags.

Although very little quantitative information is available on the influence of temperature, several authors stressed the possibility that increased temperatures might lead to rougher blast furnace operation due to more severe reduction of TiO_2. Mikhailov and Belyakova[52] pointed out that TiC would form in increased quantities in the blast furnace hearth as the temperature is raised.

Shavrin et al[50] in fact reported increased production, accompanied by a reduction in the coke rate when the hearth temperature was lowered and stated that optimum thermal conditions depend on the TiO_2 content of the burden.

2.3.3.4 The effect of nitrogen on the rate of reduction of TiO_2 from titanferous slags.

Ohno and Ross[44] compared the effects of nitrogen and argon on the reduction rate of TiO_2 from a slag containing 37,63 % CaO, 32,37 % SiO_2 and 30 % TiO_2. The temperature for both experiments was 1500°C, the slag being held in a graphite crucible. The results are shown in figure 20.

2.3.4 Co-reduction of SiO_2 and TiO_2 from titaniferous slags

Although a vast volume of information is available on the rate and mechanism of reduction of SiO_2 by carbon and carbon-saturated iron

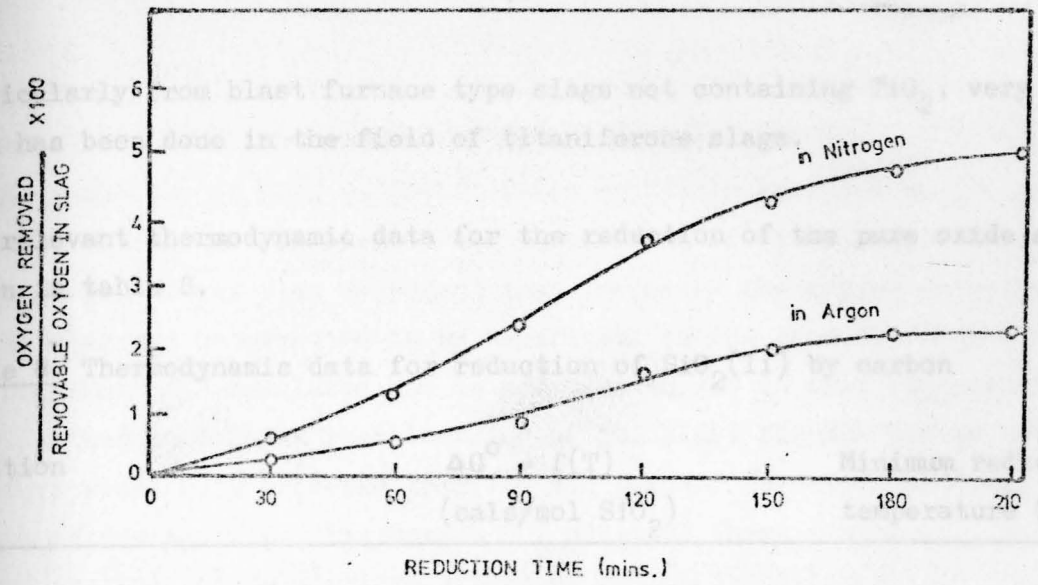


Figure 20 The influence of atmosphere on reduction of TiO_2 from a slag.(44)

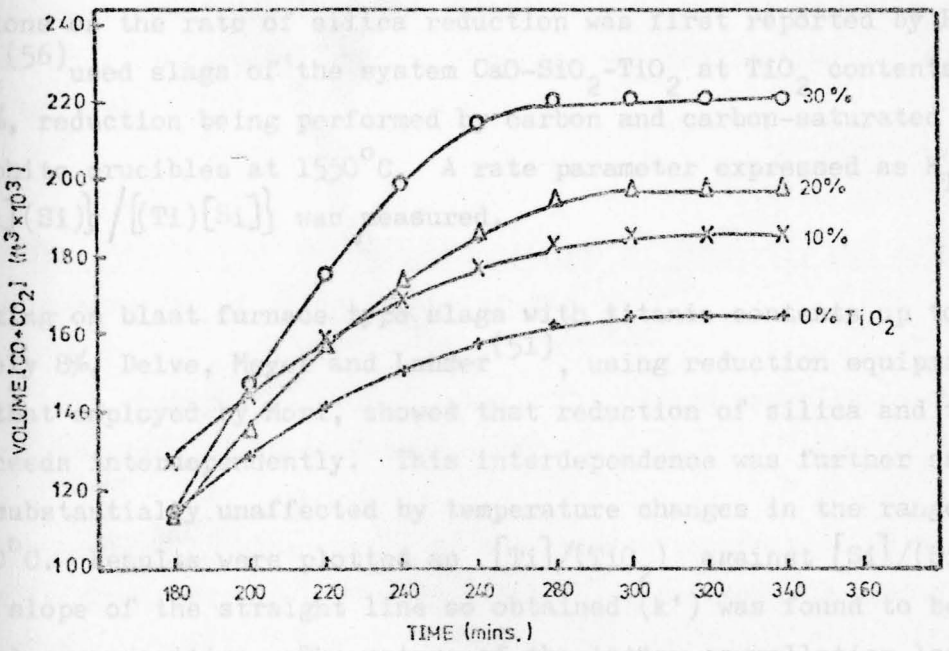


Figure 21 Volume ($CO + CO_2$) evolved at 1500°C, showing the effect of TiO_2 content, at $CaO/SiO_2 = 0,8$ (53)

particularly from blast furnace type slags not containing TiO_2, very little work has been done in the field of titaniferous slags.

The relevant thermodynamic data for the reduction of the pure oxide are given in table 8.

Table 8 Thermodynamic data for reduction of SiO_2(li) by carbon

Reaction	ΔG^o = f(T) (cals/mol SiO_2)	Minimum reduction temperature (^oC)
SiO_2(li) + C = SiO(g) + CO	163 650 - 79-96 T	1777
SiO_2(li) + 3C = SiC + 2CO	148 000 - 81,49 T	1547
SiO_2(li) +2C = Si(li) + 2CO	173 100 - 89,40 T	1664

On the diagrams of standard free energy of formation as a function of temperature, as given by eg. Darken and Gurry[54], the lines for TiO_2 and SiO_2 are virtually parallel and very close to one another.

The dependence of titania reduction under blast furnace smelting conditions on the rate of silica reduction was first reported by Faust[55]. Mori[56] used slags of the system $CaO-SiO_2-TiO_2$ at TiO_2 contents up to 35 %, reduction being performed by carbon and carbon-saturated iron in graphite crucibles at 1550°C. A rate parameter expressed as $K_{Ti,Si} = \{[Ti](Si)\} / \{(Ti)[Si]\}$ was measured.

Working on blast furnace type slags with titania contents up to approximately 8%, Delve, Meyer and Lander[51], using reduction equipment similar to that employed by Mori, showed that reduction of silica and titania proceeds interdependently. This interdependence was further shown to be substantially unaffected by temperature changes in the range 1500 to 1600°C. Results were plotted as $[Ti]/(TiO_2)$ against $[Si]/(SiO_2)$ and the slope of the straight line so obtained (k') was found to be a function of slag composition. The nature of the latter correllation led the authors to conclude that the best slag for minimizing titania reduction would be one containing high SiO_2 and correspondingly low CaO/SiO_2.

2.3.5 Co-reduction of titania and iron oxide

If the reduction of TiO_2 to lower oxides or TiC is accepted as the cause of the difficulties experienced during smelting of titaniferous burdens, the presence of any slag component that increases the oxygen potential of the slag can be expected to be beneficial to the process. Mikhailov and Belyakova[52] mentioned MnO in addition to FeO in this connection. They further postulated that lowering of the blast furnace hearth temperature would help preserve slag FeO and prevent formation of lower titanium oxides and TiC. Freidenzon[22] accepted these statements, but warned against the deleterious effect of FeO on desulphurization processes and foaming of slags, in conjunction with the thermal state of the furnace favouring high slag FeO contents.

Chukukere and Ross[53] also determined overall reduction rates of slags belonging to the $CaO-SiO_2-TiO_2-Al_2O_3-FeO$ system. The total $(CO + CO_2)$ gas volume evolved upon reduction at 1500°C was determined. At constant basicity, expressed as CaO/SiO_2, an increase in titania content was found to increase the rate of reduction and decrease the final amount of FeO retained in the slag. Their results are shown in figure 21 (p.40). The authors concluded that the effect of TiO_2 on the activity of FeO in the slag, particularly in acid slags, was qualitatively similar to that of lime.

2.4 The influence of reducing conditions on viscosity and melting temperature of titaniferous slags.

2.4.1 The possible reasons for the difficulties experienced during the smelting of titaniferous ores.

The importance of slag viscosity and melting temperature in any pyrometallurgical process producing liquid slag and metal products, is generally accepted.

It is also agreed that the reduction of titania is responsible for the problems experienced when titaniferous burdens are smelted and carbon is used as a reducing agent. It was shown in section 2.3 that a wide variety

of products can be formed during such reduction of titanium oxide. The nature of the effect of these products on furnace operation is however not yet clear and the following possibilities must me considered.

(a) Lower oxides of titanium, presumably not separating from the molten slag, may influence slag viscosity.

(b) TiC and TiN and solid solutions of these compounds may separate from the slag in finely dispersed form and, unable to settle, increase the slag viscosity.

(c) The formation of carbides and nitrides may not influence slag viscosity as such to a great extent, but may grow in the furnace hearth to form accretions, leading to rough operation. These compounds may further coat metal droplets and prevent coalescence of such droplets. The presence of solid particles may also contribute to the phenomenon of slag foaming.

In order to illustrate the controversy existing with respect to these possibilities, the conclusions of several investigators will be reviewed.

2.4.2 Mikhailov and Belyakova[52] (1939)

The acid slags tested by these authors contained 19,20 % SiO_2, 0,09 - 25,65 % TiO_2, 18,37 - 30,20 % Al_2O_3, and 26,7 - 36,12 % CaO. Basic slags were made up of 6,58 - 8,60 % SiO_2, 0,76 - 24,20 % TiO_2, 17,8 % Al_2O_3 and 37,5 - 49,72 % CaO. While addition of TiO_2 increased the fluidity of acid slags, it had the opposite effect on basic slags. Both TiO and Ti_2O_3 were found to raise the viscosity of both acid and basic slags. TiC markedly thickened all slags.

Fluidity was measured as the ratio of the length of the slag stream to the mass of the poured slag, so that by modern standards, the validity of the conclusions may be doubted. While the effect of TiC on apparent viscosity cannot be vizualized to be any other than one of reducing the fluidity, the possibility of TiO and Ti_2O_3 affecting also the melting temperature of the slag, cannot be neglected.

2.4.3 Semik[57] (1941)

Research work was carried out on blast furnace type slags. While the effect of TiO_2 was concluded to be qualitatively similar to that of lime, but quantitatively much less pronounced, holding the slag in a graphite crucible in a CO atmoshere was found to alter the slag viscosity. Addition of TiO_2 to blast furnace slags under these conditions initially rendered the fluidity slightly higher. Upon extension of the holding time, the viscosity increased. However, the increase was slight in the case of slags containing up to 20 % TiO_2, but increasing the TiO_2 content up to 30 % caused severe thickening at constant temperature. For holding times exceeding 6 hours, the amount of TiC produced was deemed sufficient to be responsible for the increases of viscosity reported.

2.4.4 Delve, Meyer and Lander[51] 1961

The work of these investigators was confined to the measurement of titanium solubility in carbon and carbon-nitrogen saturated iron and to measurement of TiO_2 reduction rates from low titania blast furnace slags, as described in section 2.3.

However, based on the findings of Semik[57], their own conclusion that low CaO/SiO_2 ratios did not favour TiO_2 reduction from slags, and the relatively high oxygen potential of slags in the bosh region of the blast furnace, they concluded that titania reduction was unlikely to cause trouble above the tuyere line in a furnace operating on burdens of such low TiO_2 contents as those considered in their paper (below about 8 %). Further, led by the slowness with which an increase in the TiO_2 content of the burden made itself apparent, they suggested that factors of slag viscosity were not of primary significance.

The authors based their statements on their own findings of low titanium solubility in iron, the low content of TiO_2 in the slag that will make precipitation possible (1 - 3 %), the nature of the precipitated phases and practical observation of massive titanium carbo-nitride in the hearth of a blown out blast furnace. They suggested that increase in the titania content of the slag could lead very readily to growth of TiC-TiN solid solutions in the hearth, the resulting accretions eventually growing

outward and upward into the slag layer. The constriction formed in this manner would cause a higher than normal slag level, leading to the normal symptoms of trouble. Further deterioration of the condition would interfere with the flow of materials above the tuyere line.

2.4.5 Ohno and Ross[18] (1963)

Slags of the $CaO-SiO_2-Al_2O_3-TiO_2$ system were subjected to viscosity measurements under reducing conditions.

When carbon was to serve as the reductant, viscosity measurement was performed isothermally in a graphite crucible, using a molybdenum viscometer plunger. The furnace atmosphere was argon. Slag thickening occurred in all instances.

An increased temperature was found to increase the thickening rate. Figure 22 illustrates this as a plot of time at temperature for the slag to reach a viscosity of 5 poise, against temperature. The compositions of the slags are given in table 9.

Table 9

Slag	Composition (mass %)		
	CaO	SiO_2	TiO_2
A	32,25	27,75	40,0
B	26,25	33,75	40,0

Figure 23 shows that, for a particular slag, containing 50 % TiO_2, the thickening rate at 1600°C is gradual, while at all temperatures of 1550°C and lower, the viscosity rises very suddenly.

It was further shown that an increase in the titania content of a slag increases the thickening rate very substantially (figure 24). The same graph also illustrates the effect of basicity (expressed as CaO/SiO_2) on the thickening rate. These experiments were conducted at 1600°C.

In another series of tests at 1600°C, the authors replaced the argon

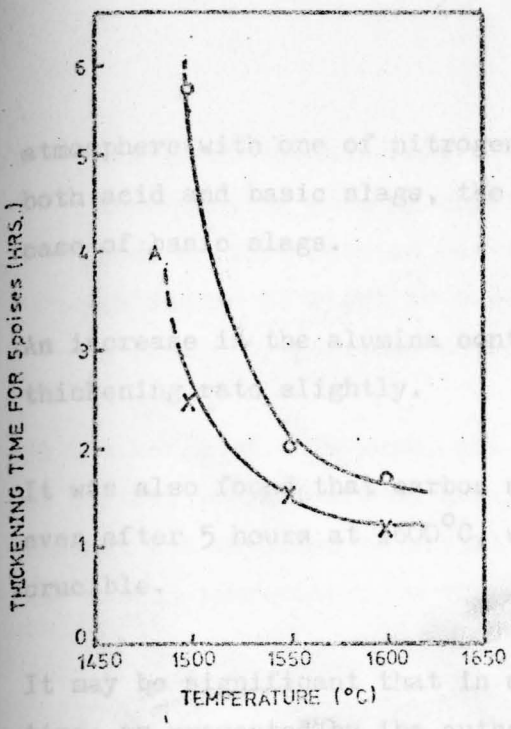


Figure 22 Effect of temperature on slag thickening (18)

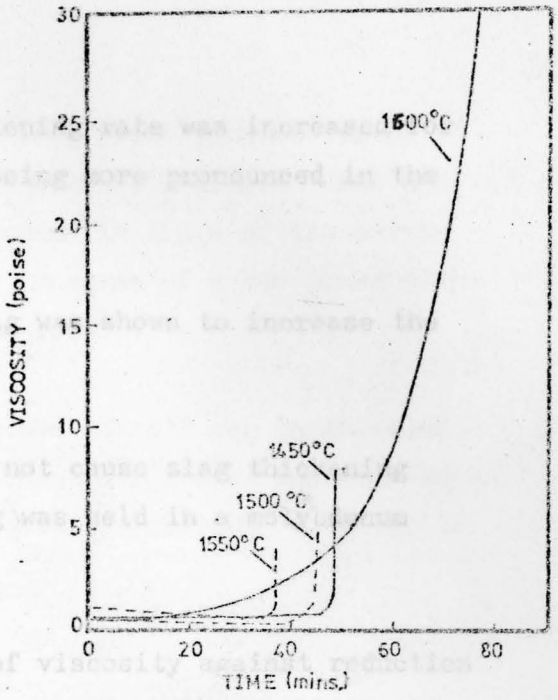


Figure 23 Isothermal viscosity measurements for a slag containing 50% TiO_2. (18)

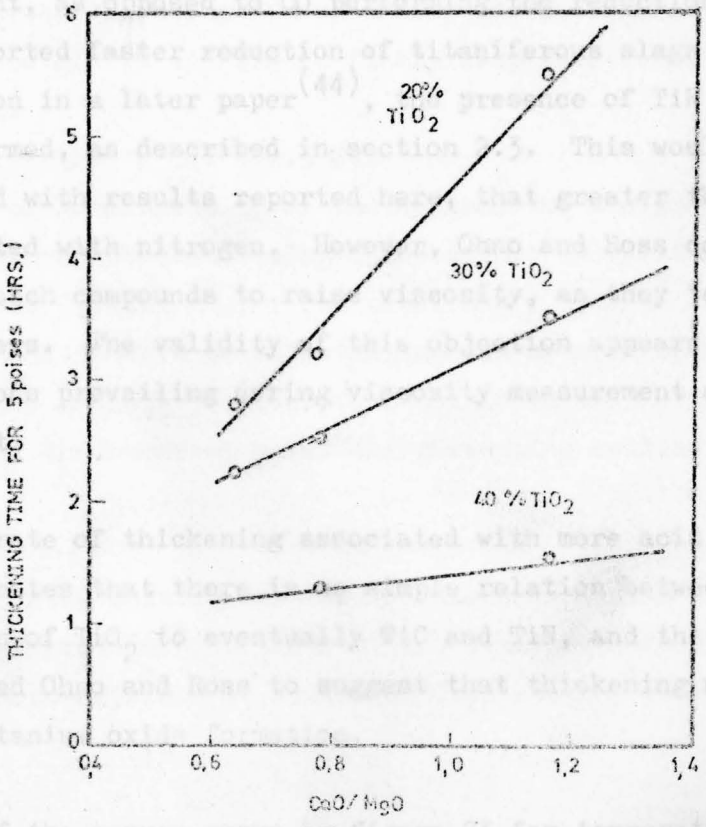


Figure 24 Effect of basicity and TiO_2 content on thickening rate. (18)

atmosphere with one of nitrogen. The thickening rate was increased for both acid and basic slags, the difference being more pronounced in the case of basic slags.

An increase in the alumina content of a slag was shown to increase the thickening rate slightly.

It was also found that carbon monoxide did not cause slag thickening even after 5 hours at 1600°C, when the slag was held in a molybdenum crucible.

It may be significant that in most graphs of viscosity against reduction time, as presented by the authors, there appears to be a slight decrease of viscosity initially.

Considering the results described above, thickening may still be the result of one or more of several causes:

(a) The possibility that high melting titanium compounds may be responsible for the phenomenon is indicated by the requirement of carbon being present, as opposed to CO performing the reduction. The same authors reported faster reduction of titaniferous slags in nitrogen than in argon in a later paper[44], the presence of TiN in fact being confirmed, as described in section 2.3. This would appear to be in accord with results reported here, that greater thickening rates are associated with nitrogen. However, Ohno and Ross doubted the ability of such compounds to raise viscosity, as they tend to form surface layers. The validity of this objection appears doubtful if the conditions prevailing during viscosity measurement are taken into account.

(b) The faster rate of thickening associated with more acid slags essentially indicates that there is no simple relation between the rate of reduction of TiO_2 to eventually TiC and TiN, and the thickening rate. It led Ohno and Ross to suggest that thickening might be due to lower titanium oxide formation.

(c) The shape of the curves shown in figure 23 for temperatures of 1550°C

and lower reminds very strongly of the very rapid rise in viscosity accompanying primary crystallization of high TiO_2 slags. Ohno and Ross in fact pointed out that the differnce in shape of the curves in figure 23 might be explained by the presence of a new phase with a fusion temperature between 1550°C and 1600°C.

On the basis of this work, not one of the above effects can be isolated, as neither the appearance nor the manner of distribution of any reduced product was reported at any stage of the reduction process. A change in the fusion temperature is merely implied.

2.4.6 Freidenzon et al[22] (1965) and Shavrin et al[50] (1966)

The slags examined by Freidenzon belonged to the system $CaO-MgO-Al_2O_3-SiO_2-TiO_2$. For titania contents up to 10 %, very little change in viscosity was recorded after holding the slag in a graphite crucible at 1600°C for 2½ hours. The slag containing 15 % TiO_2 became considerably thicker under these conditions.

Freidenzon attributed the change in viscosity to heterogeneity in the slag due to the presence of TiC and TiN in finely dispersed form. Using the Einstein equation:

$$\eta = \eta_o (1 + 2{,}5\,\phi),$$

where ϕ = degree of heterogeneity of the system, the analyses of slag and metal fractions of the "buckshot slag", the author calculated approximate viscosity values of 0,04 Ns/m^2 for the metal and 2,8 Ns/m^2 for the slag. This very viscous slag could be expected to coat metal droplets very effectively, preventing the diffusion processes necessary for completion of the refining of the buckshot metal and preventing coalescence of the metal droplets.

Shavrin et al[50] also pointed out the increased formation of TiC and TiN under the high temperature conditions of the blast furnace hearth, and the ability of the carbo-nitrides to coat iron droplets and prevent their coalescence.

2.4.7 McRae[23] (1968)

The compositions of some slags tested under reducing conditions are given in table 10:

Table 10 Slag compositions investigated by McRae[23]

Slag No.	Composition (mass %)				
	CaO	MgO	SiO_2	Al_2O_3	TiO_2
14C 16M	14,00	16,00	19,69	13,12	37,19
18C 12M	18,00	12,00	19,69	13,12	37,19

These two slags were treated as follows: The temperature of the slag held in a graphite crucible, was raised to the liquidus temperature of the oxidized slag. (The inner cylinder of the viscometer was made of platinum). The temperature was raised, viscosity being measured during this period, and again lowered until an approximate freezing temperature was reached. The temperature was then raised again and the procedure repeated. The results are shown in figure 25. Viscosity values measured above the progressively increasing liquidus temperature were found to be slightly lower than those of the oxidized slag at the same temperature.

Examination of a sample of slag 18C 12M reduced in a graphite crucible for two hours at 1440°C failed to reveal the presence of either TiC or TiN. The primary and subsequent products of crystallization were found to be same as those reported by Jochens et al[8] (see figure 1) for a slag of the same composition tested under oxidizing conditions, i.e. $4(MgO.2TiO_2).Al_2O_3.TiO_2$, $CaO.TiO_2$ and $CaO.MgO.2SiO_2$. Conspicuous black lath-like crystals were separated from a sample of a same slag which had been used for liquidus determination under reducing conditions. These crystals were found to be the magnesium-aluminium titanate mentioned above. However, heating the crystals under oxidizing conditions either to above their melting point or 1000°C produced rutile as an additional phase. The latter phase does not appear in the crystallization sequence of the overall slag composition under oxidizing conditions.

Partially reduced samples of slags 18C 12M and 14C 16M were re-oxidized and

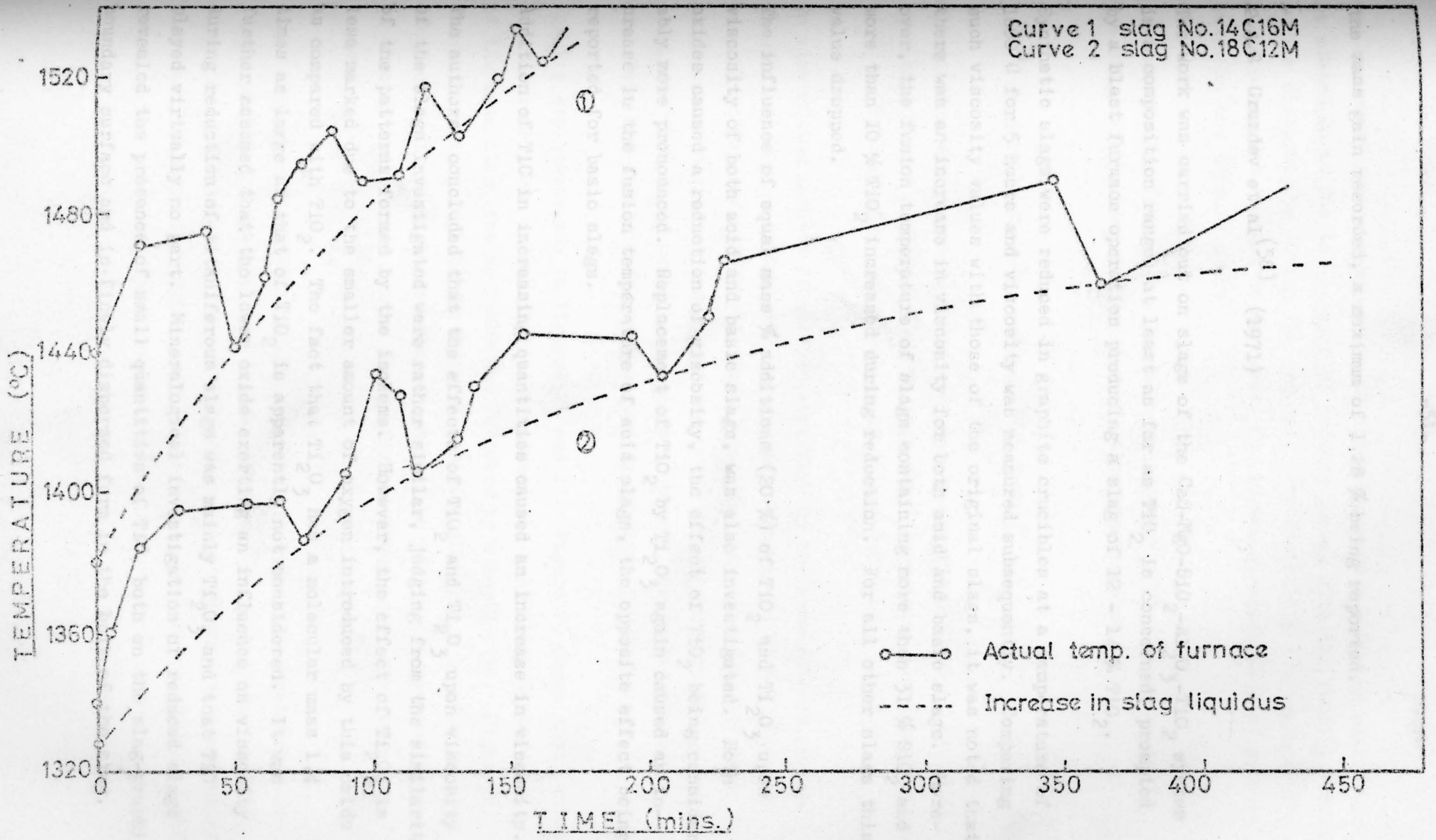


Figure 25 Effect of reduction by carbon upon liquidus temperature.[23]

the mass gain recorded, a maximum of 1,28 % being reported.

2.4.8 Gruzdev et al[58] (1971)

The work was carried out on slags of the $CaO-MgO-SiO_2-Al_2O_3-TiO_2$ system in a composition range, at least as far as TiO_2 is concerned, prompted by a blast furnace operation producing a slag of 12 - 14 % TiO_2.

Synthetic slags were reduced in graphite crucibles at a temperature of 1600°C for 5 hours and viscosity was measured subsequently. Comparing such viscosity values with those of the original slags, it was noted that there was an increase in viscosity for both acid and basic slags. Moreover, the fusion temperature of slags containing more than 31 % SiO_2 and more than 10 % TiO_2 increased during reduction. For all other slags this value dropped.

The influence of equal mass % additions (20 %) of TiO_2 and Ti_2O_3 upon viscosity of both acid and basic slags, was also investigated. Both oxides caused a reduction of viscosity, the effect of TiO_2 being considerably more pronounced. Replacement of TiO_2 by Ti_2O_3 again caused an increase in the fusion temperature of acid slags, the opposite effect being reported for basic slags.

Addition of TiC in increasing quantities caused an increase in viscosity.

The authors concluded that the effects of TiO_2 and Ti_2O_3 upon viscosity of the slags investigated were rather similar, judging from the similarity of the patterns formed by the isokoms. However, the effect of Ti_2O_3 is less marked due to the smaller amount of oxygen introduced by this oxide as compared with TiO_2. The fact that Ti_2O_3 has a molecular mass 1,4 times as large as that of TiO_2 is apparently not considered. It was further assumed that the lower oxide exerting an influence on viscosity during reduction of titaniferous slags was mainly Ti_2O_3 and that TiO played virtually no part. Mineralogical investigation of reduced slags revealed the presence of small quantities of TiC, both on the slag-graphite boundary surface and in finely dispersed form in the bulk of the slag.

The increased fusion temperature of acid slags under reducing conditions is stated to be due to a change of primary phase, with the readily fusible augite disappearing during the process. The fusibility temperature of basic slags was thought to decrease due to the disappearance of perovskite as the primary phase.

It is also significant that the authors reported a 25 % decrease in Ti (as TiO_2) in the slag during the reduction experiments.

2.4.9 Handfield, Charette and Lee[59] (1972)

A base slag was prepared, containing mainly CaO (35,0 %), SiO_2 (37,0 %), MgO (18,0 %) and Al_2O_3(4,0 %). To this slag, increasing amounts of either Ti_2O_3 or TiO (as appropriate ratios of Ti and TiO_2) were added.

In view of the results of earlier work done by the same authors, which showed that high titanium oxide slags containing up to 65 % Ti_2O_3 were very fluid (approximately 0,03 Ns/m^2) and that highly reduced titania slagspossessed greater desulphurizing power than slags with TiO_2, they concluded that Ti_2O_3 could be expected to have a more basic character than TiO_2 and should reduce the viscosity of blast furnace slags.

Results are summarized in figures 26 and 27. Figure 26 shows that, while additions of lower oxides initially reduced the fusibility temperature of the base slag, the decrease was followed by a rapid rise. Figure 27 shows that Ti_2O_3 is a better network modifier than TiO_2, bearing in mind the fact that expression of the concentrations of the titanium oxides on a molar basis would render the difference shown here, even more pronounced.

It is also significant that Ti_2O_3 was found to be a better network modifier than TiO and again mole % instead of mass % concentrations would enhance the difference. Moreover, viscosity was not related to temperature rigorously through the Arrhenius relationship in the case of TiO i.e. the graph of log η against inverse absolute temperature is curved.

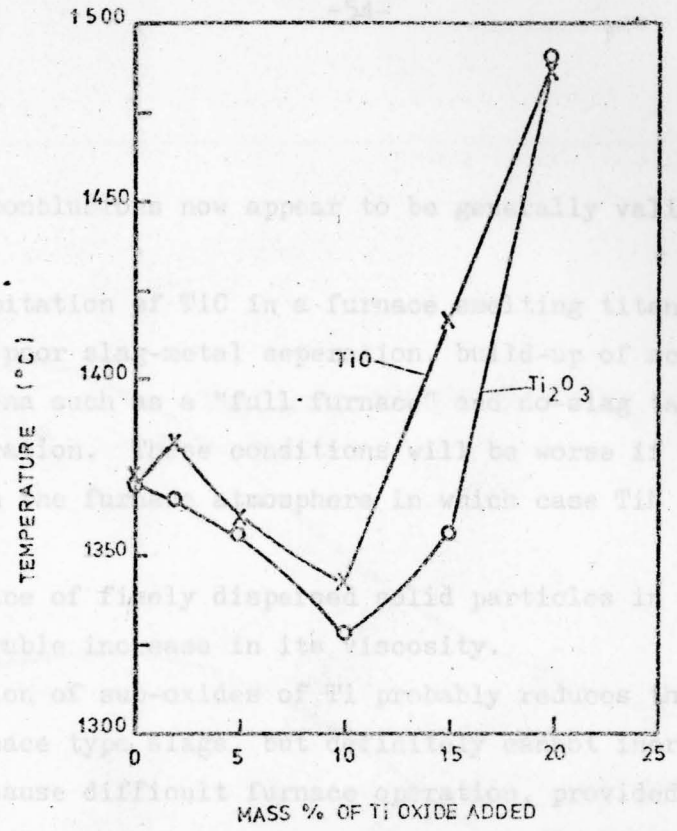


Figure 26 The effect of addition of TiO and Ti_2O_3 on the fusing temperature of a blast furnace slag. (59)

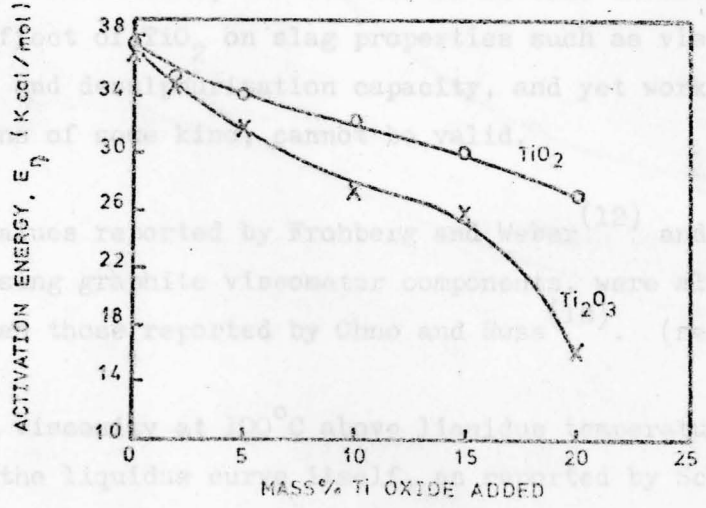


Figure 27 The effect of addition of TiO_2 and Ti_2O_3 on the activation energy for viscous flow of a blast furnace slag. (59)

2.4.10 Summary

The following conclusions now appear to be generally valid:

(a) The precipitation of TiC in a furnace smelting titaniferous burdens can cause poor slag-metal seperation, build-up of accretions leading to phenomena such as a "full furnace" and no-slag taps, and general rough operation. These conditions will be worse if nitrogen is present in the furnace atmosphere in which case TiN and Ti(C,N) are formed.

(b) The presence of finely dispersed solid particles in a slag can cause a considerable increase in its viscosity.

(c) The addition of sub-oxides of Ti probably reduces the viscosity of blast furnace type slags, but definitely cannot increase it to a level that can cause difficult furnace operation, provided the slag is truly liquid.

(d) Reduction of TiO_2 to lower oxides in titaniferous slags has an influence on the melting temperature of the slag. The exact nature of this influence is however not yet clear.

(e) The relative effects of TiO_2, Ti_2O_3 and TiO upon viscosity are still the topic of contradicting reports. Neither the influence of slag basicity, nor the effect of replacement of CaO by MgO has been agreed upon, the latter parameter having received very little attention.

In view of these conclusions, the results of several investigators examining the effect of TiO_2 on slag properties such as viscosity, liquidus temperature and desulphurization capacity, and yet working under reducing conditions of some kind, cannot be valid.

The viscosity values reported by Frohberg and Weber[12] and Schenk and Frohberg[14], using graphite viscometer components, were already shown to be higher than those reported by Ohno and Ross[18]. (see table 2)

The tendency of viscosity at 100°C above liquidus temperature to follow the contour of the liquidus curve itself, as reported by Schenk and Frohberg[14] (figure 10) may not be valid, due to a possible greater increase in liquidus temperature for slags richer in titanium oxide.

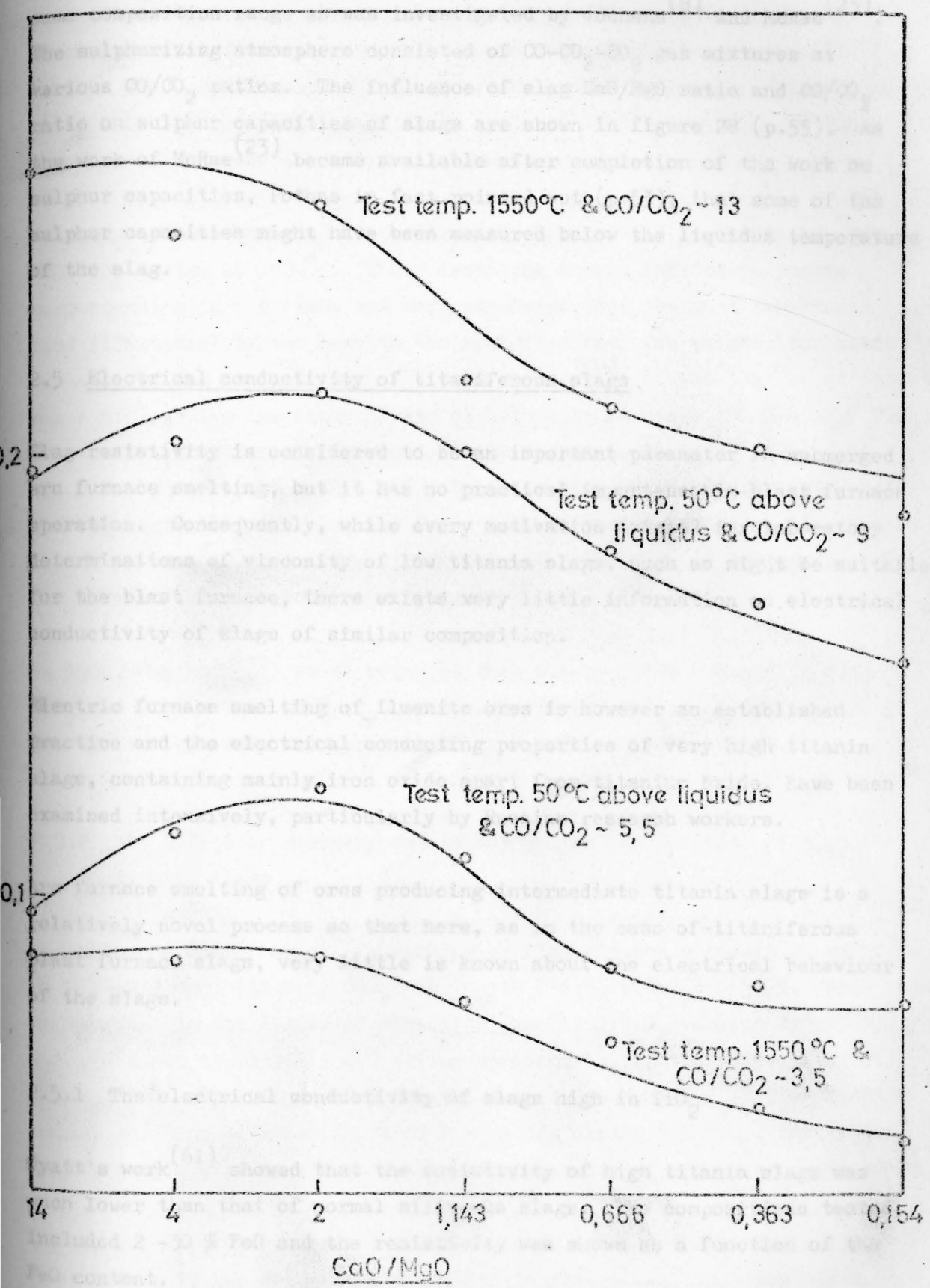


Figure 28 Effect of CaO/MgO ratio on sulphur capacity of slag, using indicated test temperatures. (60)

Pothas[60] measured the sulphur capacities of titaniferous slags in the same composition range as was investigated by Jochens[8] and McRae[23]. The sulphurizing atmosphere consisted of $CO-CO_2-SO_2$ gas mixtures at various CO/CO_2 ratios. The influence of slag CaO/MgO ratio and CO/CO_2 ratio on sulphur capacities of slags are shown in figure 28 (p.55). As the work of McRae[23] became available after completion of the work on sulphur capacities, Pothas in fact pointed out (p.53), that some of the sulphur capacities might have been measured below the liquidus temperature of the slag.

2.5 Electrical conductivity of titaniferous slags

Slag resistivity is considered to be an important parameter in submerged arc furnace smelting, but it has no practical importance in blast furnace operation. Consequently, while every motivation existed for laboratory determinations of viscosity of low titania slags, such as might be suitable for the blast furnace, there exists very little information on electrical conductivity of slags of similar composition.

Electric furnace smelting of ilmenite ores is however an established practice and the electrical conducting properties of very high titania slags, containing mainly iron oxide apart from titanium oxide, have been examined intensively, particularly by Russian research workers.

Arc furnace smelting of ores producing intermediate titania slags is a relatively novel process so that here, as in the case of titaniferous blast furnace slags, very little is known about the electrical behaviour of the slags.

2.5.1 The electrical conductivity of slags high in TiO_2

Wyatt's work[61] showed that the resistivity of high titania slags was much lower than that of normal siliceous slags. The compositions tested, included 2 -30 % FeO and the resistivity was shown as a function of the FeO content.

Denisov and Moriz[62] measured the conductivity in the solid state of

materials such as $Fe_2O_3.TiO_2$, $2FeO.TiO_2$, $FeO.TiO_2$ and $FeO.2TiO_2$. The increase in conductivity while the samples were heated, was reported. Although the conductivity was shown to be low at room temperature (10^{-3} to 10^{-8} S/m), it increased by 6 - 9 orders as the temperature was raised to 1300°C. The corresponding liquid slags at 1700°C were 10 - 30 times more conductive than the solids at 1300°C.

Balikhin and Reznichenko[63] constructed conductivity isotherms for the $FeO-TiO_2$ system at 1900°C. These isotherms showed inflection points corresponding to the ortho and meta titanates, but the most important fact illustrated by the results was again the very low values, for oxide systems, of the resistivity. The same authors[64] showed that an effective means of lowering the conductivity of high titania slags (80 % - 90 % TiO_2) was the introduction of lime or dolomite fluxes up to a CaO content of 4 - 6 %. This resulted in a 2 - 3 fold lowering of the conductivity values. The FeO content of the slag was found to have little effect on slag resistivity up to a concentration of 5 % by mass. Increase of FeO up to 15 % was however found to lower the conductivity.

In 1969, Musikhin[65] et al reported that binary melts containing 80 % TiO_2 and 20 % CaO or 20 % Al_2O_3 had conductivity values of approximately 1200 and 840 S/m respectively and appeared to be N-type semi-conductors.

2.5.2 The effect of reducing conditions on the conductivity of high titania slags

Balikhin and Reznichenko[64], working on slags in the composition range 26 % (CaO + MgO), $Al_2O_3 = SiO_2 = 8$ % with $(Fe_2O_3 + TiO_2) = 50$ %, found that an increase in the degree of reduction, as Ti_2O_3/TiO_2 varying from 0 to 0,8 , did not appreciably affect the conductivity of the melt. However, Musikhin[65] et al found that for the system $CaO-MgO-Al_2O_3-SiO_2$ + titanium oxide, addition of metallic Ti to a slag containing 5 % TiO_2, the resistivity was lowered due to the apparent appearance of electronic conduction.

If the degree of reduction of titanium oxide is accepted to be an important factor in the conductivity of titania rich slags, the iron oxide content of the slag must necessarily have a marked influence on the conducting properties. Indeed, Degtyarev et al[66] reported that the

resistivity of FeO-TiO_2 slags depended entirely on the amount of FeO present and that the relationship could be used as a control parameter.

In a series of papers, Denisov, Degtyarev, Reznichenko et al[67,68] reported quantitatively the effect of oxidation potential in the slag (as FeO) on conductivity. At 1700°C, values of 2500 - 3000 S/m and 15 000 - 17 000 S/m were given for high FeO contents (20 - 25 %) and for low FeO contents (4 - 5 %) respectively. These slags had overall titanium oxide contents in the range 63,40 to 89,85 %. The FeO content, which included Fe_2O_3, varied from 23,90 to 3,77 %, while the total lower oxides of titanium increased from 0 to 30,03 %.

Reznichenko[69] pointed out that a characteristic feature of commercial high titania slags is the relatively small change in electrical conductivity as the slag passes from the liquid to the solid state, implying only small changes in short range order during the melting process. This led to a mineralogical investigation of the phases present in these slags in the solid state, as an attempt to explain the phenomena of very high fluidity and electrical conductivity exhibited by such slags in the molten state. No satisfactory conclusion could be reached.

2.5.3 Electrical conductivity of low titania slags

Kato and Minowa investigated the effect of addition of several oxides including TiO_2, to a base slag containing 43 % CaO, 43 % SiO_2 and 14 % Al_2O_3, upon viscosity[70], electrical conductivity[71] and the relationship between these properties[72].

For titanium oxide additions up to approximately 8 mol % TiO_2, the viscosity of the base slag at constant temperature was reduced, but $E\eta$ was increased. At the same time the conductivity increased, accompanied by a decrease in E_k. Consequently, the ratio of $E\eta/E_k$ was increased to approximately 1,76 as compared with 1,36 for the base slag. E_k increased slightly as the TiO_2 content rose, giving a value of 131 KJ/mole at 7,9 mol % TiO_2. The slags containing TiO_2 were also found to deviate from the Arrhenius relationship slightly.

2.6 The influence of variable oxidation states in analogous systems

Two oustanding properties of siliceous slags containing titanium oxide, are:

(a) Although TiO_2 is classified as an intermediate oxide, it lowers both the viscosity and resistivity of such slags.

(b) The slags show semi-conducting properties in the molten state which evidently influences at least the electrical behaviour.

Physico-chemical properties of other siliceous slags containing oxides of intermediate or acidic nature, which also impart semi-conducting properties on the slag due to variable valence states, will therefore be mentioned, in order to stress the fact that systems containing titanium oxide are not unique with respect to the above properties.

2.6.1 Systems containing iron oxides

Hansen[73] measured the conductivity of phosphate glasses with 5 - 55 mol % iron oxides. The molar ratio $Fe^{3+}/Fe = x$, was varied from 0,15 to 0,88. The conductivity (k) increased, reaching a shallow maximum at x = 0,5, beyond which k decreased.

Engell and Vygen[74] investigated the system $CaO-SiO_2-FeO/Fe_2O_3$ at a molar ratio $CaO/SiO_2 = 0,79$, with the total iron oxide content N_{Fe} varying from 0 to 44 mol %. The temperature was 1600°C. The ratio x at every value of N_{Fe} was varied by equilibration with a gas phase, from 0,25 to 0,77.

The conductivity (k) was found to be a linear function of x at low values of N_{Fe}. In general, conductivity was described by the equation:

$$k = k_o - ax + bx\,(1 - x),$$

where k_o, a and b are constants, k_o being the conductivity of the system $CaO-SiO_2-FeO$, with pure ionic conduction. Similarly $(k_o - a)$ is the conductivity of the other extremity $CaO-SiO_2-Fe_2O_3$, which shows no electronic conduction either. The function $(k_o - x)$ describes the contribution of ionic conduction and $bx(1 - x)$ that of electronic conduction, to the value of k.

Ionic mobilities (u) of Fe^{2+} and Fe^{3+} in the systems $CaO-SiO_2-FeO$ and $CaO-SiO_2-Fe_2O_3$ could be calculated. The former was larger at a given value of N_{Fe}, but the figures for $u_{Fe^{3+}}$ indicated that even at N_{Fe} as low as 0,25, it is doubtful whether Fe^{3+} can still be tetrahedrally coordinated.

Regarding the electronic conduction over the range $0 < x < 1$, where conduction takes place by charge transfer between Fe^{2+} and Fe^{3+}, two models were tested:

(a) Stationary conducting centres with electron exchange by tunnel effect;

(b) Collision number dependent bimolecular reaction of Fe^{2+} and Fe^{3+}.

The experimental results were best described in terms of the latter model.

Higgins and Jones[75] made additions of FeO, Fe_2O_3 and Fe_3O_4 to master slags of the system $CaO-SiO_2-Al_2O_3$-"FeO", keeping the total iron oxide content in the region of 30 % by mass. Addition of FeO and Fe_2O_3 both lowered the viscosity, without major effect on the melting temperature of the slag, determined as the point of inflection of the $\log \eta$ against 1/T plot. The addition of synthetic magnetite also lowered the viscosity, and addition of 10 % doubled the fluidity at 1250°C. However, this addition raised the temperature of the inflection point from 1180°C to 1270°C

In the composition range 16,3 % CaO, 12,8 - 14,8 % MgO , 40,1 - 41,9 % SiO_2 , 12,2 - 16,5 % total iron oxide, Hejja[76] found both the liquidus temperature which never exceeded 1370°C, and the viscosity at two temperatures (1400°C and 1450°C), to decrease slightly initially and then to increase fairly rapidly as the ratio x was raised. The viscosity or temperature minimum occurred at x approximately equal to 0,5. The conductivity of the slags similarly passed through a region of virtual independence of x for low values of x, and subsequently decreased at higher values of x.

Ossin[77] studied slags of the system $CaO-MgO-SiO_2$-iron oxide, with total iron oxide content between 30,82 and 59,03 %. For slags with constant CaO, MgO and SiO_2 (11,5 % , 8 % and 29 % respectively), an increase in x at 1400°C caused an increase in viscosity from approximately 0,03 Ns/m^2 to approximately 0,042 Ns/m^2, the corresponding values of x being 0,114 and 0,160 respectively. Further increase in x to 0,284 had little effect on viscosity. Over the entire interval of x values from 0,114 to 0,284

the conductivity decreased from ± 425 to ±360 S/m. The approximate liquidus temperatures corresponding to values of x of 0,114 , 0,160 and 0,284 were 1230°C, 1320°C and 1310°C.

Apart from the influence of x upon viscosity, conductivity and liquidus temperature, the outstanding features illustrated by Ossin's work, are the very low values of viscosity and resistivity associated with these slags of high iron oxide content.

2.6.2 Other systems

Munakata[78], working on vanadate glasses, found a maximum in the k - x relationship at $V^{4+}/V = 0,2$, similar to what was reported by Hansen[73] for iron-phosphate glasses. This again appears to indicate pure ionic conduction at extreme values of x, with mixed conduction at all concentrations inbetween.

From their investigations of the system SiO_2-MgO-Al_2O_3-chromium oxide, Liutikov and Tsylev[79] concluded that in melts corresponding to the cordierite phase field on the MgO-SiO_2-Al_2O_3 diagram, chromium occurs as Cr^{2+}, in which state it is capable of increasing the conductivity and the fluidity of the melt. However, in melts whose composition correspond to the spinel region of the diagram, Cr is present as predominantly Cr^{3+}, and increases viscosity and resistivity.

2.6.3 Conclusion

Upon addition of each of the intermediate oxides mentioned above, to siliceous melts, there is a variation of physico-chemical properties with overall concentration of added oxide. There is also variation of these properties at a given overall oxide content, with the oxidation state.

In this sense, titanium oxide appears to be rather unique since it possesses a relatively large number of possible lower oxides, the majority of which exhibit non-stoichiometric behaviour.

3. EXPERIMENTAL WORK

The general procedure adopted during this work was reduction of synthetic slags in graphite crucibles in an inert atmosphere, followed by the measurement of physico-chemical properties of the reduced products in inert surroundings, molybdenum replacing carbon as crucible material. The state of reduction of the slag, as tested, was consequently not the state finally attained in the graphite crucible. It was the intention only to assess the effect of the presence of sub-oxides of Ti on viscosity and conductivity. It will be shown that any possible "over-reduction" of TiO_2 to non-equilibrium TiC, was satisfactorily converted into a degree of reduction in terms of sub-oxide formation, prior to the measurement of the physico-chemical properties.

All other determinations reported for "reduced slags" eg. approximate liquidus temperature, degree of reduction and primary crystallization product, apply to the equilibrated carbon-free slags.

3.1 Selection of slag compositions

In this selection the author was guided, in the first place, by the requirements of the iron plant of the Highveld Steel and Vanadium Corporation at Witbank. Average analytical figures reported by the plant before research work was started, were 20,0 -22,5 % SiO_2 , 27,0 - 31,0 % TiO_2, 13,0 - 14,0 % Al_2O_3 , 16,0 - 17,0 % CaO, 14,5 - 16,0 % MgO, 1,5 - 5,0 % FeO and 0,5 - 2,0 % V_2O_5.

The only source of TiO_2 and Al_2O_3 is the unfluxed charge of ore and coal. A constant ratio of TiO_2/Al_2O_3 was consequently considered a means to reduce the number of slag compositions to be tested. Based on the analyses received from the plant, a ratio of 2,21 was decided upon. As the degree of dilution, indicated by mass % (TiO_2 + Al_2O_3) content quoted above, was the result of prolonged plant scale optimization, it was agreed that the majority of the synthetic slags for research work should contain 30,2 % TiO_2 and 13,8 % Al_2O_3, (TiO_2 + Al_2O_3) amounting to 44%. A limited number of slags having higher or lower (TiO_2 + Al_2O_3) contents was included, at such ratios of $CaO:MgO:SiO_2$ as would make them comparable with selected members of the main series having (TiO_2 + Al_2O_3) = 44 %.

Due to the complexity of even the 5-component system CaO-MgO-Al_2O_3-TiO_2-SiO_2, when changes of physico-chemical properties have to be interpreted in terms of compositional variables, the oxides of vanadium and iron were omitted from the main group of synthetic slags.

Continued usage of dolomite as a flux was preferred to the more costly limestone. However, the addition of either lime or serpentine in addition to dolomite, made possible the variation of the ratio CaO/MgO at a particular value of basicity, which was to be expressed as the mass % ratio $(CaO + MgO)/SiO_2$.

The final variable would be the basicity index itself.

The main series of slag compositions is shown in table 11. All concentrations and parts of concentration ratios are expressed as mass per cent.

Based on the results of test work conducted on slags of table 11 by the author and also on investigations of Hejja[9], a further series of slags (table 12) was suggested, all these having $CaO/MgO = 1$ and possessing all the features common to members of group B, with small changes in basicity, from 1,30 to 1,65.

Other slag compositions used for assessing the effect of small additions of iron and vanadium oxides upon viscosity and primary crystallization temperature, are given in table 13.

3.2 Preparation of synthetic slags

The chemically pure reagents TiO_2, SiO_2, MgO, CaO and Al_2O_3 were sintered in vitreous silica dishes at 1100°C for 1 hour in a "glo-bar" furnace. The powders were allowed to cool in a dessicator.

The appropriate quantities of the sintered, pulverized oxides were thoroughly mixed and then pressed into tablets of 31 mm diameter. These tablets were melted in two batches in a molybdenum crucible of height, inside and outside diameter, 80 mm, 38 mm and 50 mm respectively, to give a total sample mass per crucible of 200 gm. Premelting was carried out

Table 11 Compositions of initial selection of synthetic slags used in this investigation

TiO_2/Al_2O_3 = 2,21

Slag group	Slag No.	(TiO_2+Al_2O_3)	TiO_2	Al_2O_3	SiO_2	CaO	MgO	(CaO+MgO)/SiO_2	CaO:MgO:SiO_2
		(mass per cent)							
A	2	36,00	24,80	11,20	23,62	20,19	20,19	1,707	0,852:0,852:1
	5	36,00	24,80	11,20	26,65	18,675	18,675	1,400	0,701:0,701:1
	8	36,00	24,80	11,20	35,55	14,225	14,225	0,800	0,400:0,400:1
B	10	44,00	30,20	13,80	20,75	23,50	11,75	1,700	1,132:0,566:1
	11	44,00	30,20	13,80	20,75	17,625	17,625	1,700	0,848:0,848:1
	12	44,00	30,20	13,80	20.75	11,75	23,50	1,700	0,566:1,132:1
	13	44,00	30,20	13,80	23,33	21,78	10,89	1,400	0,933:0,467:1
	14	44,00	30,20	13,80	23,33	16,335	16,335	1,400	0,701:0,701:1
	15	44,00	30,20	13,80	23,33	10,89	21,78	1,400	0,467:0,933:1
	16	44.00	30,20	13,80	31,10	16,60	8,30	0,801	0,533:0,267:1
	17	44,00	30,20	13,80	31,10	12,45	12,45	0,801	0,400:0,400:1
	18	44,00	30,20	13,80	31,10	8,30	16,60	0,801	0,267:0,533:1
C	23	54,00	37,18	16,82	19,19	13,405	13,405	1,400	0,699:0,699:1

Table 12 Additional group of synthetic slags

TiO_2/Al_2O_3	=	2,21
$(TiO_2 + Al_2O_3)$	=	44,00 %
TiO_2	=	30,20 %
Al_2O_3	=	13,80 %

Slag No.	SiO_2	CaO	MgO	$(CaO + MgO)/SiO_2$
	(mass per cent)			
B28	24,350	15,825	15,825	1,300
B29	23,830	16,085	16,085	1,350
B30	22,860	16,570	16,570	1,450
B31	22,410	16,795	16,795	1,500
B32	21,970	17,015	17,015	1,550
B33	21,540	17,230	17,230	1,600
B34	21,130	17,435	17,435	1,650

Table 13 Miscellaneous synthetic and plant slags used in the investigation

Slag No.	TiO_2	Al_2O_3	SiO_2	MgO	CaO	FeO	V_2O_5	Mn_3O_4	Cr_2O_3	Fe_2O_3
	(mass per cent)									
HV	30,94	13,04	20,32	14,64	16,43		0,73	0,72	0,18	3,76
HV-HV	32,54	13,66	21,25	15,33	17,22					
HV+FV	31,03	13,05	20,32	14,66	16,45		0,73			3,76
HV-FV(60M)	Same composition as HV-FV									
HV-FV (60M)+FV	Same composition as HV+FV									
M1/1	26,95	11,54	20,13	16,40	16,35	5,88	2,75			

in a carbon resistance furnace in a spectrographically pure argon atmosphere. The temperature was maintained at 1600 $\pm$ 10°C for 1 hour.

The premelted slag was removed from the molybdenum crucible by means of a diamond core drill, the resulting core diameter being 35 mm. Cores of the same composition were then combined into a bulk sample of approximately 500 gm which was crushed to be 100 % (-10 mesh). The fraction (-10 mesh +70 mesh) was retained for subsequent reduction experiments, while the (-70 mesh) fraction was used for viscosity measurements of the unreduced slags.

3.3 The furnace assembly used for measurements of viscosity and electrical conductivity and for reduction experiments

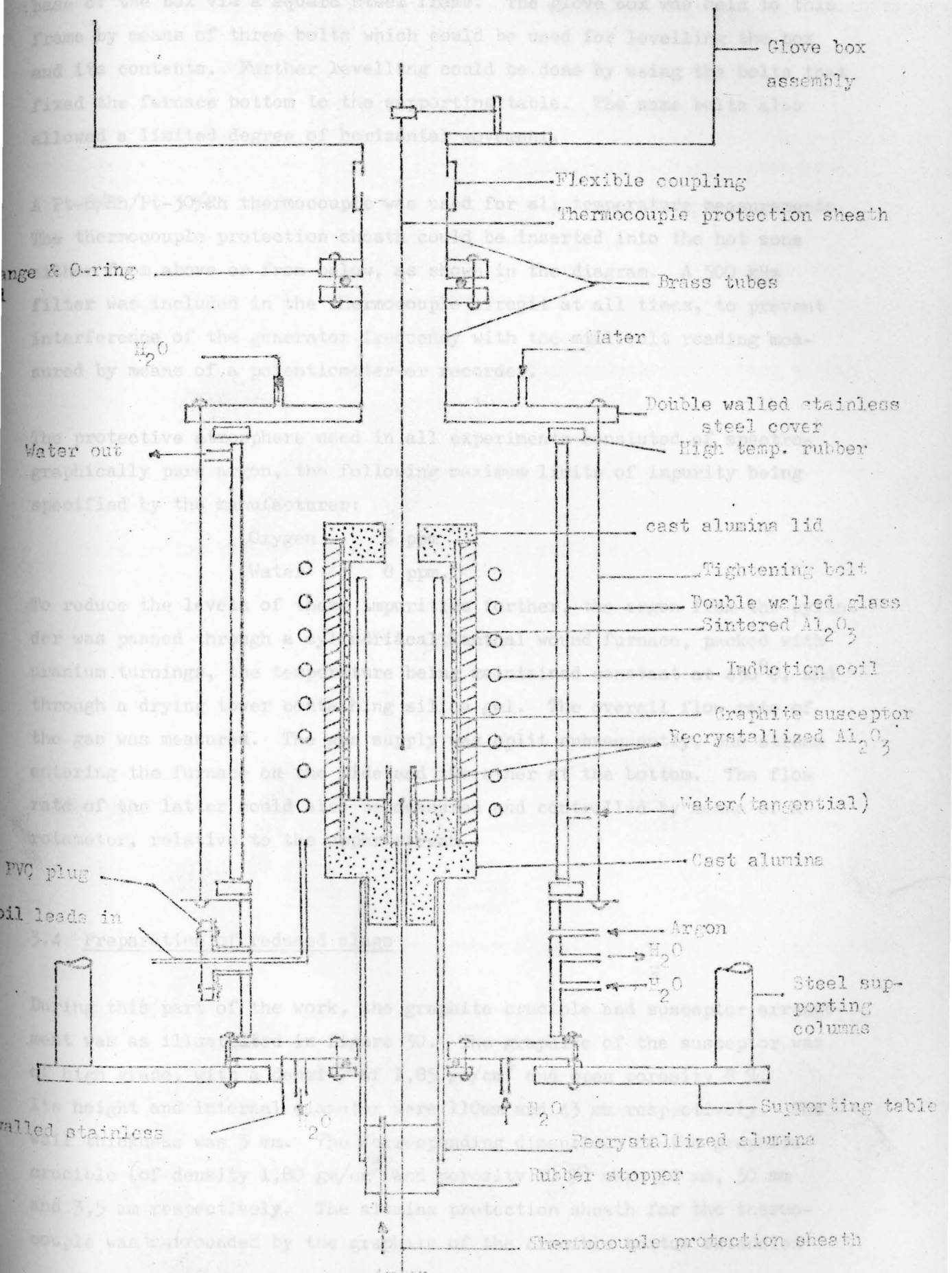
The furnace was powered by an 18 kVA output "Intertherm" induction generator, operating at a frequency of 500 kHz. The coil had an inductance of 6 mh and its diameter and height were 100 mm and 90 mm respectively. The 8-turn coil was made of 6 mm diameter annealed copper tubing.

The actual furnace constructed for the purpose of the experiments which were to be conducted in a protective atmosphere, is shown schematically in figure 29.

The entire assembly was supported on a fixed steel table. The latter also carried the four steel supporting columns bolted to a steel plate above the glove box that housed the viscometer. The two chains carrying the glove box on one side and a lead counterweight at the back of the furnace assembly, passed through slots in the top supporting plate over two pairs of gears bolted to the plate.

The front and top panels of the glove box were made of perspex, all the remaining panels being constructed of steel plate. The front and top panels were screwed onto the steel flanges of the metal part through a gas tight rubber seal. The transparent front wall contained the glove attachment, as well as the brass terminals for the thermocouple leads and the electrode extension leads. One of the steel side walls contained the gas tight entrance attachment for the viscometer lead and the protective gas exit port. The movement of the glove box was guided by brass

Figure 29 Schematic representation of the furnace



sleeves round the front supporting columns, which were attached to the base of the box via a square steel frame. The glove box was held to this frame by means of three bolts which could be used for levelling the box and its contents. Further levelling could be done by using the bolts that fixed the furnace bottom to the supporting table. The same bolts also allowed a limited degree of horizontal movement.

A Pt-6%Rh/Pt-30%Rh thermocouple was used for all temperature measurements. The thermocouple protection sheath could be inserted into the hot zone either from above or from below, as shown in the diagram. A 500 kHz filter was included in the thermocouple circuit at all times, to prevent interference of the generator frequency with the millivolt reading measured by means of a potentiometer or recorder.

The protective atmosphere used in all experiments consisted of spectrographically pure argon, the following maximum limits of impurity being specified by the manufacturer:

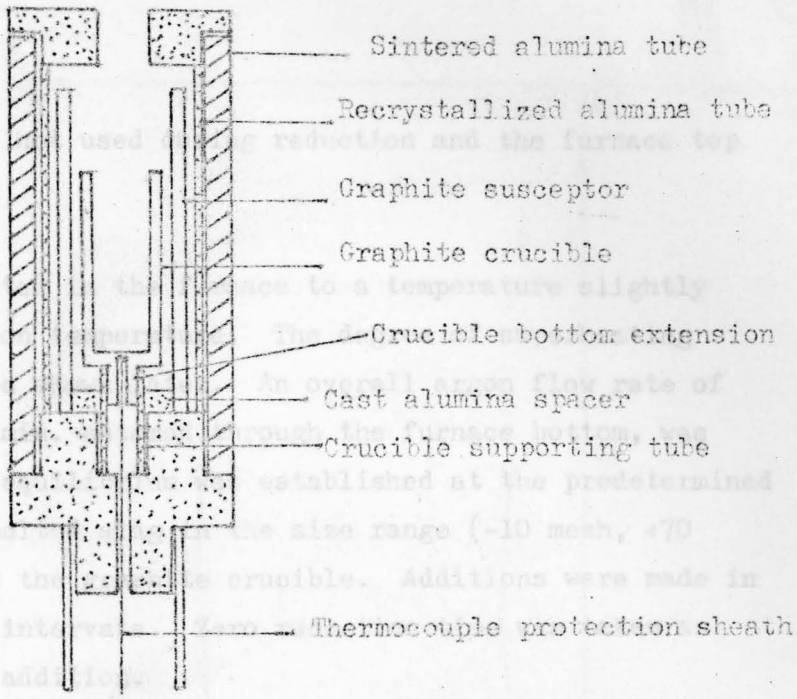
Oxygen	6 ppm
Water	8 ppm.

To reduce the levels of these impurities further, the argon from the cylinder was passed through a cylindriacal Kanthal wound furnace, packed with uranium turnings, the temperature being maintained constant at 450°C, and through a drying tower containing silica gel. The overall flow rate of the gas was measured. The gas supply was split subsequently, one stream entering the furnace on the side and the other at the bottom. The flow rate of the latter could also be measured and controlled by means of a rotameter, relative to the upper stream.

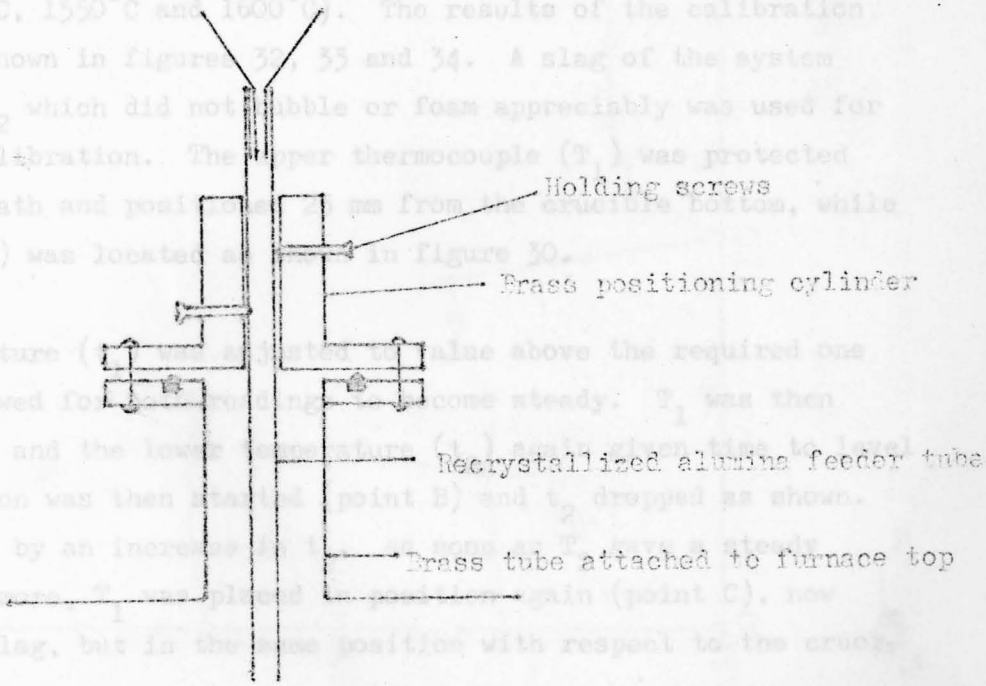
3.4 Preparation of reduced slags

During this part of the work, the graphite crucible and susceptor arrangement was as illustrated in figure 30. The graphite of the susceptor was of high grade, with a density of 1,85 gm/cm^3 and open porosity 8 %. Its height and internal diameter were 110mm and 43 mm respectively. The wall thickness was 3 mm. The corresponding dimensions of the graphite crucible (of density 1,80 gm/cm^3 and porosity 10 %) were 78 mm, 30 mm and 3,5 mm respectively. The alumina protection sheath for the thermocouple was surrounded by the graphite of the crucible bottom extension

ure 30 The crucible assembly used for reduction experiments



ure 31 Furnace top arrangement during reduction experiments



over a distance of 25 mm.

The glove box assembly was not used during reduction and the furnace top was as shown in figure 31.

The empty crucible was heated in the furnace to a temperature slightly above the intended reduction temperature. The degree of superheating was standardized as will be shown later. An overall argon flow rate of 1,5 l/min. of which 0,5 l/min. entered through the furnace bottom, was maintained. When thermal equilibrium was established at the predetermined temperature, 70 gm of premelted slag in the size range (-10 mesh, +70 mesh), was introduced into the graphite crucible. Additions were made in 10 gm batches at 1-minute intervals. Zero reduction time was taken as 5 minutes after the final addition.

Apart from the fact that the steady temperature after slag addition was lower than the one measured at the same point before addition, it was found that the temperature measured at the crucible bottom lagged the one recorded by a thermocouple immersed in the slag. To take these differences into account, calibrations were carried out at the three reduction temperatures used (1500°C, 1550°C and 1600°C). The results of the calibration experiments are shown in figures 32, 33 and 34. A slag of the system $CaO-MgO-Al_2O_3-SiO_2$ which did not bubble or foam appreciably was used for the purpose of calibration. The upper thermocouple (T_1) was protected by a platinum sheath and positioned 25 mm from the crucible bottom, while the lower one (T_2) was located as shown in figure 30.

The upper temperature (t_1) was adjusted to value above the required one and time was allowed for both readings to become steady. T_1 was then removed (point A) and the lower temperature (t_2) again given time to level out. Slag addition was then started (point B) and t_2 dropped as shown. This was followed by an increase in t_2. As soon as T_2 gave a steady temperature once more, T_1 was placed in position again (point C), now immersed in the slag, but in the same position with respect to the crucible as before.

These calibrations were used for all subsequent reduction experiments, although the one for 1550°C was repeated from time to time, using both the quiescent slag and two different titaniferous slags (B11 and B17).

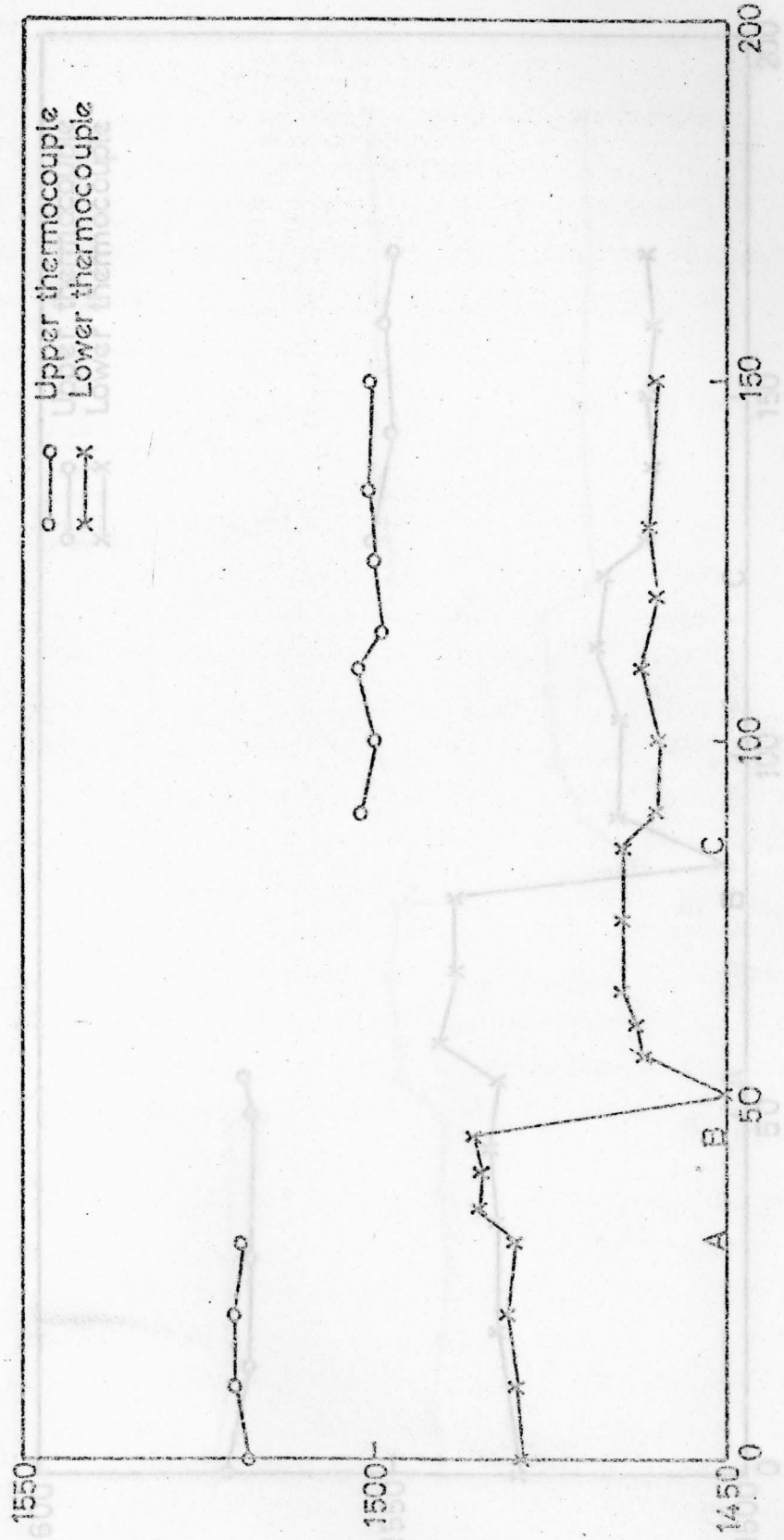


Figure 32 Calibration for reduction at 1500°C

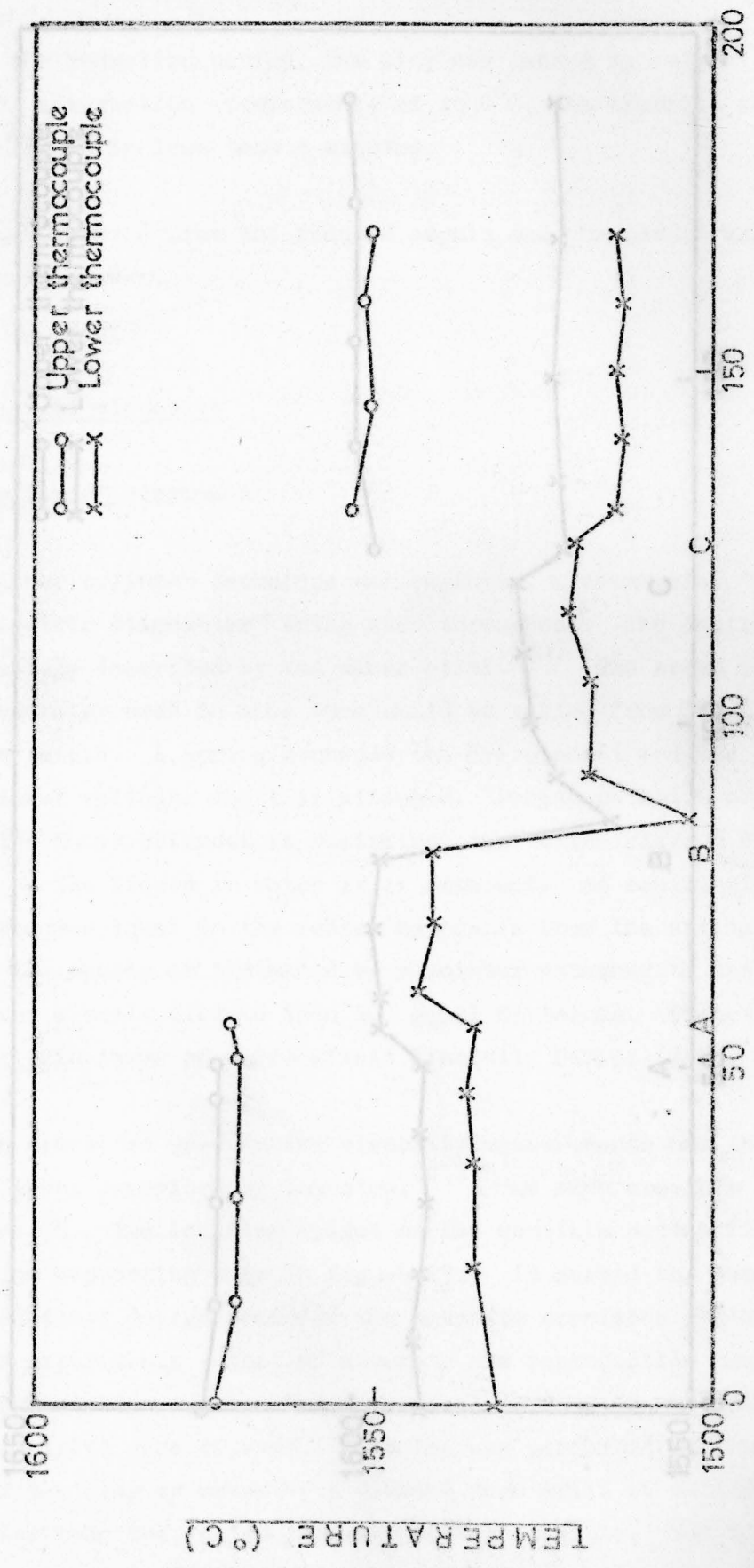


Figure 33 Calibration for reduction at 1550°C

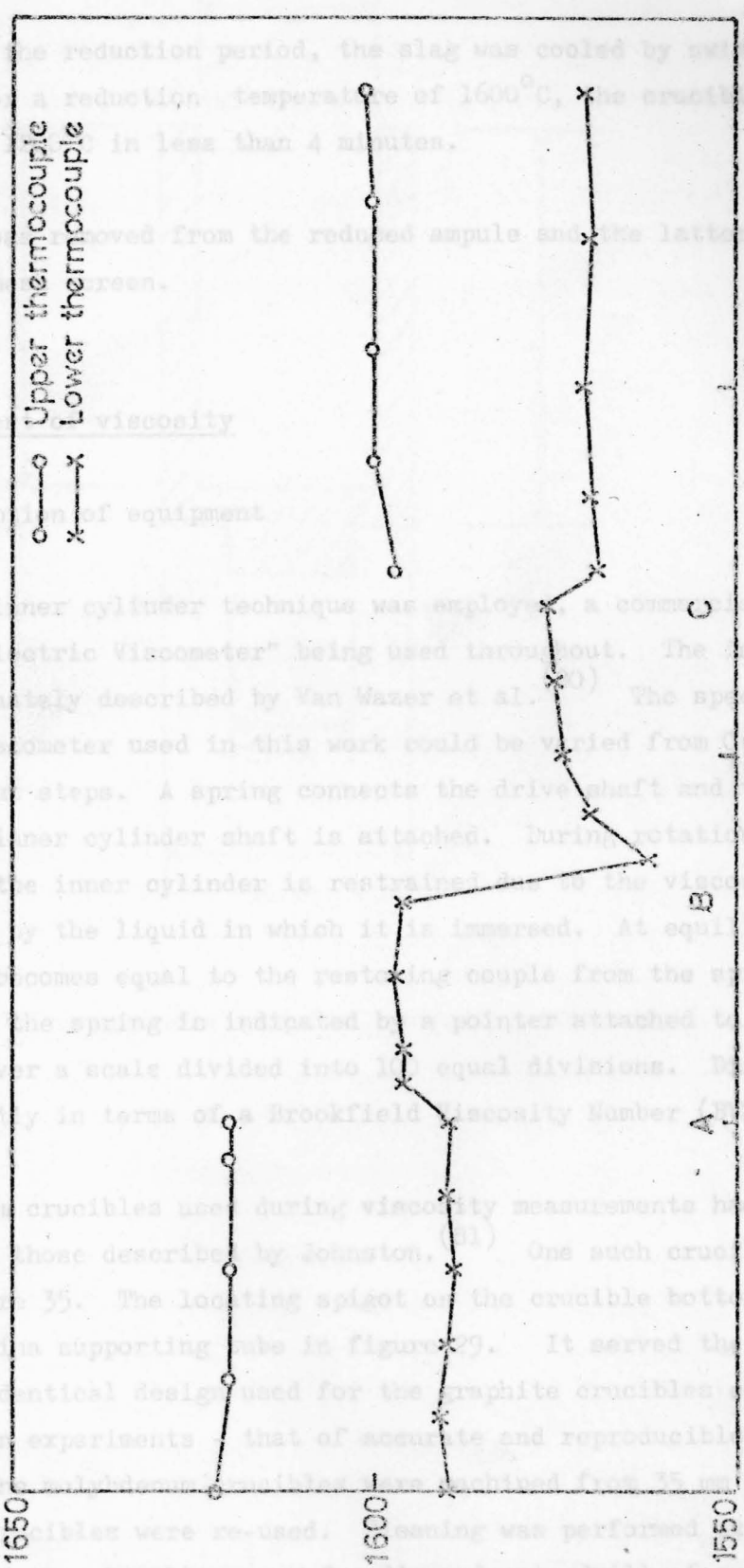


Figure 34 Calibration for reduction at 1600°C

No significant changes could be detected during these control experiments.

At the end of the reduction period, the slag was cooled by switching off the power. For a reduction temperature of 1600°C, the crucible temperature fell to below 1200°C in less than 4 minutes.

The graphite was removed from the reduced ampule and the latter was crushed to pass a 70-mesh screen.

3.5 Measurement of viscosity

3.5.1 Description of equipment

The rotating inner cylinder technique was employed, a commercial "Brookfield Synchrolectric Viscometer" being used throughout. The instrument has been adequately described by Van Wazer et al.[80] The speed of the particular viscometer used in this work could be varied from 0,5 to 100 r.p.m. in eight steps. A spring connects the drive shaft and the coupling on which the inner cylinder shaft is attached. During rotation of the drive shaft, the inner cylinder is restrained due to the viscous drag exerted on it by the liquid in which it is immersed. At equilibrium this viscous drag becomes equal to the restoring couple from the spring. The deflection of the spring is indicated by a pointer attached to the spring, which moves over a scale divided into 100 equal divisions. Direct readings are consequently in terms of a Brookfield Viscosity Number (BVN).

The molybdenum crucibles used during viscosity measurements had the same dimensions as those described by Johnston.[81] One such crucible is shown in figure 35. The locating spigot on the crucible bottom fitted into the alumina supporting tube in figure 29. It served the same purpose as the identical design used for the graphite crucibles employed during reduction experiments - that of accurate and reproducible crucible alignment. The molybdenum crucibles were machined from 35 mm diameter rod. These crucibles were re-used. Cleaning was performed by removal of the bulk of the slag by means of a diamond core drill of outside diameter slightly smaller than the inside diameter of the crucible. The remaining "skin" if slag was removed with a tungsten carbide tipped boring tool.

Figure 35 Molybdenum crucible for viscosity and electrical conductivity measurements

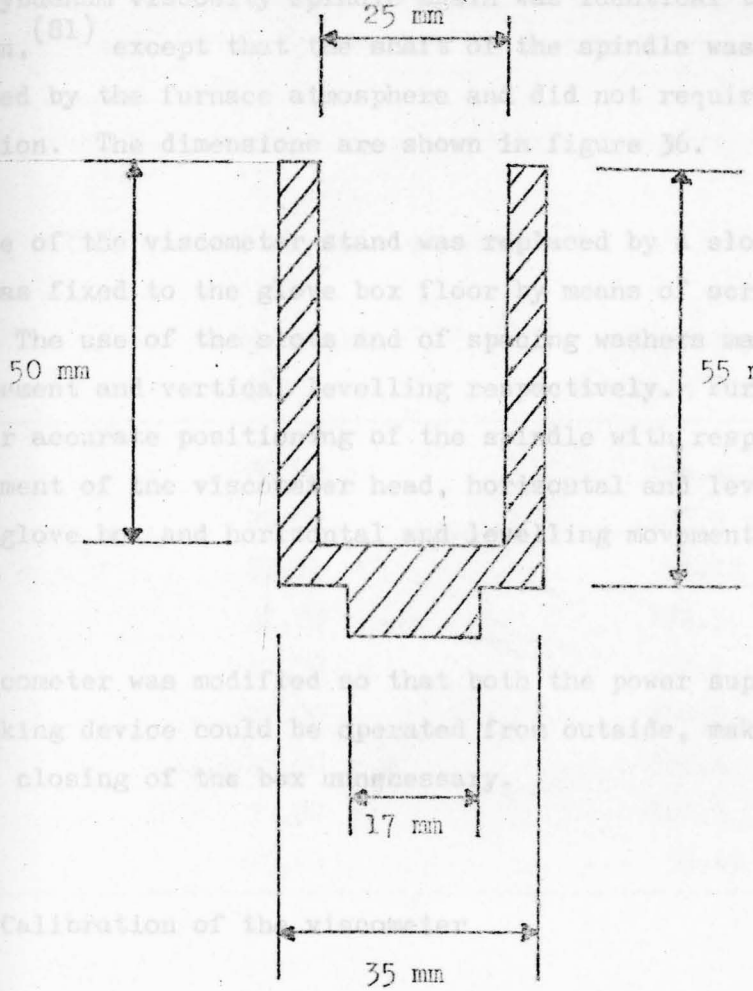
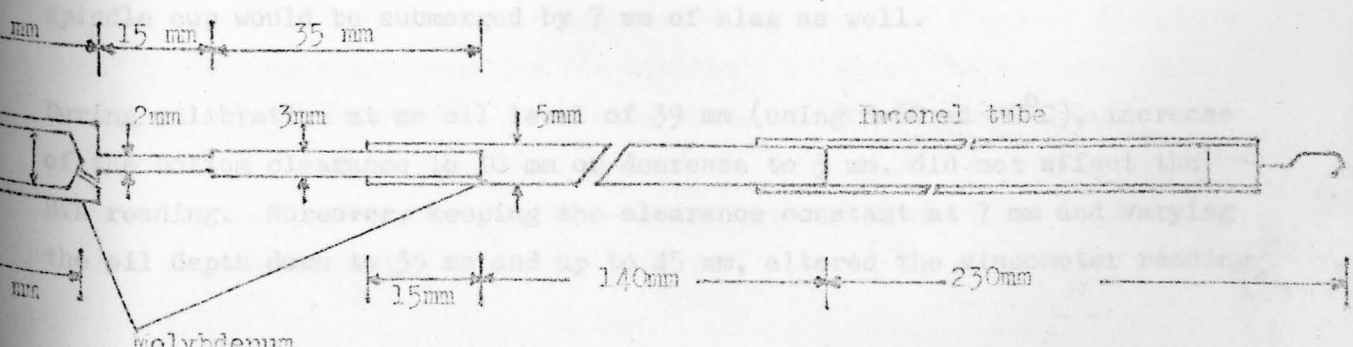


Figure 36 Molybdenum spindle used for viscosity measurement



The molybdenum viscosity spindle again was identical to that used by Johnston,[81] except that the shaft of the spindle was now adequately protected by the furnace atmosphere and did not require extra refractory protection. The dimensions are shown in figure 36.

The base of the viscometer stand was replaced by a slotted brass disc which was fixed to the glove box floor by means of screws welded to the floor. The use of the slots and of spacing washers made possible horizontal movement and vertical levelling respectively. Further provision was made for accurate positioning of the spindle with respect to the crucible by movement of the viscometer head, horizontal and levelling movement of the glove box and horizontal and levelling movement on the furnace itself.

The viscometer was modified so that both the power supply switch and the locking device could be operated from outside, making repeated opening and closing of the box unnecessary.

3.5.2 Calibration of the viscometer

Calibration was performed at a constant speed of 50 r.p.m., using three calibrating oils: S-600, S-60 and S-20 types ASTM oil standards. (Cannon Instrument Co., U.S.A.) For the low temperature work a brass crucible and viscometer spindle combination of the same dimensions as the molybdenum components was used. A constant temperature water bath was used to attain accurately the low temperature involved during calibration.

During preliminary experiments it was found that a slag charge of 55 gm would fill the standard molydenum crucible to a level of $\pm$ 39 mm at 1600°C, indicating a slag density of $\pm$ 2,9 gm/cm^3. A spindle - to - crucible bottom clearance of 7 mm would then imply that the top of the spindle cup would be submerged by 7 mm of slag as well.

During calibration at an oil level of 39 mm (using S-60 at 20°C), increase of the bottom clearance to 10 mm or decrease to 5 mm, did not affect the BVN reading. Moreover, keeping the clearance constant at 7 mm and varying the oil depth down to 35 mm and up to 45 mm, altered the viscometer reading

by less than 3 %. Off-centre rotation of the spindle with respect to the crucible axis of up to 2 mm led to an identical error.

Details of the calibration are given table 11 and figure 37.

Table 11 Calibration of the viscometer

Oil	Temperature (^{o}C)	Viscosity ($Ns/m^2 x10^3$)	BVN
S-60	20,00	146,4	22,3
	25,00	105,9	18,0
	37,78	51,13	13,2
S-200	37,78	174,5	25,0
	32,00	251,2	33,0
	27,00	350,0	42,5
	25,00	393,4	45,8
	20,00	561,5	62,4
S-20	25,00	30,69	11,0

3.5.3 Procedure of viscosity measurement

The procedure outlined below, was used for both reduced and unreduced slags:

The spindle was positioned with respect to the centre and bottom of the crucible and tested for concentricity with the furnace open. The final position of the spindle was fixed by means of a brass stop on the viscometer stand. The molybdenum crucible, charged with 55 gm of slag powder was located in the furnace as shown for the graphite crucible in figure 30.

The thermocouple in this case, entered the hot zone from above, the protective sheath being held by an adjustable clamp on the floor of the glove box. The thermocouple junction was located 2 mm above the crucible wall, vertically in line with it. This site of temperature measurement is justified by the close agreement between the approximate liquidus temperature determined viscosimetrically and the liquidus temperature as measured by hot stage microscopy. (section 3.7)

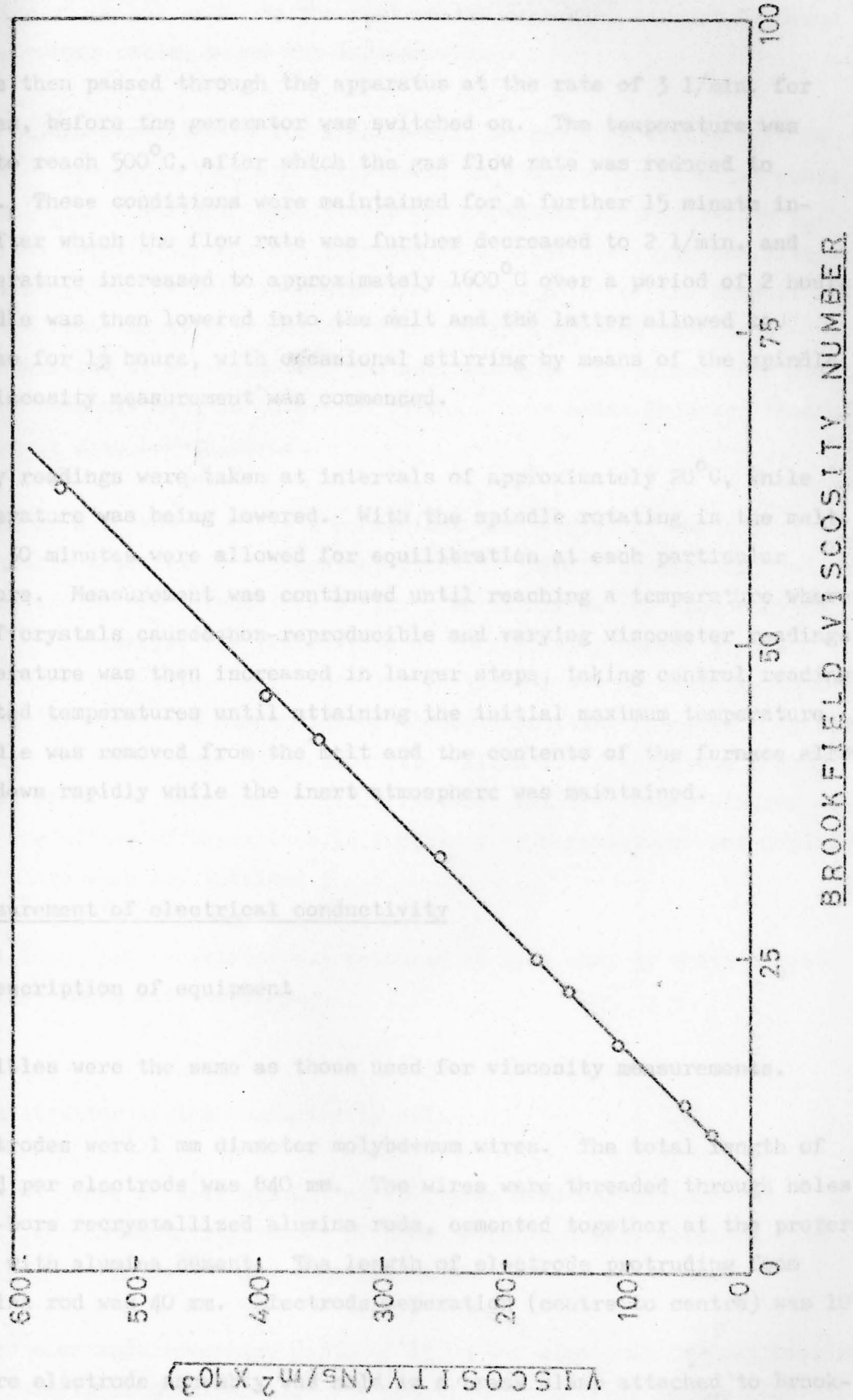


Figure 37 Calibration of viscometer

With the spindle in the raised position and the thermocouple and crucible in measuring position, the furnace was closed and connected to the glove box.

Argon was then passed through the apparatus at the rate of 3 l/min. for 15 minutes, before the generator was switched on. The temperature was allowed to reach 500°C, after which the gas flow rate was reduced to 2½ l/min. These conditions were maintained for a further 15 minute interval after which the flow rate was further decreased to 2 l/min. and the temperature increased to approximately 1600°C over a period of 2 hours. The spindle was then lowered into the melt and the latter allowed to homogenize for 1½ hours, with occasional stirring by means of the spindle, before viscosity measurement was commenced.

Viscosity readings were taken at intervals of approximately 20°C, while the temperature was being lowered. With the spindle rotating in the melt, at least 30 minutes were allowed for equilibration at each particular temperature. Measurement was continued until reaching a temperature where growth of crystals caused non-reproducible and varying viscometer readings. The temperature was then increased in larger steps, taking control readings at selected temperatures until attaining the initial maximum temperature. The spindle was removed from the melt and the contents of the furnace allowed to cool down rapidly while the inert atmosphere was maintained.

3.6 Measurement of electrical conductivity

3.6.1 Description of equipment

The crucibles were the same as those used for viscosity measurements.

The electrodes were 1 mm diameter molybdenum wires. The total length of wire used per electrode was 840 mm. The wires were threaded through holes in two 2-bore recrystallized alumina rods, cemented together at the proper spacing, with alumina cement. The length of electrode protruding from the alumina rod was 40 mm. Electrode seperation (centre to centre) was 10 mm.

The entire electrode assembly was held in a brass clamp attached to Brookfield viscometer stand that was positioned inside the glove box. The

stand was fitted with a vernier scale which allowed vertical positioning of the electrodes to within 0,05 mm. The molybdenum wires were connected, through the glove box wall, to the rest of the measuring circuit by means of 15 amp copper cable, wound non-inductively.

The A.C. bridge circuit used for measurement, is shown in figure 38. It consisted of two equal standard resistances (R_s) and a non-reactive resistance box (R_m). A variable capacitance was connected in parallel to R_m. A sinusoidal input at 10 kHz was provided by a transistor type oscillator. An oscilloscope was used to determine the balance point of the circuit. Because the experiments were conducted in a high frequency induction furnace operating at approximately 500 kHz, an oscilloscope was used with a frqucncy response between 60 Hz and 60 kHz. Thus mains frequency interference would also be minimized.

The choice of a 10 kHz input is a convenient one in view of the values of undesirable interfering frequencies present, and with respect to the rapid increase of the capacitance of ionic solutions as the frequency is lowered. Consequently, the resistivity or conductivity values reported here, have absolute value only under the particular set of conditions, and not at the low operating frequencies of electric smelting furnaces. As the primary aim was comparison of conductivity values of titaniferous slags with those of slags belonging to other systems, measured under similar conditions, the effect of variations in frequency upon resistance and capacitance of slags were not examined.

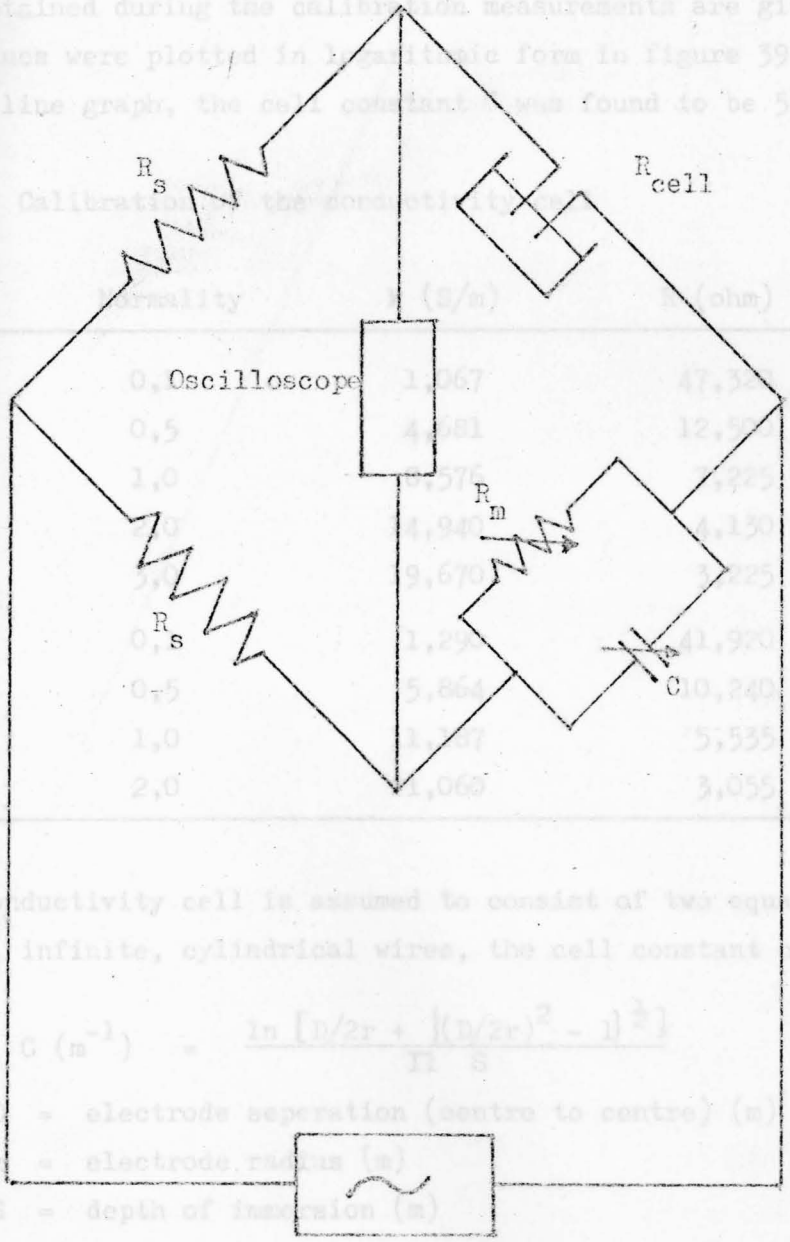
The total lead wire resistance was measured as 0,27 ohm, by short circuiting the electrodes with mercury.

3.6.2 Calibration of the conductivity cell

Standard solutions of NaCl and KCl at 25°C were used for calibration purposes. The conductivity values of these solutions were obtained from the work of Shedlovsky[82] and Chambers et al.[83]

A standard electrode immersion depth of 15 mm was used both for calibration and slag resistance measurement. The overall liquid level in the crucible was again 39 mm.

Figure 38 Bridge circuit used for resistance measurement



The resistance of the ionic liquid in the cell is related to its electri-conductivity by $R\,k = G$, where

R = resistance of the liquid (ohm)

k = conductivity of the liquid (S/m)

G = cell constant (m^{-1})

Thus $\log k = \log G - \log R$, so that a plot of log R against log k should be a straight line with a slope of -1, intersecting the log R axis at a point where $G = R$.

Values obtained during the calibration measurements are given in table 12. These values were plotted in logarithmic form in figure 39. From the straight line graph, the cell constant G was found to be 51,9 m^{-1}.

Table 12 Calibration of the conductivity cell

Solution	Normality	k (S/m)	R (ohm)
NaCl	0,1	1,067	47,320
	0,5	4,681	12,500
	1,0	8,576	7,225
	2,0	14,940	4,130
	3,0	19,670	3,225
KCl	0,1	1,290	41,920
	0,5	5,864	10,240
	1,0	11,187	5,535
	2,0	21,060	3,055

If the conductivity cell is assumed to consist of two equally charged parallel, infinite, cylindrical wires, the cell constant can be calculated from:

$$G\ (m^{-1}) = \frac{\ln\left[D/2r + \left\{(D/2r)^2 - 1\right\}^{\frac{1}{2}}\right]}{\Pi \quad S}$$

where D = electrode seperation (centre to centre) (m)

r = electrode radius (m)

S = depth of immersion (m)

For the particular cell geometry used in this investigation, $D = 10^{-2}$ m, $r = (0,5 \times 10^{-3})$m, $S = 15 \times 10^{-3}$ m and $G = 62,4\ m^{-1}$.

This calculated value of G is larger than the measured one (51,9 m^{-1}).

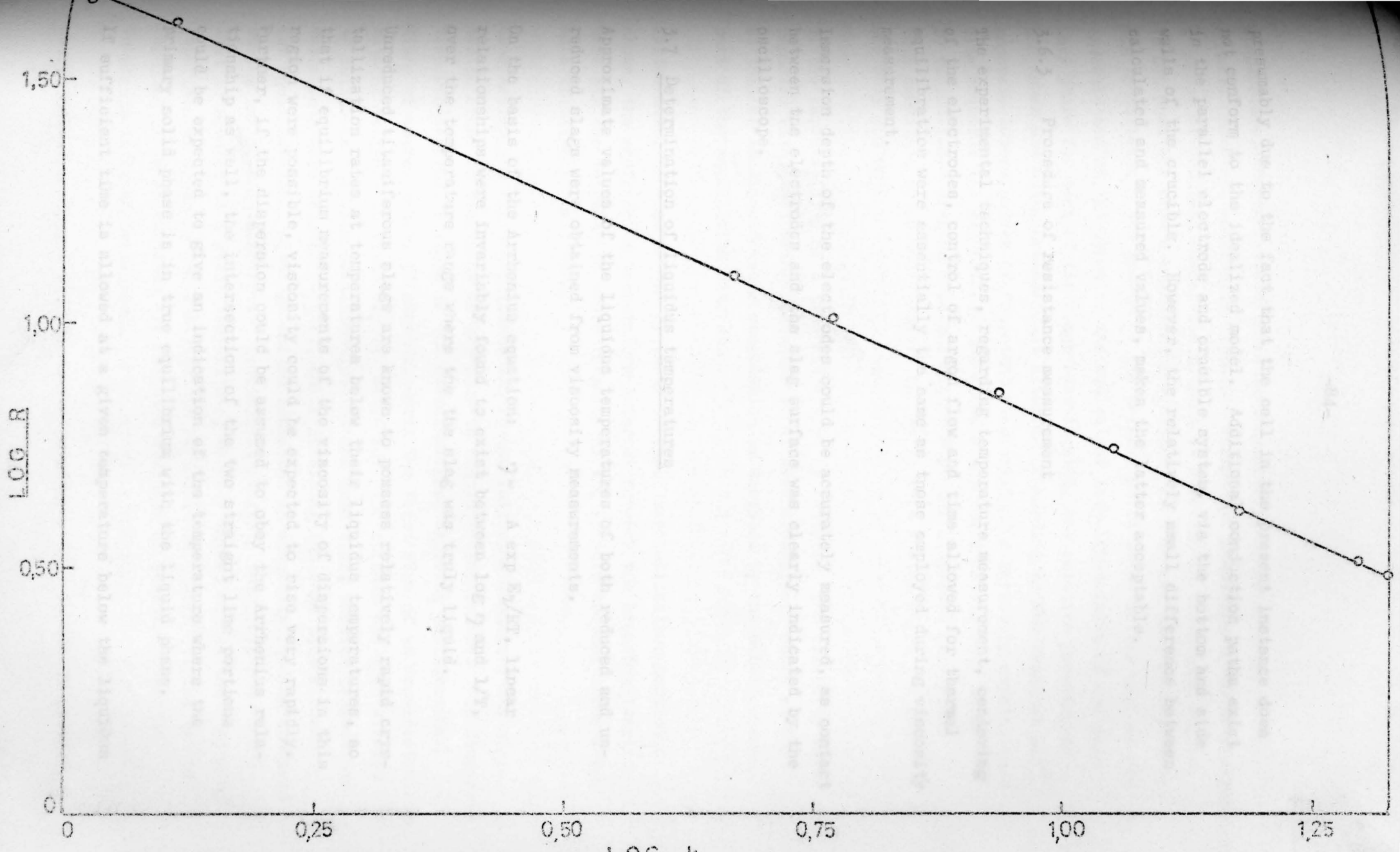


Figure 39 Calibration of the conductivity cell

presumably due to the fact that the cell in the present instance does not conform to the idealized model. Additional conduction paths exist in the parallel electrode and crucible system, via the bottom and side walls of the crucible. However, the relatively small difference between calculated and measured values, makes the latter acceptable.

3.6.3 Procedure of resistance measurement

The experimental techniques, regarding temperature measurement, centering of the electrodes, control of argon flow and time allowed for thermal equilibration were essentially the same as those employed during viscosity measurement.

Immersion depth of the electrodes could be accurately measured, as contact between the electrodes and the slag surface was clearly indicated by the oscilloscope.

3.7 Determination of liquidus temperatures

Approximate values of the liquidus temperatures of both reduced and unreduced slags were obtained from viscosity measurements.

On the basis of the Arrhenius equation: $\eta = A \exp E_\eta/RT$, linear relationships were invariably found to exist between $\log \eta$ and $1/T$, over the temperature range where the the slag was truly liquid.

Unreduced titaniferous slags are known to possess relatively rapid crystallization rates at temperatures below their liquidus temperatures, so that if equilibrium measurements of the viscosity of dispersions in this region were possible, viscosity could be expected to rise very rapidly. Furtner, if the dispersion could be assumed to obey the Arrhenius relationship as well, the intersection of the two straight line portions could be expected to give an indication of the temperature where the primary solid phase is in true equilibrium with the liquid phase.

If sufficient time is allowed at a given temperature below the liquidus

temperature, chemical equilibrium must eventually be established between phases. However, meaningful "apparent viscosity" measurement, to be assigned a degree of accuracy comparable to what is obtained in the liquid region, is not possible with a measuring arrangement such as was used in this work. Due to nucleation and growth of the primary solid phase on the wall of the crucible and on the spindle, and due to the lath-like nature of the primary phase for most of the slags investigated, the relative geometry of the inner and outer cylinders is altered. According to Van Wazer et al[80] accurate determination of "apparent viscosity" of a partially crystallized slag requires the gap between the spindle and the crucible wall to be 10 to 100 times greater than the diameter of the dispersed particles. This condition could not possibly be met in this system where the gap was only 7,5 mm.

If the improbability of a true dispersion is accepted, the viscosity value reported with a measuring mechanism of altered dimensions, could at best be that of the liquid whose composition is dictated by the sub-liquidus part of the equilibrium diagram.

Furthermore, in view of the property of rapid crystallization mentioned above, the equilibrium temperature interval between the liquidus temperature and the temperature where rotation of the spindle becomes impossible, is a relatively small one.

Considering the factors outlined above, the following procedure was adopted in order to determine an approximate liquidus temperature. The temperature was lowered in steps in the normal manner, allowing equilibration times of approximately 30 minutes, until the first sign of an accelerated rate of increase in viscosity was detected. The spindle was then allowed to rotate in the slag continuously. At the same time, smaller temperature decrements were adopted ($\pm$ 5°C), while retaining the same time allowed for equilibration. Although marked increases in viscosity reading occurred during the 30-minute interval, readings at 2-minute intervals over the last 10 minutes at a given temperature, usually varied within the limits of experimental error in the sub-liquidus region ($\pm$ 10^{-2} Ns/m^2). The values reported in later sections are weighted averages of readings over the 10-minute interval mentioned.

Measurement was stopped when excessive jerking of the viscometer needle

indicating advanced growth of primary cryatals, rendered instrument readings meaningless.

It is important that values obtained on the basis of measurements done while the temperature was then raised from its final value in the solidus-liquidus region, approached those reported while lowering the temperature, to within the positive limit of experimental error, after holding times at temperature of up to 4 hours. However, if the temperature was rapidly increased to a level, 50°C or more above the liquidus temperature, $1\frac{1}{2}$ hours were normally sufficient for a return of the viscosity value to that reported during cooling of the liquid.

It is further significant that reproducibility of results was good ($\pm 10^{-2}$ Ns/m^2) in the sub-liquidus region, during successive cooling cycle determinations.

The approximate liquidus temperature was consequently determined as the point of intersection of the $\log \eta$ - $1/T$ line for the liquid region and a straight line drawn through the points obtained in the sub-liquidus region during cooling.

Confidence in the technique of approximate liquidus temperature measurement is instilled by the close agreement between values determined in this manner, for unreduced slags (slags premelted in argon) and liquidus temperatures obtained for the corresponding oxidized slags (slags premelted in argon and subsequently heated in oxygen at 1100°C) by hot stage microscopy. The approximate liquidus temperature of one reduced slag was also confirmed by a quench technique, followed by X-ray analysis, as will be described in a later section.

Use of the hot stage microscope for liquidus temperature determination was possible only in the case of fully oxidized slags, due to the opacity even of slags premelted in an argon atmosphere.

The technique employed by Cavalier[84] involved the use of separate heating and thermocouple circuits. Welch[85] developed the arrangement in which the thermocouple functions as a generator of thermal e.m.f., sample holder and heating element. The instrument used in this work also employed half-cycle heating, and was constructed by Jochens[86]. The per-

formance of the unit was assessed by the same author in the reference quoted as well as in later publications.[8]

The thermocouple arms were made of 6%Rh - Pt and 30%Rh - Pt wires of 0,35 mm diameter and 18 mm length. The seperation between the arms was normally slightly less than the arm diameter. Each arm was butt welded to an 18 mm length of wire of the same composition, but greater diameter (0,5 mm). These supporting wires were connected by screw contact to the rest of the circuit.

An accuracy of $\pm$ 5°C is claimed for the instrument.

The slag bead was heated to a point well above its expected liquidus temperature (usually 1600°C) and held at this temperature for approximately 15 minutes. The slag was then cooled to a temperature below the crystallization temperature, noting the approximate temperature where crystallization appeared to start. It was re-heated to the latter temperature and soaked for 15 minutes. The temperature was then increased slowly (2°C/min.) and the approximate liquidus temperature taken as the point where the last solid material disappeared. The cycle was then repeated twice, each time narrowing the gap between liquidus temperature and subliquidus soaking temperature and lowering the heating rate from the soaking temperature to liquidus temperature.

The samples for liquidus temperature determination were taken from the bulk quantities of unreduced slags on which viscosity measurement had been performed. A 20 gm sample of this material in the size range (-70 mesh, +140 mesh) was heated in an atmosphere of pure oxygen at 1100°C for 1 hour. Such treatment was found to be sufficient for complete re-oxidation of even the most severely carbon-reduced slags. The resulting oxidized sample was then crushed in an agate mortar and used for measurement of liquidus temperature.

3.8 Determination of primary phases

All samples for X-ray analysis were prepared by means of the high temperature microscope.

Oxidized slags were homogenized at 1600°C for 15 minutes. The beads were then soaked at 50°C below the predetermined liquidus temperature for 60 minutes.

For the small number of determinations of primary crystallization products of reduced slags, the after-viscosity products were also generally used. The cell of the hot stage microscope was modified to be gas tight, by incorporation of silicone rubber seals at the junction between the two main cell parts, and at the observation windows. Spectrographically pure argon was passed through the cell at the rate of 1,0 l/min.

The slag powder was wetted with CCl_4, in which form an appropriate quantity was transferred to the thermocouple. The bead was again heated to a temperature above the approximate liquidus temperature, as determined during viscosity measurement and held there for 15 minutes. This was followed by soaking at 50°C below the approximate crystallization temperature. The slag was quenched, as in the case of oxidized slags, either by merely switching off the power or by simultaneous power cut and injection of a water jet into the cell. The slag bead was removed from the thermocouple, and crushed in an agate mortar under water free alcohol. The primary phase was then identified by means of a Debye-Scherrer X-ray diffraction camera, using Cu-Kα radiation with a Ni filter at 30 kV and 10 mA. The time of exposure was 8 hours in all instances.

3.9 Determination of a degree of reduction of reduced slags

The possible products of reduction in the slags after treatment in a graphite crucible include the lower oxides of titanium, titanium oxycarbide and titanium carbide. Apart from gaseous silicon monoxide which would have been removed from the system, silicon could also be present as the carbide. Moreover, any carbon reporting in the slag, would be distributed between the carbon containing compounds mentioned above and free carbon entrained in the slag.

Any assessment of an overall degree of reduction would involve differentiation between free carbon and combined carbon, an accurate measure of the amount of silicon removed from the system during reduction and an exact determination of the oxidation state of Ti. If in addition, it

must be distinguished between silica and titania reduction states, knowledge of the relative quantities of carbides and oxy-carbides of Ti and of silicon carbide is required.

Although means were initially considered to distinguish between bound and free carbon, mainly by low temperature selective sulphurization of the latter, the very low levels of carbon content (never exceeding 0,1 %) would render such determinations meaningless.

The amount of Si leaving the melt as SiO can only be calculated by analysis for Si, in conjunction with a mass balance based on eg. MgO, or an accurate determination of the decrease in mass occurring during reduction. In view of the inaccuracy of analytical results particularly, meaningful decrease in silicon content of the slag could only be quoted for highly siliceous slags.

If the emphasis is to be on the oxygen content of the reduced slags as compared with that of the unreduced slags, as it was in this study, various techniques are available for determination of oxygen content. Neutron activation methods gave completely erratic results as might be expected since it was attempted to measure very small differences in a large quantity. Methods involving complete carbonaceous reduction of all oxides present, suffered from the same drawback.

The simple technique adopted in this work was aimed at determining a degree of reduction of titanium oxide in terms of lower oxides. The starting material was the reduced slag after viscosity had been determined in a molybdenum crucible. This product was crushed to pass a 70 mesh screen but to be retained by a 140 mesh screen. A 10 gm sample of the powder of the most severely reduced derivative of a particular slag, reduced by graphite at a given temperature, was re-oxidized in a recrystallized alumina crucible in an atmosphere of pure oxygen in a thermal balance. The initial temperature was 1100°C and the mass gain was recorded over a period of 1 hour. The temperature was subsequently raised to 1200°C, maintained constant for 1 hour and then raised further to 1300°C, where isothermal conditions were maintained for a further period of 1 hour. Oxidation was always complete after 1 hour at 1100°C, although in most instances all mass increase stopped after 30 minutes at this temperature. The flow rate of oxygen was kept constant at 1,0 l/min.

Samples of the same slag that were reduced for shorter times were subsequently oxidized under conditions identical to those described above, but in a separate furnace. The mass gain was obtained by weighing the crucible and its contents before and after the oxidation period. An oxidation time of two hours was used in all cases. The oxidation temperature was 1100°C.

The use of this technique appears justified in view of the following findings:

(a) Although the reduction of SiO_2 did not form part of this investigation, it must be noted that the reaction: $SiO_2 + C = SiO + CO$ only proceeded to any significant extent in the case of the most acidic slags. The analytical results reported in table 13 were obtained for the slags after viscosity measurements had been performed on them.

Table 13 Compositions of selected slags before and after reduction by carbon

Slag No.	Reduction time (mins)	Reduction temp. (°C)	TiO_2	Al_2O_3	SiO_2	CaO	MgO
			(m a s s	p e r	c e n t)		
B14	0		30,20	13,80	23,33	16,335	16,335
	120	1550	30,85	13,31	23,53	16,85	15,39
	120	1600	30,50	13,10	23,10	16,37	16,93
B11	0		30,20	13,80	20,75	17,625	17,625
	120	1550	30,80	13,11	21,65	18,45	16,14
B17	0		30,20	13,80	31,10	12,45	12,45
	120	1550	36,29	13,26	27,02	11,55	11,61

Although Ti and Si might have been present in the slags in other forms, they were reported as TiO_2 and SiO_2 respectively.

(b) Carbon was found to be present in the slags after removal from the graphite crucible and before determination of viscosity or resistivity, in very small amounts, as shown in table 14.

(c) It is theoretically possible that some of the carbon present in the reduced slags upon removal from the graphite crucible might be in

the form of carbide. Thin- and polished sections were prepared of the slags B11, B14 and B17 after reduction at 1550°C for two hours (the longest reduction time used in this work). No carbide could be detected. Moreover, the same three slags were treated in the following manner: Minute particles were scraped off the surfaces (both free surface and where the slag was in contact with the graphite crucible) by means of a 1 mm diameter diamond drill. The complex pattern obtained from X-ray analysis of these particles will be discussed in a later section, but no SiC or TiC could be detected.

Table 14 Carbon contents of reduced slags

Slag No.	$(CaO+MgO)/SiO_2$	TiO_2 (mass%)	Reduction temp(°C)	Reduction time(mins)	C (mass%)
B11	1,700	30,20	1550	90	0,07
			1550	120	0,05
B14	1,400	30,20	1550	60	0,05
			1550	90	0,08
			1550	120	0,05
			1600	120	0,06
B17	0,800	30,20	1550	90	0,04
			1550	120	0,07
C23	1,400	37,18	1550	60	0,04

(d) It is reasonable to assume that all carbon present in the slag after reduction, will disappear during viscosity measurement by reactions of the type: $TiO_2 + C = TiO + CO$.....(1) (for free carbon)

$2TiO_2 + TiC = 3TiO + CO$....(2) (for combined carbon)

No carbon was found present in samples of the three slags mentioned above, after viscosity measurement. Moreover, a sample of B11, reduced for 120 minutes and then given the normal treatment prior to viscosity measurement, and sampled at this stage from the molybdenum crucible, contained no carbon either. This seems to prove that in whatever form the carbon was present after reduction, the slag on which viscosity measurement was performed, contained no carbon. It must further be assumed that the carbon originally present, was eventually incorporated in the degree of reduction of Ti in terms of

lower oxides, as determined after viscosity measurement.

Samples of slag B14, reduced at 1550°C, were also subjected to re-oxidation prior to viscosity measurement. The gains in mass recorded during this set of experiments were very close to those reported for the same series of samples when oxidation was performed after viscosity determination. This is illustrated in figure 40.

(e) Gruzdev et al[58] reported a decrease in the titanium content of the slag during reduction in graphite crucibles. The figures in table 13 show no such decrease for the present work.

It is concluded that any changes in properties of slags during reduction reported hereafter, must be due solely to the reduction of TiO_2 to lower oxides, except possibly in the case of very acidic slags, where reduction of SiO_2 to SiO may be significant. Further, as reduction state determinations and viscosity measurements were performed on the same product, correllation between these parameters must be rigorously valid.

3.10 Critical appraisal of experimental techniques

The two stages in which reduction and measurement of physico-chemical properties were performed here, are to be preferred to a single stage measurement of eg. viscosity in a graphite crucible, as the effects of viscosity change and variation in crystallization temperature are effectively separated.

When viscosity is determined, using a metallic inner cylinder and a graphite outer cylinder, the results must necessarily be doubtful on an absolute basis. There are indications that these slags initially do not wet the graphite crucible, but succeed in doing so after prolonged contact. Moreover, the speed of rotation of the viscometer spindle cannot be varied without altering the rate of reduction. If solid particles of TiC are indeed eventually formed in the graphite crucible, the effect of these on viscosity will once again be influenced by the speed of rotation of the spindle.

The measurement of electrical conductivity in a graphite crucible

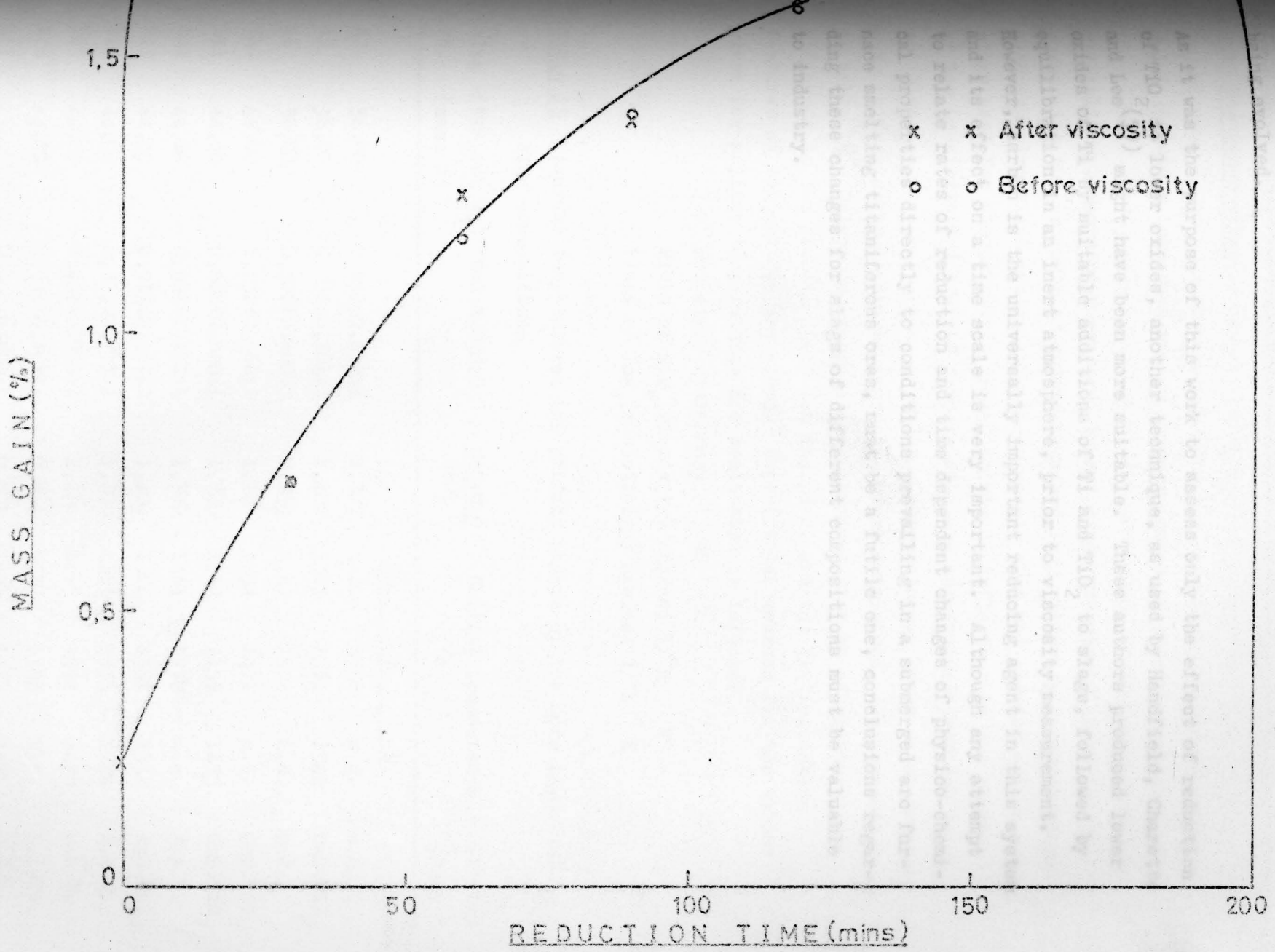


Figure 40 Reoxidation of reduced derivatives of slag B14

would be practically meaningless in a fluid from which gas bubbles are being evolved.

As it was the purpose of this work to assess only the effect of reduction of TiO_2 to lower oxides, another technique, as used by Handfield, Charette and Lee[59] might have been more suitable. These authors produced lower oxides of Ti by suitable additions of Ti and TiO_2 to slags, followed by equilibration in an inert atmosphere, prior to viscosity measurement. However, carbon is the universally important reducing agent in this system and its effect on a time scale is very important. Although any attempt to relate rates of reduction and time dependent changes of physico-chemical properties directly to conditions prevailing in a submerged arc furnace smelting titaniferous ores, must be a futile one, conclusions regarding these changes for slags of different compositions must be valuable to industry.

4. RESULTS

4.1 Unreduced slags

4.1.1 Liquidus temperatures and primary phases of unreduced slags

All melting temperatures measured by hot stage microscopy could be compared with the approximate values obtained from viscosity determinations. Although electrical resistivity measurements were not carried out on all slags used for viscosimetric tests, points of inflection in the plots of log (resistivity) against inverse absolute temperature provided an additional approximate value of melting temperature. These data, together with primary crystallization products, where determined, are presented in table 15. Only those compositions considered to be of greater significance in the present study are included, and the distinguishing features of composition are shown. Experimental sources for the values given for melting temperatures are designated as follows:

Hot stage microscopy HS

Plots of $\log_e$(viscosity) against $1/^oK$ V

Plots of $\log_e$(resistivity) against $1/^oK$ R

Table 15 Liquidus temperatures and primary phases of the more important slag compositions

Slag No.	$(TiO_2+Al_2O_3)$ (mass %)	CaO:MgO:SiO_2	$\frac{CaO+MgO}{SiO_2}$	Melting temperature (^oC)			Primary phase *
				HS	V	R	
A2	36,00	0,852:0,852:1	1,707	n.d.	1388	n.d.	n.d.
A5	36,00	0,701:0,701:1	1,400	1383	1361	1342	$CaO.TiO_2$
A8	36,00	0,400:0,400:1	0,800	n.d.	1322	n.d.	n.d.
B10	44,00	1,132:0,566:1	1,700	1454	1472	n.d.	$CaO.TiO_2$
B11	44,00	0,848:0,848:1	1,700	1460	1455	1475	$CaO.TiO_2$
B12	44,00	0,566:1,132:1	1,700	1461	1478	n.d.	M.A.T.
B13	44,00	0,933:0,467:1	1,400	1360	1337	1334	$CaO.TiO_2$
B14	44,00	0,701:0,701:1	1,400	1365	1335	1340	M.A.T.
B15	44,00	0,467:0,933:1	1,400	1499	1492	1478	M.A.T.
B16	44,00	0,533:0,267:1	0,801	1377	1388	n.d.	M.A.T.
B17	44,00	0,400:0,400:1	0,801	1405	1420	1401	M.A.T.
B18	44,00	0,267:0,533:1	0,801	1455	1473	n.d.	M.A.T.
C23	54,00	0,699:0,699:1	1,400	1473	1447	1461	M.A.T.

* M.A.T. = $4(MgO.2TiO_2).Al_2O_3.TiO_2$

Table 16 shows a comparison of liquidus temperatures measured by Hejja[9] (figure 3) with the values obtained by the author through viscosity measurements in most instances and by hot stage microscopy in a few cases. The slag compositions differed from one another only in basicity ratio $(CaO + MgO)/SiO_2$ and had the following features in common:

$(TiO_2 + Al_2O_3)$ = 44,00 mass %
TiO_2 = 30,20 mass %
TiO_2/Al_2O_3 = 2,21
CaO/MgO = 1,00

The experimental sources are designated in the following manner :
Determined by hot stage microscope (Hejja) - H
Determined by hot stage microscope (Author) - HS
Determined through viscosity measurement (Author) - V

Table 16 Correllation between melting temperatures from different sources

Slag No.	SiO_2 (mass %)	$(CaO+MgO)/SiO_2$	Melting temperature (°C)		
			H	HS	V
B17	31,100	0,801	n.d.	1405	1420
B28	24,350	1,300	1427	n.d.	1440
B29	23,830	1,350	1360	n.d.	1366
B14	23,330	1,400	1356	1365	1335
B30	22,860	1,450	1372	n.d.	1358
B31	22,410	1,500	1350	n.d.	1358
B32	21,970	1,550	1364	n.d.	1369
B33	21,540	1,600	1358	n.d.	1373
B34	21,130	1,650	1400	n.d.	1402
B11	20,750	1,700	1460	1460	1455

As is evident from the tables, the agreement between liquidus temperatures obtained from measurement of particularly viscosity, and the values obtained from high temperature microscopy, is such that meaningful comparative values could be expected from measurement of melting temperatures of reduced slags by the former technique. As will be shown in later sections the magnitude of variation of melting temperature of a given starting

slag composition due to reduction by carbon lies well outside what could be considered as the limits of experimental error, in the cases where the variation is of true industrial significance.

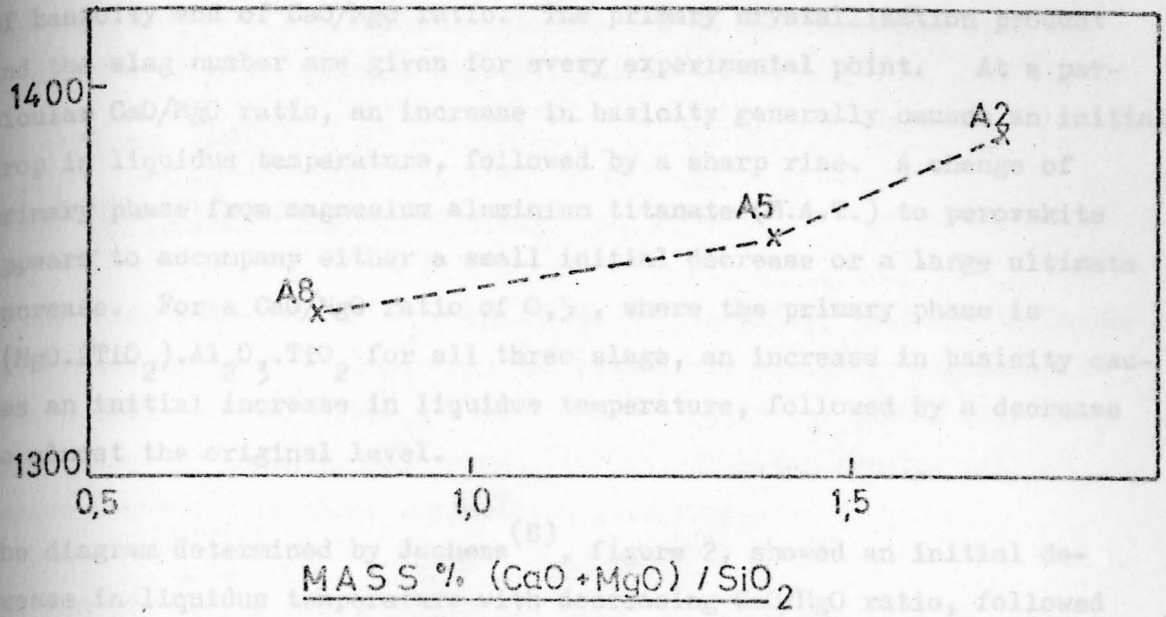
It must however be borne in mind that values obtained from hot stage microscopy and those from viscosity or resistivity measurements do not refer to slags in strictly the same condition of oxidation with respect to Ti. The material used for the former technique was fully oxidized. Values derived from viscosity measurement apply to a slag in a pure argon atmosphere. These slags exhibit a small but measurable degree of reduction in terms of a mass gain during complete re-oxidation in an atmosphere of pure oxygen. This fact must be coupled with the inherent error in viscosimetrically determined temperatures, due mainly to a certain degree of supercooling. The complexity of the two effects, together with the inconsistancy of the sign of the error (relative to the microscopically determined value) render error analysis impossible.

The selection of the slags shown in table 16 for liquidus temperature determination is well motivated by established operation at the iron plant of the Highveld Steel and Vanadium Corporation. The degree of dilution represented by ($TiO_2 + Al_2O_3$) = 44 mass % was giving satisfactory results. The ratio TiO_2/Al_2O_3 = 2,21 is mainly a function of the ore, while the CaO/MgO ratio of approximately unity is indicated chiefly by the most economical fluxing additions. Within these practical limitations, there exists a region of low liquidus temperature over a relatively wide basicity range of 1,35 to 1,60.

Closely supplementing or meaningfully interlinking liquidus temperature data are not available in the literature. Moreover, in the present work composition variable intervals are generally too large for acceptable correllation of liquidus temperature with such variables. However, certain general trends may be pointed out.

Members of series A (A2, A5 and A8), all possessing a CaO/MgO ratio = 1, show a gradual decrease in melting temperature with decrease in basicity (figure 41). The temperatures on the chart are those obtained through viscosity measurements. The slag numbers are shown next to the experimental points.

Figure41 Liquidus temperatures of series A slags



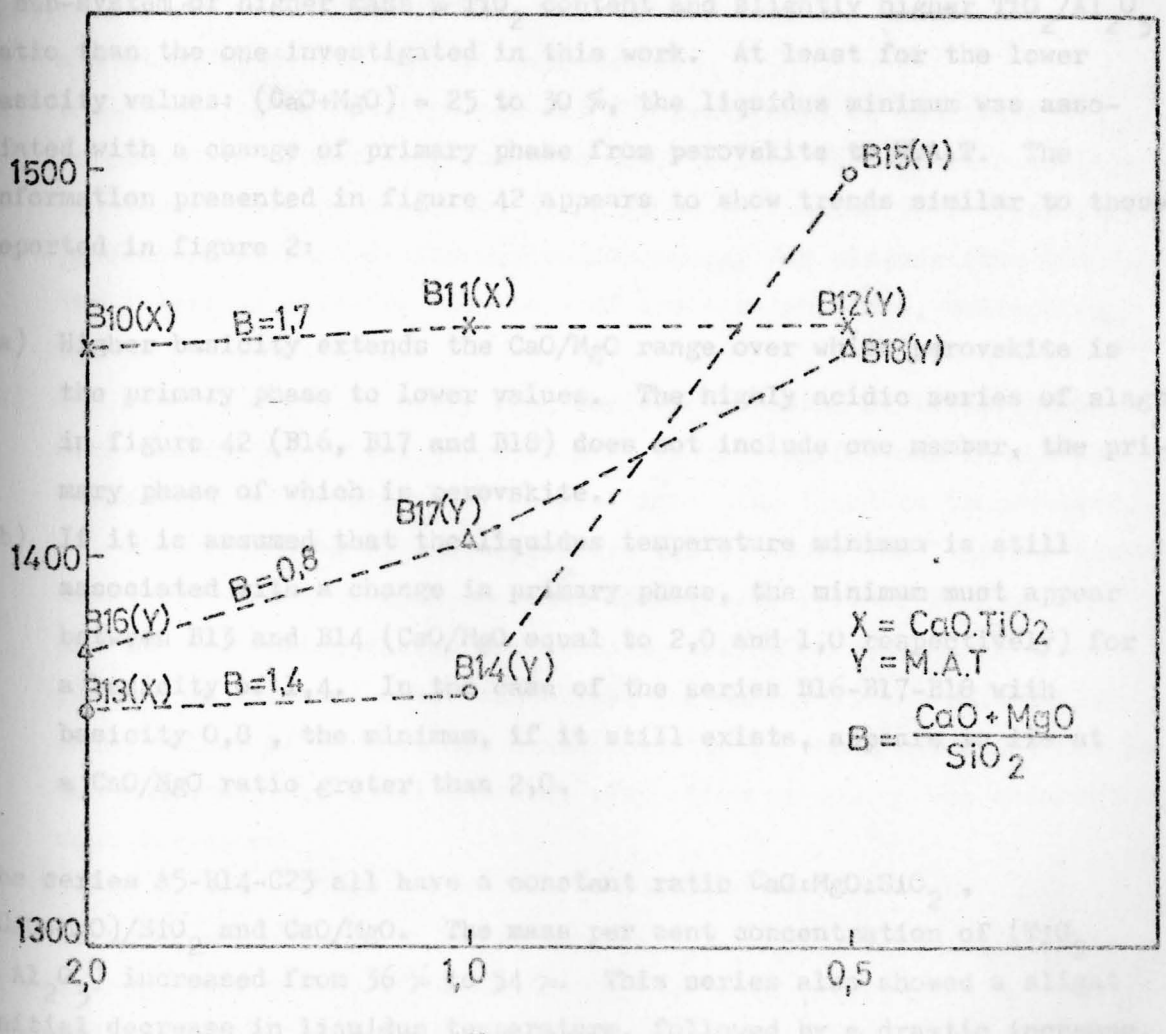


Figure 42 Effect of basicity and CaO/MgO ratio on liquidus temperatures of series B slags.

Figure 42 shows the liquidus temperatures of series B slags as a function of basicity and of CaO/MgO ratio. The primary crystallization product and the slag number are given for every experimental point. At a particular CaO/MgO ratio, an increase in basicity generally causes an initial drop in liquidus temperature, followed by a sharp rise. A change of primary phase from magnesium aluminium titanate (M.A.T.) to perovskite appears to accompany either a small initial decrease or a large ultimate increase. For a CaO/MgO ratio of 0,5 , where the primary phase is $4(MgO.2TiO_2).Al_2O_3.TiO_2$ for all three slags, an increase in basicity causes an initial increase in liquidus temperature, followed by a decrease to almost the original level.

The diagram determined by Jochens[8], figure 2, showed an initial decrease in liquidus temperature with decreasing CaO/MgO ratio, followed by a more gradual rise, for any constant basicity. His data applied to a sub-system of higher mass % TiO_2 content and slightly higher TiO_2/Al_2O_3 ratio than the one investigated in this work. At least for the lower basicity values: (CaO+MgO) = 25 to 30 %, the liquidus minimum was associated with a change of primary phase from perovskite to M.A.T. The information presented in figure 42 appears to show trends similar to those reported in figure 2:

(a) Higher basicity extends the CaO/MgO range over which perovskite is the primary phase to lower values. The highly acidic series of slags in figure 42 (B16, B17 and B18) does not include one member, the primary phase of which is perovskite.

(b) If it is assumed that the liquidus temperature minimum is still associated with a change in primary phase, the minimum must appear between B13 and B14 (CaO/MgO equal to 2,0 and 1,0 respectively) for a basicity of 1,4. In the case of the series B16-B17-B18 with basicity 0,8 , the minimum, if it still exists, appears to lie at a CaO/MgO ratio greter than 2,0.

The series A5-B14-C23 all have a constant ratio $CaO:MgO:SiO_2$, $(CaO+MgO)/SiO_2$ and CaO/MgO. The mass per cent concentration of (TiO_2 + Al_2O_3) increased from 36 % to 54 %. This series also showed a slight initial decrease in liquidus temperature, followed by a drastic increase. Again there is a change of primary phase between A5 and B14 from perovskite to magnesium aluminium titanate, and the similarity of liquidus

temperatures of A5 and B14 (1383°C and 1365°C) may indicate a minimum between (TiO_2 + Al_2O_3) contents of 36 % and 44 %, associated with the appearance of a new primary crystallization product.

4.1.2 Viscosity of unreduced slags

As the slag compositions were chosen in such a manner that the influence of relatively drastic changes in the parameters basicity, expressed as mass % ratio (CaO+MgO)/SiO_2, mass % CaO/MgO ratio and mass % (TiO_2+Al_2O_3) upon viscosity could be determined, the experimental results will be presented according to these composition variables.

The results of the measurements are given in graphical form in figures 43 to 60. The effects of composition in terms of any of the variables mentioned above, are shown by means of three successive diagrams:

(X) A plot of viscosity against temperature;

(Y) A plot of $\log_e$(viscosity) against the reciprocal of the absolute temperature. These diagrams were used to find the approximate liquidus temperature of the slag, as outlined in section 3.7. They also provided a measure of the activation energy for viscous flow ($E\eta$). The latter is given by the slope of the straight line, multiplied by the gas constant R.

(Z) The data relating to every slag series consisting of three compositions, were summarized in the third diagram to show variations in the following parameters, as functions of composition: the liquidus temperature, the viscosity at a fixed temperature (50°C) above the liquidus temperature, the viscosity at a constant temperature (either 1500 or 1550°C) and the activation energy for viscous flow. The results were not plotted as lines of equal viscosity, due mainly to the relatively small values of $E\eta$ that are characteristic of the system, and due to the comparatively small interval over which viscosity was measured in most instances.

This sequence was adhered to until the basic viscosity-temperature data of all slags were given, after which only the summarizing plot (Z) was retained.

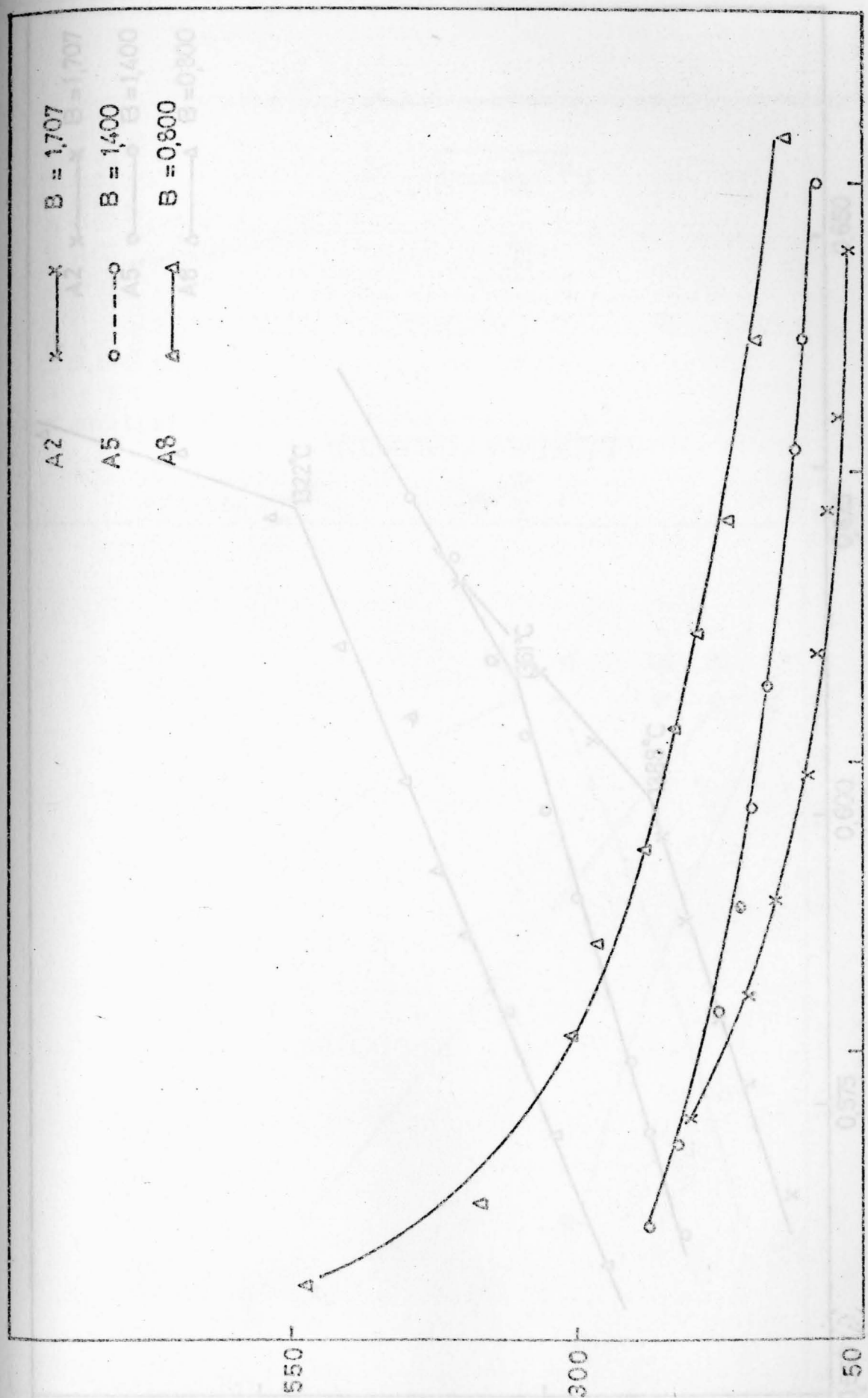


Figure 43 The effect of basicity upon viscosity for slags of series A.

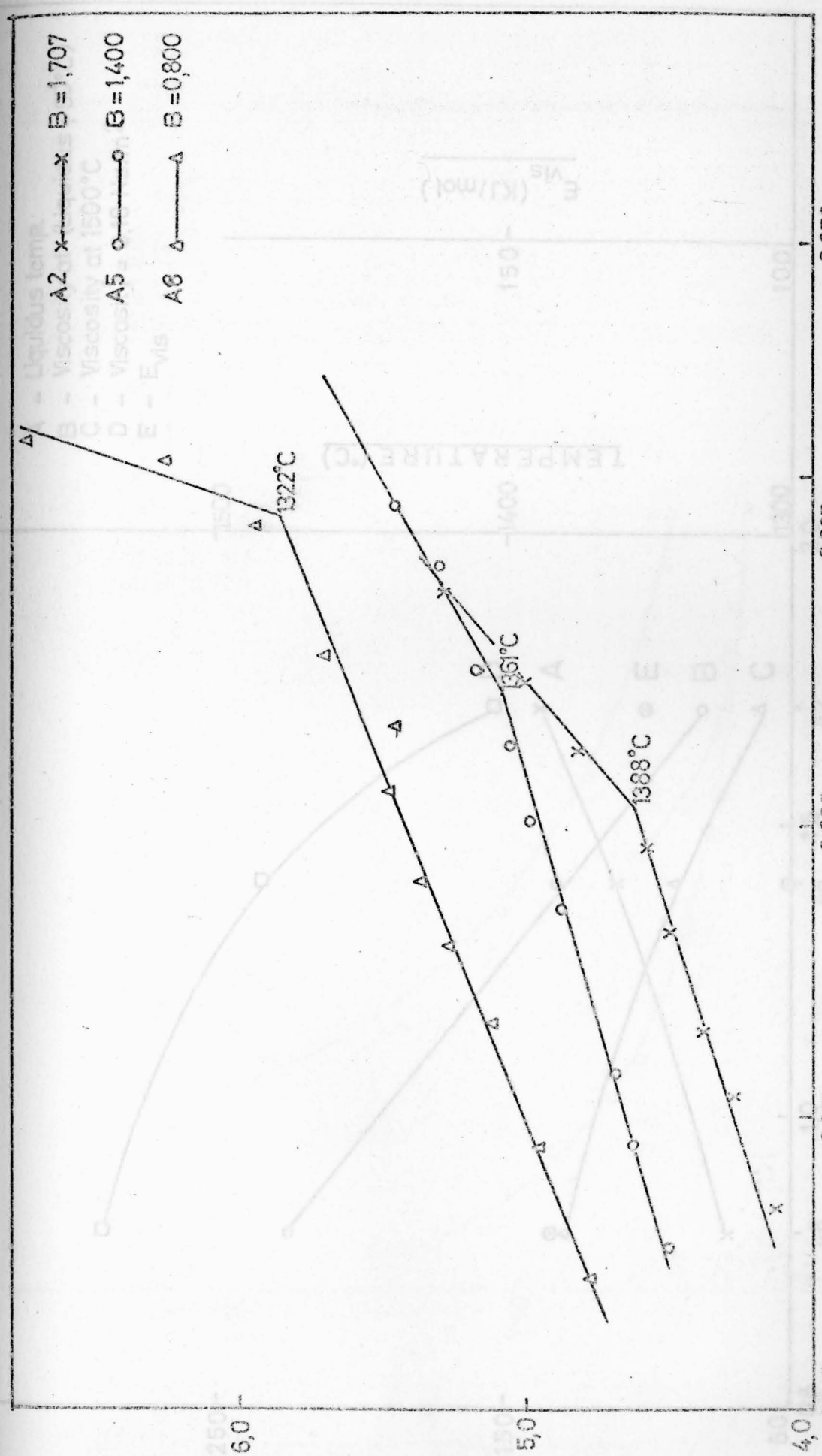


Figure 44 The effect of basicity upon viscosity for slags of series A.

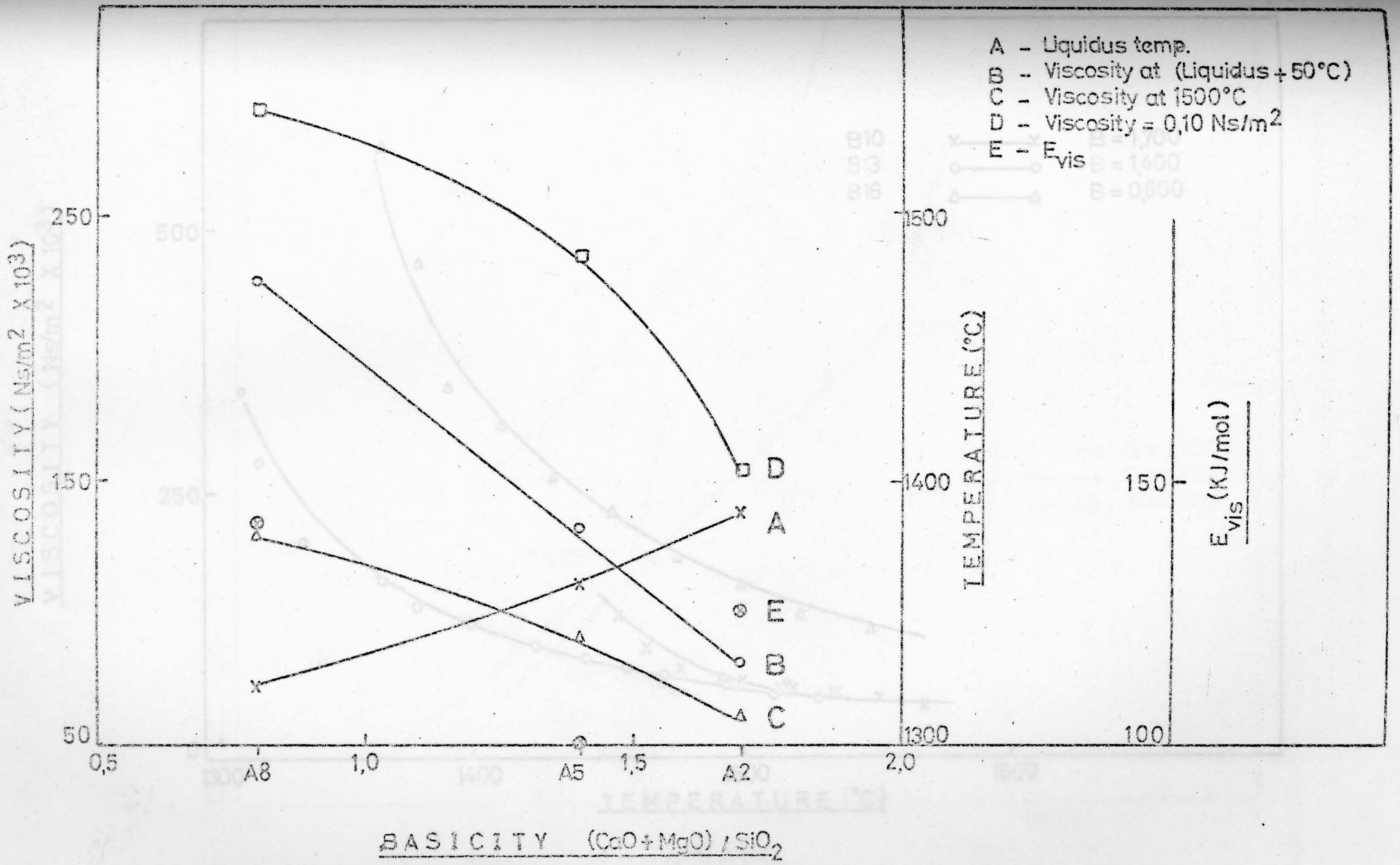


Figure 45 The effect of basicity upon viscosity for slags of series A - Summary

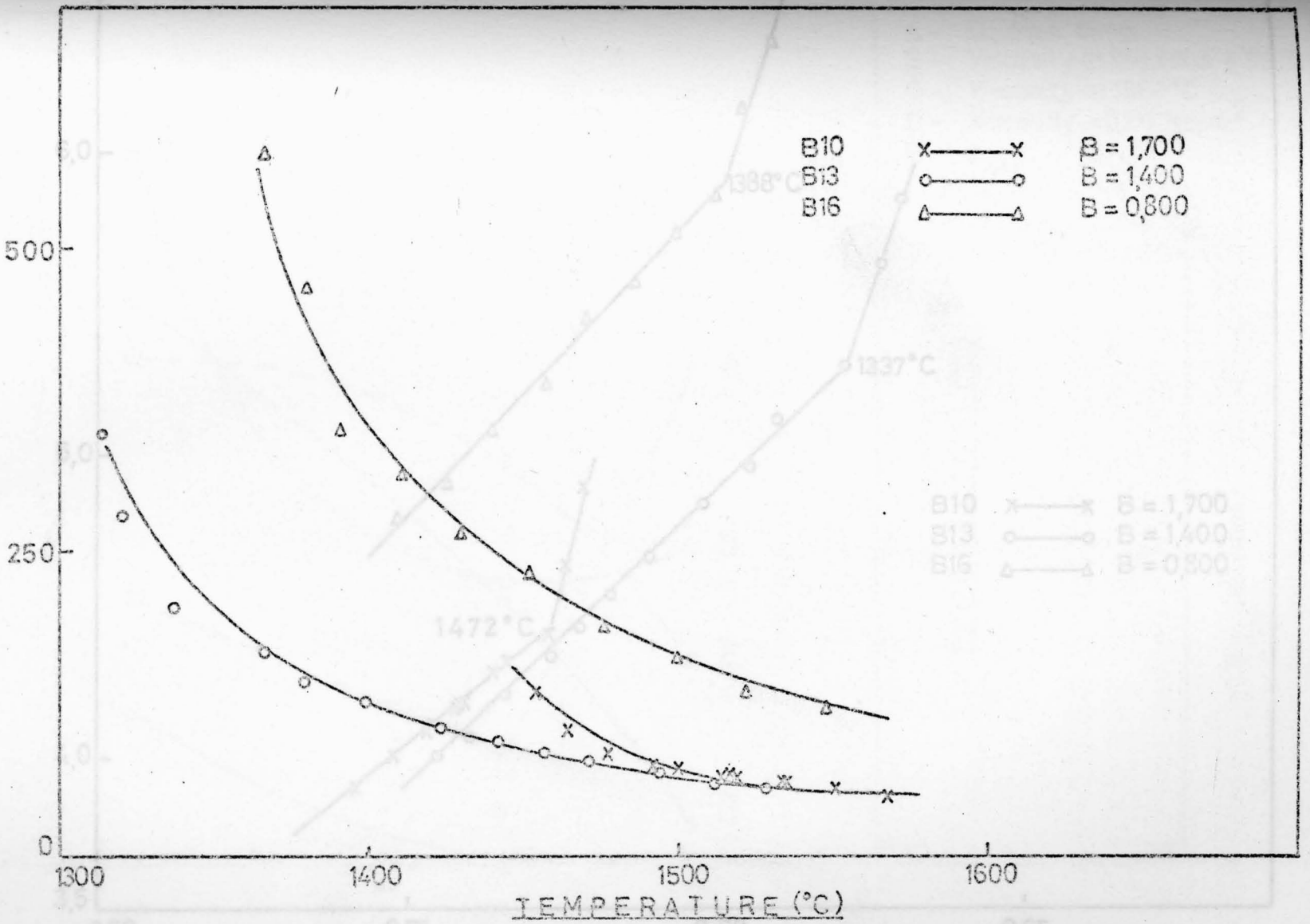


Figure 46 The effect of basicity upon viscosity for slags of series B. CaO/MgO = 2,0

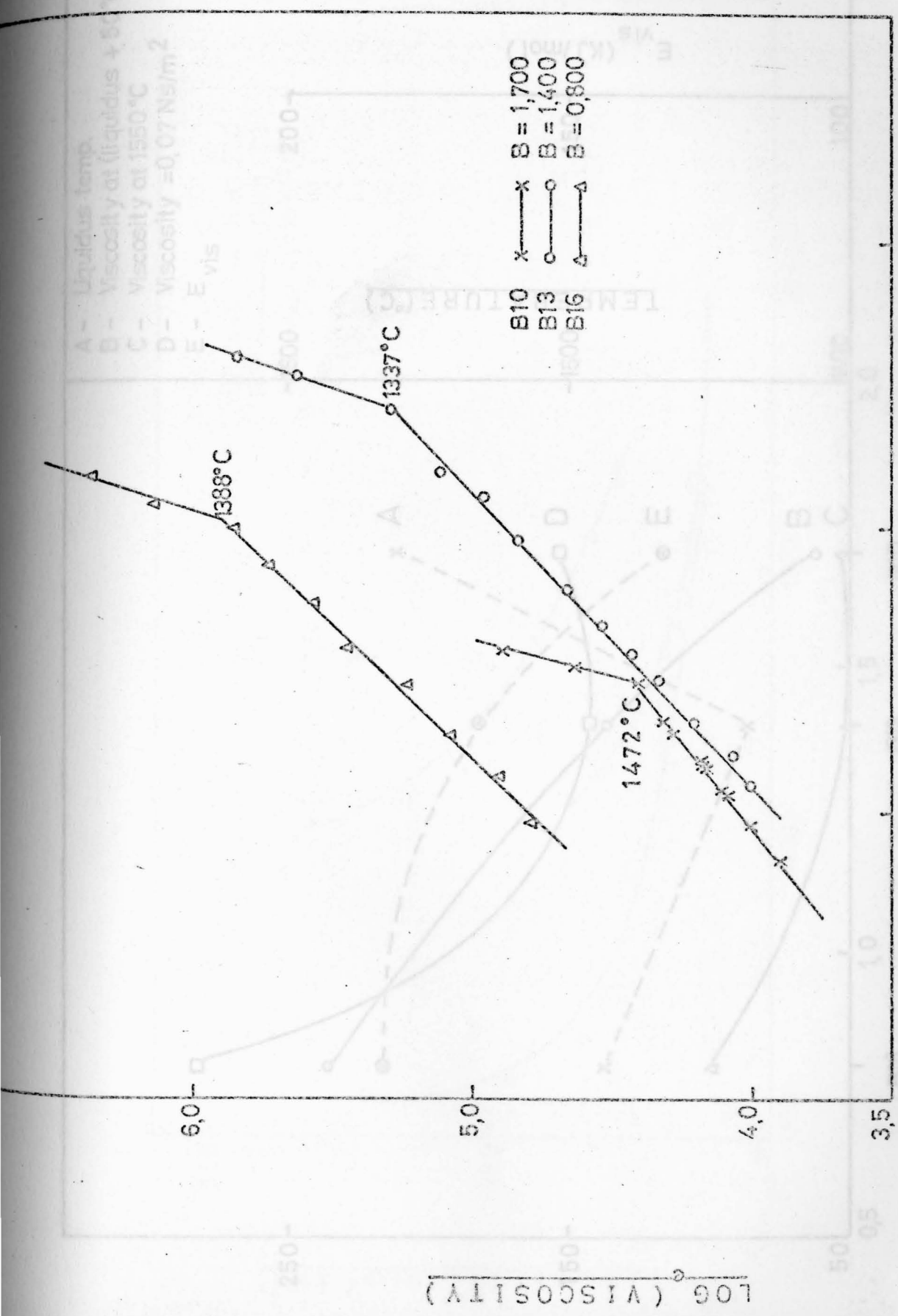


Figure 47 The effect of basicity upon viscosity for slags of series B, CaO/MgO = 2,0

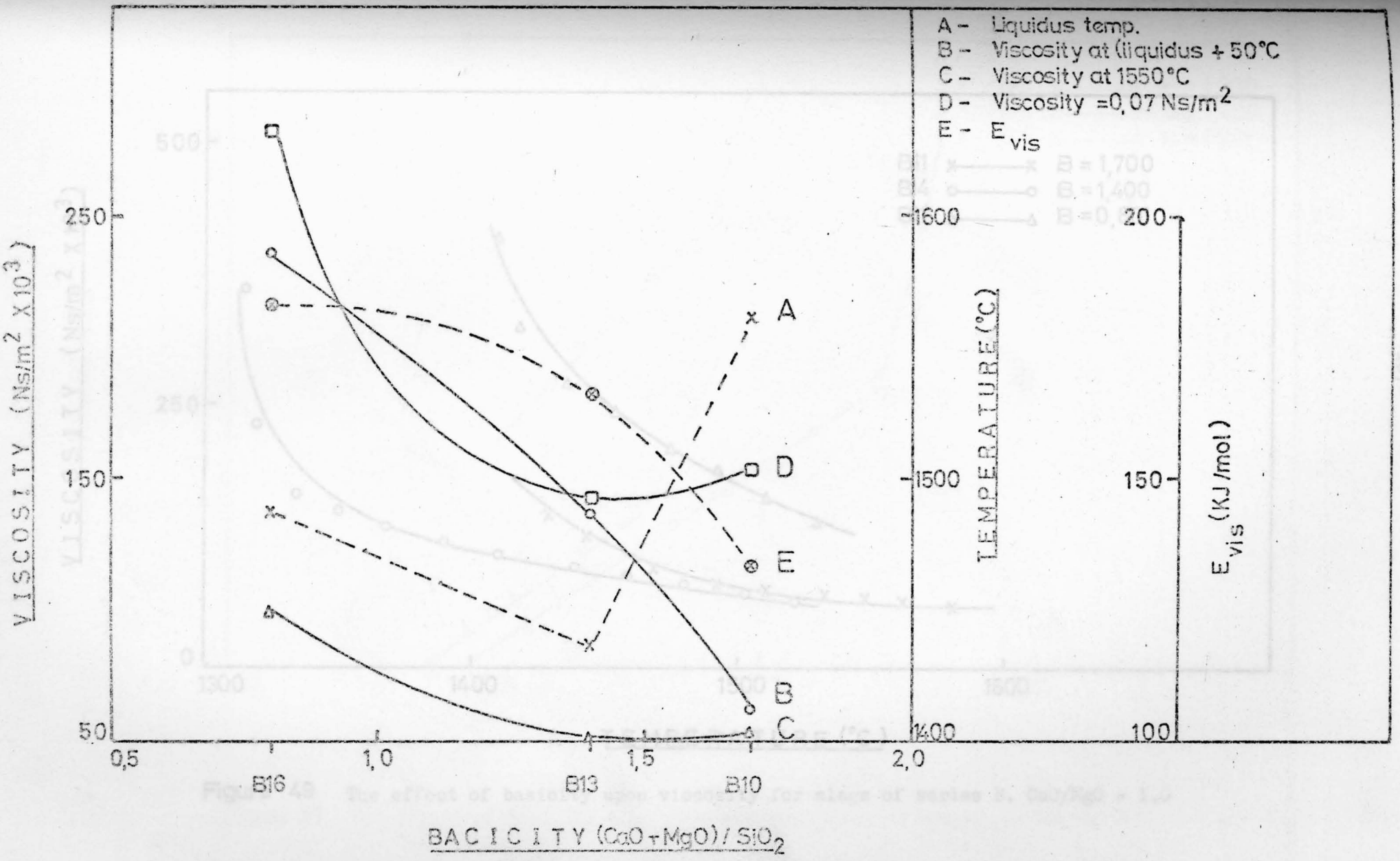


Figure 48 Theeffect of basicity upon viscosity for slags of series B, CaO/MgO = 2,0 - Summary

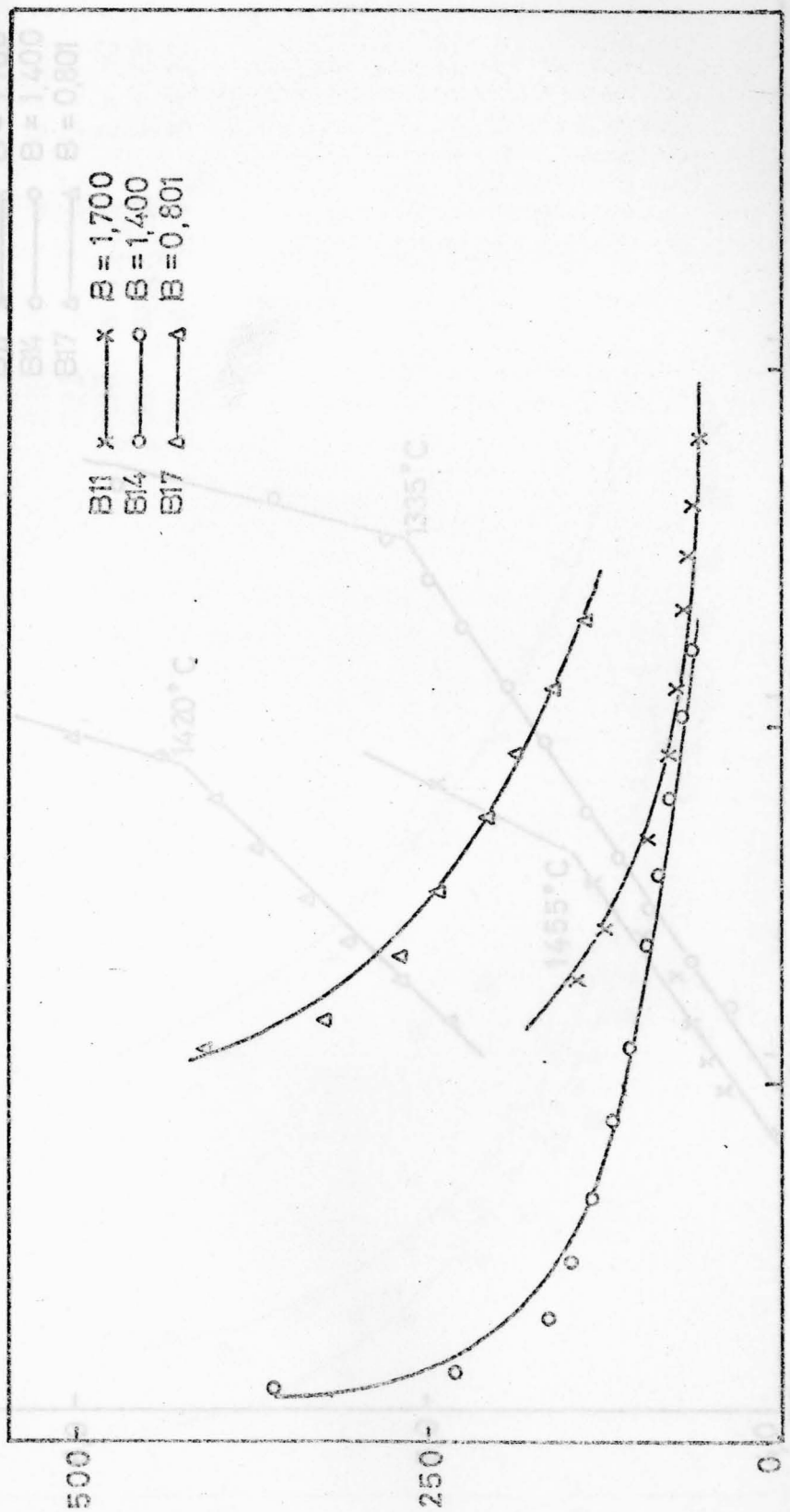


Figure 43 The effect of basicity upon viscosity for slags of series B, CaO/MgO = 1,0

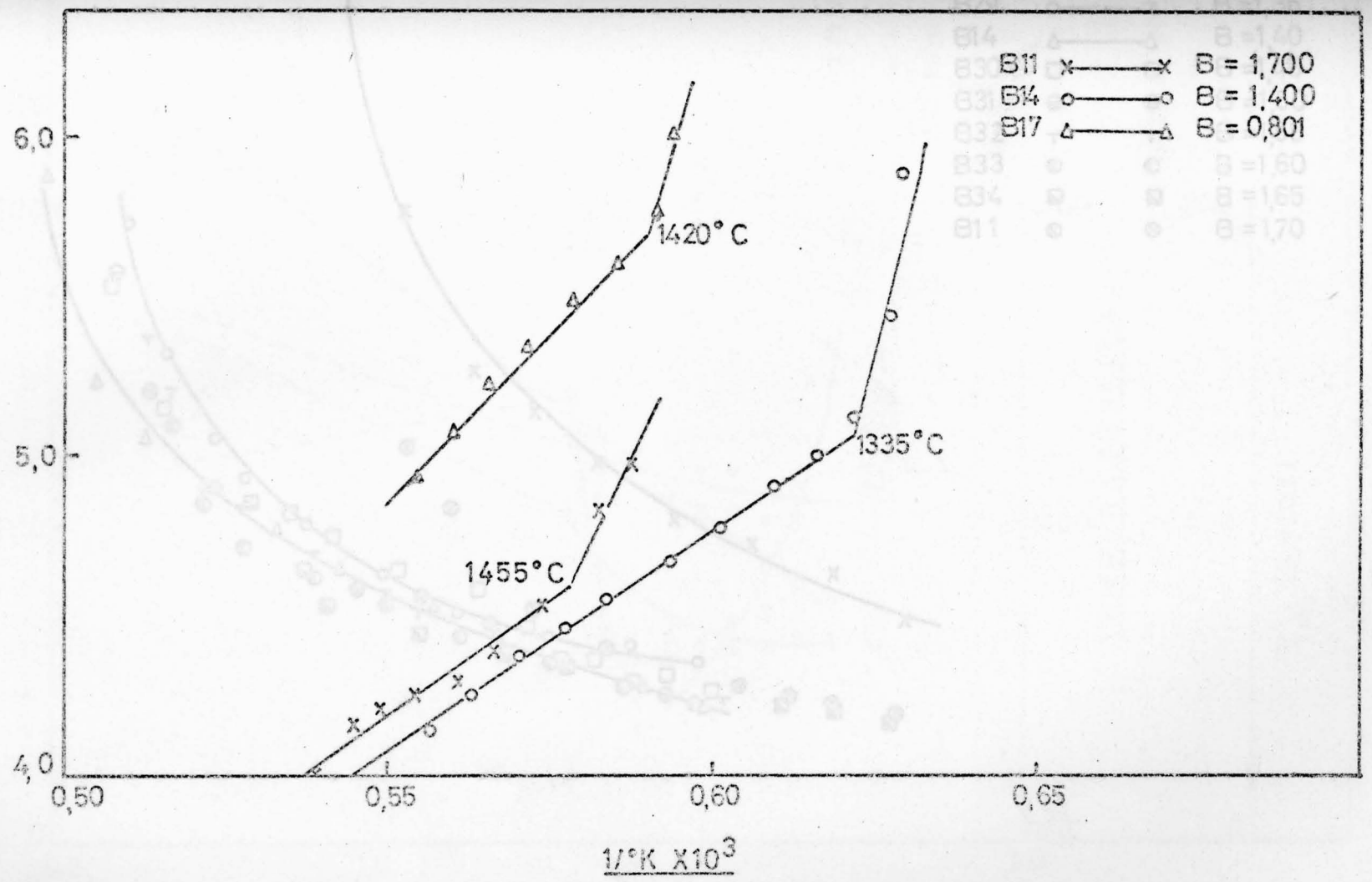


Figure 50 The effect of basicity upon viscosity for slags of series B, CaO/MgO = 1

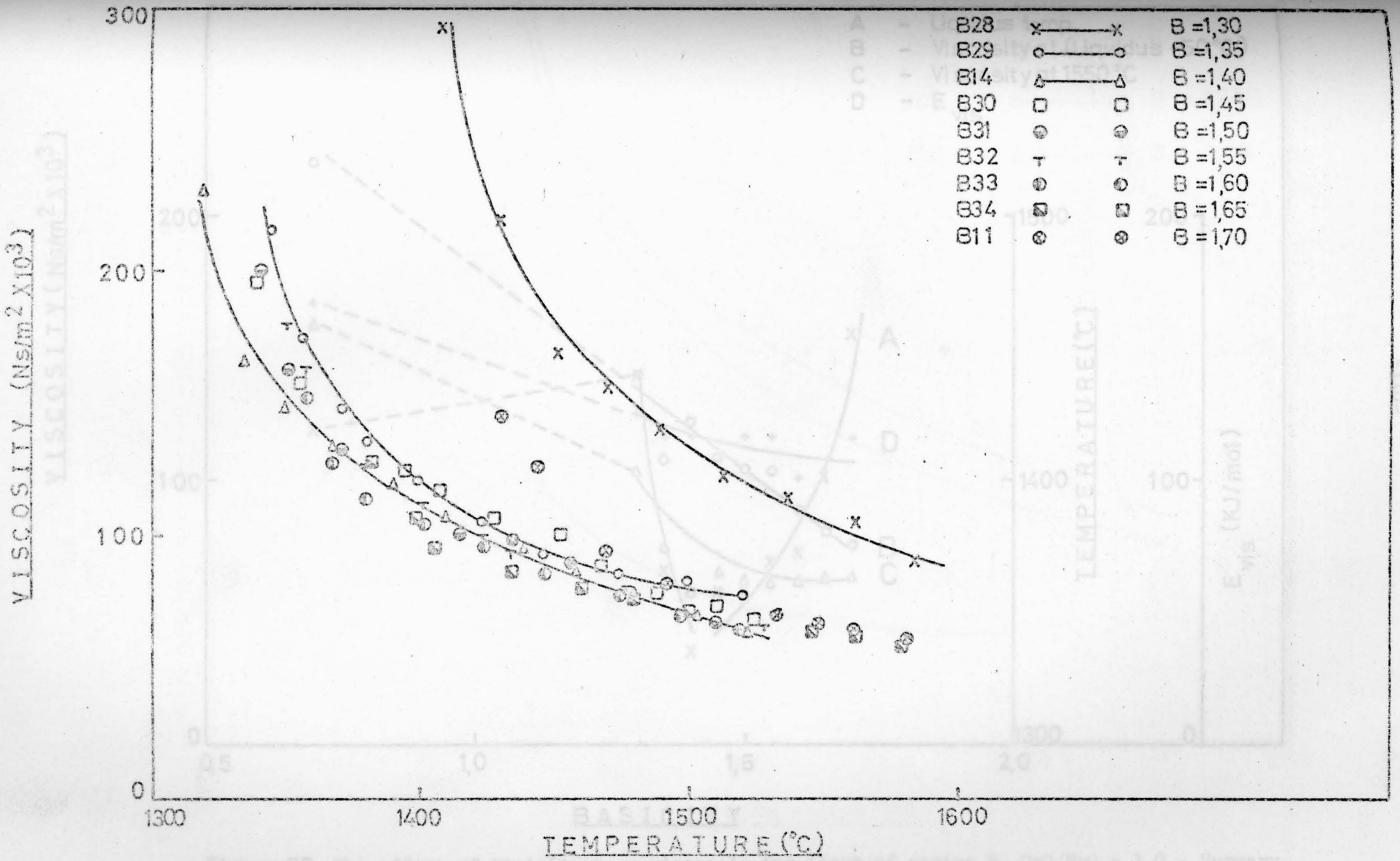


Figure 51 The effect of basicity upon viscosity for slags of series B, CaO/MgO = 1,0

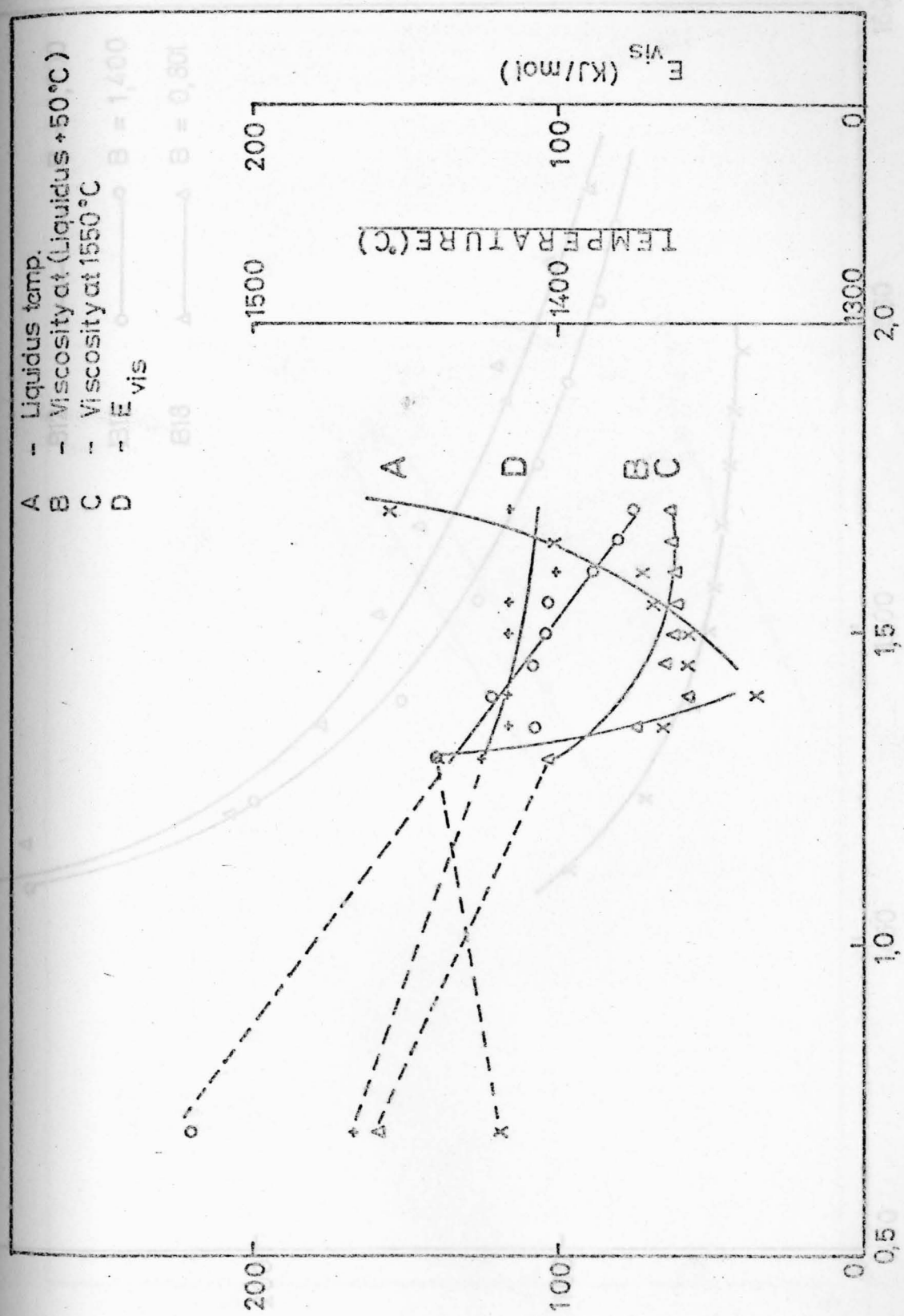


Figure 52 The effect of basicity upon viscosity for slags of series B, CaO/MgO = 1,0 - Summary

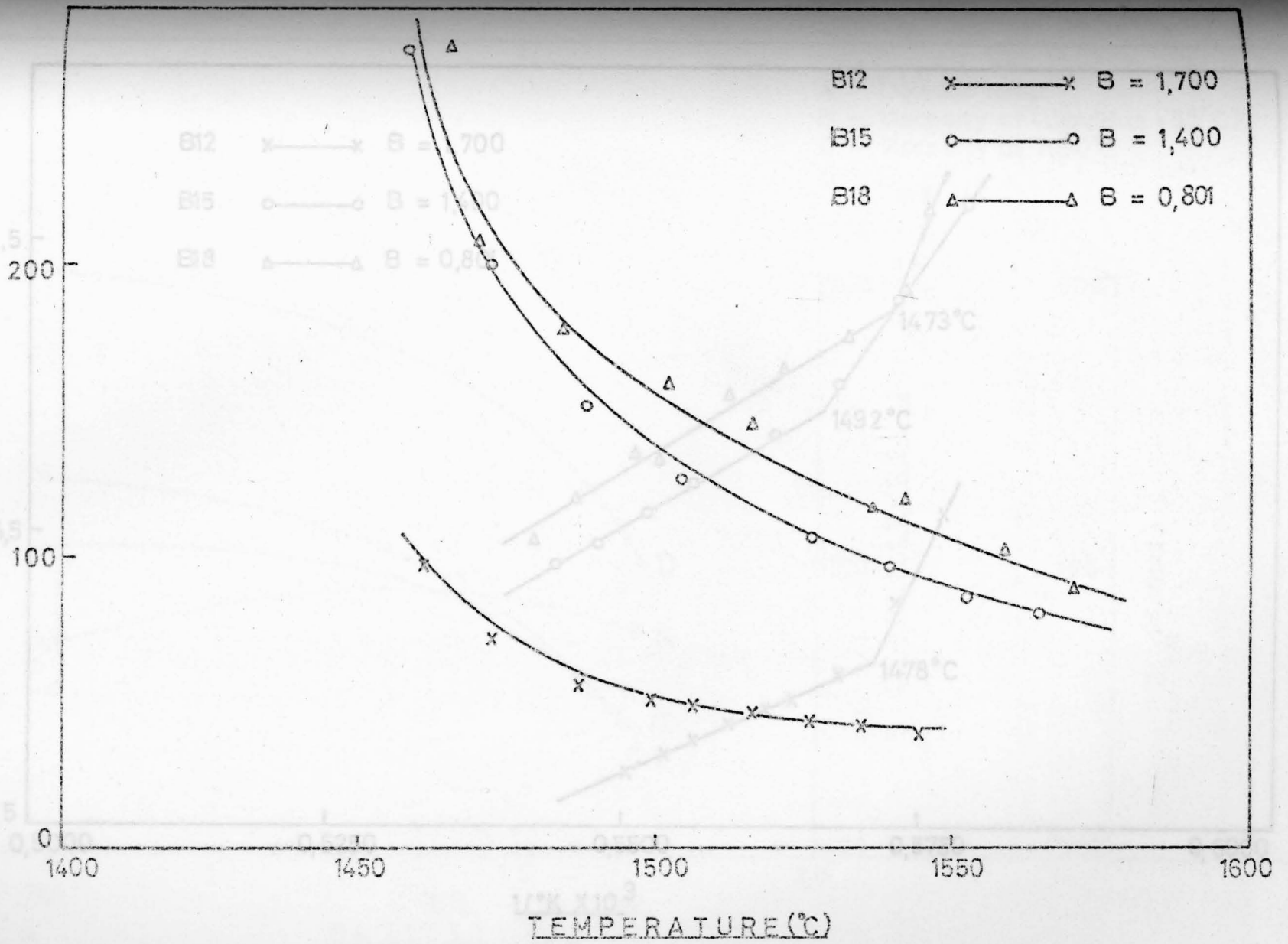


Figure 53 The effect of basicity upon viscosity for slags of series 5, CaO/MgO = $\frac{1}{2}$

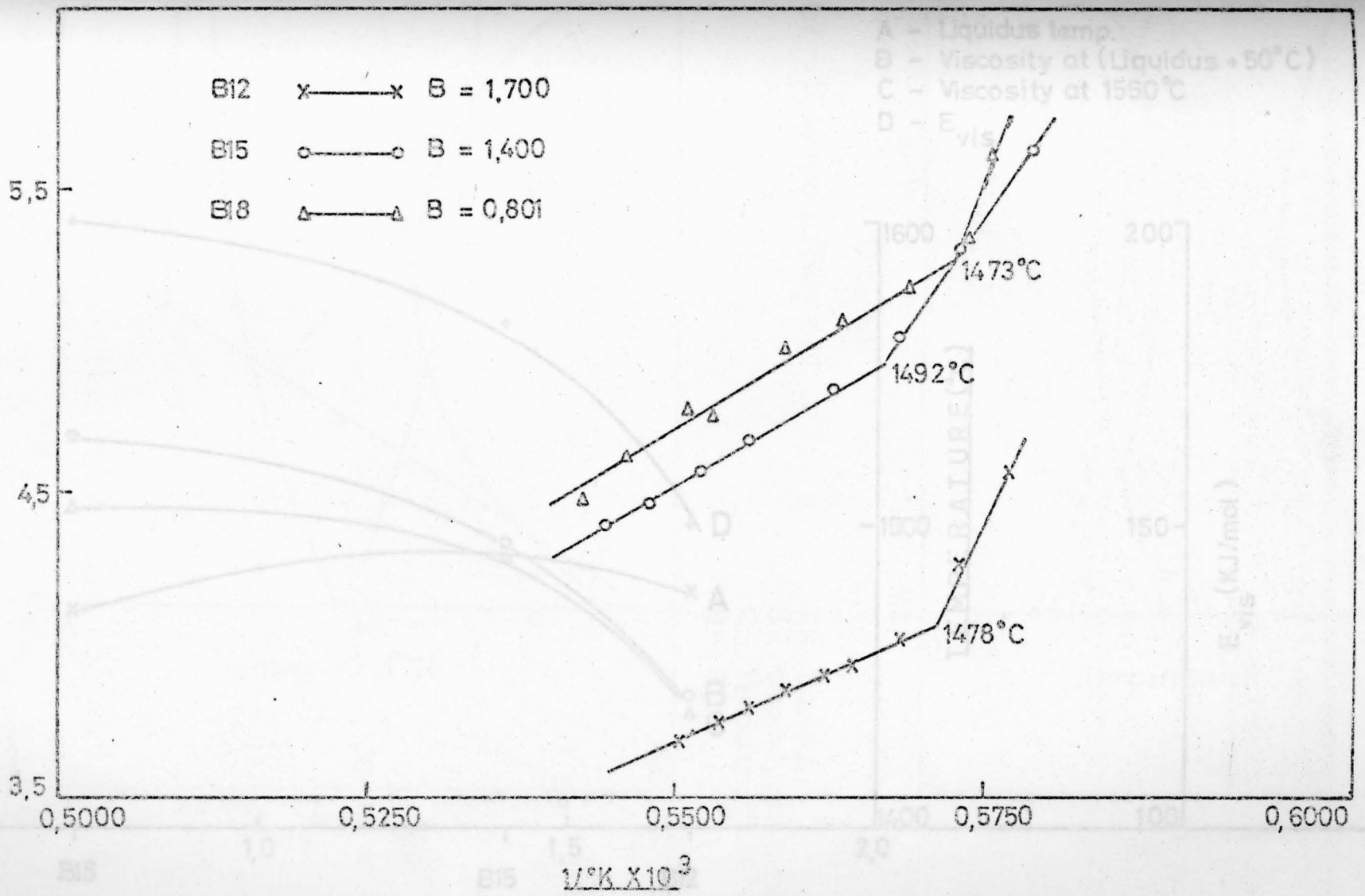


Figure 54 The effect of basicity upon viscosity for slags of series B, $CaO/MgO = \frac{1}{2}$

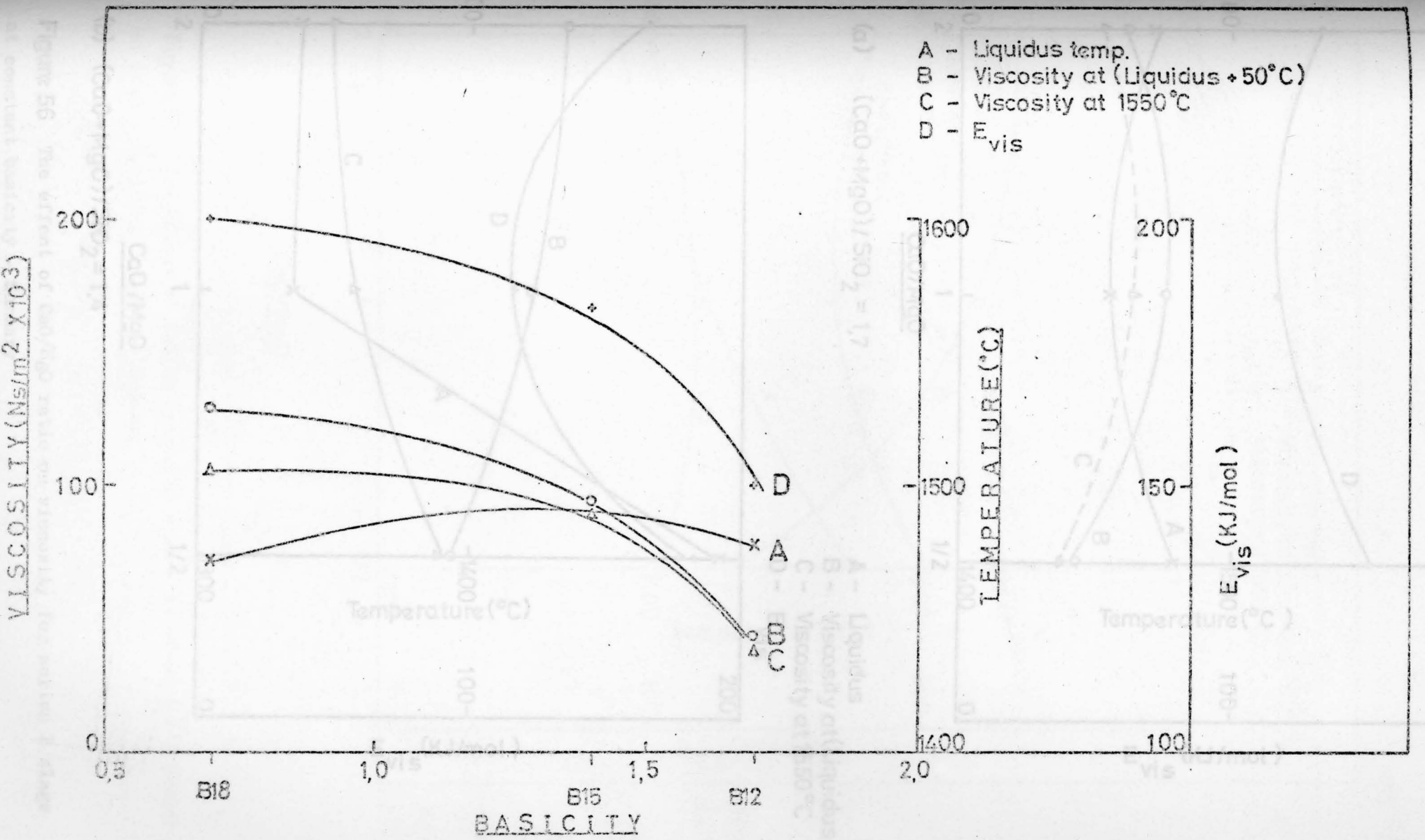
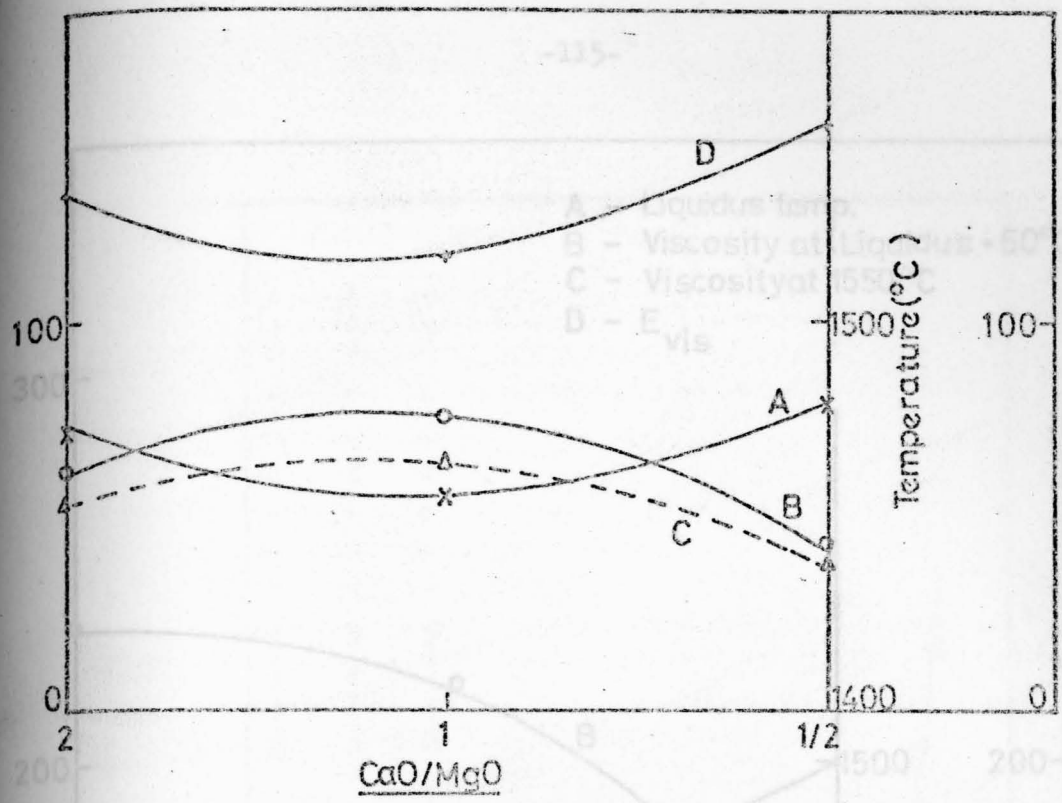
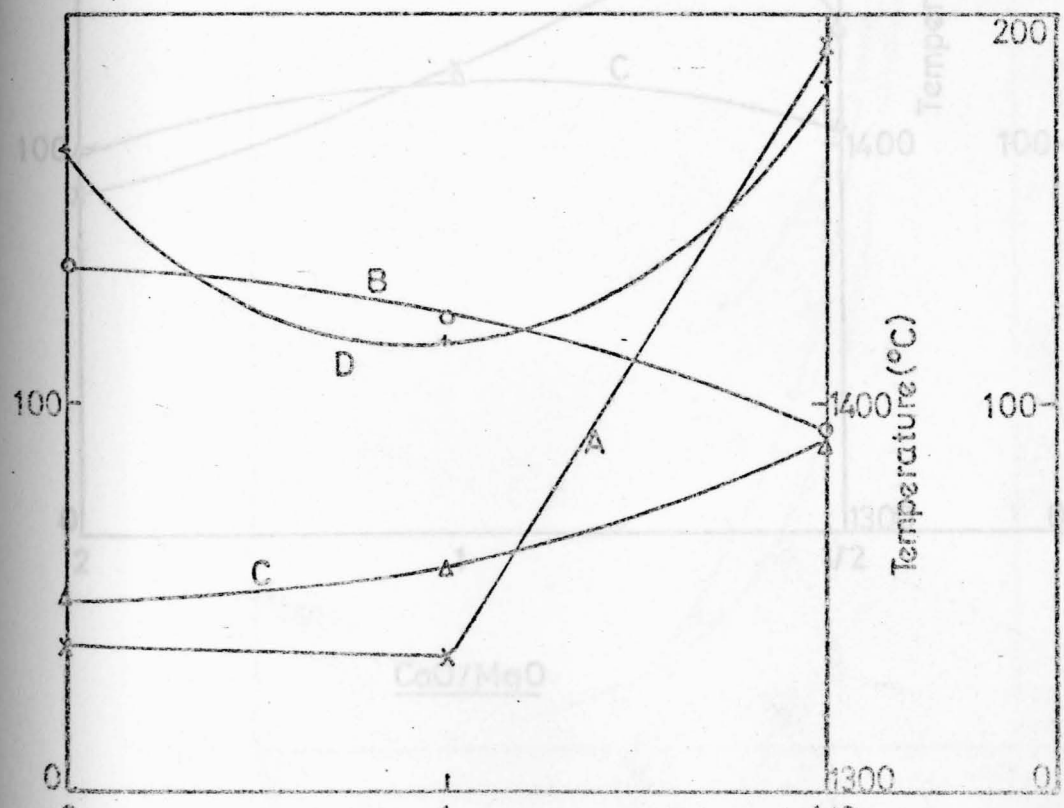


Figure 55 The effect of basicity upon viscosity for slags of series B, $CaO/MgO = \frac{1}{2}$ - Summary



(a) $(CaO+MgO)/SiO_2 = 1,7$

A – Liquidus
B – Viscosity at (Liquidus + 50°C)
C – Viscosity at 1550°C
D – E_{vis}



(b) $(CaO+MgO)/SiO_2 = 1,4$

Figure 56 The effect of CaO/MgO ratio on viscosity for series B slags at constant basicity - Summary

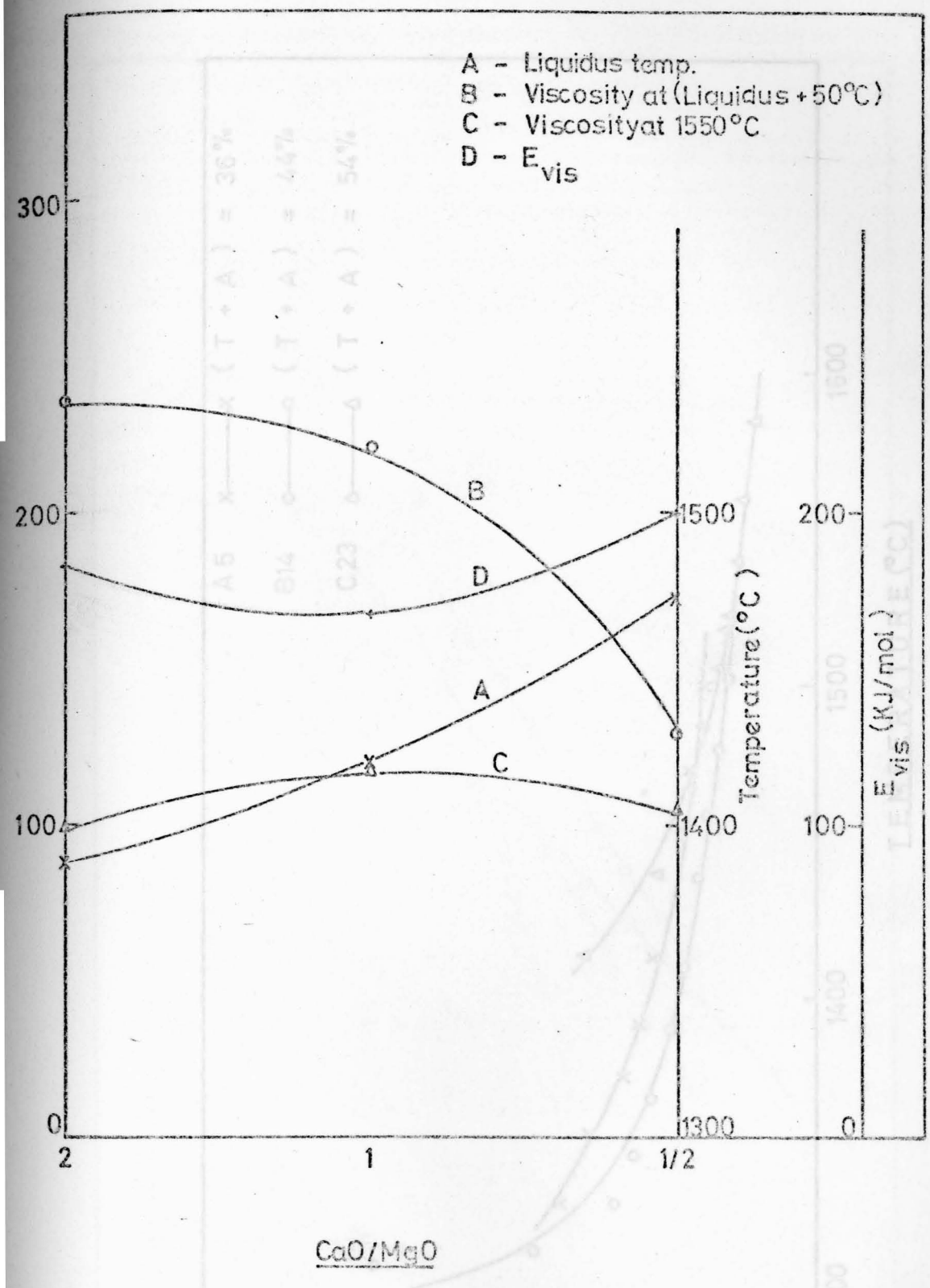


Figure 57 The effect of CaO/MgO ratio on viscosity of series B slags at $(CaO + MgO)/SiO_2 = 0,8$ - Summary

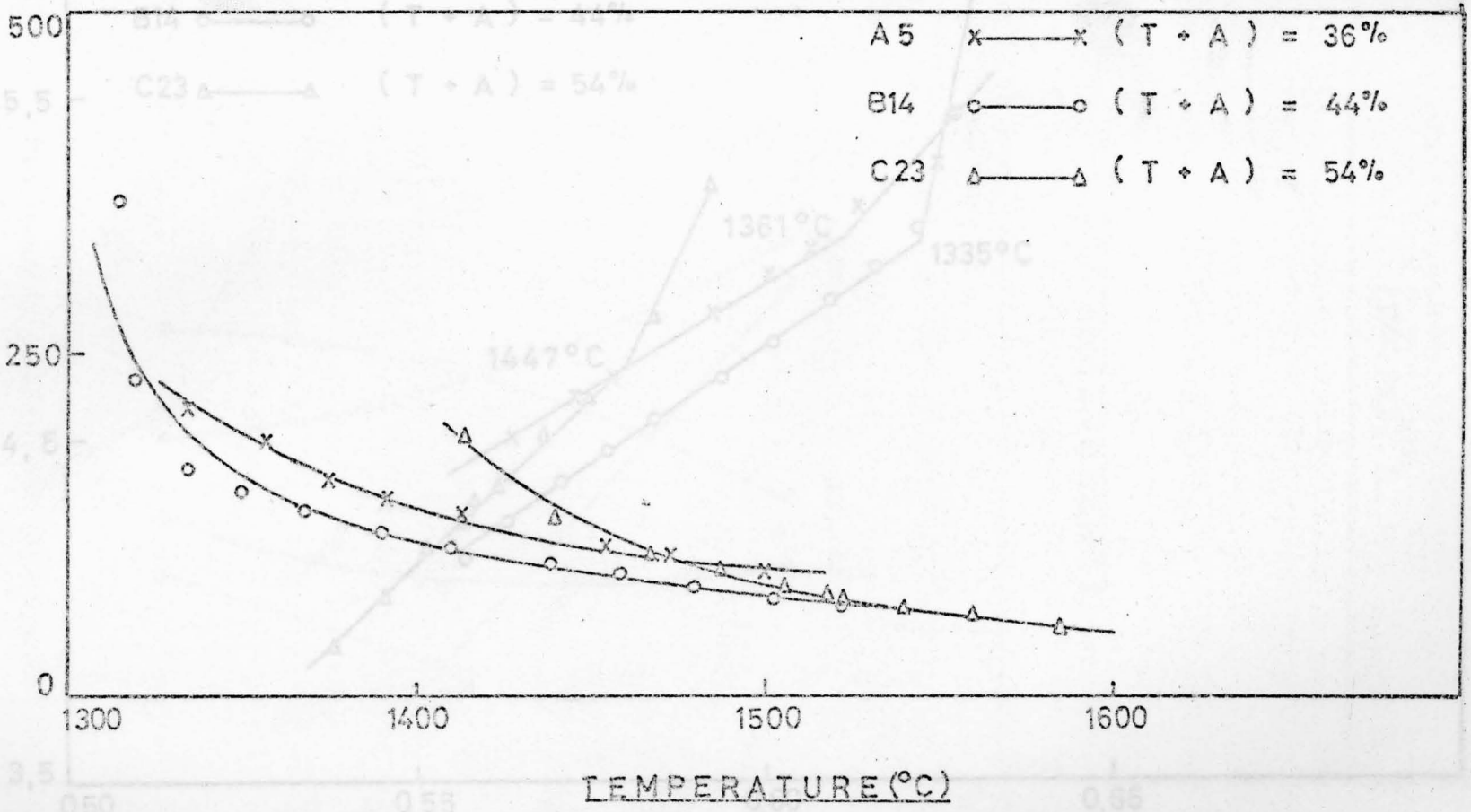


Figure 58 The effect of (TiO_2 + Al_2O_3) content on viscosity at $CaO/MgO/SiO_2$ = 0,7/0,7/1

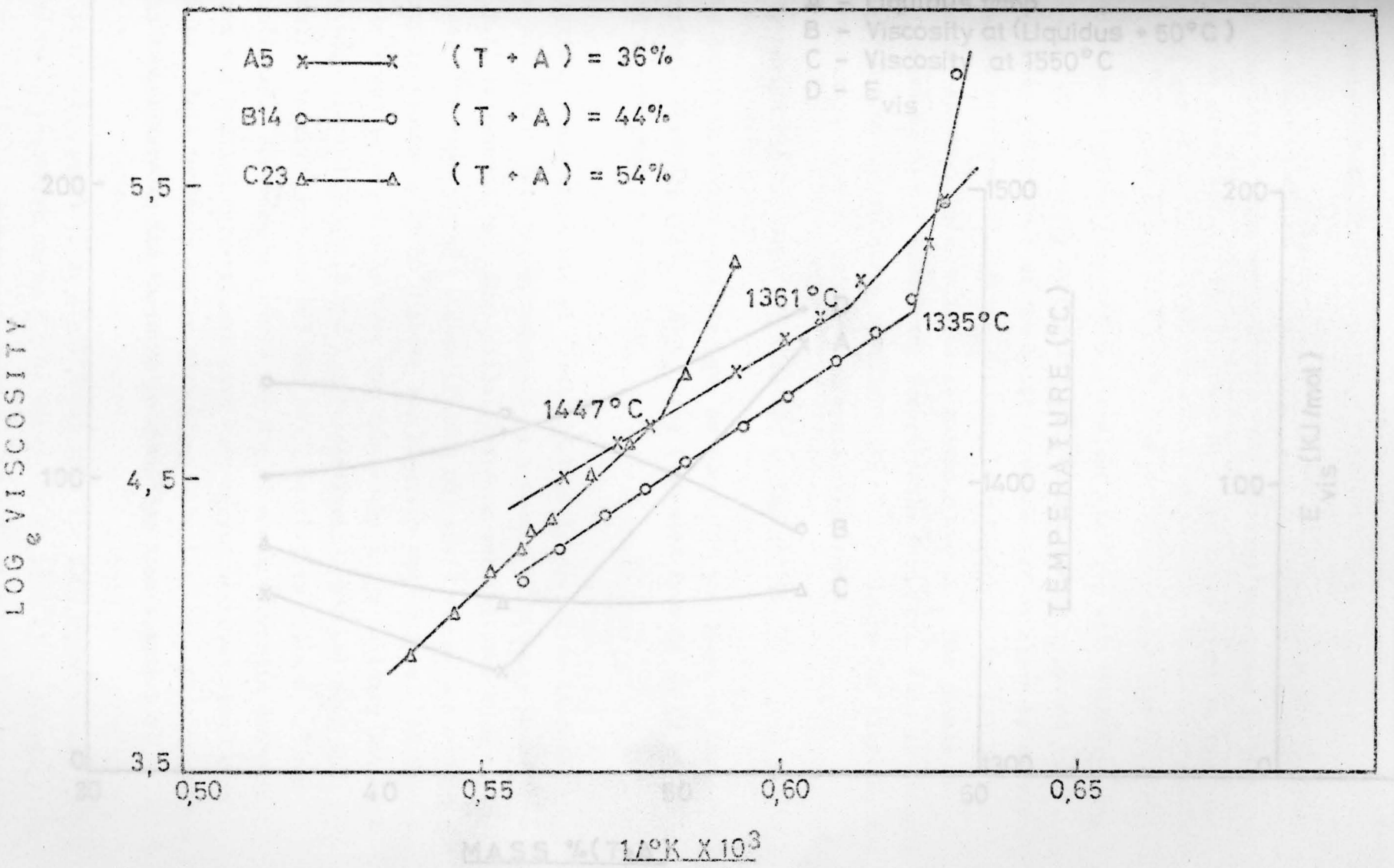


Figure 59 The effect of (TiO_2 + Al_2O_3) content on viscosity at $CaO/MgO/SiO_2$ = 0,7/0,7/1

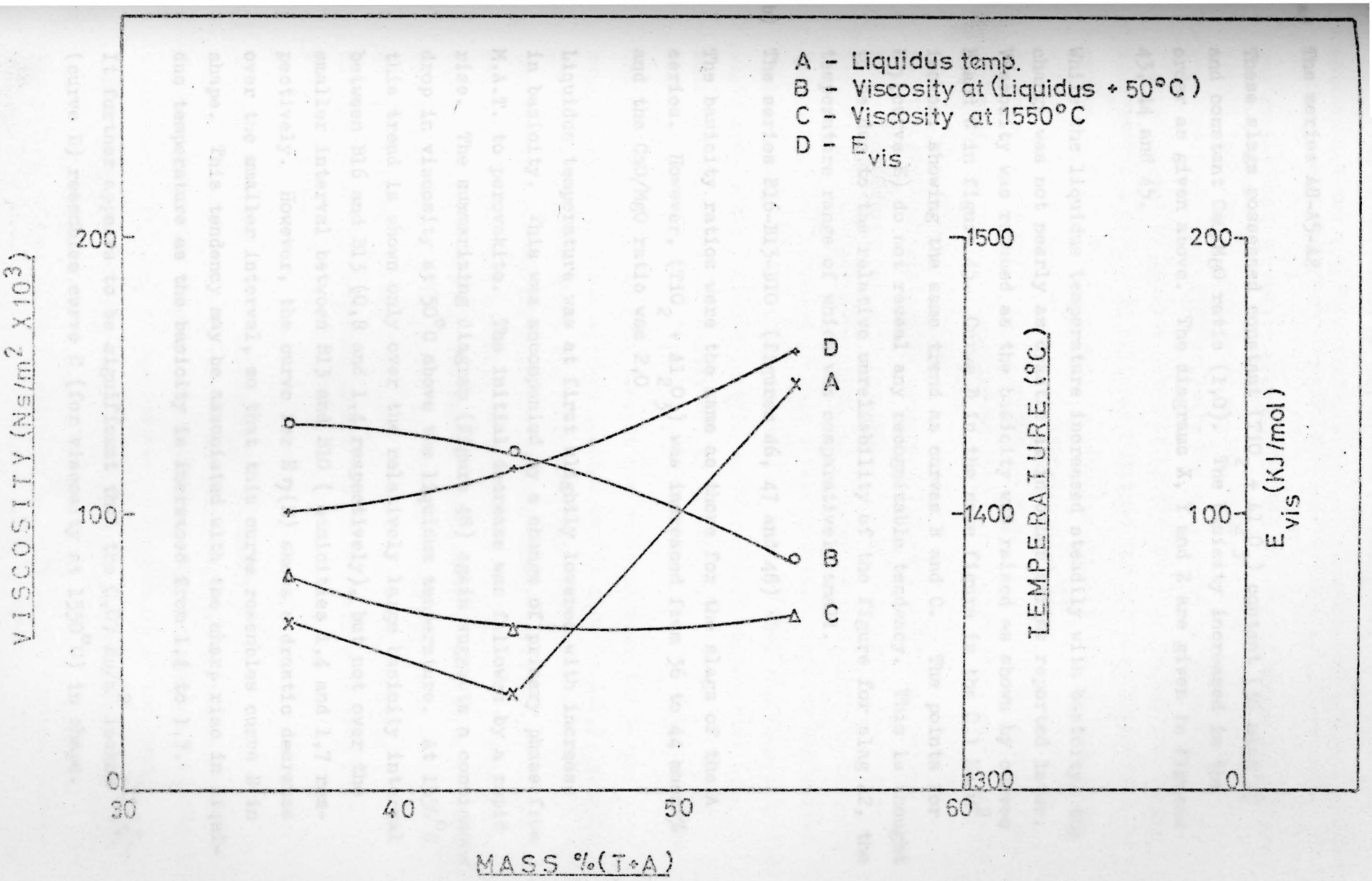


Figure 60 The effect of (TiO_2 + Al_2O_3) content on viscosity at $CaO/MgO/SiO_2$ = 0,7/0,7/1 - Summary

4.1.2.1 The effect of basicity upon viscosity

(a) The series A8-A5-A2

These slags possessed constant (TiO_2 + Al_2O_3) content (36 mass %) and constant CaO/MgO ratio (1,0). The basicity increased in the order as given above. The diagrams X, Y and Z are given in figures 43, 44 and 45.

While the liquidus temperature increased steadily with basicity, the change was not nearly as drastic as in other series reported later. Viscosity was reduced as the basicity was raised as shown by curves B and C in figure 45. Curve D in the same figure is the 0,1 Ns/m^2 isokom, showing the same trend as curves B and C. The points for $E\eta$ (curve E) do not reveal any recognizable tendency. This is thought to be due to the relative unreliability of the figure for slag A2, the temperature range of which was comparatively small.

(b) The series B16-B13-B10 (figures 46, 47 and 48)

The basicity ratios were the same as those for the slags of the A series. However, (TiO_2 + Al_2O_3) was increased from 36 to 44 mass % and the CaO/MgO ratio was 2,0

Liquidus temperature was at first slightly lowered with increase in basicity. This was accompanied by a change of primary phase from M.A.T. to perovskite. The initial decrease was followed by a rapid rise. The summarizing diagram (figure 48) again suggests a continuous drop in viscosity at 50°C above the liquidus temperature. At 1550°C this trend is shown only over the relatively large basicity interval between B16 and B13 (0,8 and 1,4 respectively), but not over the smaller interval between B13 and B10 (basicities 1,4 and 1,7 respectively. However, the curve for $E\eta$ (E) shows a drastic decrease over the smaller interval, so that this curve resembles curve B in shape. This tendency may be associated with the sharp rise in liquidus temperature as the basicity is increased from 1,4 to 1,7.

It further appears to be significant that the 0,07 Ns/m^2 isokom (curve D) resembles curve C (for viscosity at 1550°C) in shape.

(c) The series B17-B14-B11 and the effect of small changes in basicity between 1,3 and 1,7

The series B17-B14-B11 correspond to B16-B13-B10 in every respect, except that the CaO/MgO ratio of the former is 1,0. If these three slags at large basicity intervals are considered by themselves, figures 49 and 50 and the summarizing diagram (figure 52) show practically the same trends as those outlined for the more lime-rich series in (b). There is again a liquidus temperature minimum associated with the slag of intermediate basicity (B14), a continuous decrease in viscosity at (liquidus temperature + 50°) and a relatively large decrease in viscosity at 1550°C only initially, with basicity.

For the reasons outlined in section 4.1.1, the additional series of slags, possessing the same parameters of composition as the series B17-B14-B11, but differing from one another only slightly in basicity ratio, were incorporated in this investigation. Basicity was varied from 1,3 (B28) to 1,7 (B11) in steps of 0,05. Slag B14 (basicity 1,4) was consequently included in this series. Their viscosities are shown as functions of temperature in figure 51.

The region of low liquidus temperature existing over the basicity range 1,35 to 1,60 was already pointed out in section 4.1.1. Figure 52 (curve A) again shows the phenomenon and also seems to indicate the relative non-validity of postulating smooth variation of liquidus temperature with basicity in the series B16-B13-B10. However, figure 52 also shows the continuous increase in viscosity at (liquidus temperature + 50°) (curve B), and the small variation in viscosity at 1550°C (curve C) and E_η (curve D) over the basicity range 1,3 to 1,7 that would be indicated by a summarizing diagram dealing only with B17, B14 and B11.

(d) The series B18-B15-B12 (figures 53, 54, and 55)

This magnesia-rich slag sequence (CaO/MgO = 0,5) again has basicity ratios equal to those of the corresponding members of the series B16-B13-B10 and B17-B14-B11.

The general effect of an increase in basicity on the various measures

of viscosity remains the same. The liquidus temperature (curve A, figure 55) is generally high and shows little variation. This probably makes the viscosity at 50° above the liquidus temperature a more reliable parameter. It is remarkable that in this instance, the increase in basicity from 1,4 to 1,7 causes relatively large reductions in viscosity (curves B and C) and in $E\eta$ (curve D). Viscosity at 1550°C also gives a more reliable assessment of the effect of basicity. In the previous two series, 1550° represented a greater degree of superheating in the case of the slag of intermediate basicity 1,4 (B13 and B14) since these slags lie in a low liquidus temperature region.

4.1.2.2 The effect of mass % CaO/MgO ratio upon viscosity

As the viscosity-temperature relationships of slags used to illustrate the effect of CaO/MgO ratio have already been reported, only summarizing diagrams are given here. All these slags belong to series B with $(TiO_2 + Al_2O_3) = 44$ %. The influence of CaO/MgO ratio could thus be assessed at different basicity ratios.

(a) The series B10-B11-B12 : $(CaO + MgO)/SiO_2 = 1,7$

Figure 56 a shows that a decrease in CaO/MgO ratio from 2 to $\frac{1}{2}$ causes very little change in liquidus temperature. It may consequently be expected that viscosity at 50° above liquidus temperature and viscosity at 1550°will vary in a similar manner. Curves B and C show that this is in fact the case. The apparent maximum in either of these two curves, occurring at CaO/MgO = 1, is thought to be a function more of the liquidus temperature, even though the variation in the latter is small, than of composition.

(b) The series B13-B14-B15 : $(CaO + MgO)/SiO_2 = 1,4$

Curve A (figure 56 b) relates liquidus temperature to CaO/MgO ratio. A very sharp increase occurs as the CaO/MgO ratio is reduced from 1 to $\frac{1}{2}$. Again viscosity at 50° above liquidus (curve B) follows an approximately reversed trend, although a smaller value would be expected for B15. Curve C (viscosity at 1550°C) rises gradually as the

CaO/MgO ratio is reduced and the increase over the range 1,0 to 0,5 at least, must be attributed to to the sharp rise in liquidus temperature over this region.

(c) The series B16-B17-B18 : $(CaO + MgO)/SiO_2 = 0,8$

Figure 57 shows a gradual rise in liquidus temperature with decrease in CaO/MgO (curve A). Curve B (viscosity at liquidus temperature + 50°) drops rather abruptly over the CaO/MgO range from 1,0 to 0,5 and curve C (viscosity at 1550°C) shows a decrease over this region, in spite of the increased liquidus temperature. This appears to indicate that at this high silica level, the composition variable CaO/MgO is becoming more important in the distortion of the network, relative to temperature.

It may also be significant that at higher levels of CaO/MgO, an increase in this ratio is always accompanied by an increase in $E\eta$. This also applies to the series B10-B11-B12 and B13-B14-B15.

4.1.2.3 The effect of mass % $(TiO_2 + Al_2O_3)$ content upon viscosity

The single series of slags to illustrate this effect include A5 (36 %), B14 (44 %) and C23 (54 %). The $CaO/MgO/SiO_2$ proportion had a constant value of 0,7/0,7/1. The results are reported graphically in figures 58, 59 and 60.

The last two diagrams show a liquidus temperature minimum in the vicinity of the intermediate level of $(TiO_2 + Al_2O_3)$, represented by slag B14. Curve B (figure 60) again illustrates the apparent relation between viscosity at 50° above liquidus and a liquidus temperature profile as represented by the A-curve in figure 60 in this case, but also by that in figure 56 b.

The shape of the C-curve (figure 60) suggests a more or less continuous increase in $E\eta$ as $(TiO_2 + Al_2O_3)$ is increased. This effect of $(TiO_2 + Al_2O_3)$ resembles that of MgO as established for series B slags at different levels of basicity.

4.1.2.4 Comparison with other results

The effect of silica additions to increase the viscosity of titaniferous oxide systems is to be expected in the light of the strong network forming tendency exhibited by SiO_2. This trend was amply illustrated by examples from existing literature in section 2.2.

It appears to be generally agreed that replacement of lime by magnesia, on a molar basis, has no effect on the viscosity. This was illustrated by eg. Turkdogan and Bills[87] in their critical review of the viscosity of $CaO-MgO-Al_2O_3-SiO_2$ melts. It may therefore be reasonably expected that a decreasing mass % ratio CaO/MgO at constant basicity will lower the viscosity. Unless very high degrees of superheating are used in conducting the experiments, the fact that MgO so frequently tends to raise the liquidus temperature of the slag will mask its effect on viscosity.

In his study of the $CaO-MgO-SiO_2-TiO_2-Al_2O_3$ system, Freidenzon[22] found that addition of MgO caused a decrease in viscosity. This is essentially the same effect as what would be obtained from a decrease in the CaO/MgO ratio at "constant basicity" - that of effectively making the slag more basic. The same author did mention that such MgO addition did not cause an appreciable increase in viscosity even when the liquidus temperature is substantially increased.

McRae[23], working on the same overall system, found that replacement of CaO by MgO did in fact cause a slight drop in viscosity at constant temperature, if concentrations were expressed as mass per cent. If viscosity was measured at constant temperature above liquidus, high fluidity appeared to be associated with high liquidus temperature (figure 15). This conclusion is in general agreement with the results illustrated in figures 56 and 57.

Kato and Minowa[70] found that additions of MgO to a base slag containing CaO, SiO_2 and Al_2O_3, caused an increase in E_η. This also appears to be the general tendency shown in figures 56 and 57.

Many examples of the effect of TiO_2 as one of lowering the viscosity of oxide melts, were given in section 2.2. It will not be attempted to draw

any conclusions regarding the effect of TiO_2 from the results of this work, which involved only very limited variation in TiO_2 concentration. Moreover, the variation was accompanied by simultaneous change in alumina content. It may be significant that increased (TiO_2 + Al_2O_3) contents caused an increase in E_η. A similar effect was reported by Kato and Minowa[70] for low titania additions to a $CaO-SiO_2-Al_2O_3$ slag.

It was pointed out in the previous section that for variation in (TiO_2 +Al_2O_3) level, there appears to be a relationship between liquidus temperature and the value of viscosity at 50° above liquidus. This trend was similar to what was observed for replacement of lime by magnesia. It was virtually absent on those diagrams which showed the effect of silica content upon viscosity. If it is assumed that a plot of viscosity at 50° above liquidus temperature will only reveal the true effect of composition upon viscosity if this effect is a very marked one, or if the variation in liquidus temperature is small, the following conclusions must be drawn from the present work:

(a) The variation of basicity is the most important single parameter influencing viscosity;
(b) The effect of a decreasing CaO/MgO ratio only becomes significant at low basicity.

Viscosimetric data on slags of approximately the same composition as those investigated here, could not be found in the literature. However, table 17 does provide some comparison of absolute values obtained for slag C23 and those reported by McRae[23] for his slags 11C 14M and 18C 12M. The compositions of the slags are given in table 18.

Table 17 Absolute viscosimetric values for slags with TiO_2 contents 37 - 40 %.

Slag No.	Liquidus temp(°C)	$\eta_{(liquidus+50°)}$ ($Ns/m^2 \times 10^3$)	$\eta_{(1500)}$ ($Ns/m^2 \times 10^3$)	E_η (kJ/mol)
C23	1473	83	80	158
11C14M	1430	70	60	108
18C12M	1340	101	65	139

Table 18 Compositions of slags referred to in table 17

Slag No.	Mass per cent concentrations				
	TiO_2	Al_2O_3	CaO	MgO	SiO_2
C23	37,18	16,82	13,405	13,405	19,19
11C14M	39,84	14,02	11,00	14,00	21,10
18C12M	37,19	13,12	18,00	12,00	19,69

4.1.3 Electrical resistivities of unreduced slags

Although the composition variables used here, were the same as for viscosity measurements, the number of slags was limited to one series per variable. All series incorporated the composition B14 which was of most immediate interest to the Highveld Steel and Vanadium Corporation at the time when the research was undertaken. Moreover, viscosity determinations revealed that little additional information was to be gained from assessing the effect of basicity at CaO/MgO ratios either higher or lower than 1,0 (for B11-B14-B17). Similarly, the effect of variation of CaO/MgO ratio at constant basicity was expected to be illustrated adequately by using only one basicity ratio. (1,4)

The results for any particular series are again presented on three successive diagrams:

(X) Resistivity against temperature;

(Y) $\log_e$(resistivity) against the reciprocal of the absolute temperature. As $\log_e \rho = \log_e(A_k)^{-1} + E_k/R \cdot (T)^{-1}$, this plot would give the value of activation energy for conduction (E_k), as the product of the slope of the line and the gas constant R. It would also provide an additional approximate value of the liquidus temperature. These values are shown next to the points of inflection on the diagrams.

(Z) A summarizing plot incorporating the following properties as functions of composition:

A. Liquidus temperature;

B. Resistivity at (liquidus temperature + 50°C);

C. Resistivity at a constant temperature (1500° or 1550°C);

D. The activation energy for conduction (E_k).

4.1.3.1 Influence of basicity on resistivity

The series B11-B14-B17 was used to illustrate this effect (figures 61, 62 and 63). The main features of composition are given on the diagrams.

The resistivity at 50°C above liquidus temperature decreases drastically as basicity is increased. Resistivity at 1500°C does however show the effect of the high liquidus temperature associated with the slag of highest basicity in the series (B11). The activation energy for conduction (E_k) is reduced by an increase in basicity.

4.1.3.2 Influence of CaO/MgO ratio on resistivity

The slags B13, B14 and B15 have CaO/MgO ratios 2, 1 and 0,5 respectively (figures 64, 65 and 66). Variation in resistivity at constant temperature above liquidus is not very drastic, but it does show a decrease as the ratio is lowered. The plot of resistivity at 1550°C (curve C in figure 66) again shows the effect of the high liquidus temperature of slag B15 with CaO/MgO = 0,5. The variation in E_k (curve D, figure 66) is too small to be truly significant.

4.1.3.3 Influence of (TiO_2 + Al_2O_3) content on resistivity

This is shown in the usual order in figures 67, 68 and 69 for slags A5, B14 and C23, having (TiO_2 + Al_2O_3) concentrations 36 %, 44 % and 54 % respectively. Although the liquidus temperature of C23 is considerably higher than those of the other two slags in the series, curve B (figure 69) shows a continuous decrease and curve C (resistivity at 1500°C) indicates that liquidus temperature is by no means the only variable exerting a pronounced effect on the resistivity. The activation energy for conduction (E_k) increases as the (TiO_2 + Al_2O_3) level is raised.

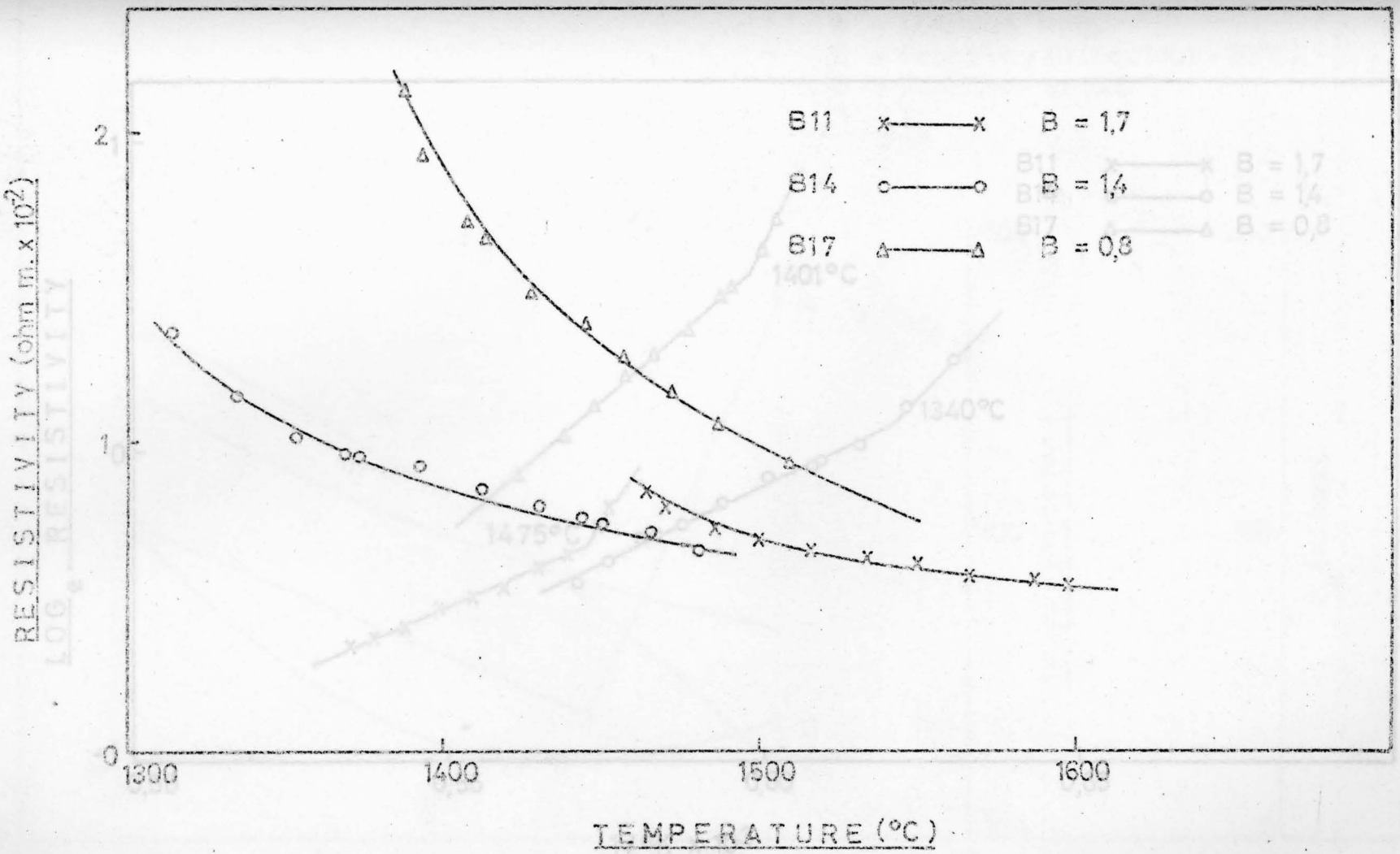


Figure 61 The effect of Basicity on Resistivity for (TiO_2 + Al_2O_3) = 44%, CaO/MgO = 1

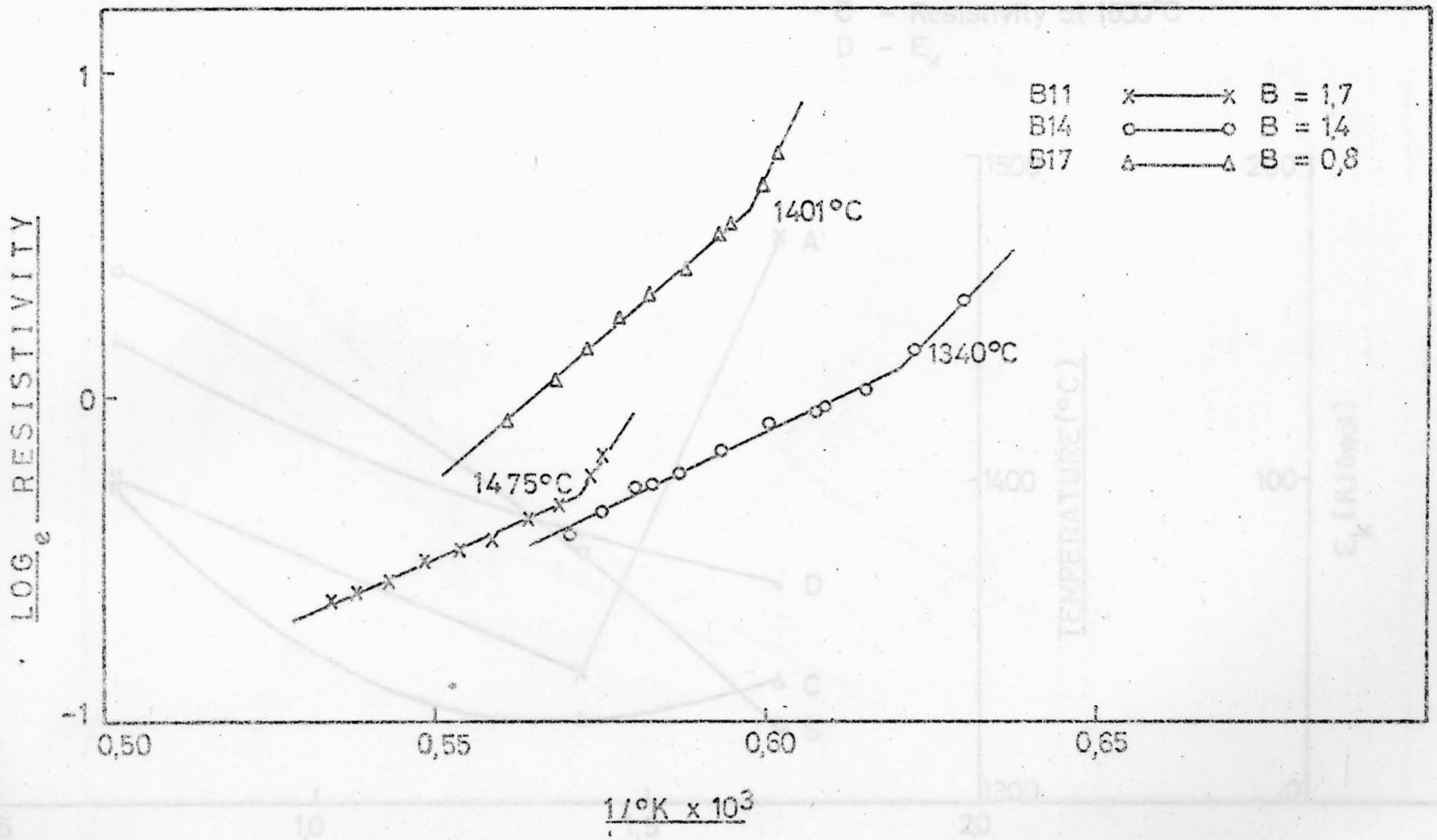


Figure 62 The effect of Basicity on Resistivity for (TiO_2 + Al_2O_3) = 44%, CaO/MgO = 1

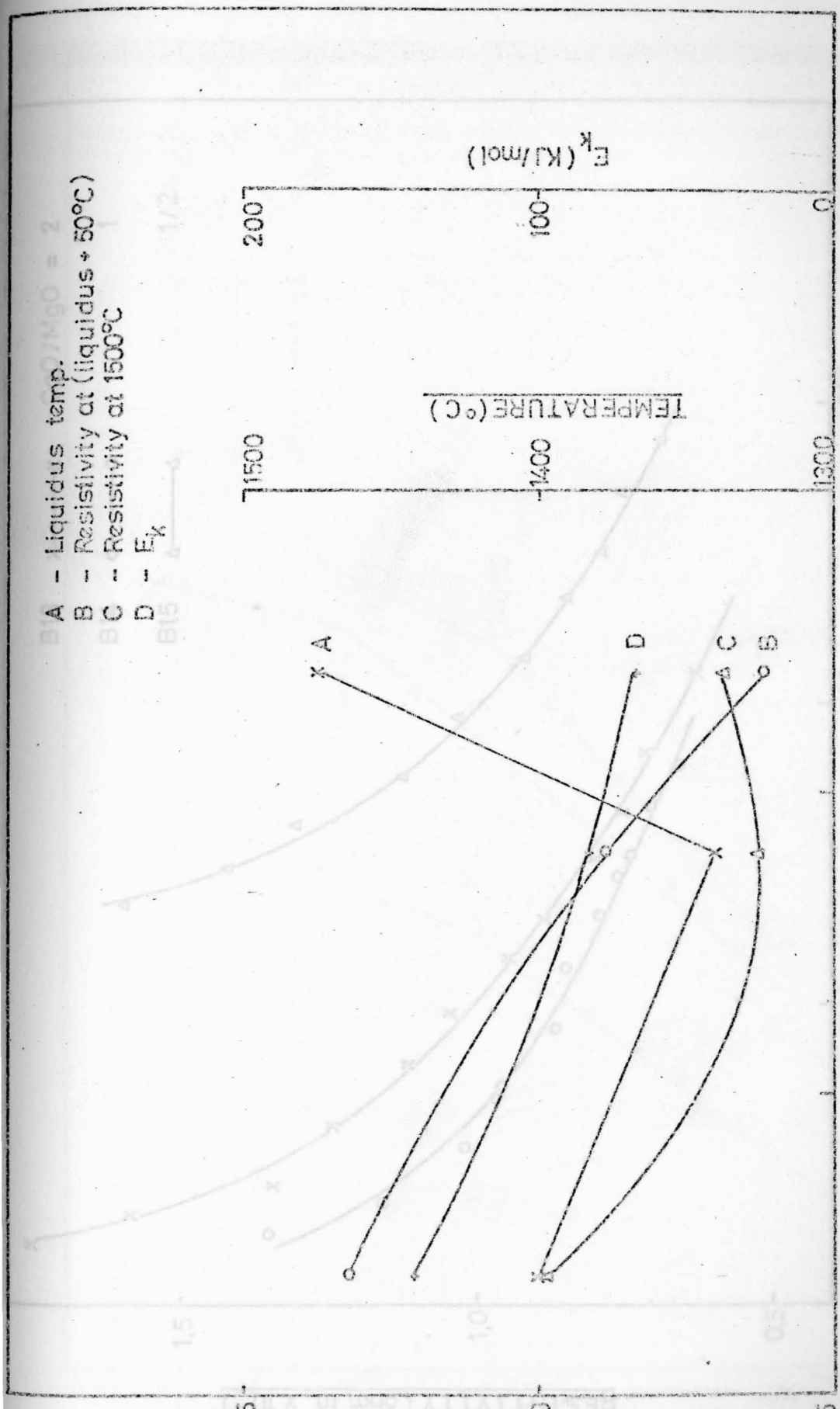


Figure 63 The effect of Basicity on Resistivity for (TiO_2 + Al_2O_3) = 44%, CaO/MgO = 1 - Summary

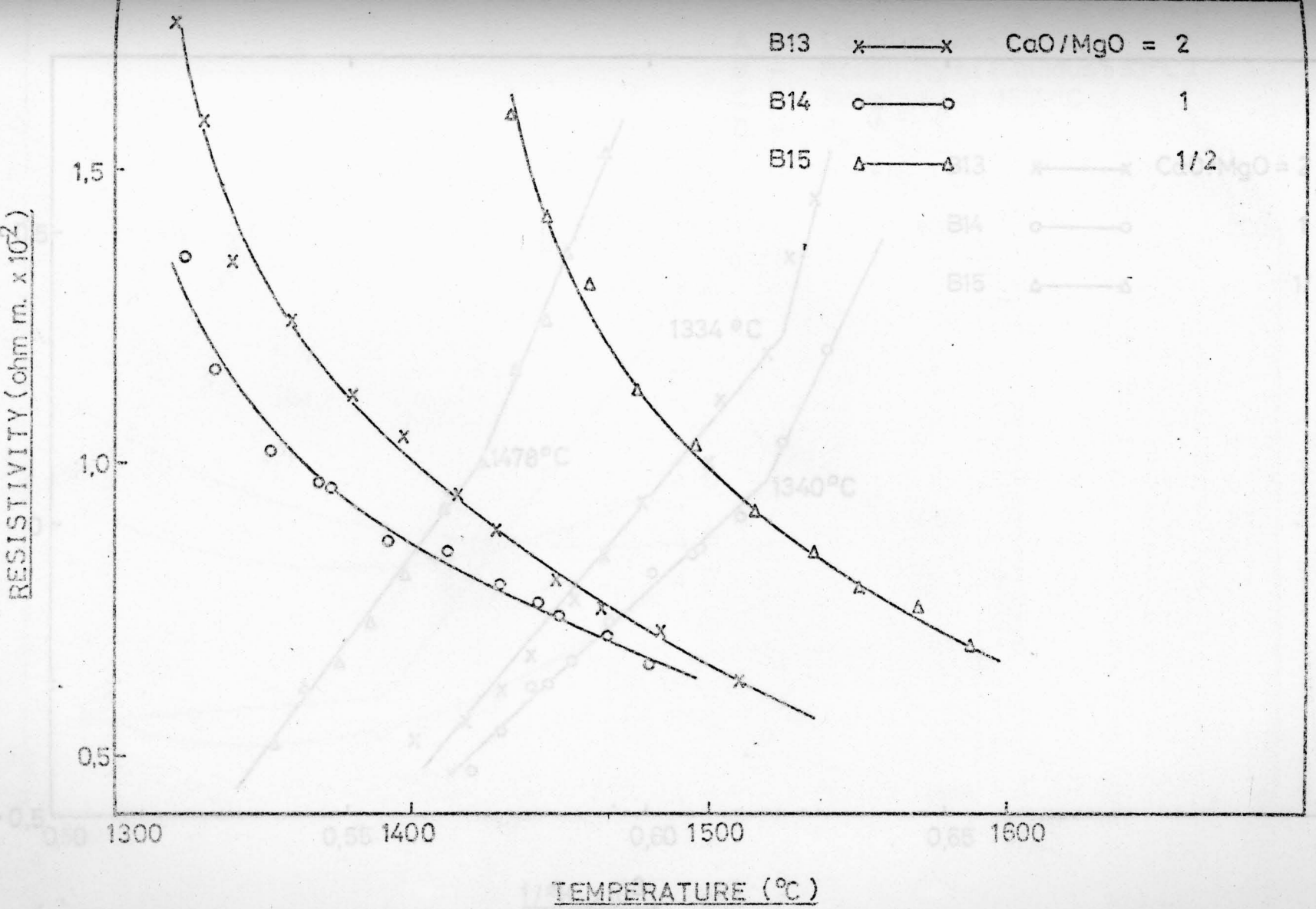


Figure 64 The effect of CaO/MgO ratio on Resistivity for (TiO_2 + Al_2O_3) = 44%, (CaO + MgO)/SiO_2 = 1,4

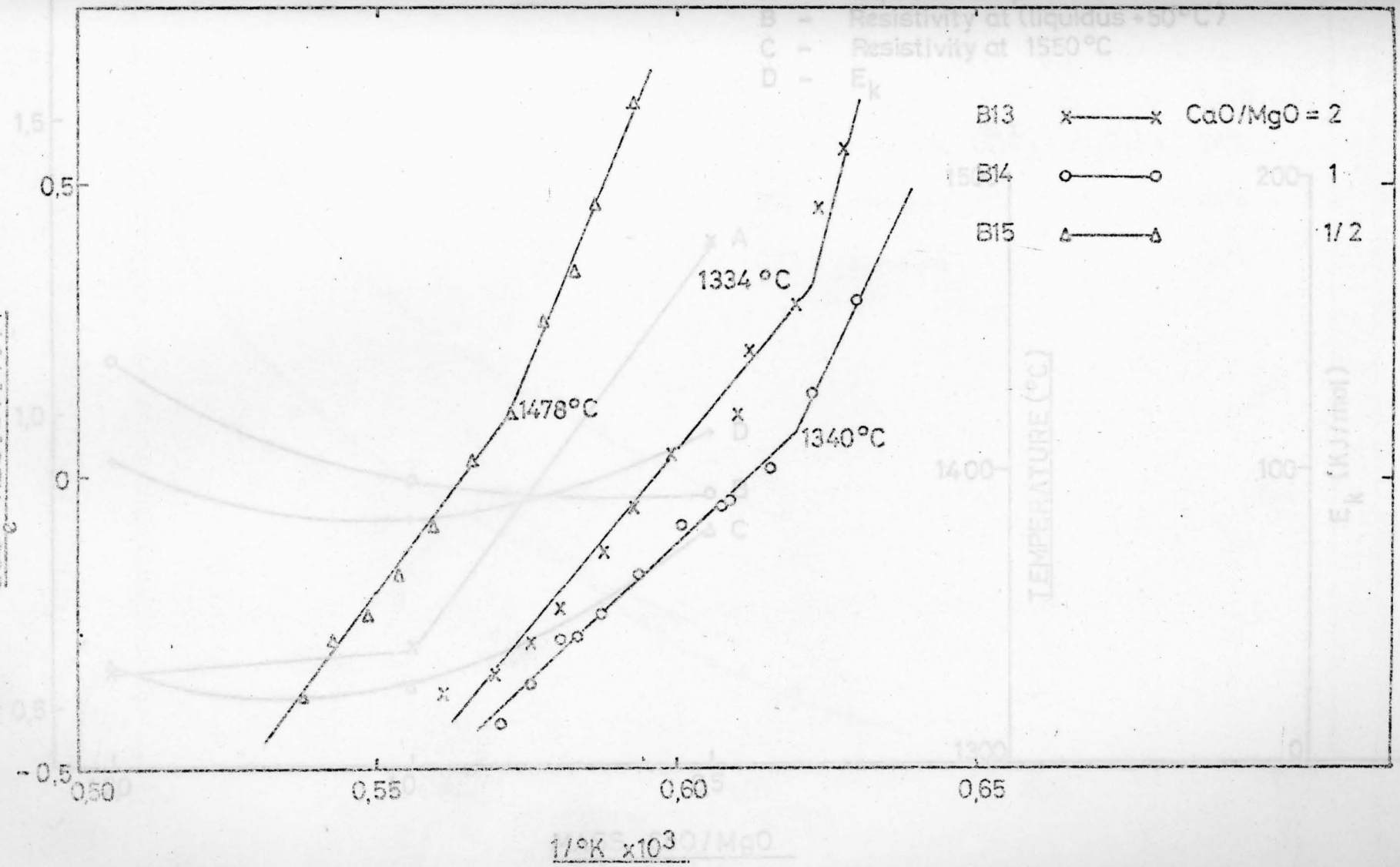


Figure 65 The effect of CaO/MgO ratio on Resistivity for (TiO_2 + Al_2O_3) = 44%, (CaO+MgO)/SiO_2 = 1,4

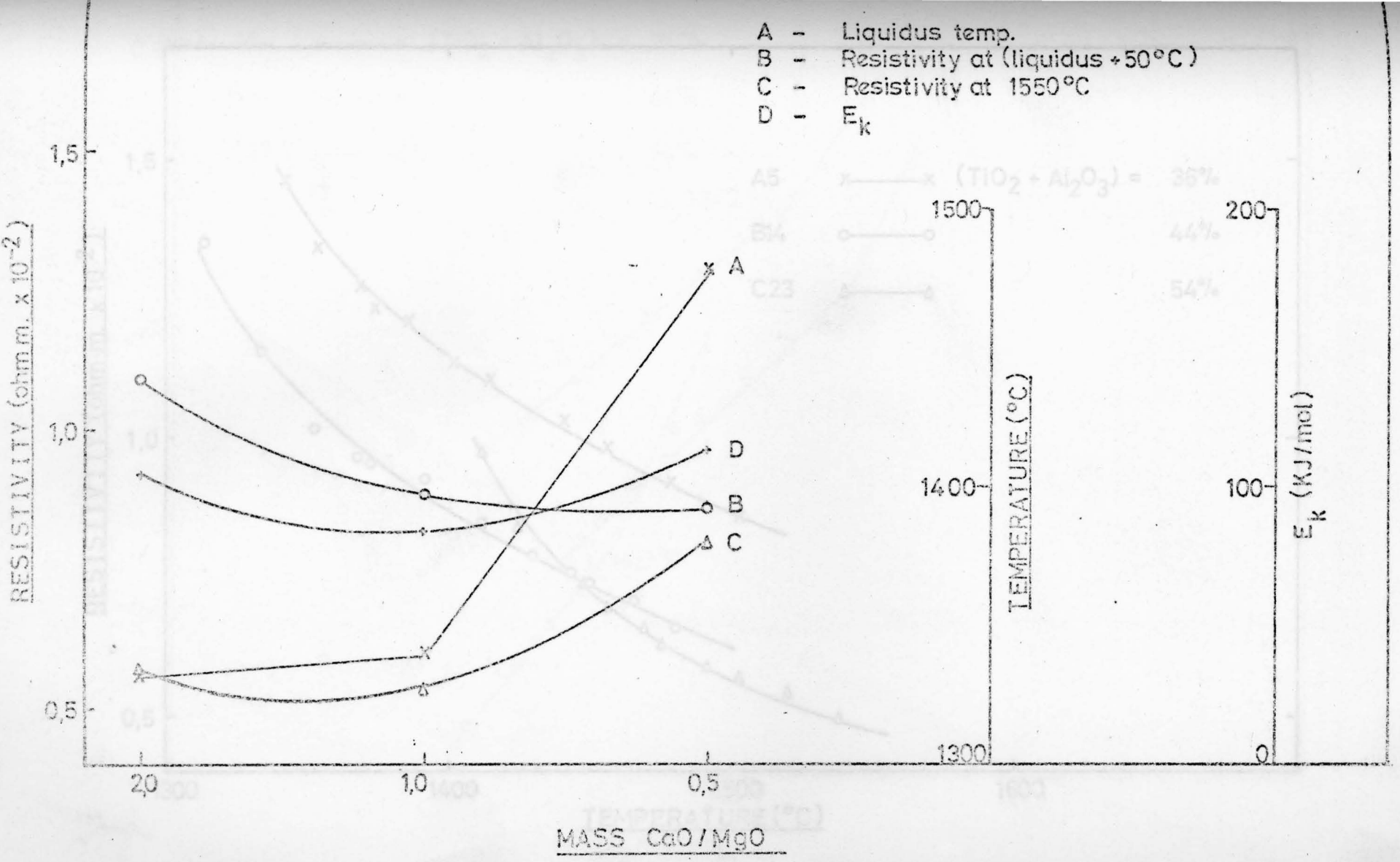


Figure 66 The effect of CaO/MgO ratio on Resistivity for $(TiO_2+Al_2O_3)$=44%, $(CaO+MgO)/SiO_2$ = 1,4 - Summary

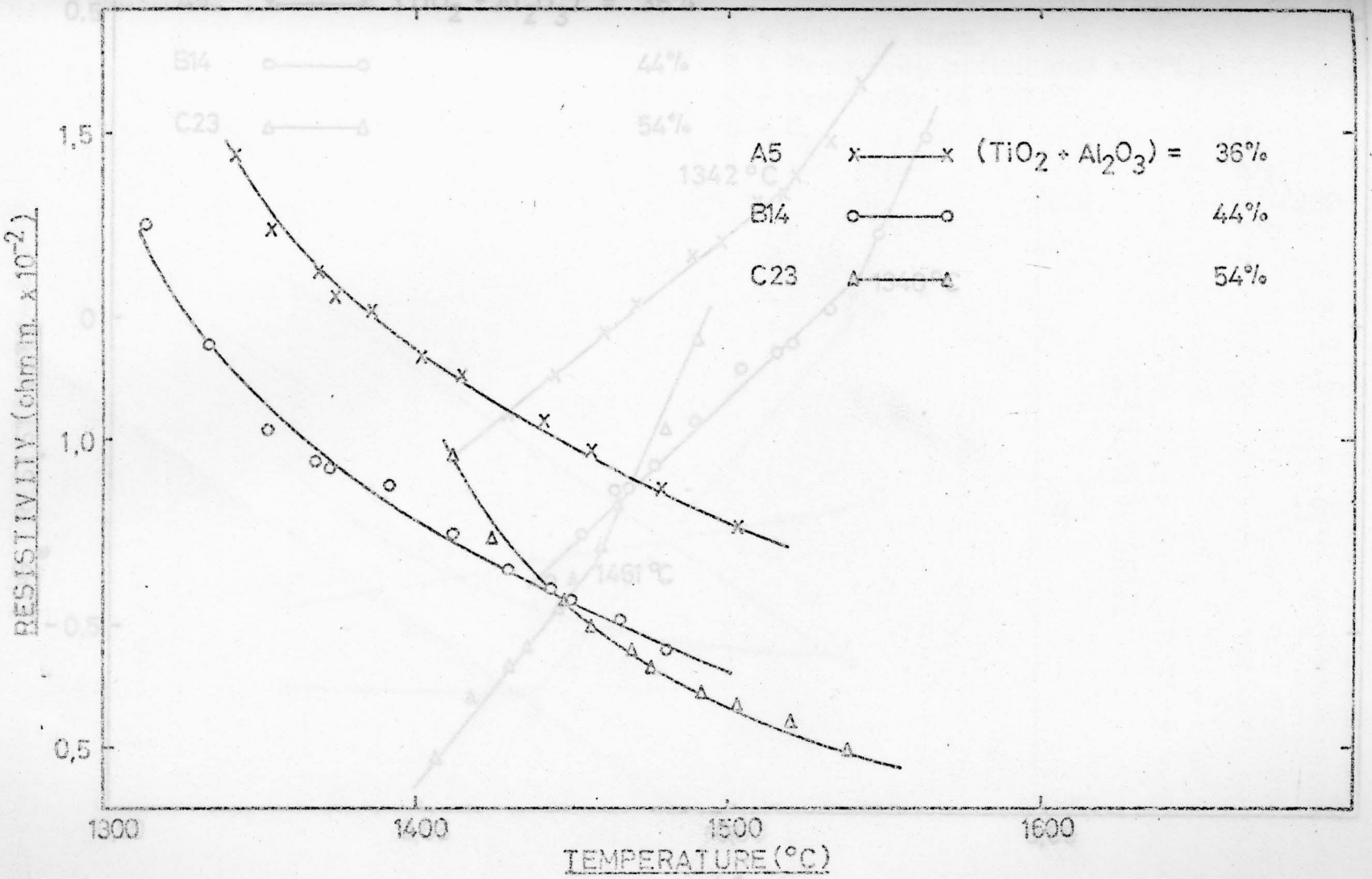


Figure 67 The effect of $(TiO_2+Al_2O_3)$ content on Resistivity at $CaO/MgO/SiO_2$ = 0,7/0,7/1

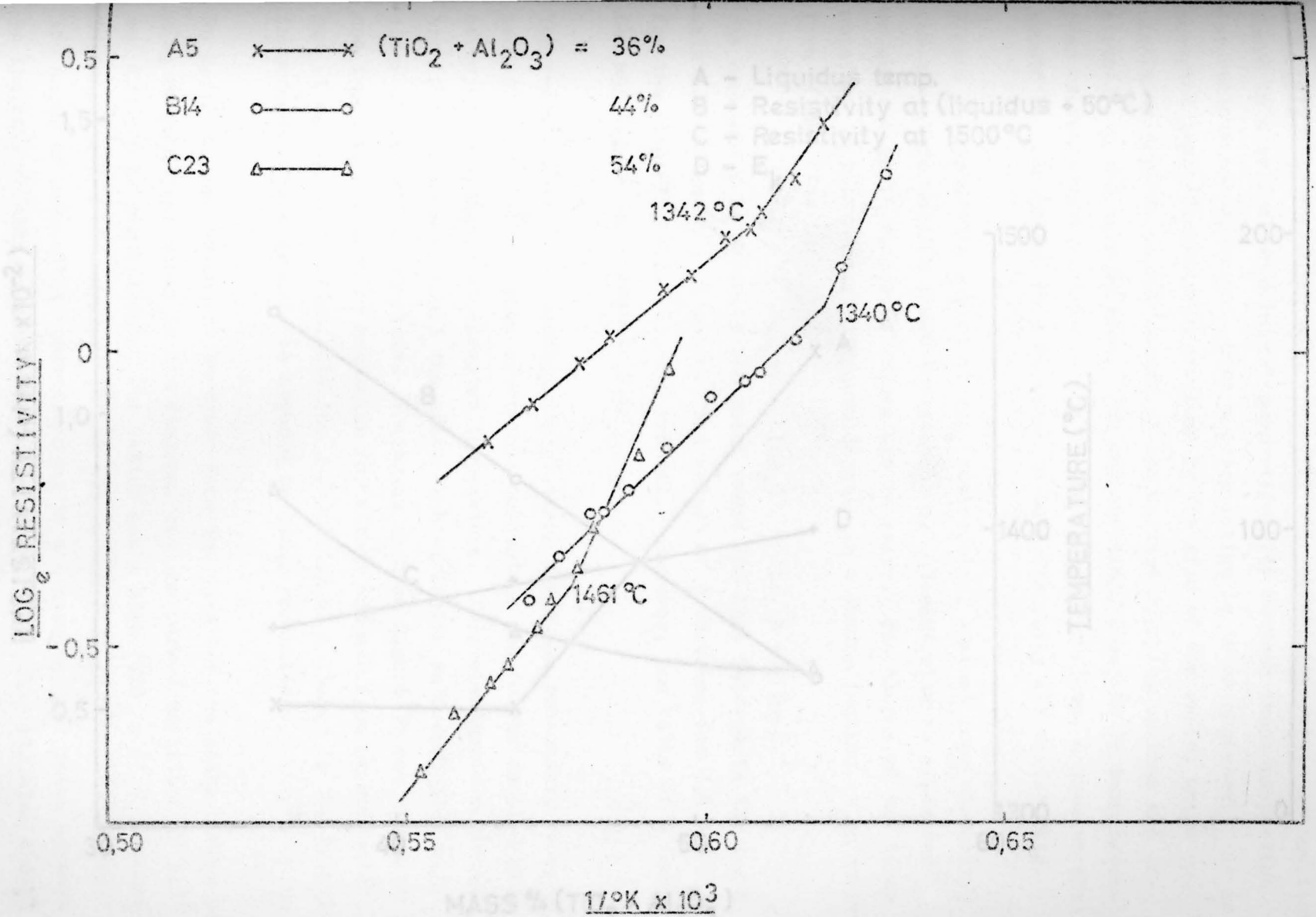


Figure 68 The effect of (TiO_2+Al_2O_3) content on Resistivity at CaO/MgO/SiO_2 = 0,7/0,7/1

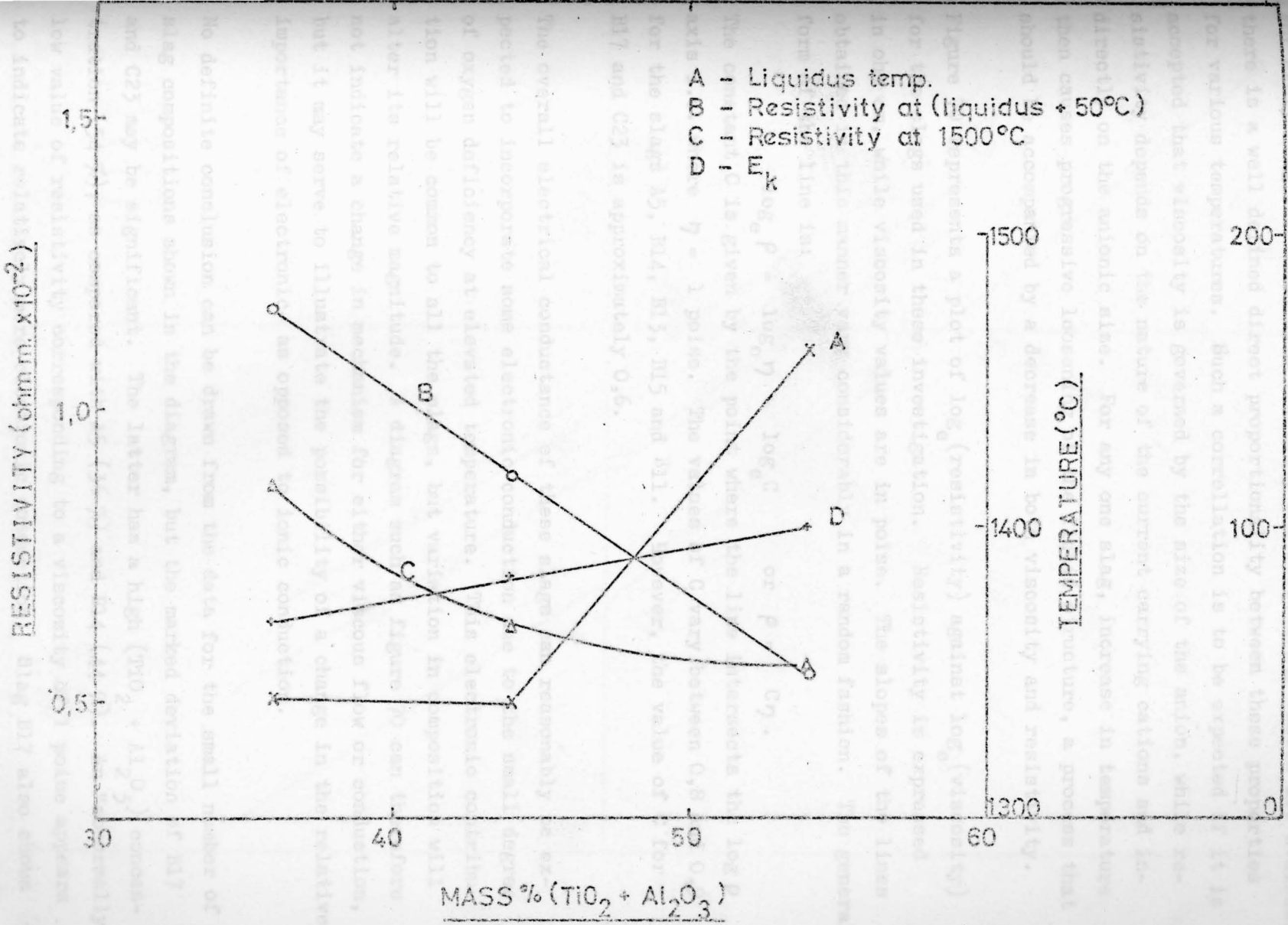


Figure 69 The effect of (TiO_2+Al_2O_3) content on Resistivity at CaO/MgO/SiO_2 = 0,7/0,7/1 - Summary

4.1.4 Relation between viscosity and resistivity

For every slag for which both viscosity and resistivity values are available, there is a well defined direct proportionality between these properties for various temperatures. Such a correllation is to be expected if it is accepted that viscosity is governed by the size of the anion, while resistivity depends on the nature of the current carrying cations and indirectly on the anionic size. For any one slag, increase in temperature then causes progressive loosening of the liquid structure, a process that should be accompanied by a decrease in both viscosity and resistivity.

Figure 70 represents a plot of $\log_e$(resistivity) against $\log_e$(viscosity) for the slags used in these investigation. Resistivity is expressed in ohm cm, while viscosity values are in poise. The slopes of the lines obtained in this manner vary considerably in a random fashion. The general form of the line is:

$$\log_e \rho = \log_e \eta + \log_e C \qquad \text{or} \qquad \rho = C\eta .$$

The constant C is given by the point where the line intersects the $\log \rho$ axis i.e. where η = 1 poise. The values of C vary between 0,8 and 0,9 for the slags A5, B14, B13, B15 and B11. However, the value of C for B17 and C23 is approximately 0,6.

The overall electrical conductance of these slags can reasonably be expected to incorporate some electronic conduction due to the small degree of oxygen deficiency at elevated temperature. This electronic contribution will be common to all the slags, but variation in composition will alter its relative magnitude. A diagram such as figure 70 can therefore not indicate a change in mechanism for either viscous flow or conduction, but it may serve to illustrate the possibility of a change in the relative importance of electronic- as opposed to ionic conduction.

No definite conclusion can be drawn from the data for the small number of slag compositions shown in the diagram, but the marked deviation of B17 and C23 may be significant. The latter has a high (TiO_2 + Al_2O_3) concentration (54 %), as compared with A5 (36 %) and B14 (44 %). An "abnormally" low value of resistivity corresponding to a viscosity of 1 poise appears to indicate relatively more electronic conduction. Slag B17 also shows appreciably lower resistivity than would be expected from its high silica content of 31,1 %, as compared with 20,75 % of B11 and 23,33 % of B14

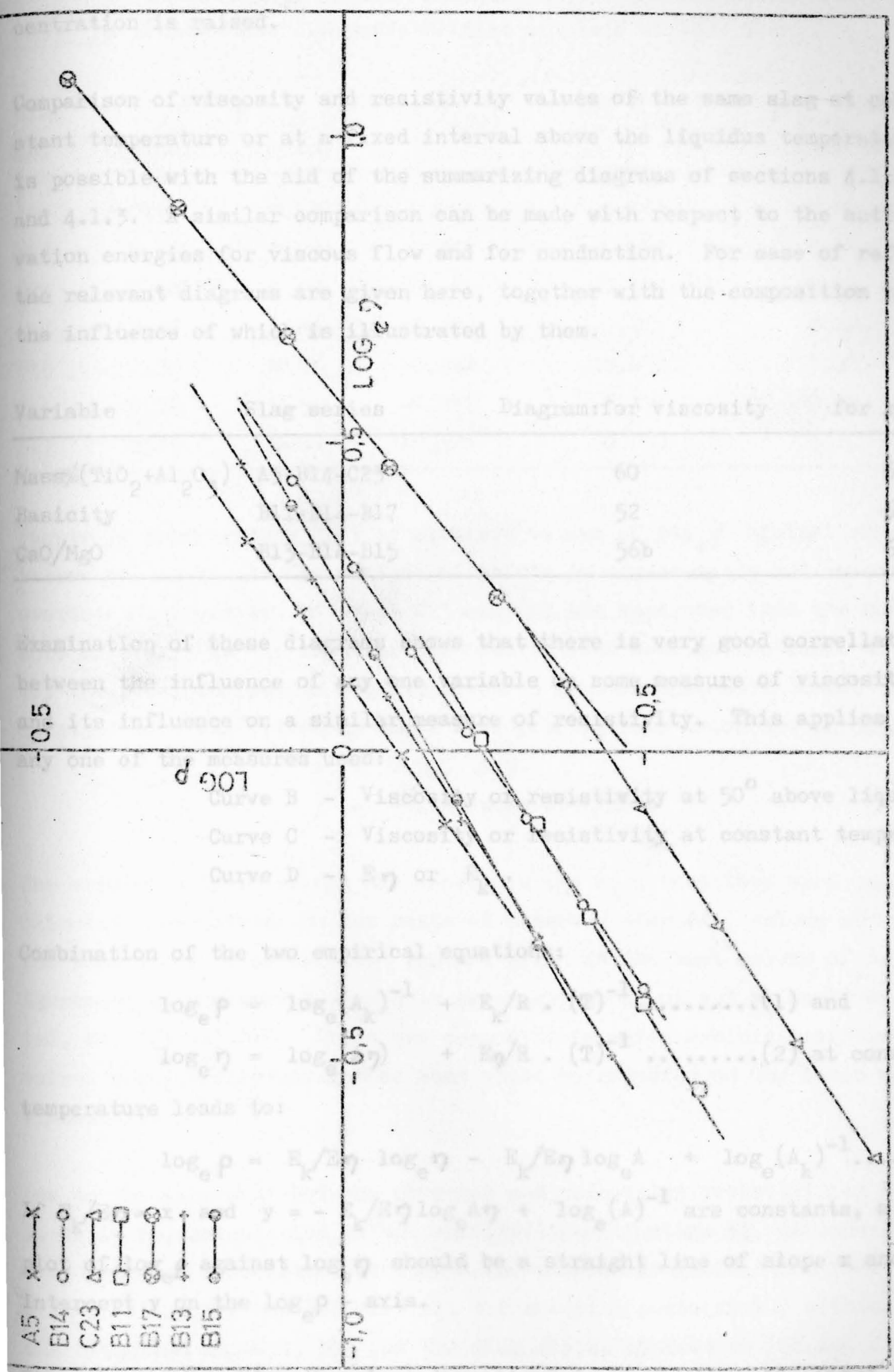


Figure 70 Relation between Viscosity (η) and Resistivity (ρ) of the same slag.

This again seems to show that electronic conduction tends to become increasingly important, relative to ionic conduction, as the silica concentration is raised.

Comparison of viscosity and resistivity values of the same slag at constant temperature or at a fixed interval above the liquidus temperature, is possible with the aid of the summarizing diagrams of sections 4.1.2 and 4.1.3. A similar comparison can be made with respect to the activation energies for viscous flow and for conduction. For ease of reference the relevant diagrams are given here, together with the composition variable the influence of which is illustrated by them.

Variable	Slag series	Diagram: for viscosity	for resistivity
Mass%(TiO_2+Al_2O_3)	A5-B14-C23	60	69
Basicity	B11-B14-B17	52	63
CaO/MgO	B13-B14-B15	56b	66

Examination of these diagrams shows that there is very good correllation between the influence of any one variable on some measure of viscosity and its influence on a similar measure of resistivity. This applies to any one of the measures used:

Curve B - Viscosity or resistivity at 50° above liquidus

Curve C - Viscosity or resistivity at constant temperature

Curve D - E_η or E_k .

Combination of the two empirical equations:

$$\log_e \rho = \log_e (A_k)^{-1} + E_k/R \,.\, (T)^{-1} \quad \ldots\ldots\ldots (1) \text{ and}$$

$$\log_e \eta = \log_e (A\eta) + E\eta/R \,.\, (T)^{-1} \quad \ldots\ldots\ldots (2) \text{ at constant}$$

temperature leads to:

$$\log_e \rho = E_k/E\eta \, \log_e \eta - E_k/E\eta \log_e A + \log_e (A_k)^{-1} \ldots\ldots (3)$$

If $E_k/E\eta = x$ and $y = - E_k/E\eta \log_e A\eta + \log_e (A)^{-1}$ are constants, a plot of $\log_e \rho$ against $\log_e \eta$ should be a straight line of slope x and intercept y on the $\log_e \rho$ - axis.

The relevant data for the slags investigated are shown in the first five

columns of table 19.

Table 19 Viscosities and resistivities of slags at 1500°C

Slag No.	η_{1500} (poise)	ρ_{1500} (ohm cm)	$\log_e \eta_{1500}$	$\log_e \rho_{1500}$	ρ_{1500}(calc) (ohm cm)
A5	0,91	0,87	-0,094	-0,139	0,80
B14	0,67	0,63	-0,400	-0,462	0,66
C23	0,80	0,56	-0,223	-0,579	0,73
B13	0,67	0,66	-0,400	-0,417	0,66
B15	1,38	0,97	+0,322	-0,030	1,05
B11	0,77	0,69	-0,261	-0,371	0,72
B17	1,75	0,99	+0,588	-0,010	1,22

Figure 71 represents a plot of observed values of $\log_e \rho$ against observed values of $\log_e \eta$. The scatter of points is considerable and cannot be overlooked. However, if slags C23 and B17 are separated from the main core of slags, in the light of the observations made on the basis of figure 70, the remaining points seem to reveal a more recognizable trend. A straight line was fitted to these five points, from which the values of

$$x = 0,65 \quad \text{and}$$

$$y = -0,16 \quad \text{were obtained.}$$

The errors in these values are uncertain and as a test they were used to calculate resistivity on the basis of observed viscosity values at 1500°C. The results of these calculations are given in the last column of table 19. Agreement with observed values is generally good, except as would be expected, for C23 and B17. These two compositions again exhibit resistivity values considerably lower than what would be expected on the basis of their viscosities.

Due to the agreement between observed and calculated resistivities shown in table 19, calculation of the resistivities of slags A2, B10 and B12 from observed viscosities at 1500°C was considered valid. The resistivities of slags B16 and B18 were not determined experimentally either, but the deviation shown by B17 (of the same silica content as B16 and B18), coupled with the small changes in resistivity or viscosity brought about

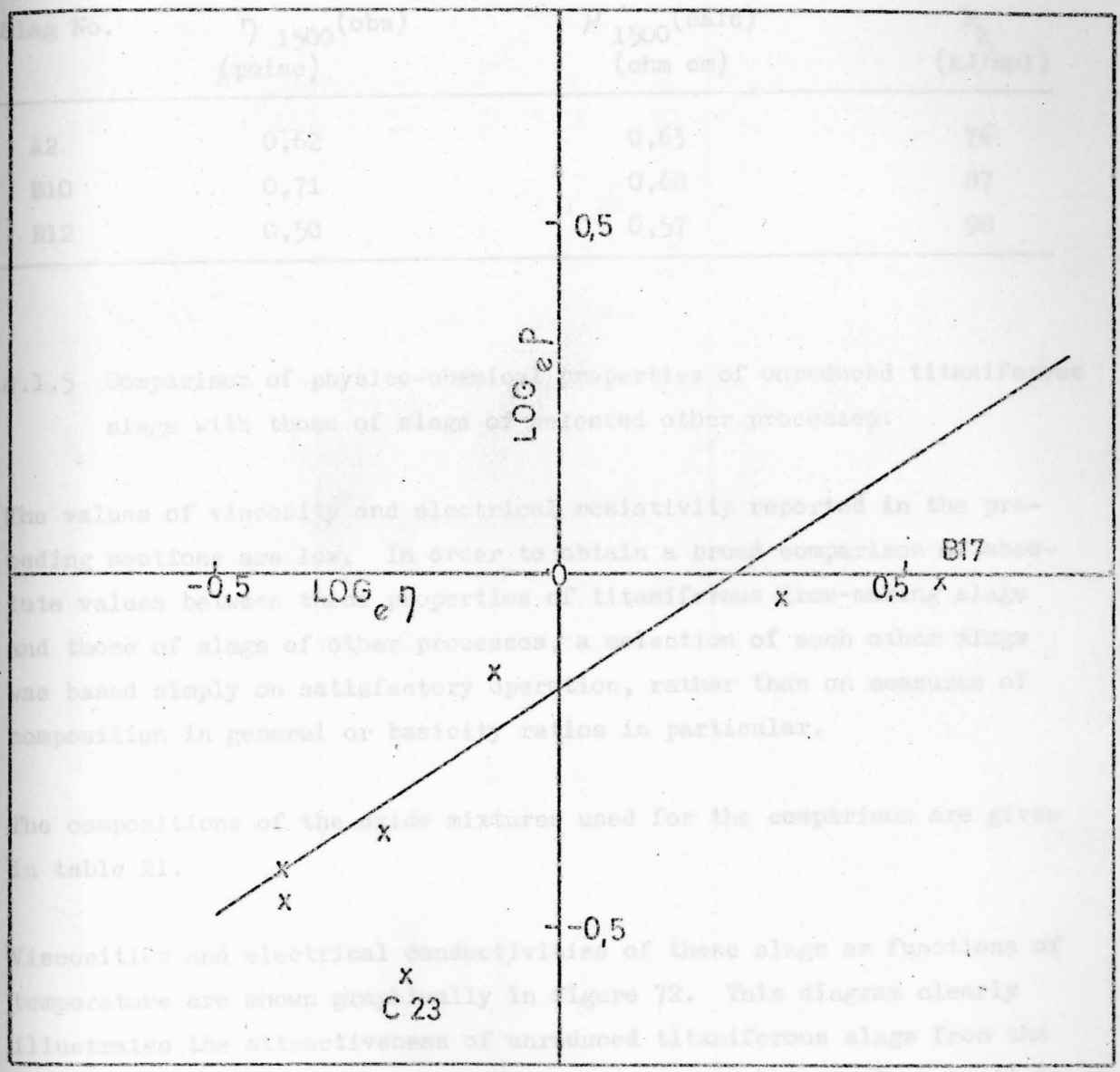


Figure 71 Relation between Viscosity (η) and Resistivity (ρ) at 1500°C

by a change in the CaO/MgO ratio at constant basicity, prevented calculation based on equation 3.

Table 20 Resistivities calculated from observed values of viscosity at 1500°

Slag No.	$\eta_{1500}^{(obs)}$ (poise)	$\rho_{1500}^{(calc)}$ (ohm cm)	E_k (kJ/mol)
A2	0,62	0,63	76
B10	0,71	0,68	87
B12	0,50	0,57	98

4.1.5 Comparison of physico-chemical properties of unreduced titaniferous slags with those of slags of selected other processes.

The values of viscosity and electrical resistivity reported in the preceding sections are low. In order to obtain a broad comparison of absolute values between these properties of titaniferous iron-making slags and those of slags of other processes, a selection of such other slags was based simply on satisfactory operation, rather than on measures of composition in general or basicity ratios in particular.

The compositions of the oxide mixtures used for the comparison are given in table 21.

Viscosities and electrical conductivities of these slags as functions of temperature are shown graphically in figure 72. This diagram clearly illustrates the attractiveness of unreduced titaniferous slags from the point of view of fluidity. At the same time, the electrical conductivity of these slags are relatively high and if this property is assumed to be an important factor in the dissipation of power in the submerged arc furnace, operations involving these slags must be expected to be difficult.

Table 21 Compositions of slags from different processes

Product	Furnace	Slag No.	Reference	Mass % Composition						
				TiO_2	Al_2O_3	SiO_2	CaO	MgO	FeO	Mn
Vanadium bearing pig iron	Arc furnace	B14	This work	30,2	13,8	23,33	16,34	16,34		
High C Fe-Mn	Arc furnace	X	88		16,75	26,65	23,65	13,91		19,
Cu-Ni matte	Arc furnace	Y	89		5.1	41,9	18,1	14,8	15,7	
Pig iron	Blast furnace	Z	90		20,0	35,0	35,0	10,0		

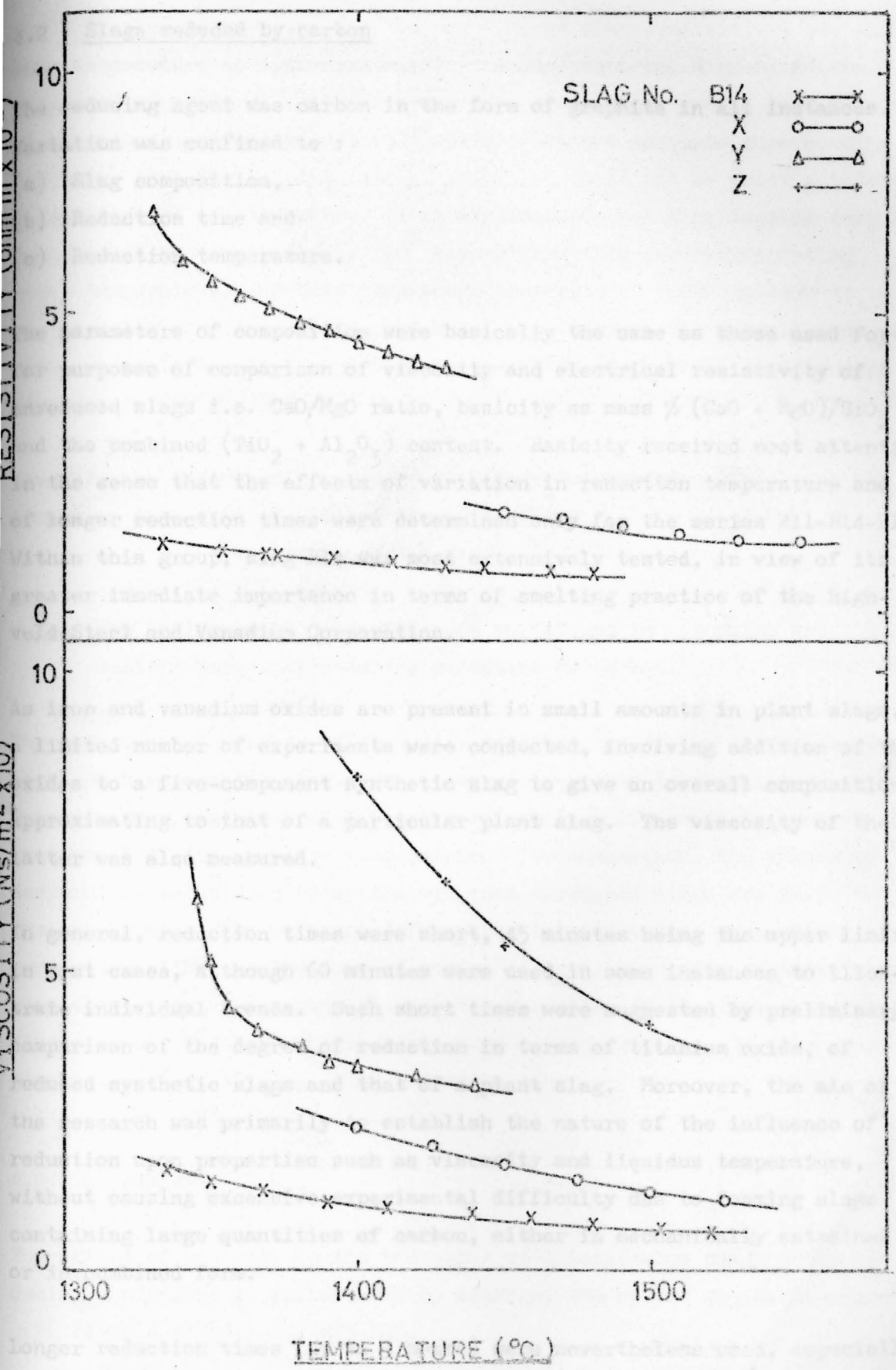


Figure 72 Comparison of physico-chemical properties of a titaniferous slag with those of other slags.

4.2 Slags reduced by carbon

The reducing agent was carbon in the form of graphite in all instances. Variation was confined to :

(a) Slag composition,

(b) Reduction time and

(c) Reduction temperature.

The parameters of composition were basically the same as those used for for purposes of comparison of viscosity and electrical resistivity of unreduced slags i.e. CaO/MgO ratio, basicity as mass % $(CaO + MgO)/SiO_2$ and the combined $(TiO_2 + Al_2O_3)$ content. Basicity received most attention in the sense that the effects of variation in reduction temperature and of longer reduction times were determined only for the series B11-B14-B17. Within this group, slag B14 was most extensively tested, in view of its greater immediate importance in terms of smelting practice of the Highveld Steel and Vanadium Corporation.

As iron and vanadium oxides are present in small amounts in plant slags, a limited number of experiments were conducted, involving addition of these oxides to a five-component synthetic slag to give an overall composition approximating to that of a particular plant slag. The viscosity of the latter was also measured.

In general, reduction times were short, 45 minutes being the upper limit in most cases, although 60 minutes were used in some instances to illustrate individual trends. Such short times were suggested by preliminary comparison of the degree of reduction in terms of titanium oxide, of reduced synthetic slags and that of a plant slag. Moreover, the aim of the research was primarily to establish the nature of the influence of reduction upon properties such as viscosity and liquidus temperature, without causing excessive experimental difficulty due to foaming slags containing large quantities of carbon, either in mechanically entrained or in combined form.

Longer reduction times (up to 3 hours) were nevertheless used, especially in the case of slag B14, in order to assess the ultimate order of change in slag properties, relative to the initial trends.

The reduction temperature for the majority of slag compositions was 1550°C. This temperature is approximately 100° higher than the highest initial liquidus temperature. As the activation energy for viscous flow of most of the slags are fairly low, 1550° would represent adequate superheating to ensure that the initial rate of reduction would not be greatly influenced by differences in viscosity. If it is accepted that slag tapping temperature should be approximately 100° higher than than the corresponding metal temperature, and that high metal temperatures (1400 to 1450°C) are normally associated with good metal chemistry during titaniferous iron ore smelting, then 1550°C also appears to represent a good average temperature for reduction.

However, the effects of lower and of higher temperatures (1500° and 1600°C) were also tested for a limited number of slags.

4.2.1 The influence of composition on variations in viscosity and melting temperature during reduction by carbon.

The experimental results of viscosity measurements of the reduced derivatives of a particular slag composition are reported graphically on separate diagrams, as plots of the natural logarithm of viscosity against the reciprocal of the absolute temperature. For comparison, the viscosity-temperature relationships of the original unreduced slags are given on the same graph. The relevant information for every slag composition is summarized either in the form of curves of equal viscosity on temperature-time charts, or as diagrams showing the variation in liquidus temperature, viscosity at 50° above the liquidus temperature or viscosity at a constant temperature (eg. 1550°C), with reduction time.

4.2.1.1 Basicity

The effect of basicity on the behaviour of titaniferous slags under reducing conditions is illustrated by means of the series A5-A8, B10-B13-B16, B11-B14-B17 and B12-B15-B18.

(a) The slag pair A5-A8

The behaviour of A5 is shown in figures 73 and 74 and that of A8 in figures 75 and 76. Figure 74 b shows that the melting temperature

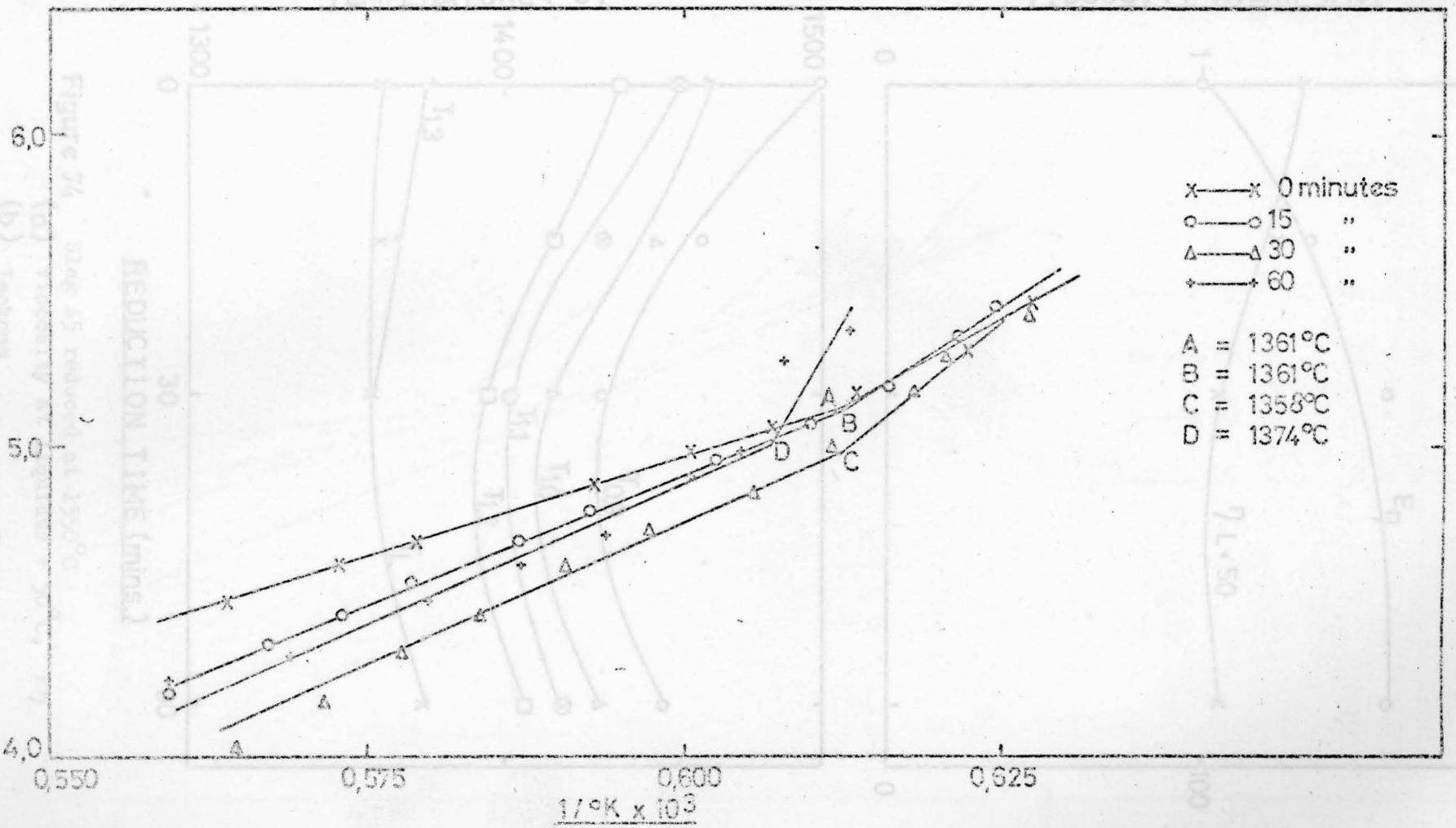


Figure 73 Viscosity of slag A5, reduced by carbon at 1550°C

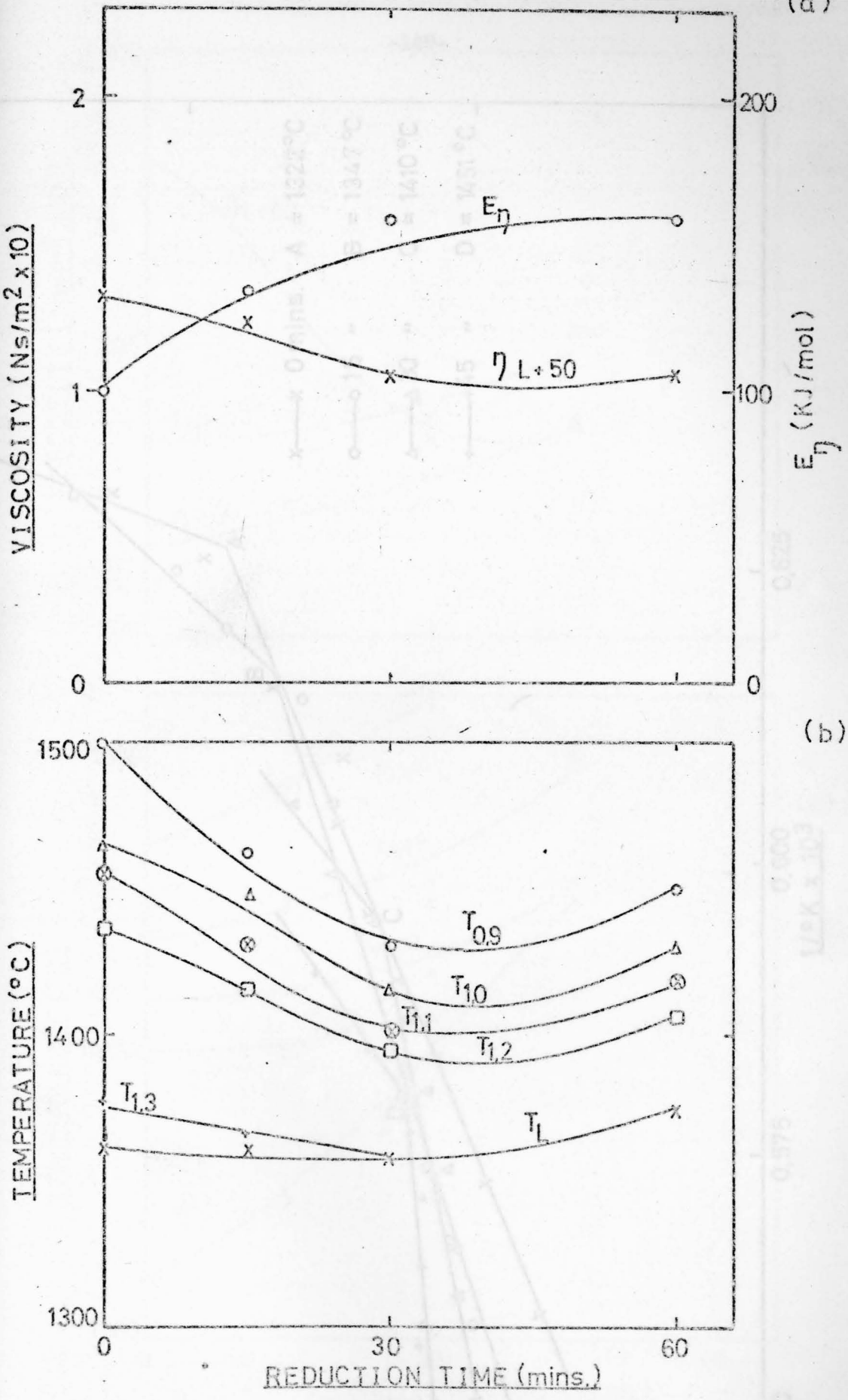


Figure 74 Slag A5 reduced at 1550°C
(a) Viscosity at liquidus + 50°C, E_η
(b) Isokoms

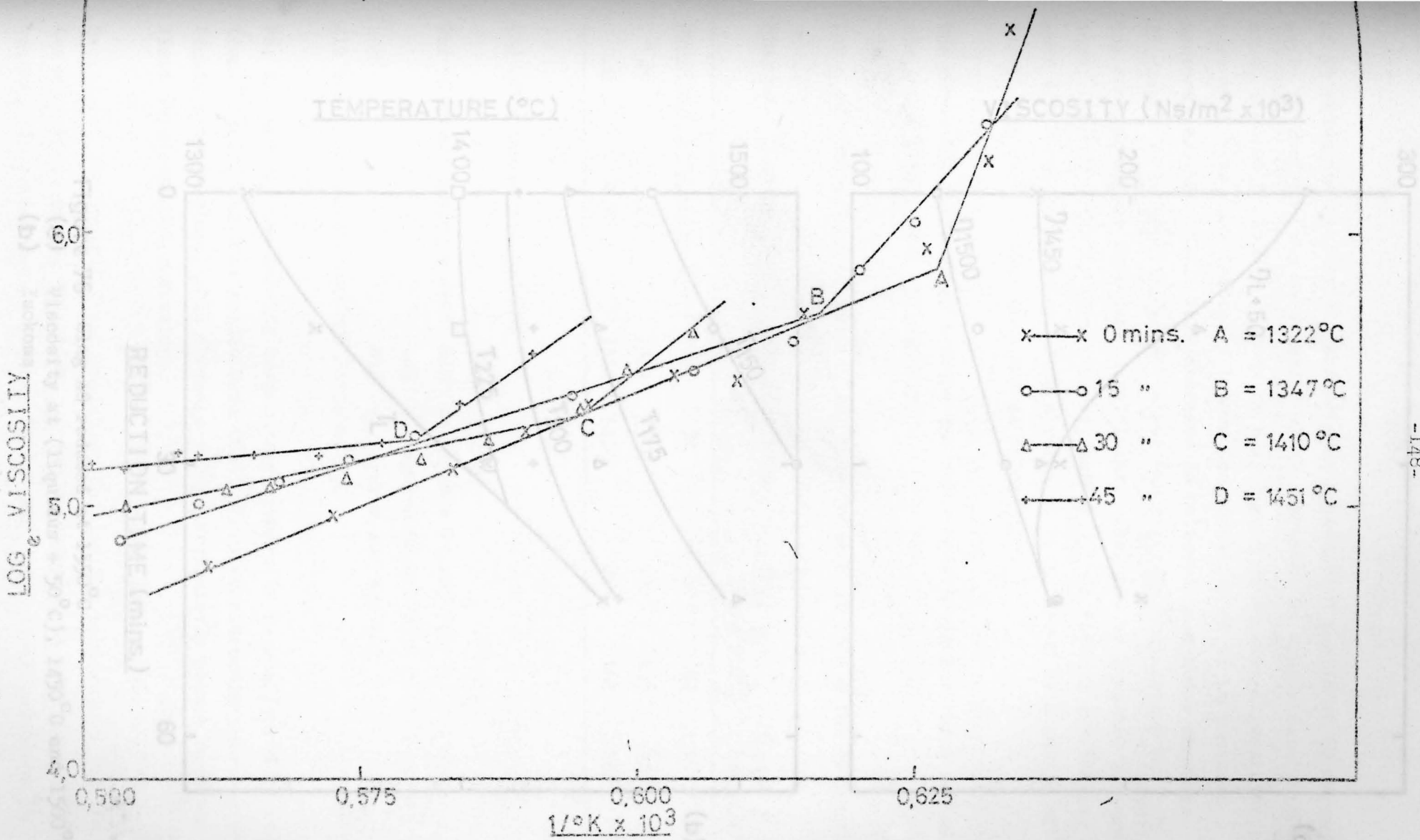


Figure 75 Viscosity of slag A8 reduced by Carbon at 1550°C

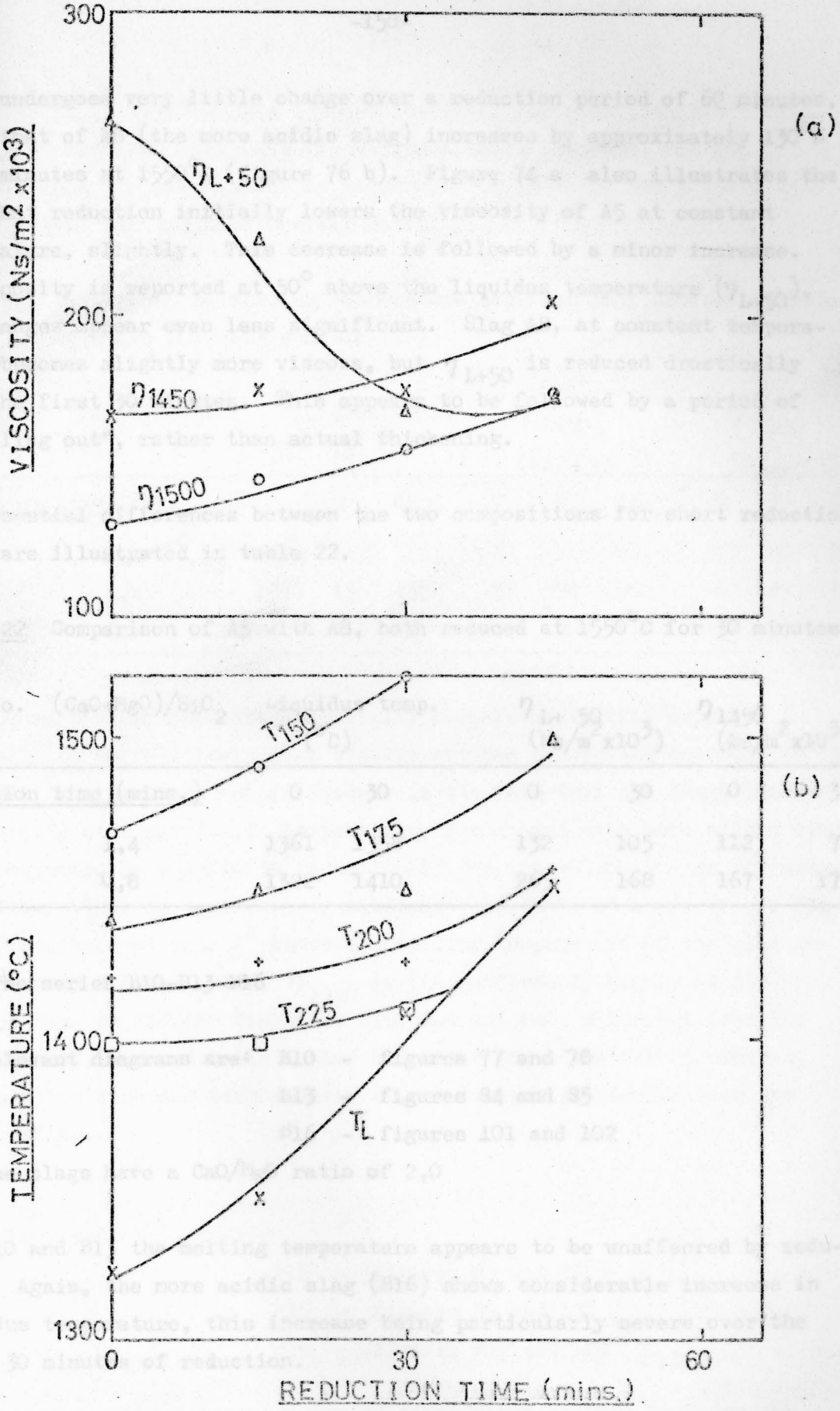


Figure 76 Slag A8 reduced at 1550°C
(a) Viscosity at (liquidus + 50°C), 1450°C and 1500°C
(b) Isokoms

of A5 undergoes very little change over a reduction period of 60 minutes, while that of A8 (the more acidic slag) increases by approximately 130°C in 45 minutes at 1550°C (figure 76 b). Figure 74 a also illustrates the fact that reduction initially lowers the viscosity of A5 at constant temperature, slightly. This decrease is followed by a minor increase. If viscosity is reported at 50° above the liquidus temperature (η_{L+50}), the changes appear even less significant. Slag A8, at constant temperature, becomes slightly more viscous, but η_{L+50} is reduced drastically over the first 30 minutes. This appears to be followed by a period of "levelling out", rather than actual thickening.

The essential differences between the two compositions for short reduction times are illustrated in table 22.

Table 22 Comparison of A5 with A8, both reduced at 1550°C for 30 minutes

Slag No.	$(CaO+MgO)/SiO_2$	Liquidus temp. (°C)		η_{L+50} ($Ns/m^2 x10^3$)		η_{1450} ($Ns/m^2 x10^3$)	
Reduction time (mins.)		0	30	0	30	0	30
A5	1,4	1361	1358	132	105	112	79
A8	0,8	1322	1410	265	168	167	175

(b) The series B10-B13-B16

The relevant diagrams are: B10 - figures 77 and 78
B13 - figures 84 and 85
B16 - figures 101 and 102

All the slags have a CaO/MgO ratio of 2,0

For B10 and B13 the melting temperature appears to be unaffected by reduction. Again, the more acidic slag (B16) shows considerable increase in liquidus temperature, this increase being particularly severe over the first 30 minutes of reduction.

Because of the insignificant variation in liquidus temperature for the two more basic slags, η_t and η_{L+50} can be expected to vary in a similar manner. This is shown in figures 78 and 85. An initial reduction in

viscosity is followed by significant increase, for reduction times exceeding 30 minutes. For B16, η_t will naturally increase, but η_{L+50} falls in much the same manner as was shown for A8 which has a lower titania content but the same overall basicity.

Table 23 Variations in melting temperature and viscosity during reduction of slags B10, B13 and B16

Slag No.	$(CaO+MgO)/SiO_2$	Liquidus temp. (°C)			η_{L+50} ($Ns/m^2 \times 10^3$)			η_{1500} ($Ns/m^2 \times 10^3$)		
Reduction time (mins.)		0	30	45	0	30	45	0	30	45
B10	1,7	1472	1479	1481	62	51	63	71	60	83
B13	1,4	1337	1337	1350	137	94	96	67	49	72
B16	0,8	1388	1489	1498	236	80	81	162	93	98

It appears that an increase in basicity causes the initial decrease in viscosity to be relatively less drastic and the subsequent increase to start earlier. Another outstanding feature is the fact that the large increases in fluidity at a particular temperature, associated with more acidic slags, is accompanied by a definite reduction in the activation energy for viscous flow. This is particularly noticeable in table 23 where η_{1500} for B16 is measured at only 2° above the melting temperature of the slag reduced for 45 minutes. Yet, η_{1500} is insignificantly higher at 45 minutes than at shorter times for B16, and not very different from the viscosity of the most basic member B10 after reduction for 45 minutes, although the liquidus temperatures of the two reduced derivatives are rather alike.

(c) The series B12-B15-B18

B12 - figures 82 and 83
B15 - figures 99 and 100
B18 - figures 107 and 108

The initial liquidus temperatures of these slags are all high due to the high magnesia content ($CaO/MgO = 0,5$) and although the increase generally occurring during reduction is not very marked, the trend is recognizable in all cases.

Again, the initial reduction in η_{L+50} is most noticeable for the most acidic slag (B18), but entirely absent in the case of the most basic one (B12), although it is possible that a minimum could occur over the first 15 minutes of reduction of B12 (figure 83). Even at basicity 1,4 (slag B15), the viscosity is already increasing after 30 minutes. Table 24 gives selected comparative data for the three slag compositions.

Table 24 Variation in melting temperature and viscosity during reduction of slags B12, B15 and B18.

Slag No.	$(CaO+MgO)/SiO_2$	Liquidus temp. (^oC)			η_{L+50} ($Ns/m^2 x10^3$)			η_{1500} ($Ns/m^2 x10^3$)		
Reduction time (mins.)		0	30	45	0	30	45	0	30	45
B12	1,7	1478	1504	1517	43	72	116	39	73	125
B15	1,4	1492	1504	1524	94	112	132	90	113	162
B18	0,8	1473	1501	1516	129	91	97	106	91	101

(d) (i) The series B11-B14-B17 reduced at 1550^oC

B11 - figures 79 and 81 a
B14 - figures 87 and 89 b
B17 - figures 103 and 104

The melting temperature of the most basic slag B11 (basicity = 1,7) is not greatly influenced by reduction, while those of B17 and B14 are severely increased. Especially in the case of B14 (basicity = 1,4), the liquidus temperature is raised very rapidly, from its initial value of $\pm 1340^o$ to $\pm 1440^oC$ within 45 minutes. B17 (basicity = 0,8) has a higher initial liquidus temperature and the increase is more gradual.

It must be pointed out that B14, after 3 hours in a graphite crucible at 1550^oC, has a liquidus temperature of 1480^oC and a viscosity at 1550^o of just over 0,2 Ns/m^2. Such a melting temperature is not abnormally high when it is compared with those of the more basic slags (B11 in this series). Neither is the viscosity high, when compared with that of eg. blast furnace type slags.

Table 25 Variation in melting temperature and viscosity during reduction of slags B11, B14 and B17

Slag No.	$(CaO+MgO)/SiO_2$	Liquidus temp. (^oC)			η_{L+50} ($Ns/m^2 x10^3$)			η_{1500} ($Ns/m^2 x10^3$)		
Reduction time (mins.)		0	30	90	0	30	90	0	30	90
B11	1,7	1455	1472	1483	75	50	208	64	46	197
B14	1,4	1335	1383	1456	122	74	180	58	40	133
B17	0,8	1420	1481	1520	220	140	100	118	136	107

(ii) The effect of small changes in basicity at $CaO/MgO = 1,0$

Although the general influence of large variations in basicity is shown by the series B11-B14-B17, the basicity range 1,3 to 1,7, being of particular practical importance mainly because of relatively low liquidus temperatures, was also tested. These slags were reduced at 1550^oC, only for 45 minutes, as such a reduction period was considered sufficient to reveal "thinning" or "thickening" tendencies that might exist. Results are summarized in table 26.

Table 26 Variation in melting temperature and viscosity during reduction of slags having $CaO/MgO = 1,0$

Slag No.	$(CaO+MgO)/SiO_2$	Liquidus temp. (^oC)		η_{L+50} ($Ns/m^2 x10^3$)		Figures
Reduction time (mins.)		0	45	0	45	
B28	1,30	1440	1520	140	85	92
B29	1,35	1366	1465	108	94	93
B14	1,40	1335	1438	122	95	87 & 89b
B30	1,45	1358	1418	108	124	94
B31	1,50	1358	1427	104	116	95
B32	1,55	1369	1395	103	113	96
B33	1,60	1373	1395	88	107	97
B34	1,65	1402	1427	80	96	98
B11	1,70	1455	1475	75	103	79 & 81a

Although the variations in viscosity reported here are too small to be important on industrial scale, the changes in melting temperature are

significant. The trends shown by means of these variations generally agree well with what would be expected from a consideration of slags B11, B14 and B17.

The increase in melting temperature is more marked for the less basic slags. These slags also generally exhibit a "thinning" tendency over the first 45 minutes of reduction. More basic slags show only small changes in liquidus temperature, but generally tend to become more viscous. The transition region between the two modes of behaviour appears to lie in the basicity range 1,45 to 1,55.

4.2.1.2 CaO/MgO ratio

(a) The series B10-B11-B12 : $(CaO + MgO)/SiO_2 = 1,7$

B10 - figures 77 and 78
B11 - figures 79 and 81 a
B12 - figures 82 and 83

All these slags, after reduction at 1550° for 45 minutes show an eventual increase in η_{L+50}. However, while the initial decrease in this value is clearly noticeable for CaO/MgO ratios 2 and 1, (slags B10 and B11) it is absent for B12 where CaO/MgO = $\frac{1}{2}$.

Melting temperatures are relatively high for all three slags in the unreduced condition, and it seems to increase slightly in all cases, the trend being most recognizable for slag B12.

Table 27 Variation in melting temperature and viscosity during reduction of slags B10, B11 and B12.

Slag No.	CaO/MgO	Liquidus temp. (°C)			η_{L+50} ($Ns/m^2 \times 10^3$)		
Reduction time (mins.)		0	15	45	0	15	45
B10	2	1472	1478	1481	62	47	63
B11	1	1455	1466	1475	75	57	103
B12	$\frac{1}{2}$	1478	1495	1517	43	50	116

(b) The series B13-B14-B15 : $(CaO+MgO)/SiO_2 = 1,4$

B13 - figures 84 and 85

B14 - figures 87 and 89 b

B15 - figures 99 and 100

The overall pattern of behaviour involving an initial drop in η_{L+50}, followed by an increase, is recognizable for all three slags. However, the decrease tends to become less marked and the increase more pronounced as the CaO/MgO ratio is lowered.

If it is assumed that a high initial liquidus temperature renders increases occurring during reduction less pronounced, a lower CaO/MgO ratio again appears to be associated with generally marked increases in melting temperature due to reduction by carbon.

Table 28 Variations in melting temperature and viscosity during reduction of slags B13, B14 and B15.

Slag No.	CaO/MgO	Liquidus temp. (^oC)			η_{L+50} ($Ns/m^2 x10^3$)		
Reduction time (mins.)		0	15	45	0	15	45
B13	2	1337	1340	1350	137	91	96
B14	1	1335	1347	1438	122	73	95
B15	$\frac{1}{2}$	1492	1492	1524	94	76	162

(c) The series B16-B17-B18 : $(CaO+MgO)/SiO_2 = 0,8$

B16 - figures 101 and 102

B17 - figures 103 and 104

B18 - figures 107 and 108

The increase in viscosity occurring within relatively short reduction times at 1550^o, that are characteristic of slags of higher basicity, is virtually absent in this series. The initial decrease is present in all cases, but again becomes less marked as the CaO/MgO ratio is decreased. It must however be borne in mind that the viscosity of the high magnesia slag in this series (B18) was considerably lower than that of the other two members, before reduction.

Table 29 Variations in melting temperature and viscosity during reduction of slags B16, B17 and B18

Slag No.	CaO/MgO	Liquidus temp. (°C)			η_{L+50} ($Ns/m^2 x10^3$)		
Reduction time (mins.)		0	15	45	0	15	45
B16	2	1388	1450	1498	236	195	81
B17	1	1420	1461	1489	220	190	134
B18	½	1473	1491	1516	129	84	97

The liquidus temperature was raised during reduction in all cases, the effect being least pronounced for the slag of highest initial liquidus temperature (B18).

4.2.1.3 (TiO_2 + Al_2O_3) content - the series A5-B14-C23 with $CaO:MgO:SiO_2$ = 0,7:0,7:1

A5 - figures 73 and 74
B14 - figures 87 and 89 b
C23 - figure 109

As slag C23 was only reduced for 60 minutes at 1550°C, this time interval was used for the purpose of comparing the properties of all the members of this series.

Table 30 Variations in melting temperature and viscosity during reduction of slags A5, B14 and C23.

Slag No.	Mass% (TiO_2+Al_2O_3)	Liquidus temp. (°C)		η_{L+50} ($Ns/m^2 x10^3$)	
Reduction time (mins.)		0	60	0	60
A5	36	1361	1374	132	106
B14	44	1335	1463	122	126
C23	54	1447	1516	83	109

If it is assumed that the general trend followed by viscosity during

reduction of other series is continued here, it must be concluded that A5 may have passed a viscosity minimum but is still more fluid than the original slag. Figure 89 b shows that the viscosity of B14 is increasing although the difference shown in the table is insignificant. C23 has apparently passed its viscosity minimum even though the reduced slag has approximately the same fluidity as the other two members of the series, after reduction for 60 minutes.

4.1.2.4 Oxides of iron and vanadium

It was in general not intended to add more composition variables in this study of an already complex five-component system. However, the viscosity of a composite plant slag was measured and found to be remarkably low. The composition of this slag, designated as HV, was given in table 13. Specifications not shown in the table are:

$$CaO/MgO = 1,12$$
$$(CaO+MgO)/SiO_2 = 1,53$$
$$TiO_2/Al_2O_3 = 2,37$$
$$(TiO_2 + Al_2O_3 = 43,98 \text{ mass } \%$$

As the composition of slag HV did not very closely resemble that of any of the five-component mixtures already discussed, its composition was re-calculated on the basis of the components CaO, MgO, SiO_2, Al_2O_3 and TiO_2 only. (HV-FV, table 13)

The viscosities of the two melts (HV and HV-FV) are shown in figure 110. The synthetic slag without iron and vanadium oxides was slightly more viscous and its liquidus temperature was significantly higher.

Iron and vanadium oxides were then added to HV-FV to give a composition very similar to that of HV. The minor quantities of manganese and chromium oxides reported in HV were not taken into account. The added oxides were in the oxidation states as reported in table 13, although these did not necessarily represent their true states. The composition of the resulting melt, HV+FV, is also given in the table and its viscosity is shown as a function of temperature in figure 110. Its fluidity was very similar to that of the plant slag, and definitely higher than that of the synthetic slag HV-FV. From this it must be concluded that even small

quantities of particularly iron oxide exert a noticeable influence upon the viscosity of slags based on the $CaO-MgO-SiO_2-Al_2O_3-TiO_2$ system.

Complete reoxidation tests carried out on the plant slag HV, showed that it was reduced with respect to titanium oxide, to a degree rather similar to that attained by slag B14 (of composition not very different from that of HV) after reduction by graphite at 1550°C for 60 minutes in the normal manner. Its viscosity and liquidus temperature was raised - results are shown graphically in figure 110 (This refers to slag HV-FV reduced as mentioned above and then designated as HV-FV(60M)). This reduced product was then treated as follows:
Iron and vanadium oxides were again added to it to return the composition to approximately that of plant slag HV. The resulting mixture, HV-FV(60M)+FV, thus had the same overall composition as slag HV+FV. The melt was homogenized at 1550°C in the inert atmosphere for two hours before its viscosity was measured. Figure 110 shows that addition of the oxides of iron and vanadium to the reduced slag again made it more fluid, so that its viscosity was practically the same as that of the original unreduced synthetic slag HV-FV and only slightly higher than that of the plant slag HV.

Although the scope of these experiments is extremely narrow, they appear to indicate the possibility that addition of oxides more readily reducible by carbon than TiO_2, to a reduced five-component titaniferous slag, tends to restore the original properties of viscosity and liquidus temperature of such a slag. It therefore seems reasonable to assume that the presence of these readily reducible oxides in titaniferous slags under reducing conditions will serve to retard the reduction of titanium oxide, the process which is thought to be responsible for the variation in liquidus temperature and viscosity, reported in the preceding sections.

4.2.2 The influence of reduction temperature on variations in viscosity and melting temperature

The selection of slag compositions to illustrate the effect of reduction temperature was based on basicity only (B11, B14 and B17), while comprehensive testing at three different temperatures was carried out only

on slag B14.

(a) Slag B11 : $(CaO+MgO)/SiO_2 = 1,7$

Viscosity-temperature relations of this slag reduced at 1550°C and at 1600°C are given in figures 79 and 80 respectively. The results are summarized in figure 81.

The immediately apparent effect of an increase in reduction temperature is the fact that at the higher temperature, the viscosity minimum is either absent altogether or appears very soon after reduction is commenced, so that it is not observed on the particular time scale used.

While it is not likely that the slag reduced for 60 minutes will be more viscous after reduction at the lower temperature, as might be concluded from the shapes of the curves drawn through the available experimental points, they do seem to indicate that the rate of "thickening" at 1600° is not much faster than at 1550°C for reduction times exceeding 30 minutes.

(b) Slag B14 : $(CaO+MgO)/SiO_2 = 1,4$

Three temperatures of reduction were used - 1500°, 1550° and 1600°C. Results of viscosity measurements are shown in figures 86, 87 and 88. The effect of reduction time is shown, for the various temperatures, in figures 89 and 90. Figure 91 illustrates the effect of variation in reduction temperature in general. The following curves were drawn:

$\eta_{L+50}(30M)$ - the value of η_{L+50} after reduction for 30 minutes at the different temperatures;

$\eta_{L+50}(90M)$ - the variation in the same parameter after reduction for 90 minutes;

$T_L(30M)$ and $T_L(90M)$ give the variation in approximate liquidus temperatures after reduction for 30 minutes and 90 minutes respectively. The liquidus temperature and η_{L+50} of the original unreduced slag are also shown on the diagram.

At 30 minutes, η_{L+50} for samples reduced at all three temperatures are below that of the original slag. The value for 1600° is only slightly below, showing that in this case, the viscosity minimum has been passed.

At 90 minutes, only the slag reduced at 1500°C has a viscosity approximating to that of the original slag. At the two higher temperatures, the melt is relatively much more viscous.

The 30 minutes liquidus curve shows the relatively greater effect of a temperature increase from 1550° to 1600°C as compared with that of an increase from 1500° to 1550°C. The fact that this difference seems to disappear at 90 minutes to some extent, indicates that there is an upper limit to the melting temperature for reduction at 1600°. This fact is shown more clearly in figures 89 b and 90 for 1550° and for 1600°C respectively. The apparent upper limits at these two reduction temperatures are approximately 1470° and 1530°C.

(c) Slag B17 - $(CaO+MgO)/SiO_2 = 0,8$

Results of viscosity determinations are reported graphically in figures 103 and 105 for reduction temperatures 1550° and 1600°C respectively. Results are summarized in figures 104 and 106.

Again the liquidus temperature rises faster and further during reduction at 1600°. There is again a liquidus temperature difference after reduction for 90 minutes, of approximately 50° to 60°C.

It is important that η_{L+50} is reduced more or less continuously when reduction is performed at 1550°. At 1600°, this measure of viscosity is beginning to increase after reduction for 90 minutes.

In general, temperature must be regarded as an important factor in the behaviour of titaniferous slags under reducing conditions, its importance possibly becoming greater as the slag becomes more acidic. While B14, reduced at 1600° for longer periods, may still be classified as a slag of good fluidity, its liquidus temperature ($\pm$1530°C) can be responsible for difficulties experienced during the tapping of an electric furnace smelting titaniferous iron ores and producing slags of composition appoximating to that of B14.

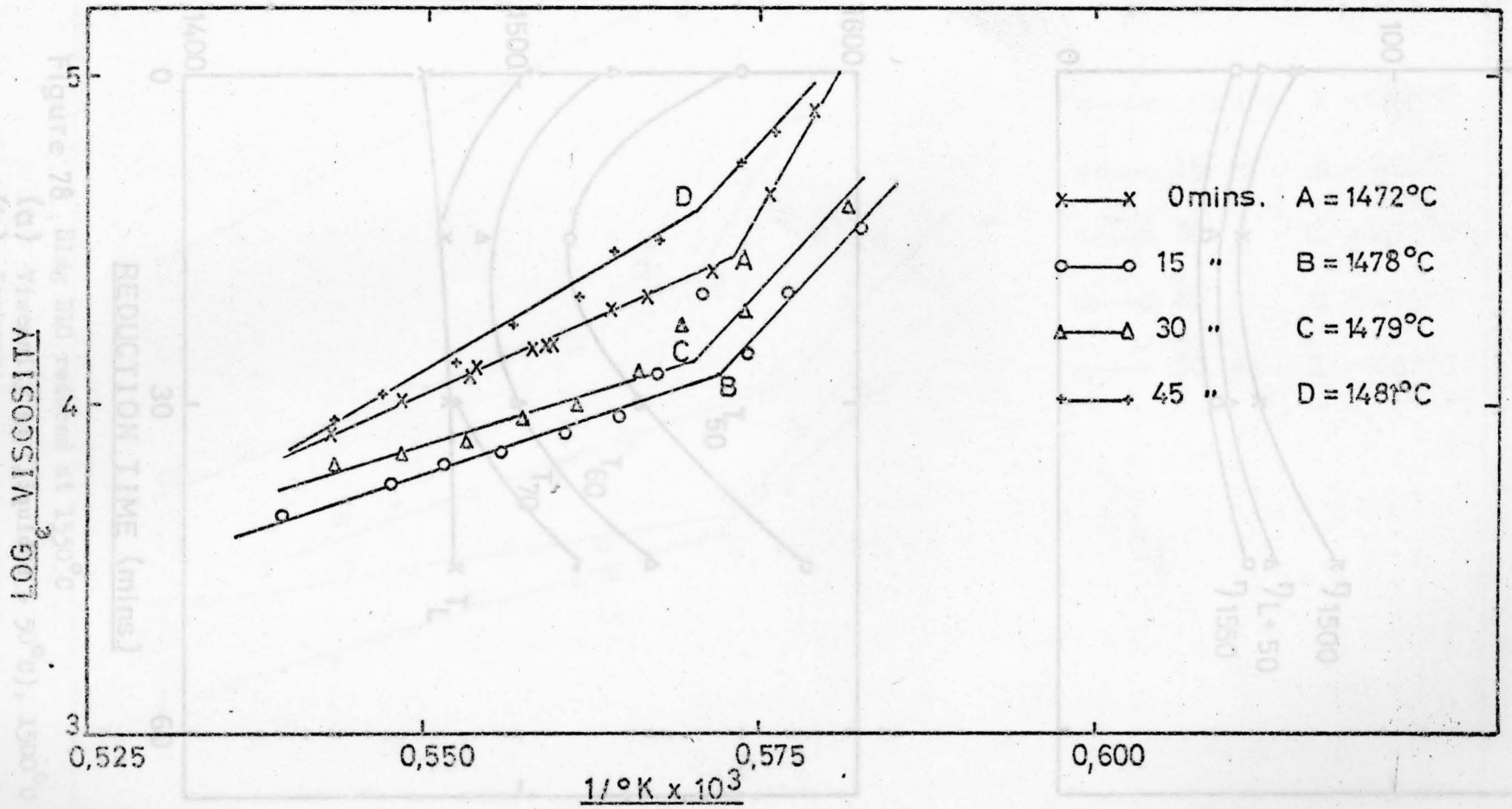
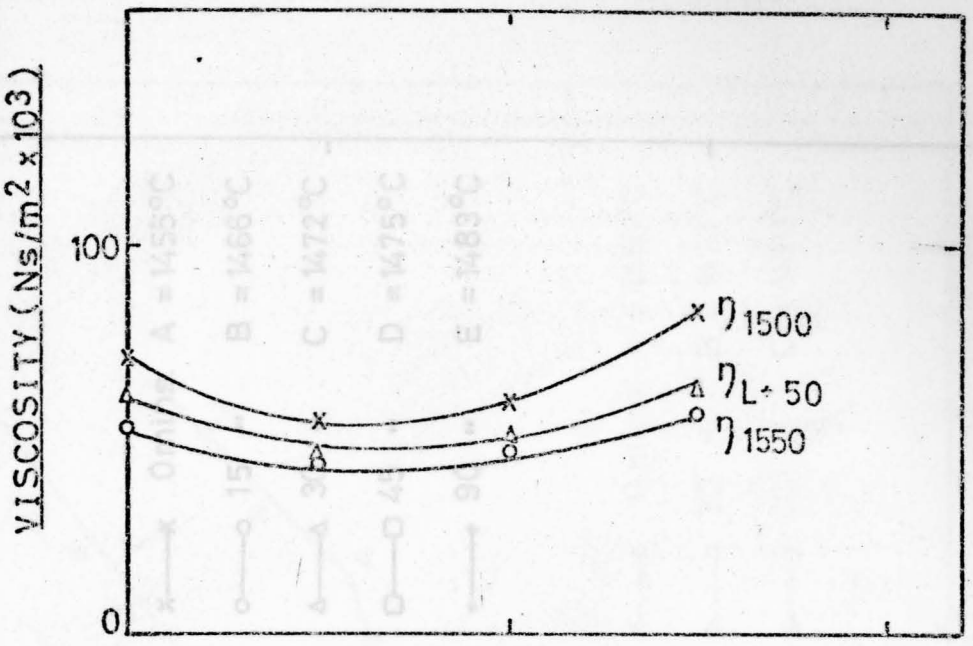


Figure 77 Viscosity of slag B10 reduced by carbon at 1550°C



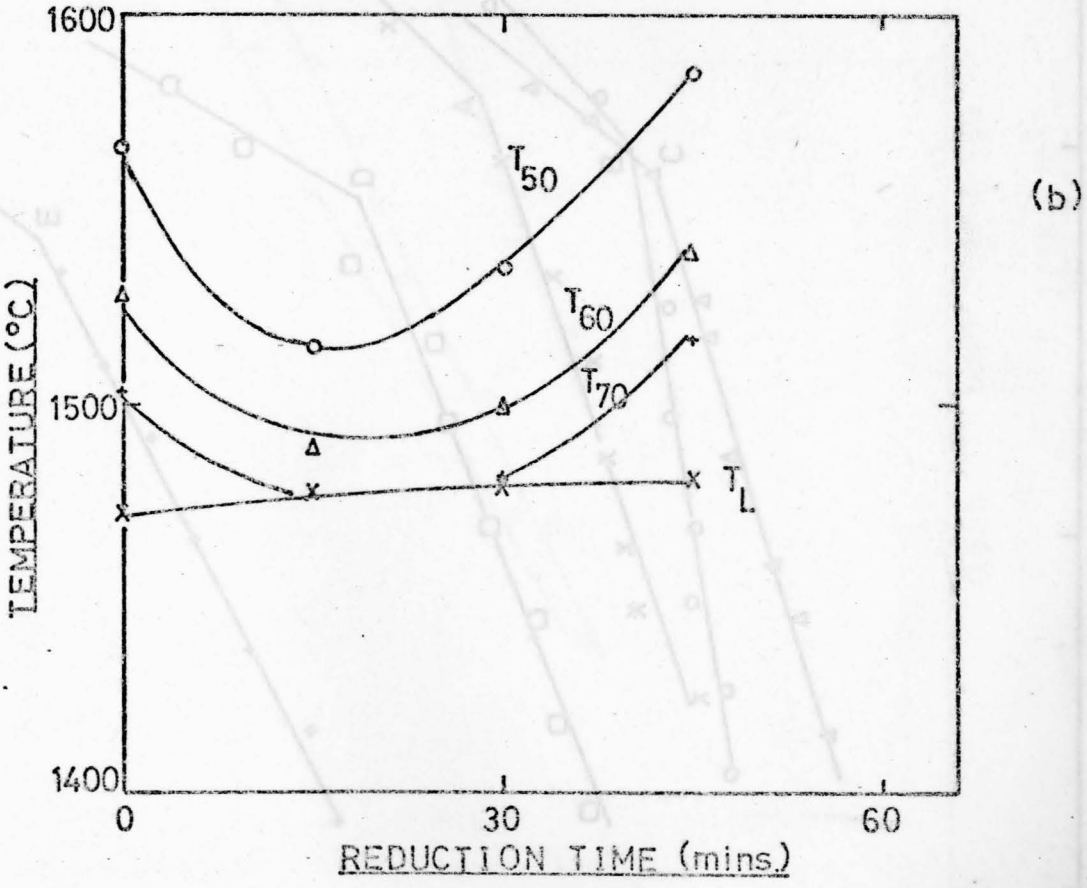


Figure 78 Slag B10 reduced at 1550°C
(a) Viscosity at (liquidus + 50°C), 1500°C and 1600°C
(b) Isokoms

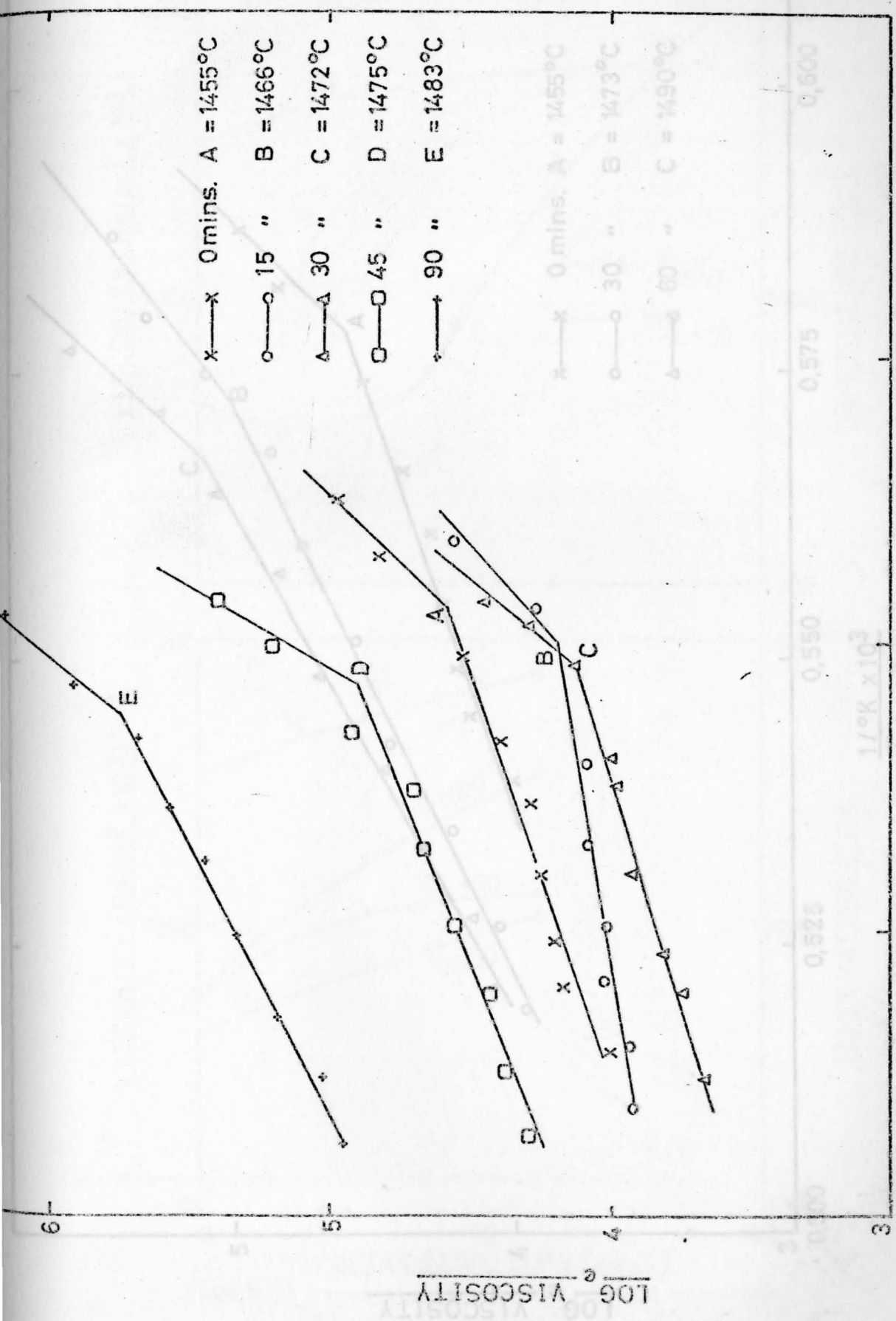


Figure 79 Viscosity of slag B11 reduced by carbon at 1550°C

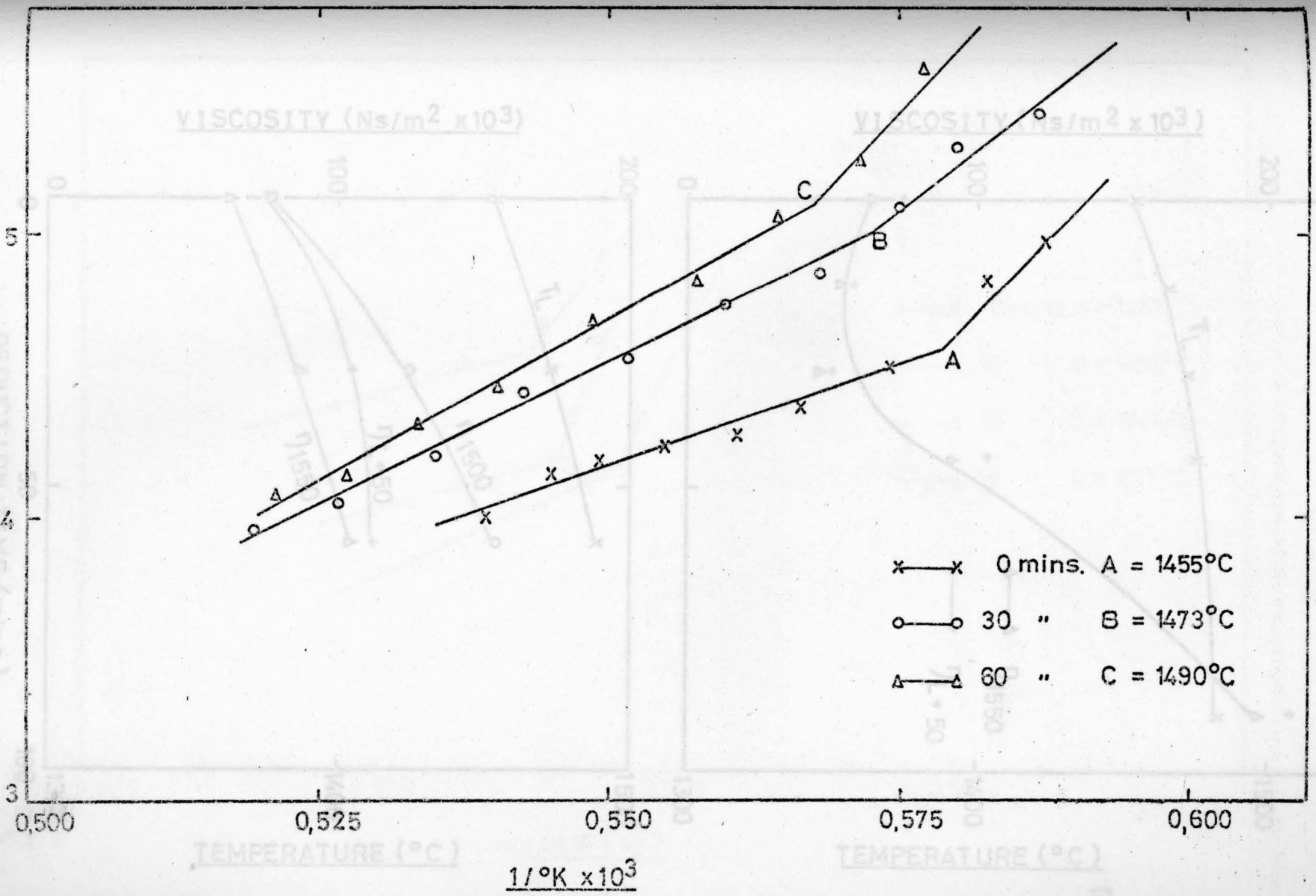


Figure 80 Viscosity of slag B11 reduced by carbon at 1600°C

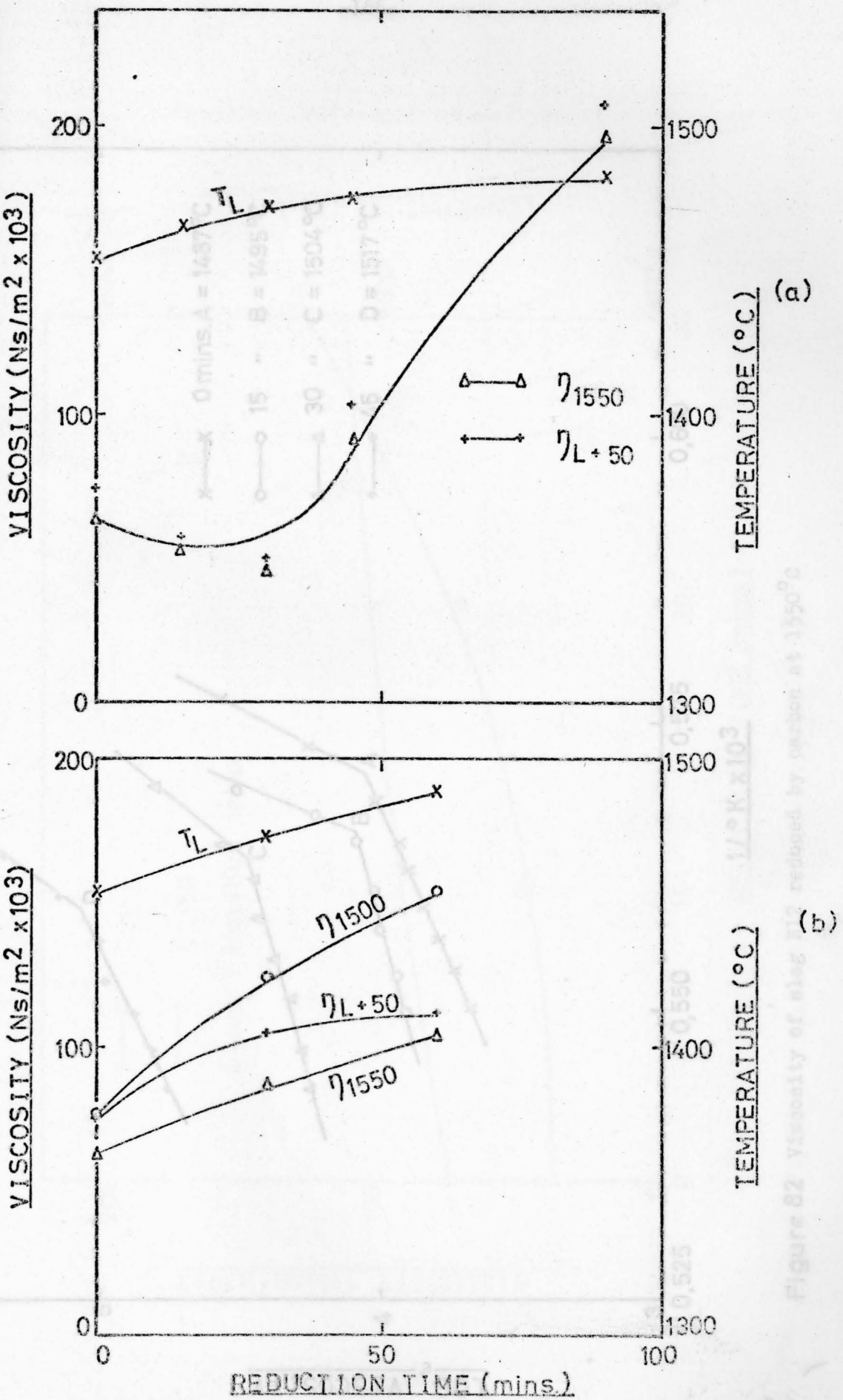


Figure 81 Viscosity of slag B11 reduced by carbon
(a) Reduction temperature = 1550°C
(b) Reduction temperature = 1600°C

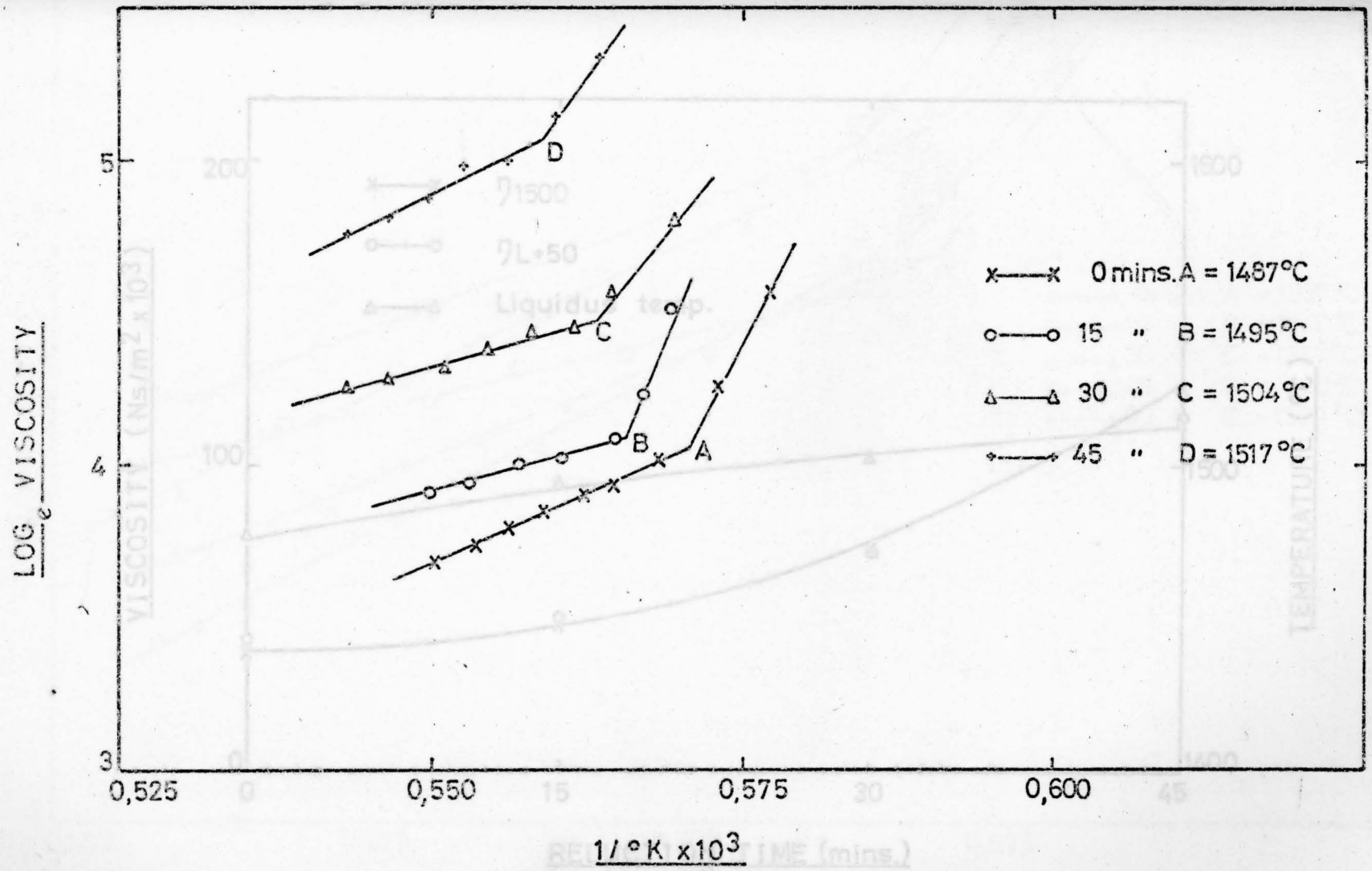


Figure 82 Viscosity of slag B12 reduced by carbon at 1550°C

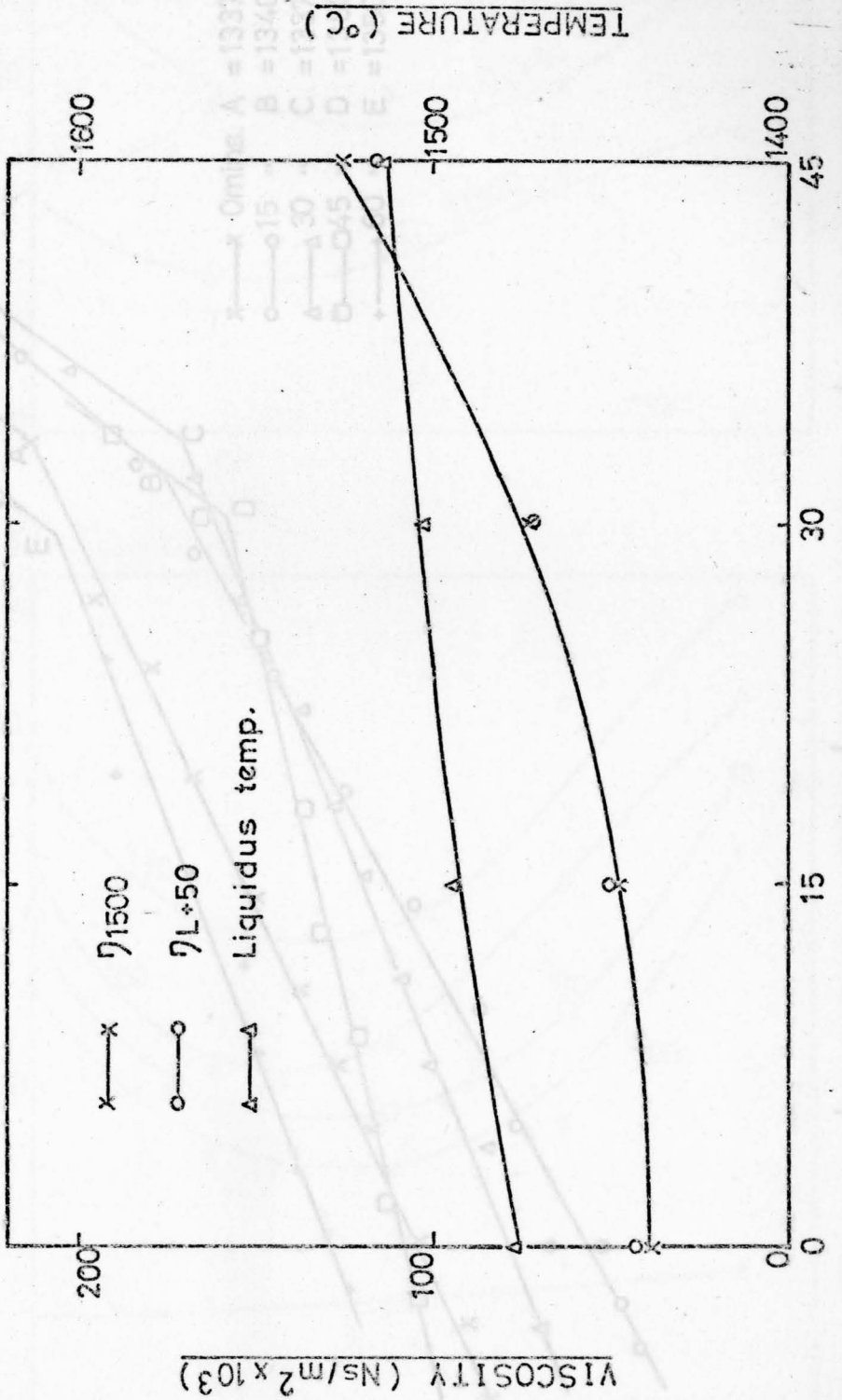


Figure 83 Viscosity of slag B12 reduced at 1550°C

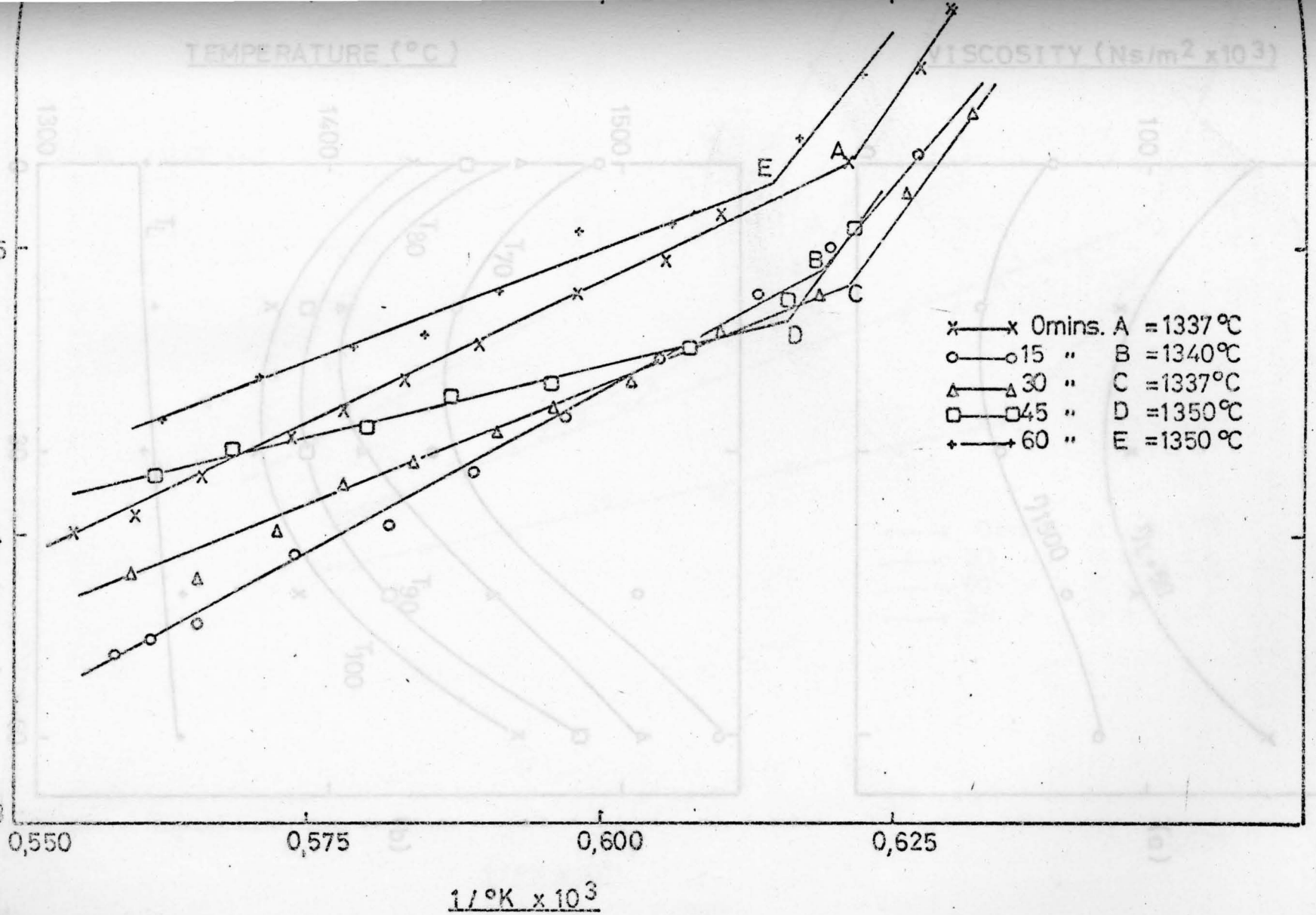


Figure 84 Viscosity of slag B13 reduced at 1550°C

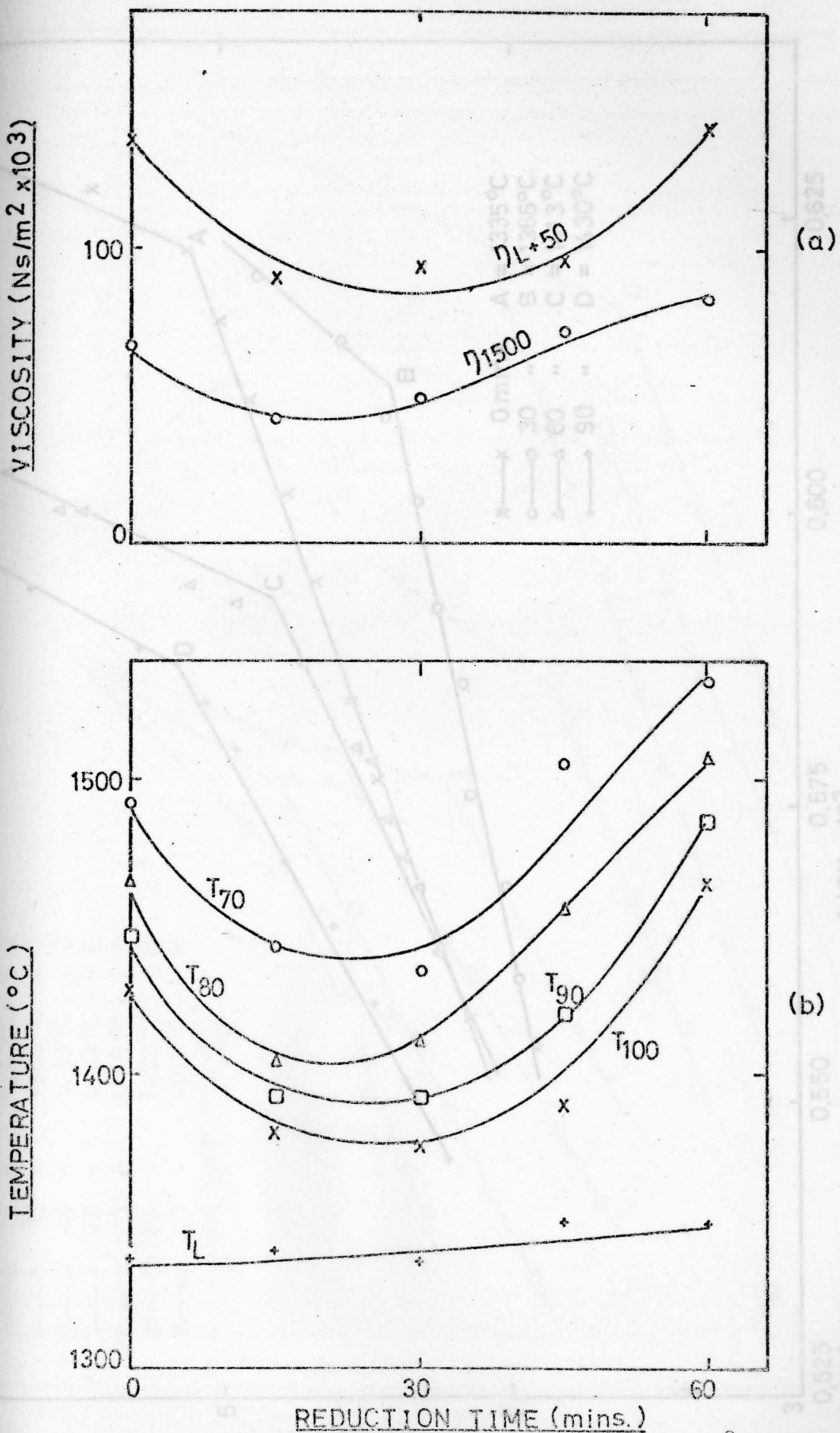


Figure 85 Viscosity of slag B13 reduced at 1550°C
(a) Viscosity at 1500°C and at 50°C above liquidus
(b) Isokoms

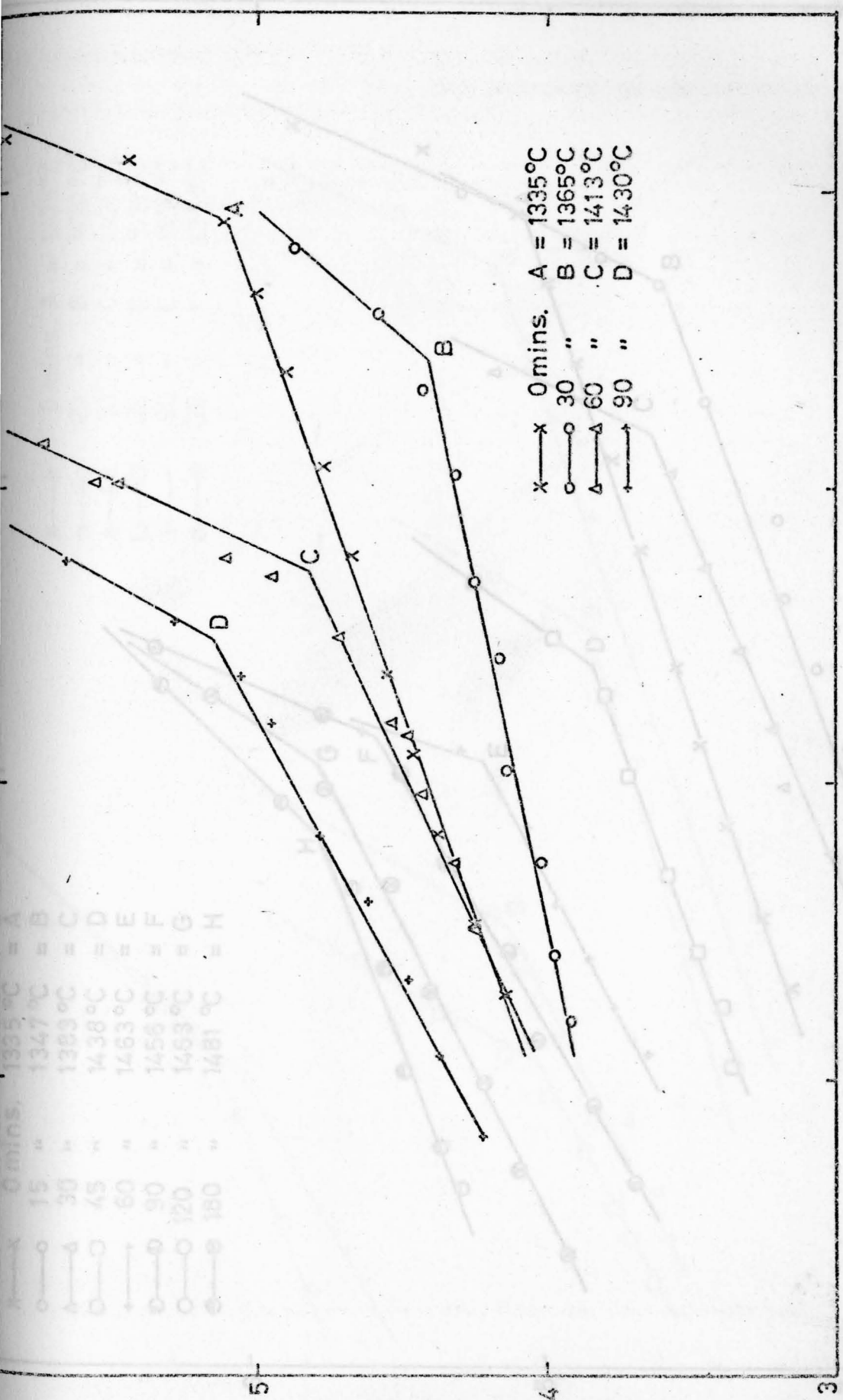


Figure 86 Viscosity of slag B14 reduced at 1500°C

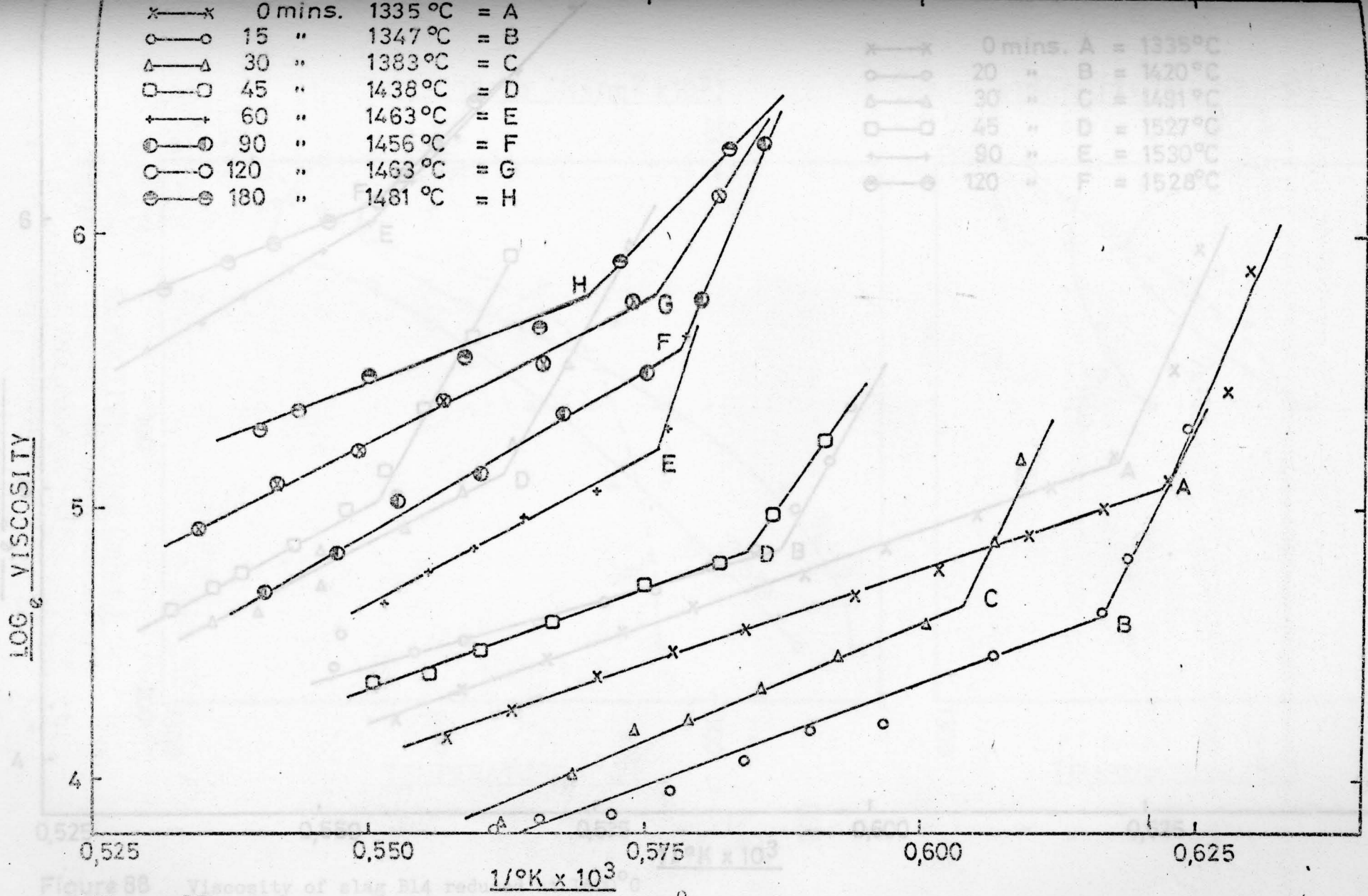


Figure 87 Viscosity of slag B14 reduced at 1550°C

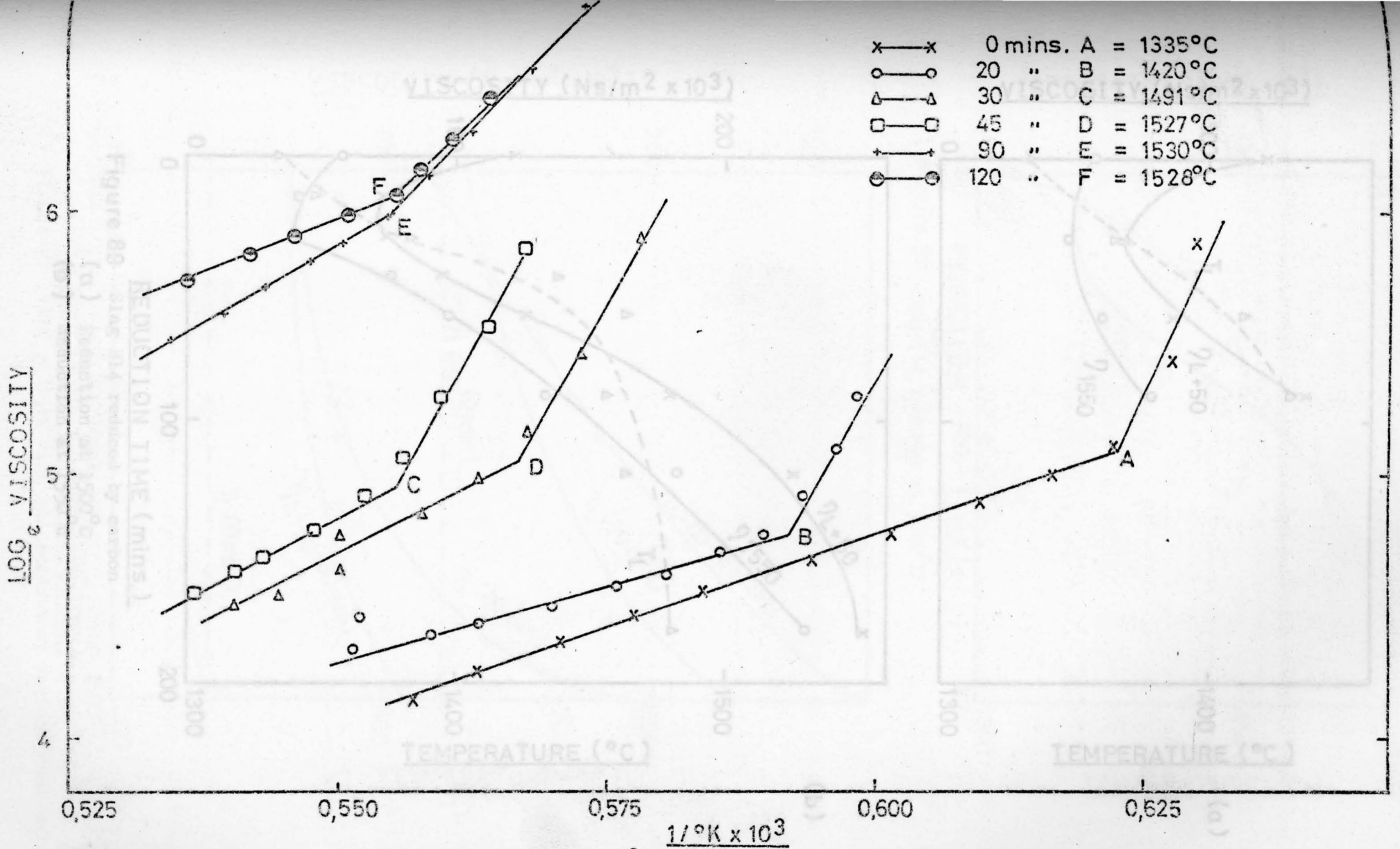


Figure 88 Viscosity of slag B14 reduced at 1600°C

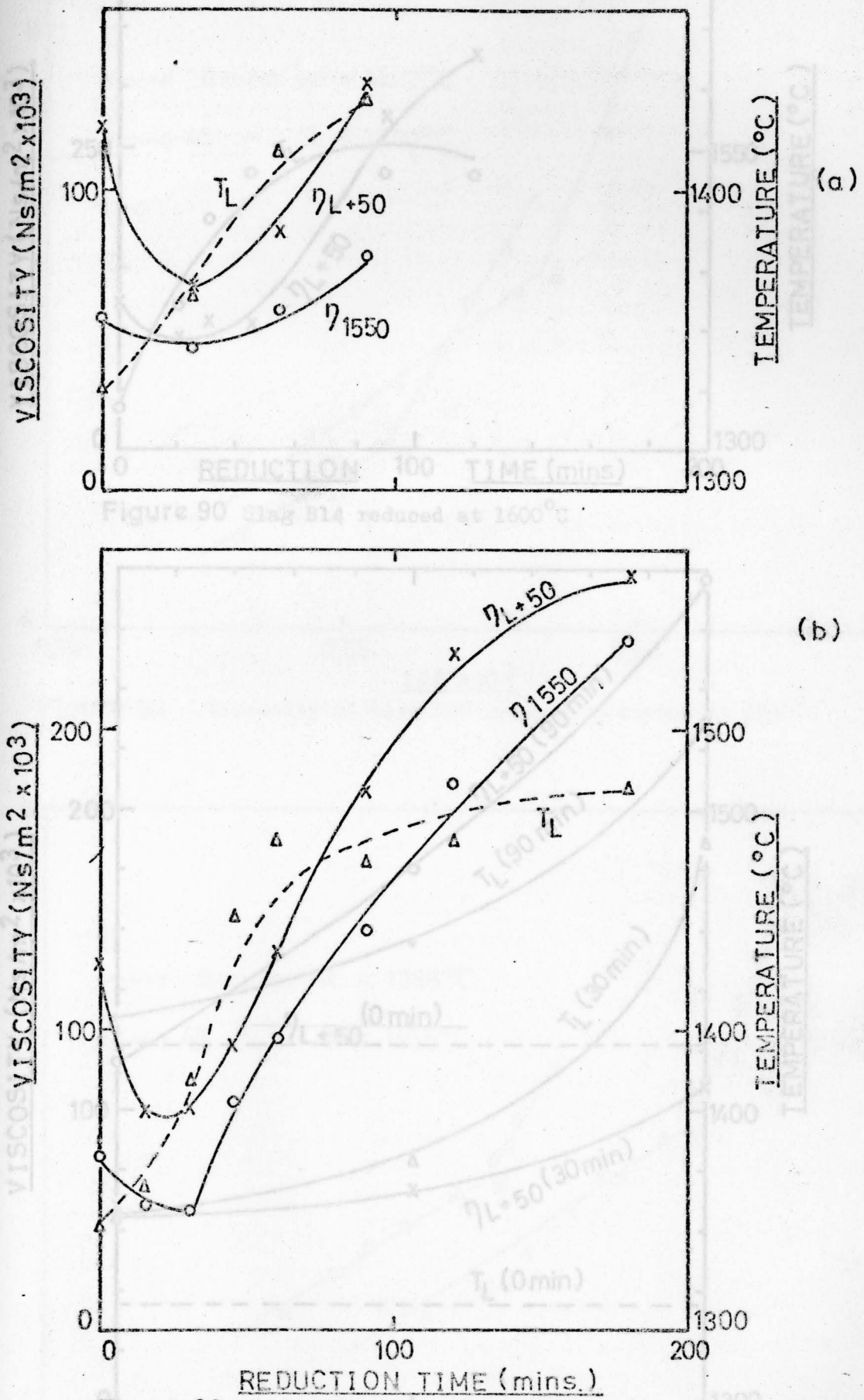


Figure 89 Slag B14 reduced by carbon
(a) Reduction at 1500°C
(b) Reduction at 1550°C

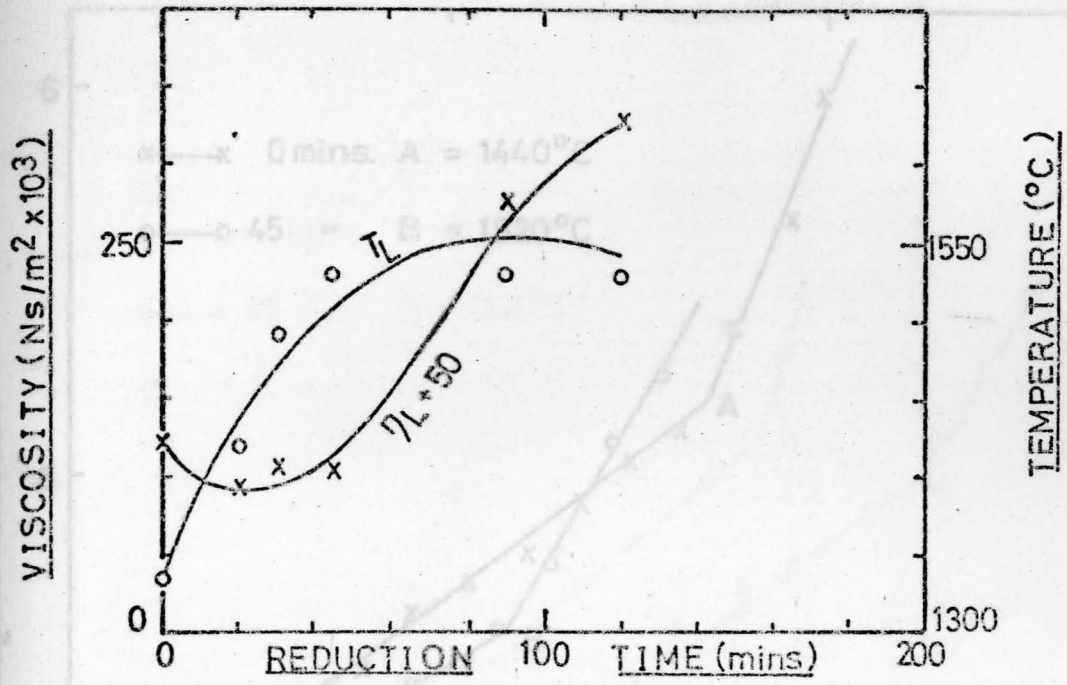


Figure 90 Slag B14 reduced at 1600°C

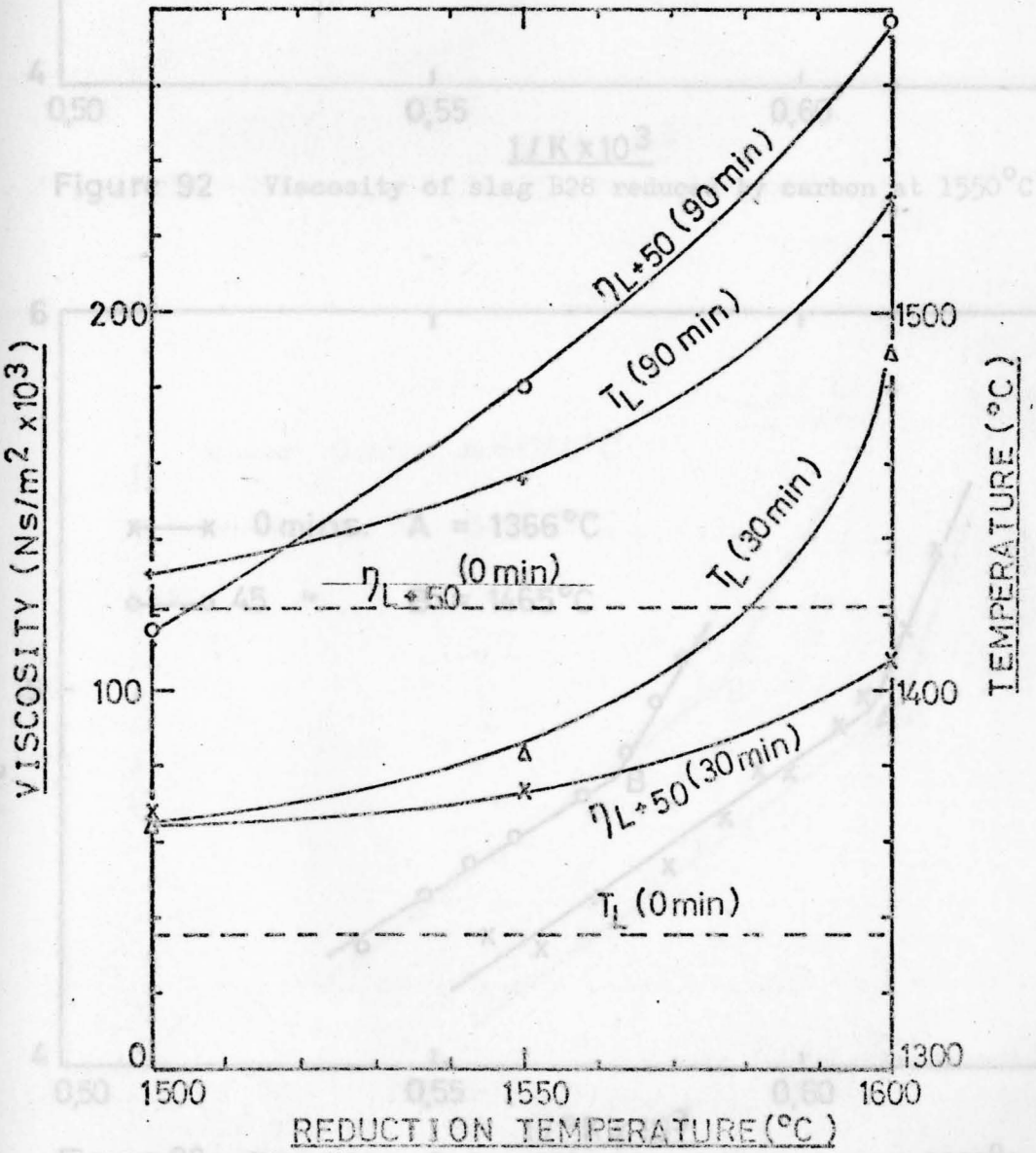


Figure 91 Viscosity of slag B14 reduced at various temperatures

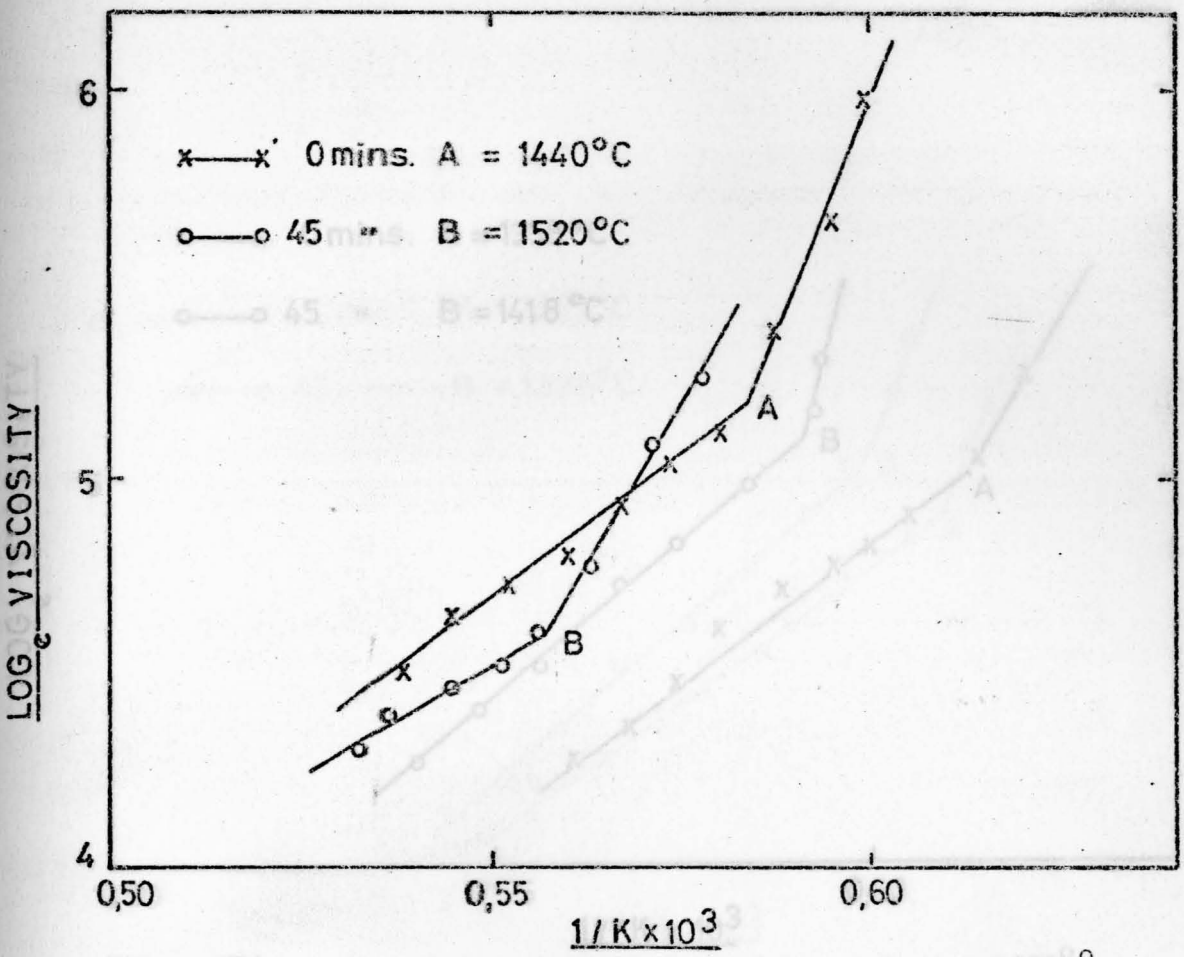


Figure 92 Viscosity of slag B28 reduced by carbon at 1550°C

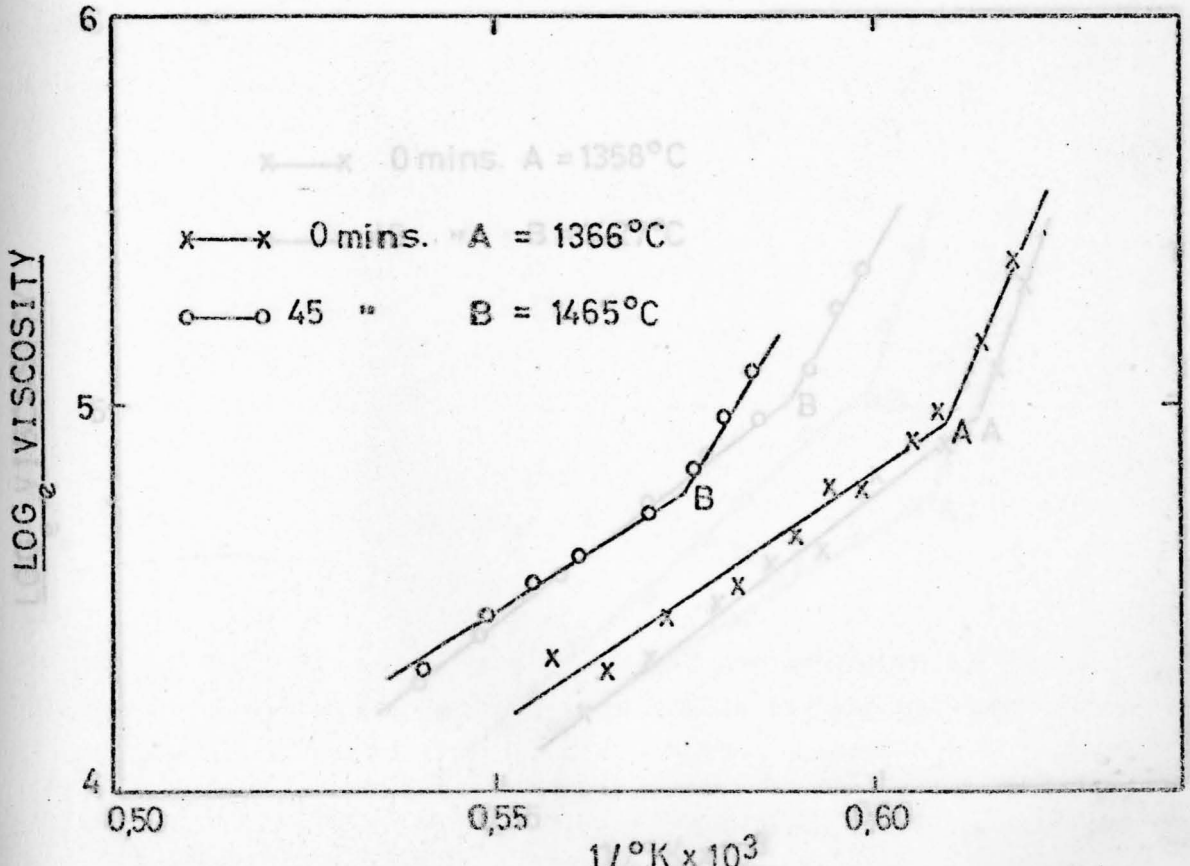


Figure 93 Viscosity of slag B29 reduced by carbon at 1550°C

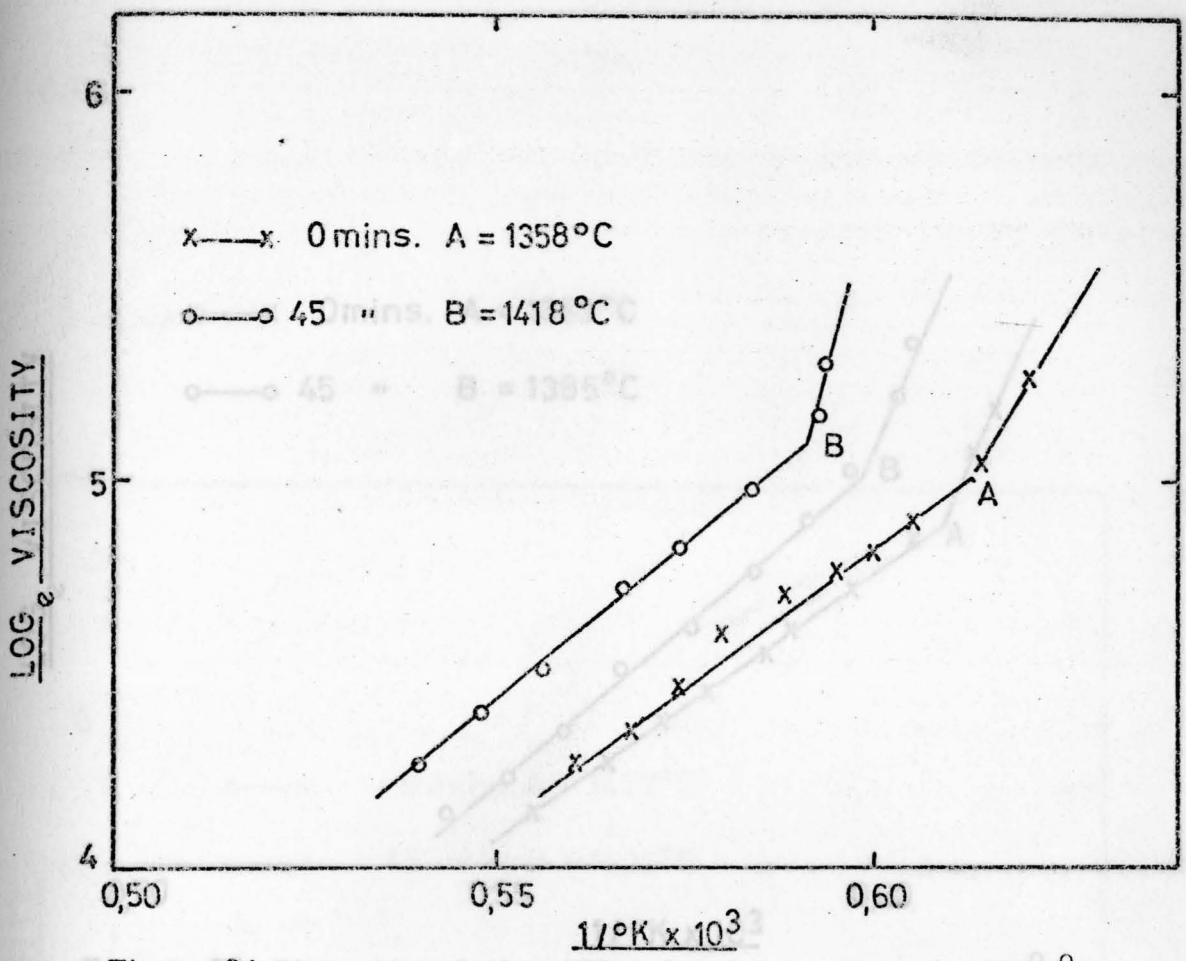


Figure 94 Viscosity of slag B30 reduced by carbon at 1550°C

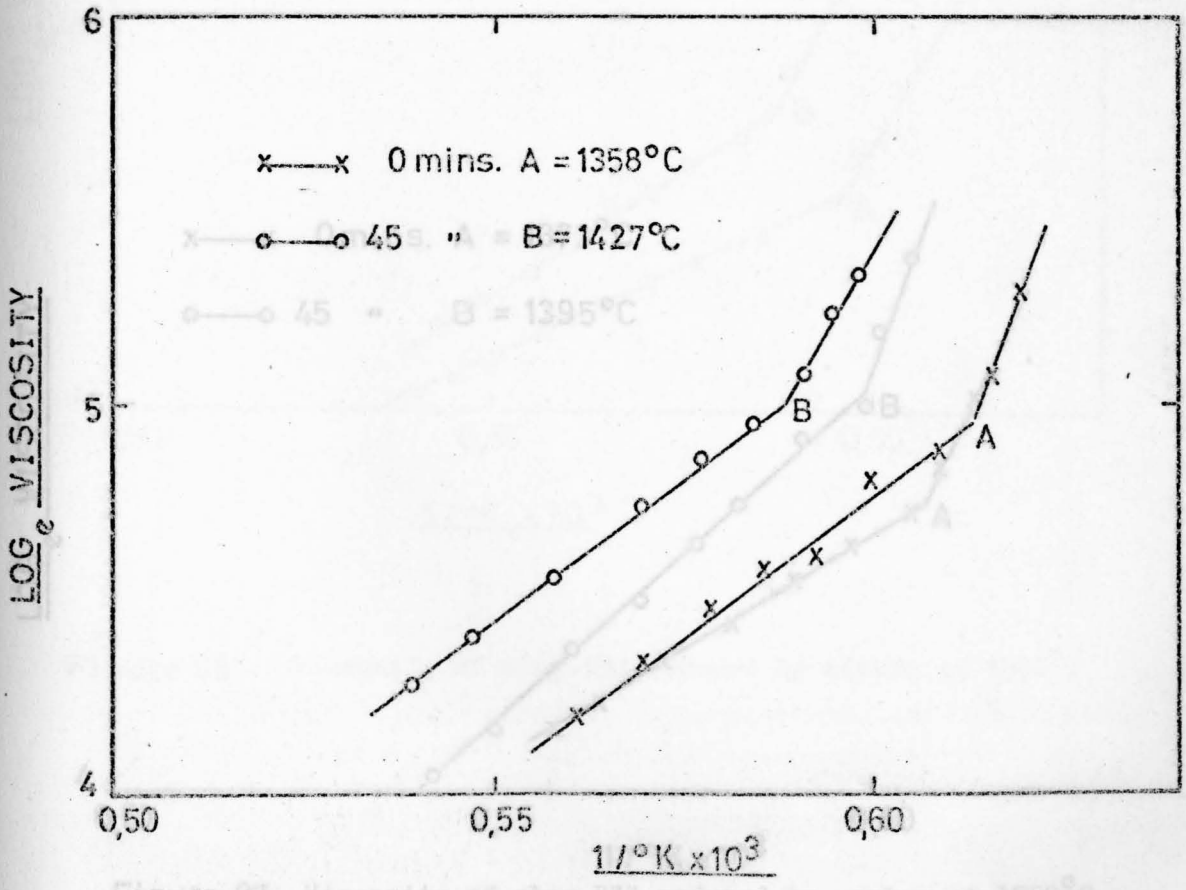


Figure 95 Viscosity of slag B31 reduced by carbon at 1550°C

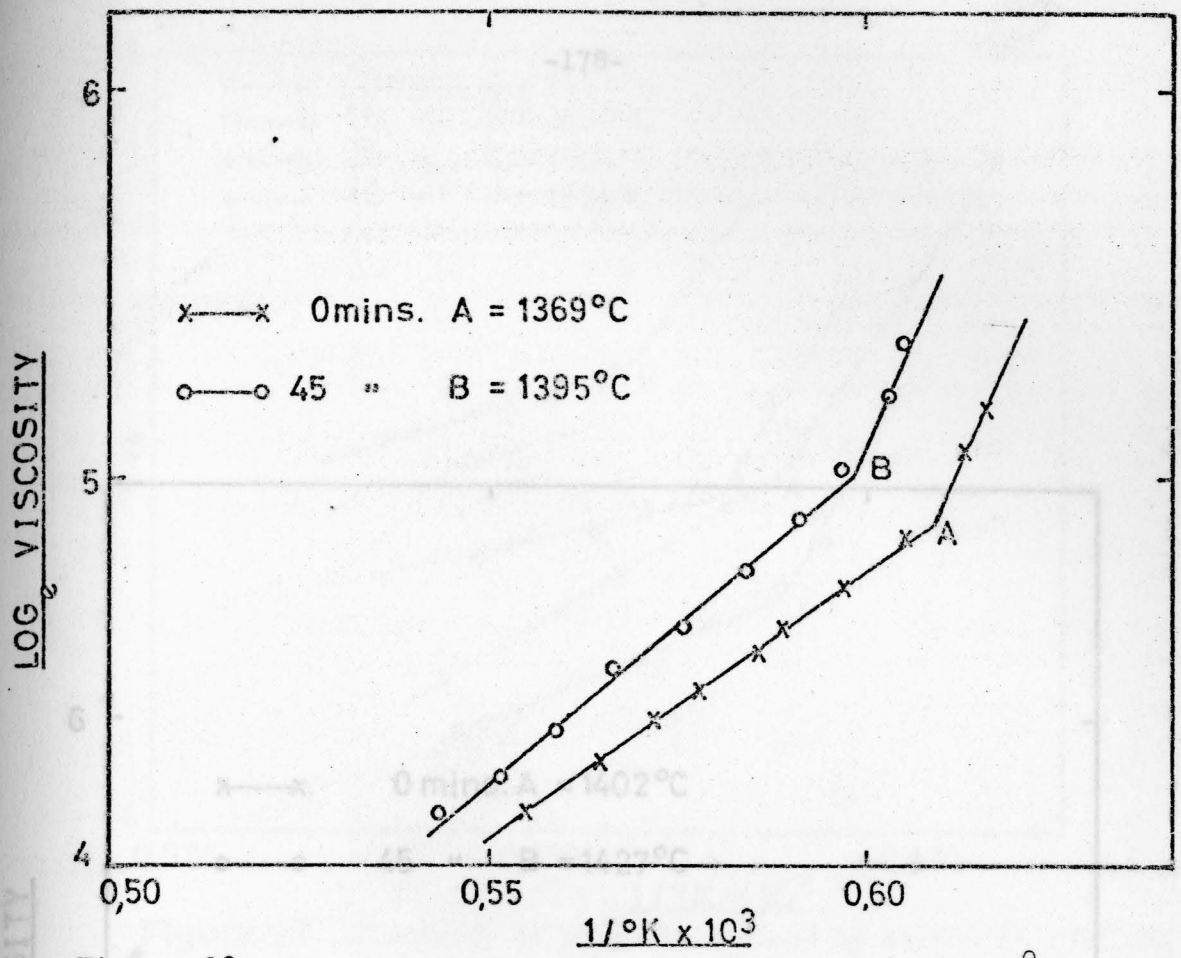


Figure 96 Viscosity of slag B32 reduced by carbon at 1550°C

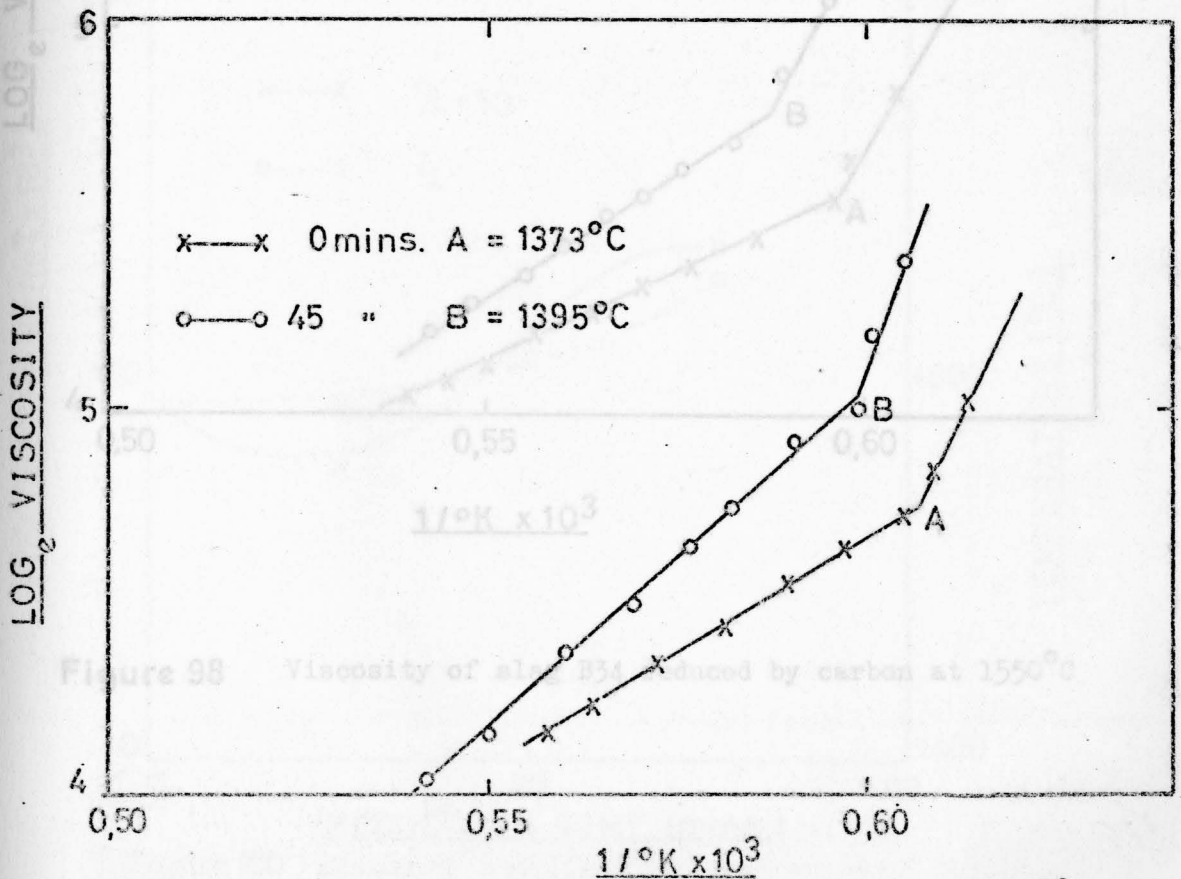


Figure 97 Viscosity of slag B33 reduced by carbon at 1550°C

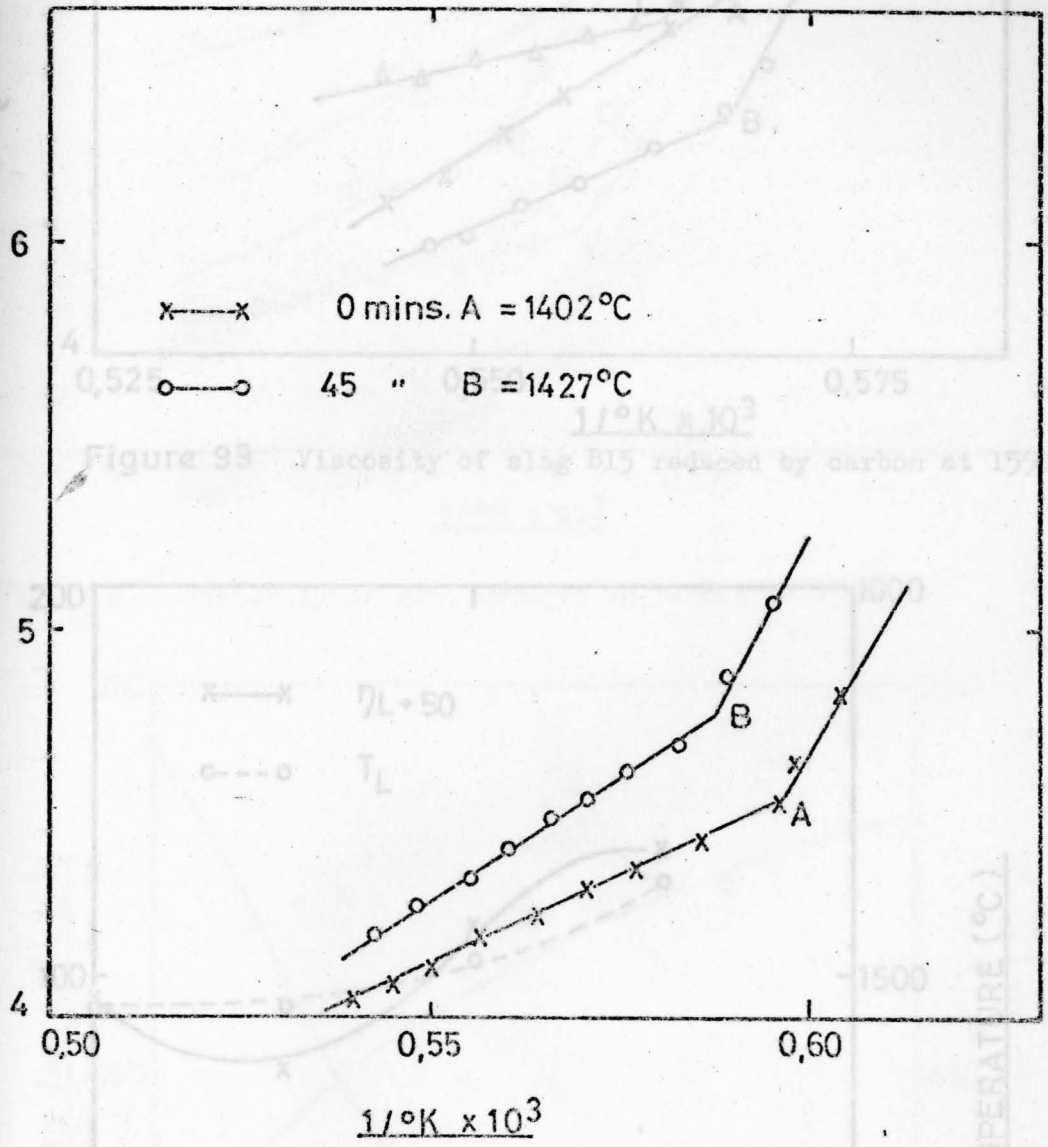


Figure 98 Viscosity of slag B34 reduced by carbon at 1550°C

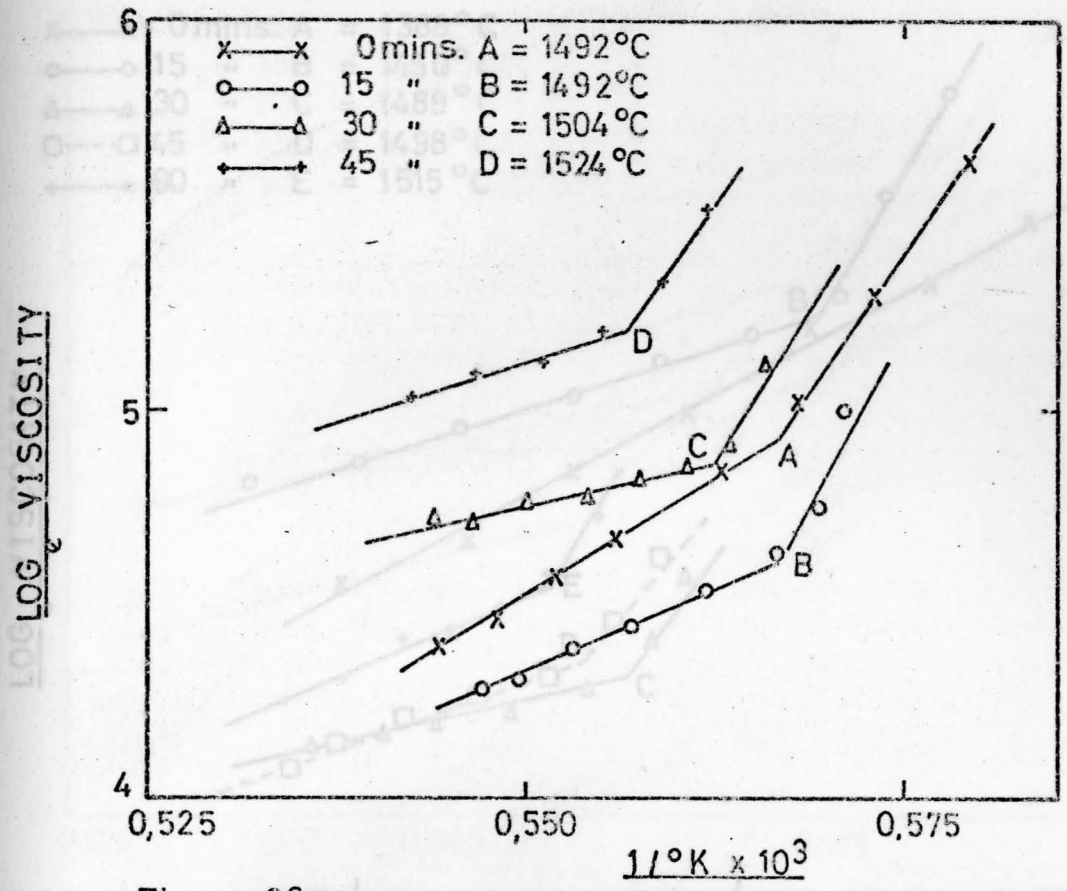


Figure 99 Viscosity of slag B15 reduced by carbon at 1550°C

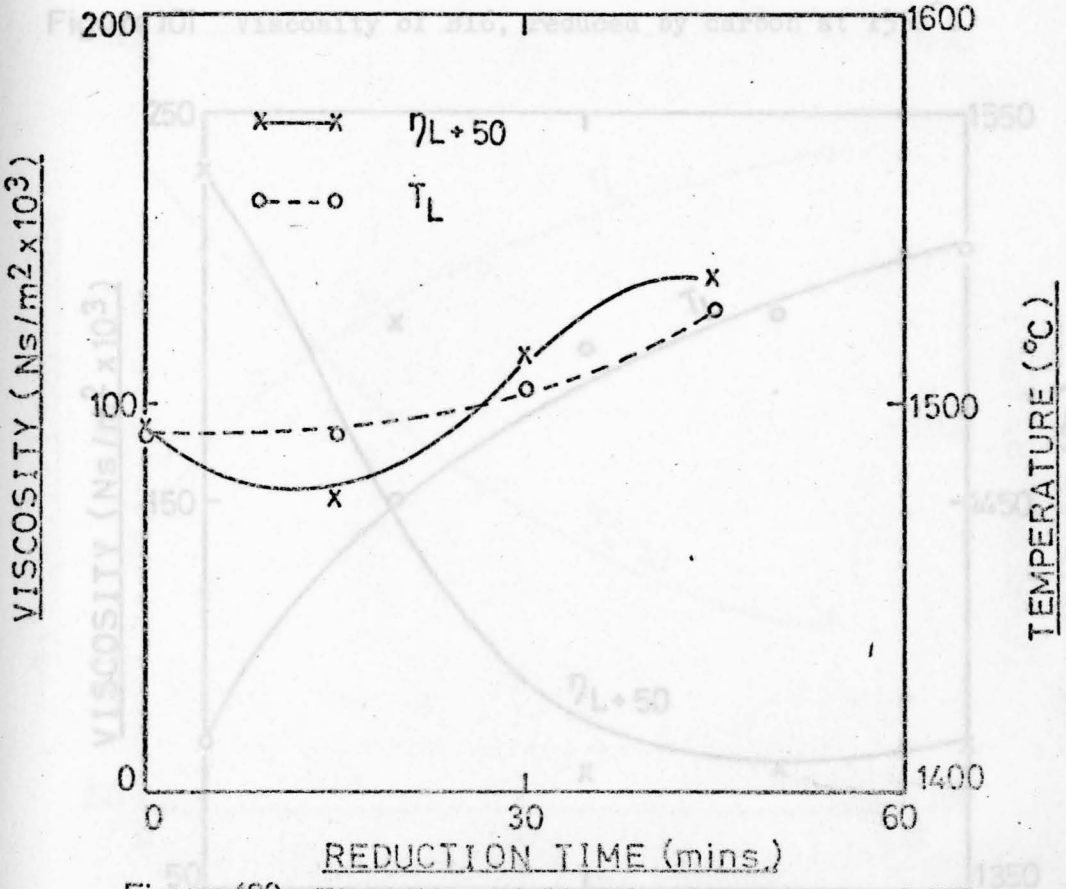


Figure 100 Viscosity and liquidus temperature of B15, reduced at 1550°C

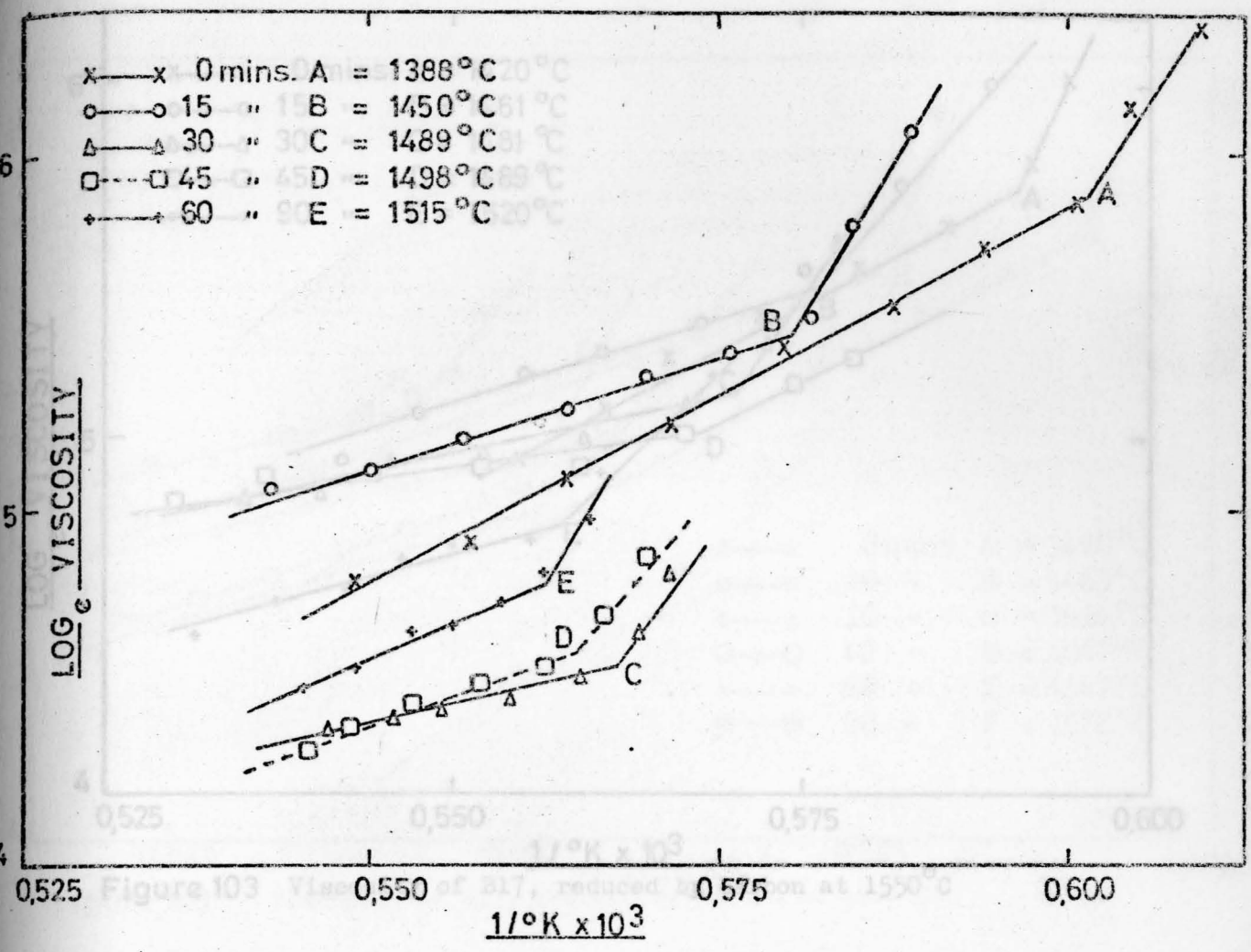


Figure 101 Viscosity of B16, reduced by carbon at 1550°C

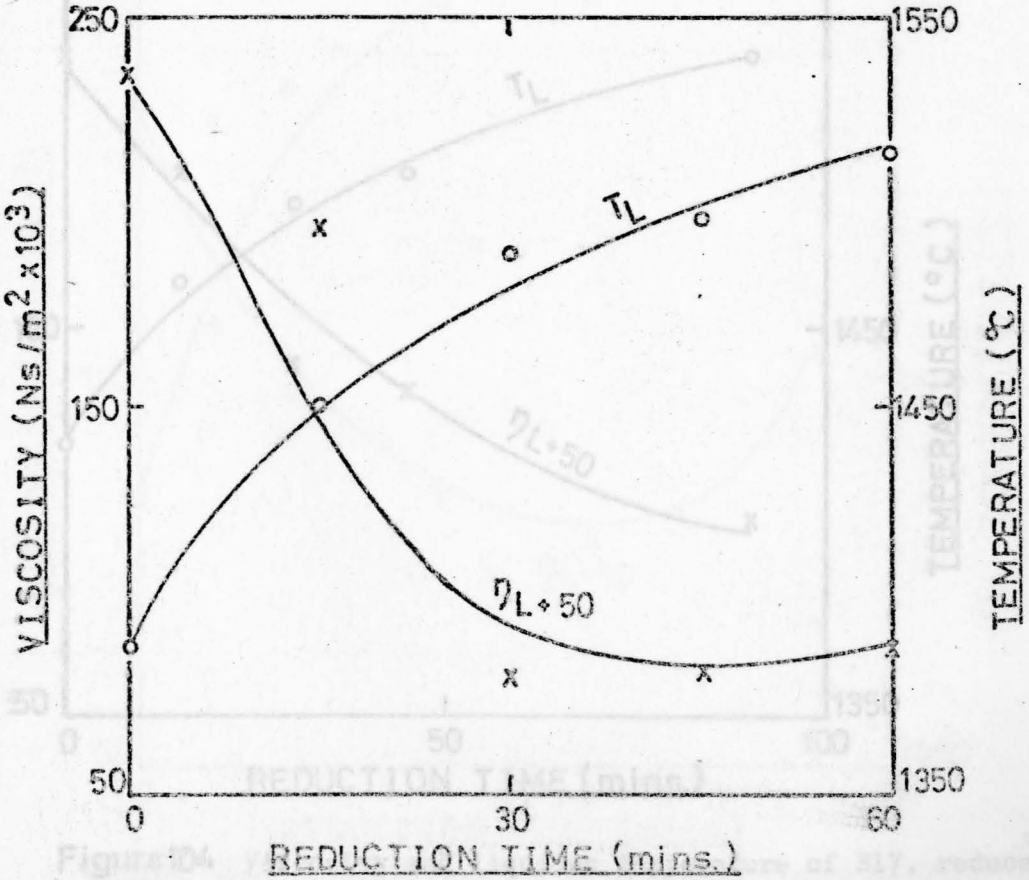


Figure 102 Viscosity and liquidus temperature of B16, reduced at 1550°C

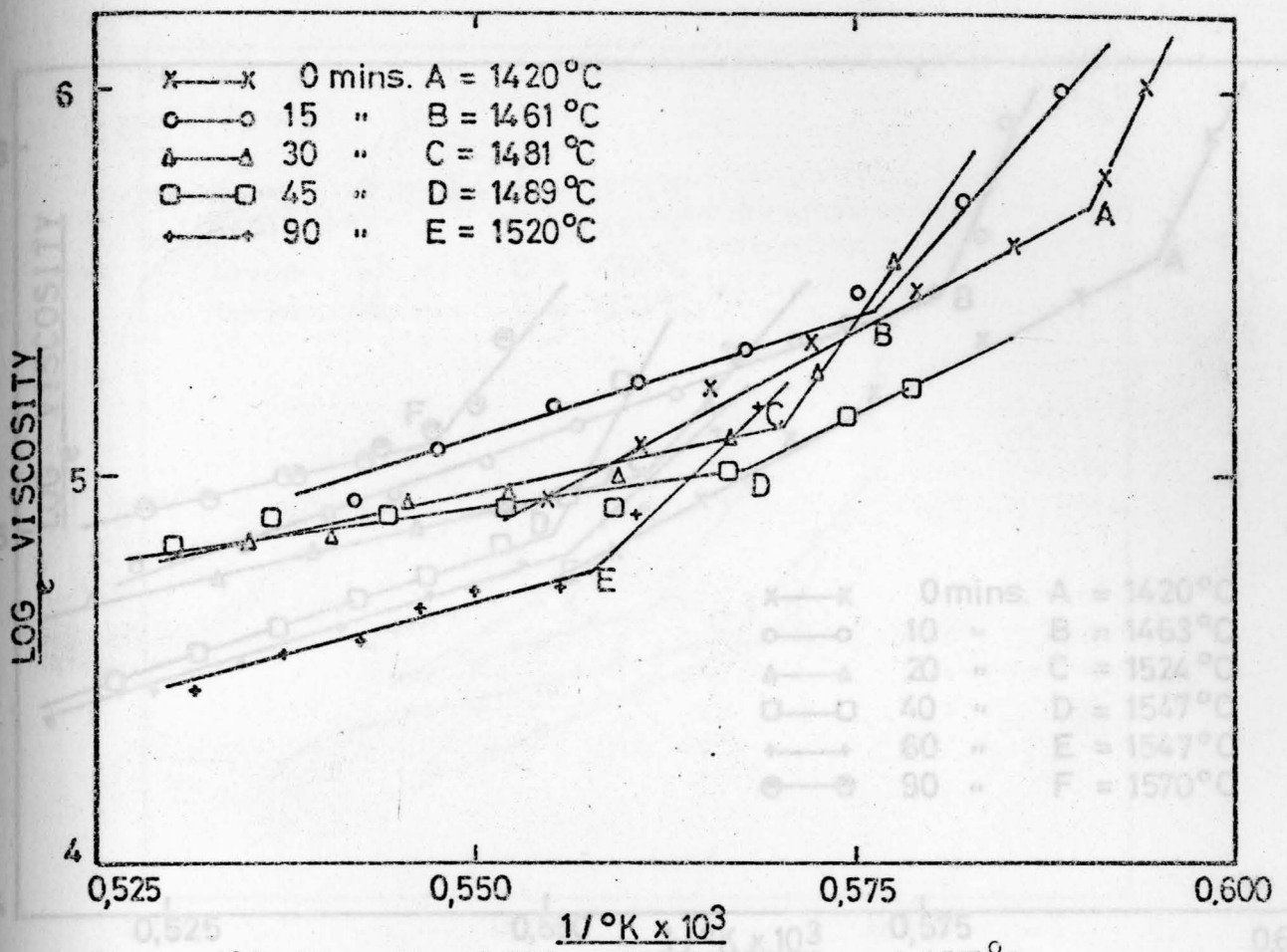


Figure 103 Viscosity of B17, reduced by carbon at 1550°C

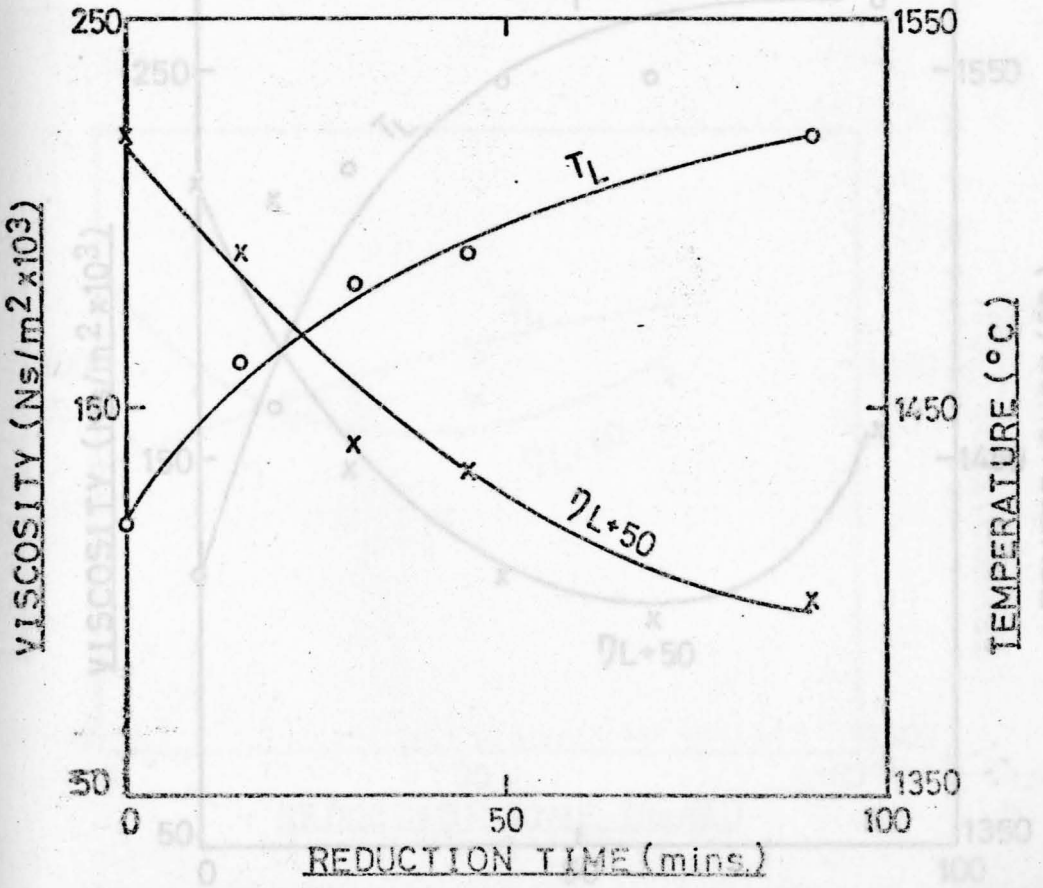


Figure 104 Viscosity and liquidus temperature of B17, reduced at 1550°C

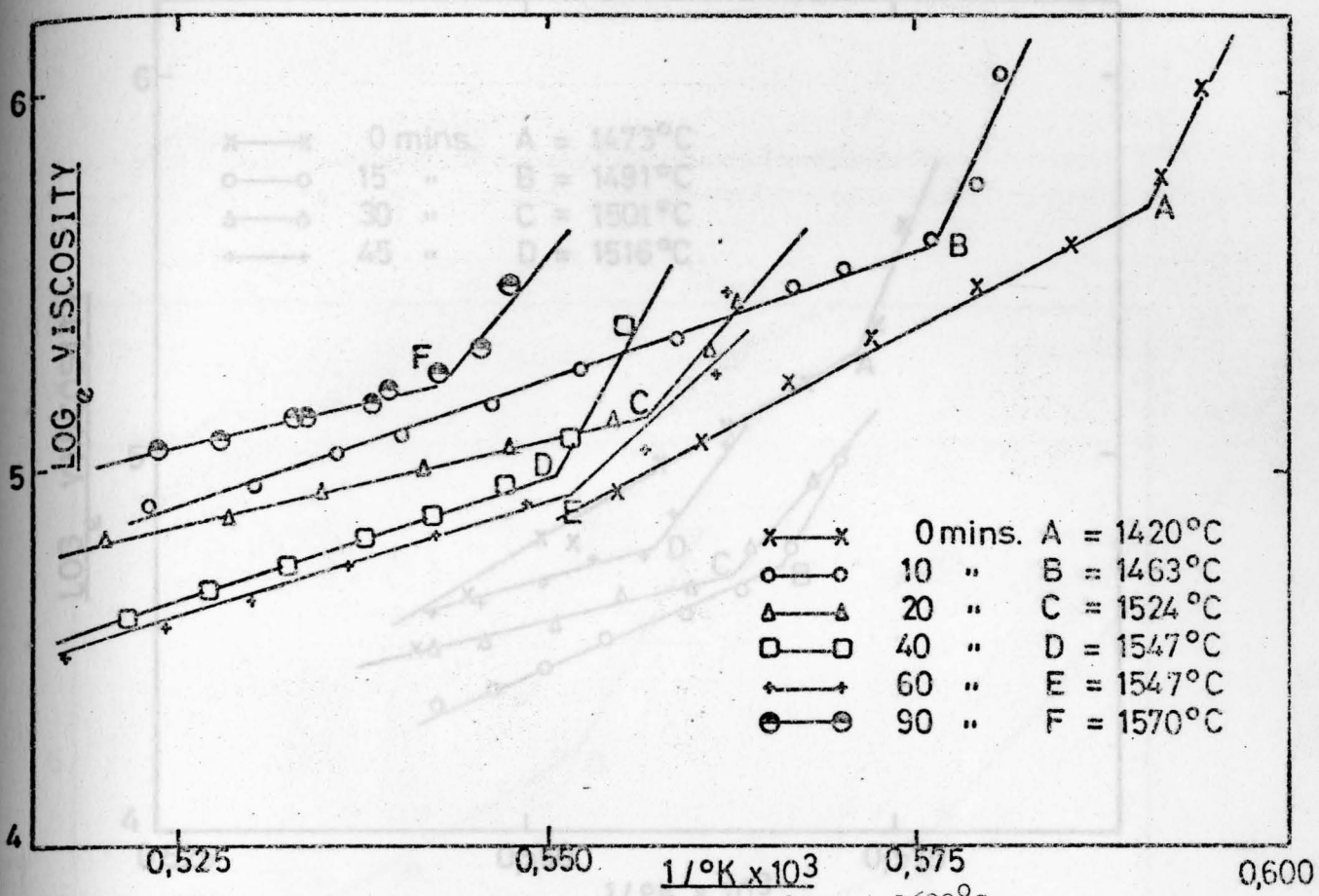


Figure 105 Viscosity of B17, reduced by carbon at 1600°C

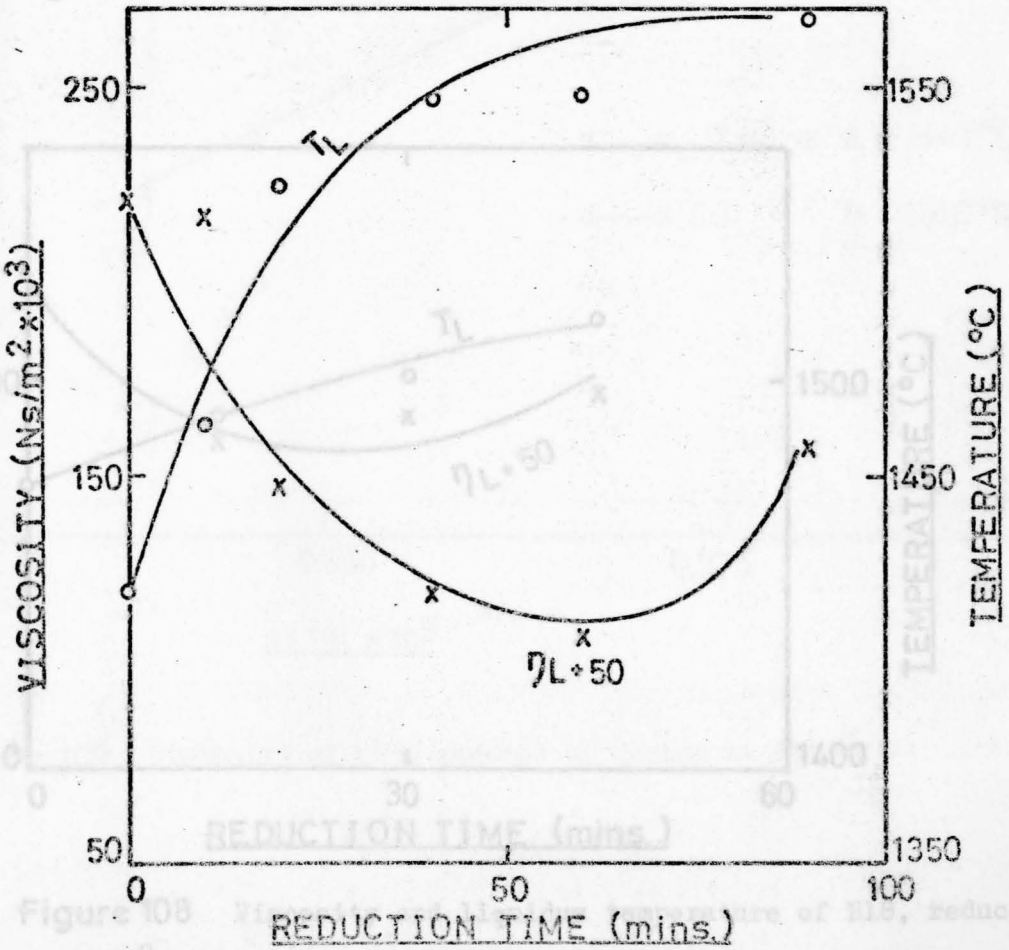


Figure 106 Viscosity and liquidus temperature of B17, reduced at 1600°C

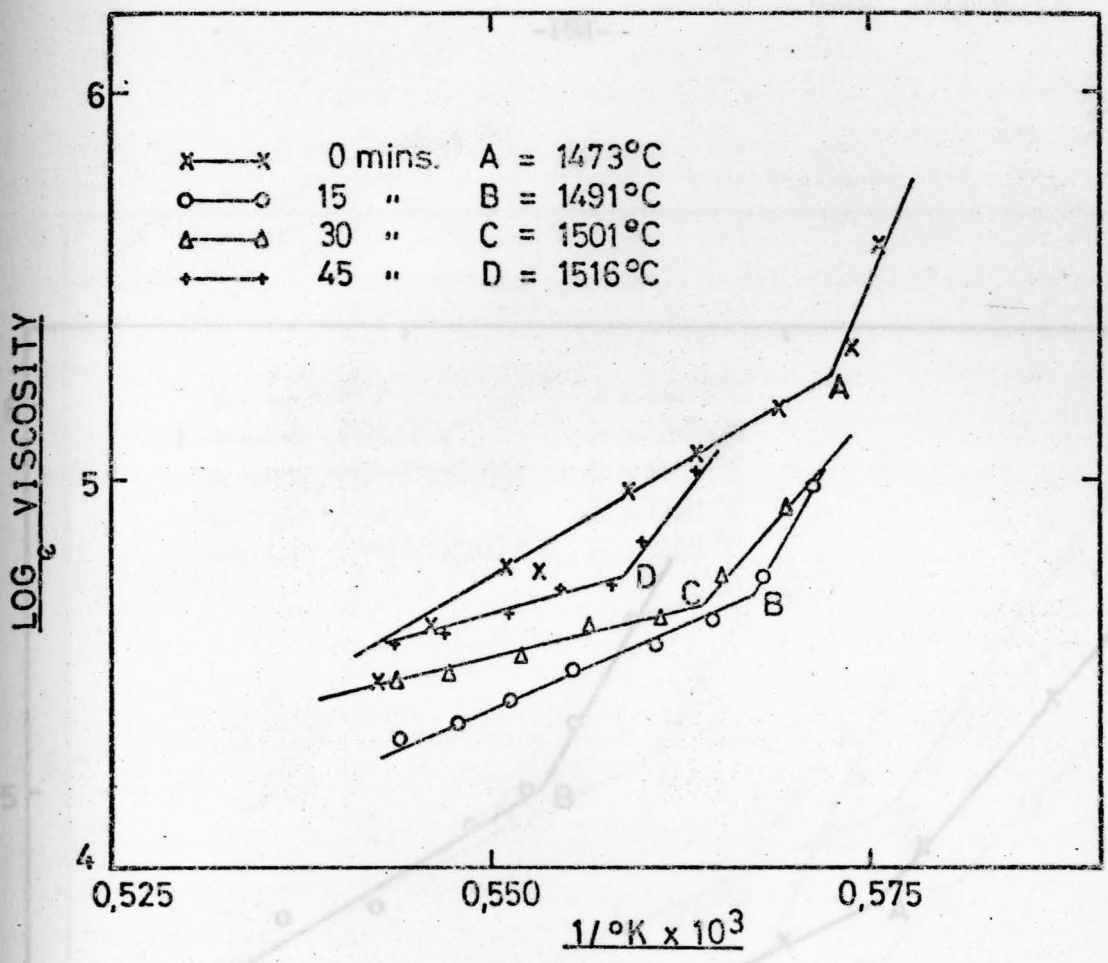


Figure 107 Viscosity of B18, reduced by carbon at 1550°C

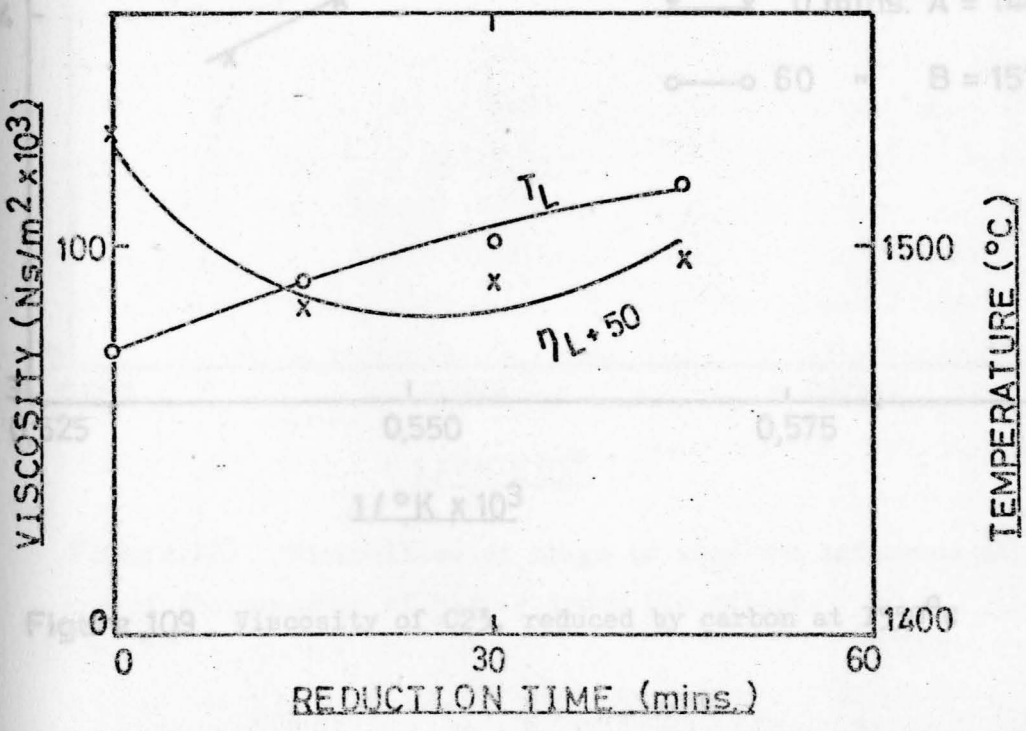


Figure 108 Viscosity and liquidus temperature of B18, reduced at 1550°C

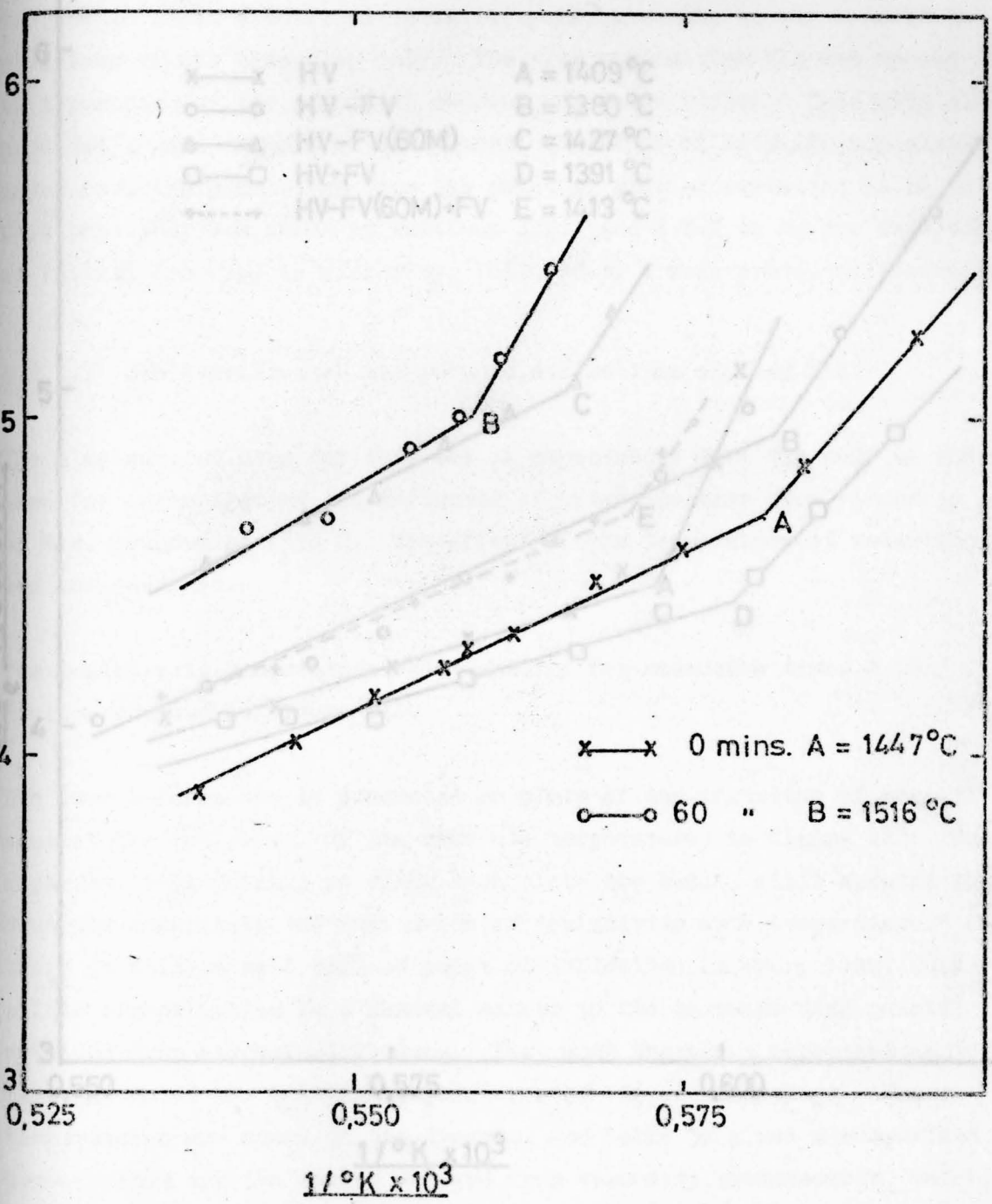


Figure 109 Viscosity of C23, reduced by carbon at 1550°C

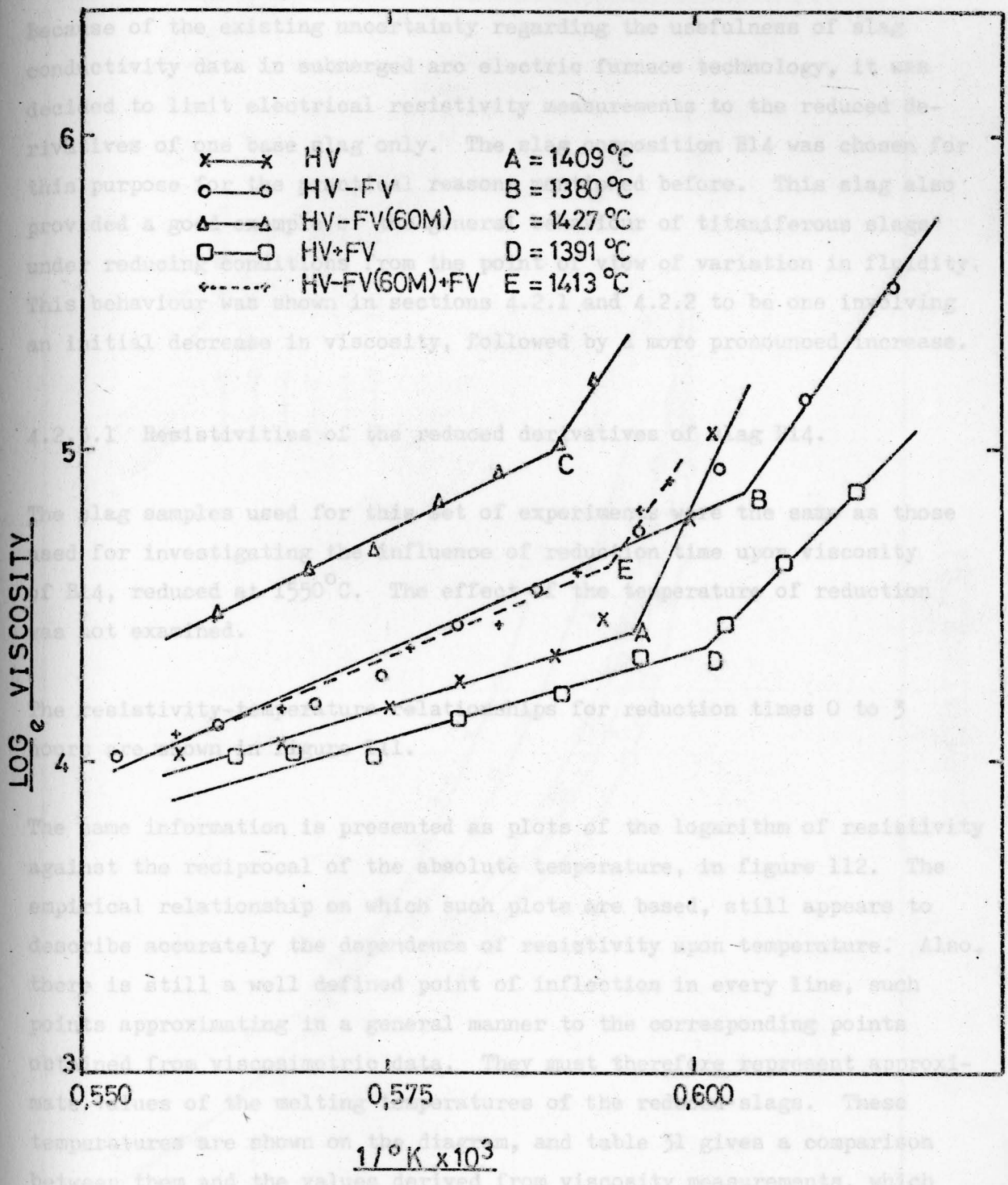


Figure 110 Viscosities of slags to show the influence of reduction and of the presence of highly reducible oxides.

4.2.3 Resistivity of reduced slags

Because of the existing uncertainty regarding the usefulness of slag conductivity data in submerged arc electric furnace technology, it was decided to limit electrical resistivity measurements to the reduced derivatives of one base slag only. The slag composition B14 was chosen for this purpose for the practical reasons mentioned before. This slag also provided a good example of the general behaviour of titaniferous slags under reducing conditions from the point of view of variation in fluidity. This behaviour was shown in sections 4.2.1 and 4.2.2 to be one involving an initial decrease in viscosity, followed by a more pronounced increase.

4.2.3.1 Resistivities of the reduced derivatives of slag B14.

The slag samples used for this set of experiments were the same as those used for investigating the influence of reduction time upon viscosity of B14, reduced at 1550°C. The effect of the temperature of reduction was not examined.

The resistivity-temperature relationships for reduction times 0 to 3 hours are shown in figure 111.

The same information is presented as plots of the logarithm of resistivity against the reciprocal of the absolute temperature, in figure 112. The empirical relationship on which such plots are based, still appears to describe accurately the dependence of resistivity upon temperature. Also, there is still a well defined point of inflection in every line, such points approximating in a general manner to the corresponding points obtained from viscosimetric data. They must therefore represent approximate values of the melting temperatures of the reduced slags. These temperatures are shown on the diagram, and table 31 gives a comparison between them and the values derived from viscosity measurements, which were shown in figure 87.

Figure 113 is a graphical representation of the variation of resistivity, as well as the variation in melting temperature, with time of reduction. Reduction by carbon causes a marked decrease in the resistivity of the slag at least over the first 90 minutes. Only thereafter there appears to be a slight increase in the resistance of the melt. The values of

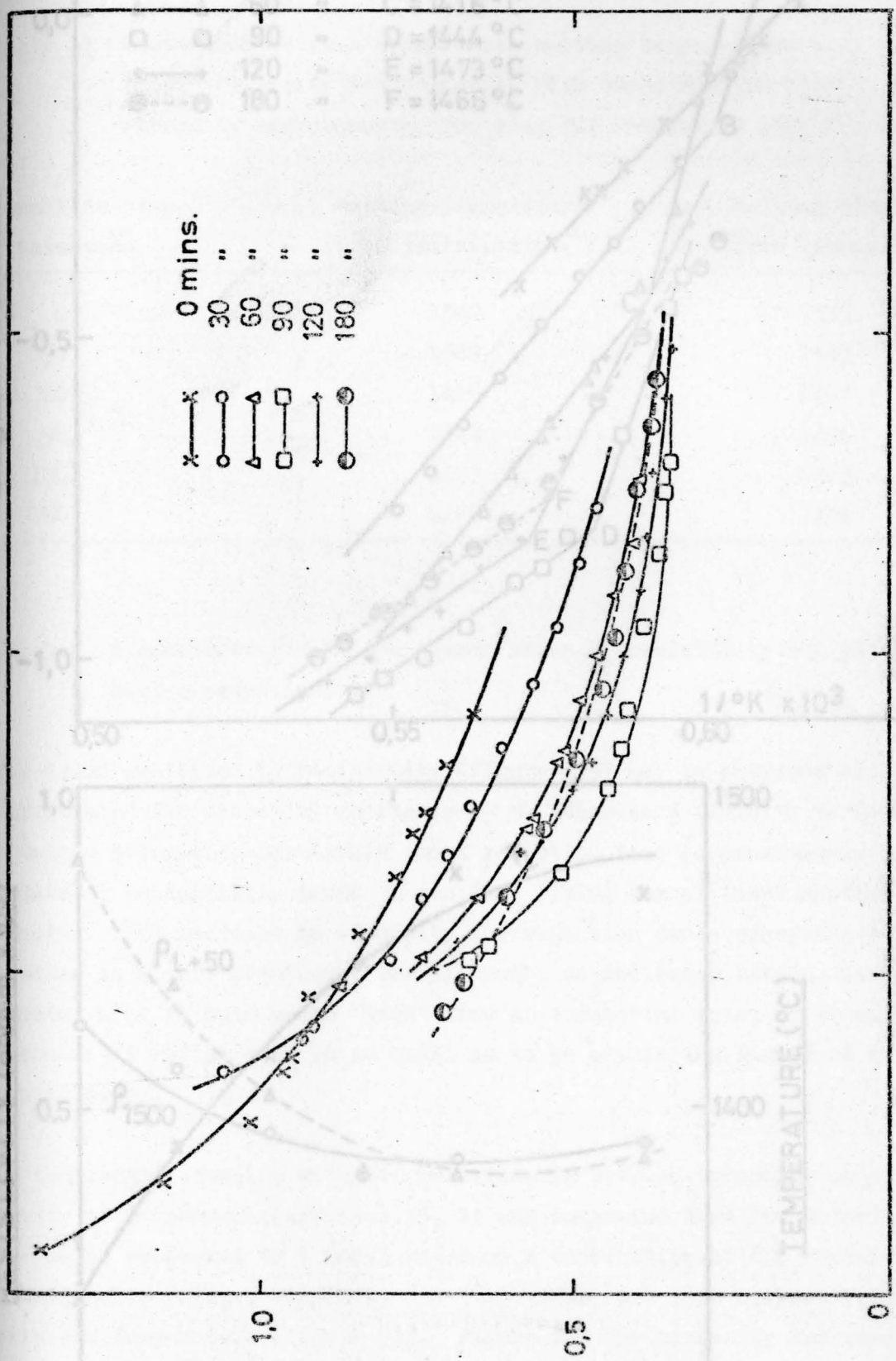
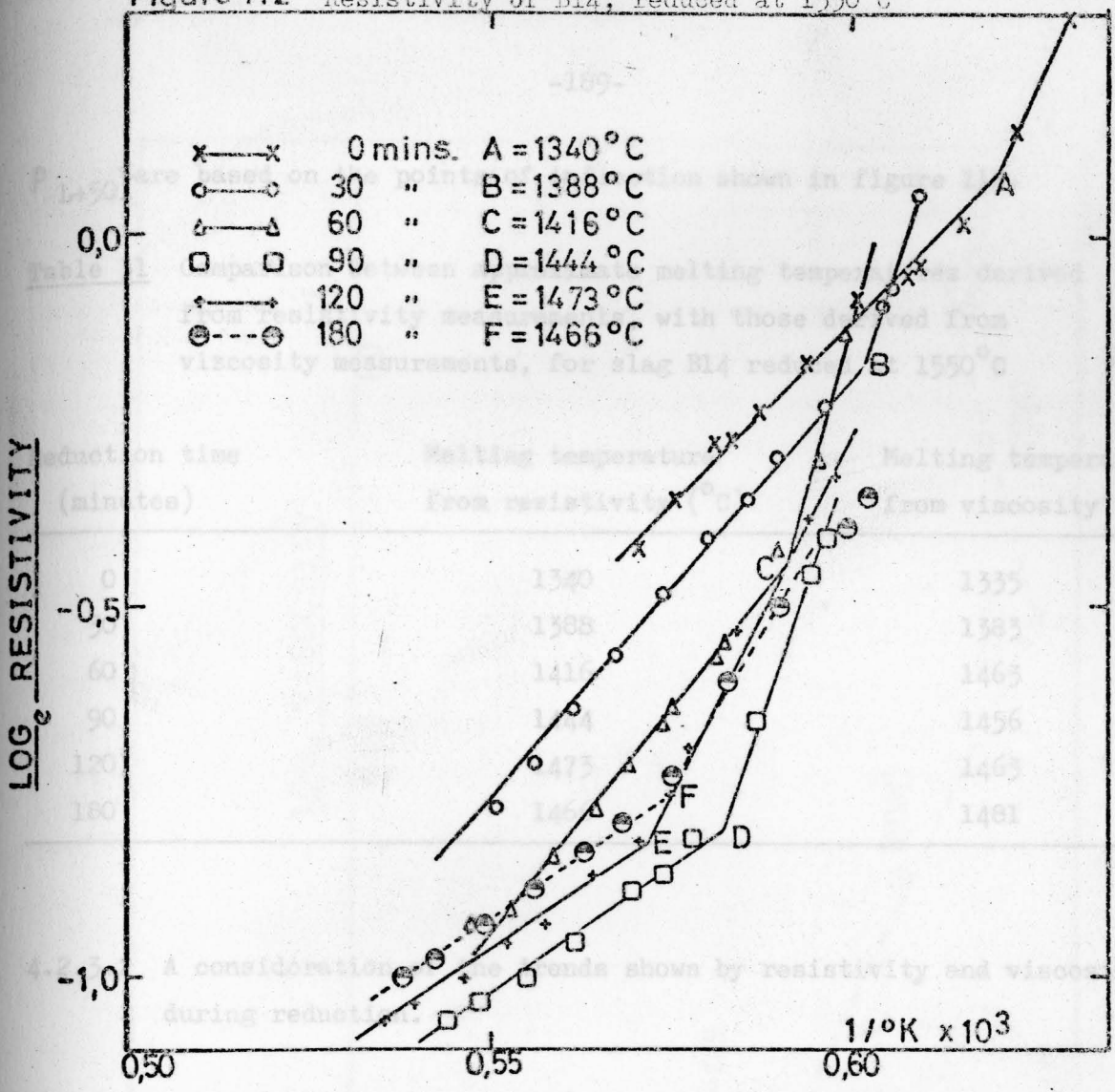


Figure 111 Resistivity of slag B14, reduced by carbon at 1550°C

Figure 112 Resistivity of B14, reduced at 1550°C



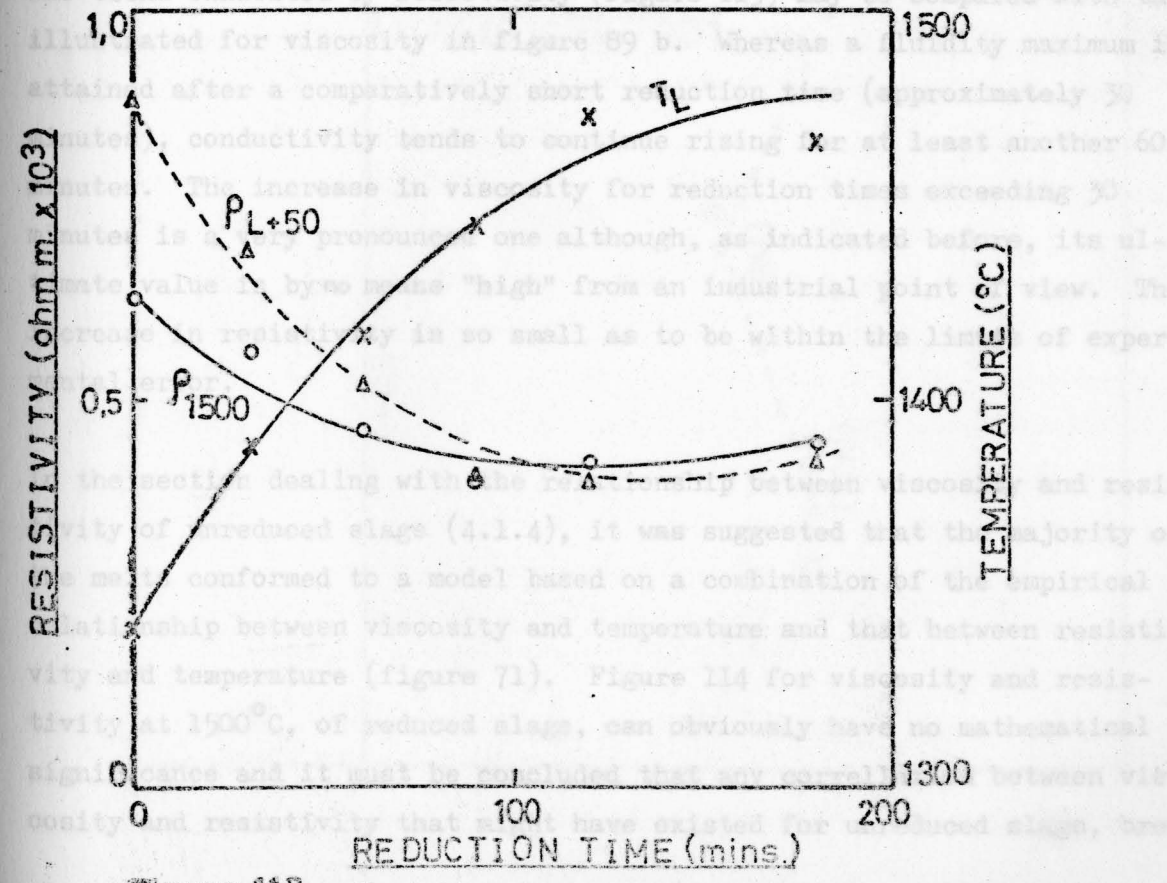


Figure 113 Variation in resistivity and melting temperature - slag B14 reduced at 1550°C

ρ_{L+50} are based on the points of inflection shown in figure 112.

Table 31 Comparison between approximate melting temperatures derived from resistivity measurements, with those derived from viscosity measurements, for slag B14 reduced at 1550°C

Reduction time (minutes)	Melting temperature from resistivity (°C)	Melting temperature from viscosity (°C)
0	1340	1335
30	1388	1383
60	1416	1463
90	1444	1456
120	1473	1463
180	1466	1481

4.2.3.2 A consideration of the trends shown by resistivity and viscosity during reduction.

The trend exhibited by resistivity (figure 113) may be compared with that illustrated for viscosity in figure 89 b. Whereas a fluidity maximum is attained after a comparatively short reduction time (approximately 30 minutes), conductivity tends to continue rising for at least another 60 minutes. The increase in viscosity for reduction times exceeding 30 minutes is a very pronounced one although, as indicated before, its ultimate value is by no means "high" from an industrial point of view. The increase in resistivity is so small as to be within the limits of experimental error.

In the section dealing with the relationship between viscosity and resistivity of unreduced slags (4.1.4), it was suggested that the majority of the melts conformed to a model based on a combination of the empirical relationship between viscosity and temperature and that between resistivity and temperature (figure 71). Figure 114 for viscosity and resistivity at 1500°C, of reduced slags, can obviously have no mathematical significance and it must be concluded that any correllation between viscosity and resistivity that might have existed for unreduced slags, breaks

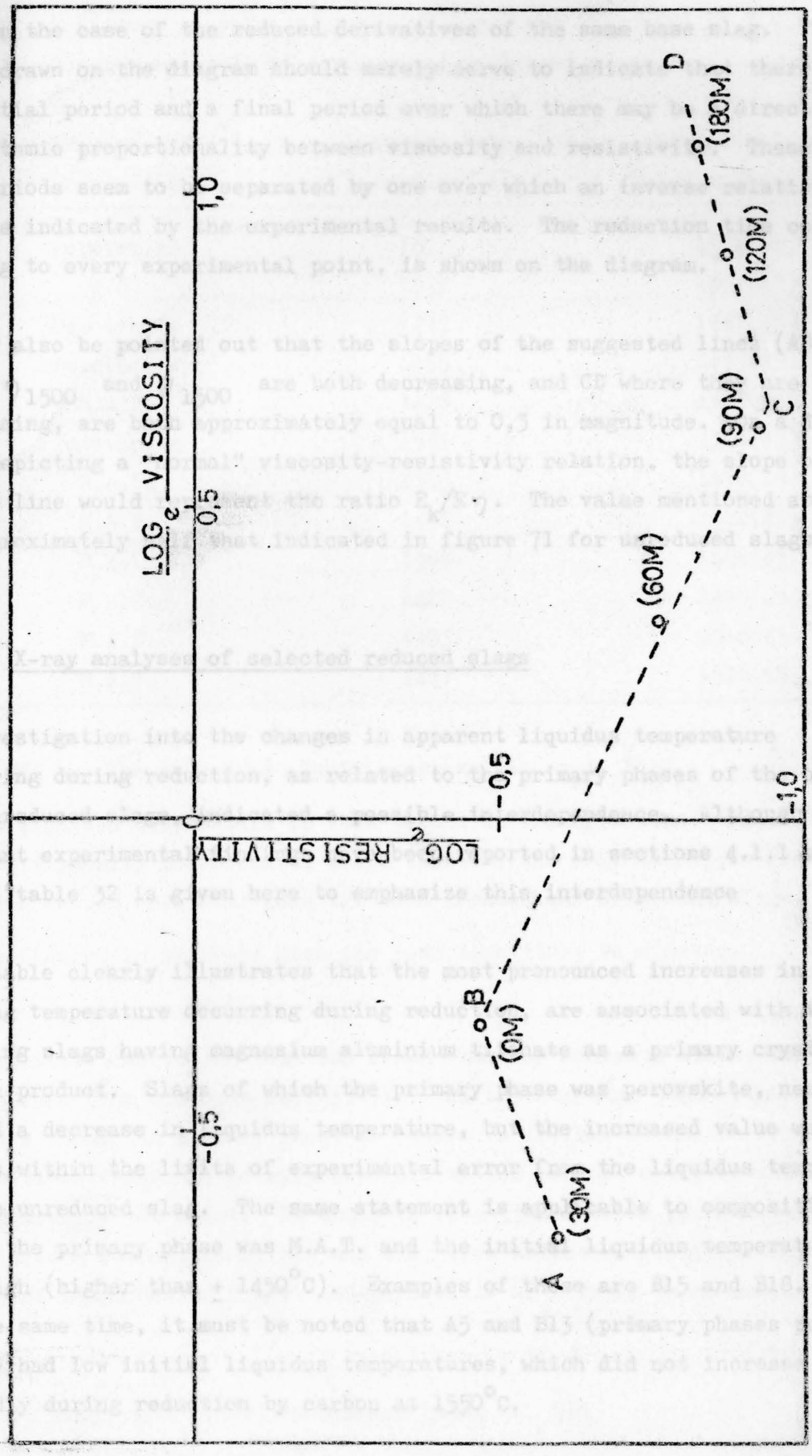


Figure 114 Viscosity and resistivity at 1500°C, for B14 reduced at 1550°C

down in the case of the reduced derivatives of the same base slag. The lines drawn on the diagram should merely serve to indicate that there is an initial period and a final period over which there may be a direct logarithmic proportionality between viscosity and resistivity. These two periods seem to be separated by one over which an inverse relationship is indicated by the experimental results. The reduction time corresponding to every experimental point, is shown on the diagram.

It may also be pointed out that the slopes of the suggested lines (AB where η_{1500} and ρ_{1500} are both decreasing, and CD where they are both increasing, are both approximately equal to 0,3 in magnitude. On a diagram depicting a "normal" viscosity-resistivity relation, the slope of such a line would represent the ratio $E_k/E\eta$. The value mentioned above, is approximately half that indicated in figure 71 for unreduced slags.

4.2.4 X-ray analyses of selected reduced slags

An investigation into the changes in apparent liquidus temperature occurring during reduction, as related to the primary phases of the original unreduced slags, indicated a possible interdependence. Although the relevant experimental findings have been reported in sections 4.1.1 and 4.2.1, table 32 is given here to emphasize this interdependence

This table clearly illustrates that the most pronounced increases in melting temperature occurring during reduction, are associated with those starting slags having magnesium aluminium titanate as a primary crystallization product. Slags of which the primary phase was perovskite, never showed a decrease in liquidus temperature, but the increased value was always within the limits of experimental error from the liquidus temperature of the unreduced slag. The same statement is applicable to compositions where the primary phase was M.A.T. and the initial liquidus temperature was high (higher than $\pm$ 1450°C). Examples of these are B15 and B18. At the same time, it must be noted that A5 and B13 (primary phases perovskite) had low initial liquidus temperatures, which did not increase markedly during reduction by carbon at 1550°C.

Table 32 A summary of primary phases of unreduced slags and of liquidus temperatures of reduced and unreduced slags.

Slag No.	Primary phase* (unreduced slag)	Liquidus temp.(°C)** (unreduced slag)	Liquidus temp.(°C)*** (slag reduced at 1550°C)
A5	Perovskite	1361	1374(60)
A8	n.d.	1322	1451(45)
B10	Perovskite	1472	1481(45)
B11	Perovskite	1455	1475(45)
B12	M.A.T.	1478	1517(45)
B13	Perovskite	1337	1350(45)
B14	M.A.T.	1335	1438(45)
B15	M.A.T.	1492	1524(45)
B16	M.A.T.	1388	1498(45)
B17	M.A.T.	1420	1489(45)
B18	M.A.T.	1473	1516(45)
C23	M.A.T.	1447	1516(60)

* M.A.T. = The magnesium aluminium titanate $Mg_4Al_2Ti_9O_{25}$

** The liquidus temperature in this column is the approximate value derived from viscosity measurement, since this was the only technique from which values were available for both reduced and unreduced slags.

*** The figures in brackets give the reduction times in minutes.

The tentative conclusion that was drawn from the comments above, was that oxygen loss from mixtures having M.A.T. as the starting primary phase, caused a change in primary phase to occur. A similar mechanism for those compositions where the primary crystallization product was perovskite, did apparently not exist. In order to investigate these possibilities, two starting compositions, B14 and B11, were selected to represent the groups of slags having M.A.T. and perovskite as primary phase respectively.

4.2.4.1 Slags with M.A.T. as primary phase - B14

It was considered possible that the precipitation of a refractory phase

such as titanium carbide during reduction, might be responsible for depletion of the bulk of the melt with respect to titanium. If such a high melting phase were to adhere to the wall of the graphite crucible, the overall composition of the slag used for either viscosity or resistivity measurement, could be different from that of the original slag. Removal of titanium to an appreciable extent in this manner could possibly give rise to a change of primary phase. However, as shown in table 13 (section 3.9), severely reduced samples of slag B14 were found to be of substantially the same composition as the unreduced slag. It was also mentioned in section 3.9 that an attempt was made to detect titanium carbide on the surface of the solid slag that was in contact with the graphite crucible during the reduction stage. The technique earlier described in this connection, was also applied to the sample reduced for 90 minutes at 1550°C. In neither case (120 or 90 minutes) did X-ray analysis of the powdered sample scraped from the surface, reveal the presence of the carbide.

Further investigations were confined mainly to the slag sample that had been reduced for 90 minutes. If an alternative product of reduction did exist, it was most likely to be concentrated in the vicinity of the slag-graphite interface, or at the free surface of the slag if density differences were appreciable. A total of four samples for X-ray analyses were removed from the slag ampule after removal from the graphite crucible, by light scraping with a diamond drill - two from the surface that was in contact with the graphite crucible wall (A), one from the surface that was in contact with the crucible bottom (B) and one from the free slag surface (C).

The X-ray patterns obtained from the samples A were complex. The lines for M.A.T. and perovskite were identified for one of the samples. The remaining lines were found to be best interpreted as belonging to a mixture of lower titanium oxides (higher than $TiO_{1,5}$), with the oxide Ti_3O_5 (anosovite) predominating. The other A-sample gave a similar pattern, except that the lines for perovskite were absent.

Sample B also consisted of a mixture of lower oxides, in addition to M.A.T. and perovskite.

Sample C gave no pattern and must have been in the glassy state.

The fact that no graphite was detected anywhere could only have been due to the manner in which the samples were taken, because it was visible with the naked eye.

The solid cylindrical slag sample as removed from the graphite crucible, had the following approximate dimensions: height = diameter = 30 mm. A 12,5 mm diameter hole was drilled into the 90-minute cylinder to a depth of approximately 20 mm. The resulting powder was ground in a tungsten carbide ball mill (agate vessel) to be 100% (-325 mesh). Two samples of the powder were then treated in the cell of the high temperature microscope, as described in section 3.8. The quenching temperature in both instances was 1440°C. (The liquidus temperature of the original slag by hot stage microscopy was 1365°, and that of the reduced slag 1456° and 1444° by viscosity and resistance measurement respectively). The simple set of lines obtained by X-ray diffraction analysis of both samples very clearly belonged to $MgO.Al_2O_3$.

It was not attempted to determine the liquidus temperature of the bulk core sample. It must be pointed out here that, although the complete sequence of crystallization products of the unreduced slag was not determined, the secondary phase, following M.A.T., was found to be perovskite. The exact temperature at which the latter phase appeared, was not determined either.

Table 33 Crystallization products of unreduced B14, quenched from different temperatures.

Quenching temperature (°C)	Solid phases present
1315	M.A.T.
1290	M.A.T. and $CaO.TiO_2$
1260	M.A.T. and $CaO.TiO_2$

Thus, although the spinel phase was not proved to be absent from the complete crystallization sequence of the unreduced slag, it definitely does not appear at temperatures above 1260°C.

The slag samples that had been reduced for 60 minutes and for 120 minutes

were subsequently also treated in the manner described above, to obtain core samples for X-ray examination. The respective quenching temperatures were 1400° and 1440°C. In both instances the primary phase was identified as $MgO.Al_2O_3$.

The approximate liquidus temperatures derived from either viscosity or resistance measurement of slag B14, reduced for 90 minutes (1456° and 1444°C respectively) do not refer to the core samples on which the experiments described above, were conducted. Measurements were carried out on reduced slags in molybdenum crucibles in an inert atmosphere after homogenization at temperatures normally in excess of 1550°C, for 1½ hours. Any segregation of solid phases that might have existed immediately after reduction, must therefore at least be altered in the melt used for viscosity or resistance measurement. It must also be borne in mind that more uncertainty attaches to the melting temperatures reported for severely reduced slags (longer than 90 minutes at 1550°C) than to those suggested for slags reduced for shorter intervals. This is shown to a certain extent by the relatively large differences reported between values from the two experimental sources, after prolonged reduction.

The sample of B14 that had been reduced for 90 minutes, on which viscosity and resistivity measurements were performed, was used for the following series of experiments. The entire 55 gm sample was drilled out of the molybdenum crucible and reduced in size as described for the core sample above. Five X-ray diffraction camera samples were prepared in the cell of the high temperature microscope as before. The results of the analyses are given in table 34.

Table 34 Crystallization products of homogenized B14 reduced for 90minutes at 1550°C, quenched from different temperatures

Quenching temperature (°C)	Solid phases present
1390	M.A.T and $MgO.Al_2O_3$
1400	M.A.T and $MgO.Al_2O_3$
1410	M.A.T and $MgO.Al_2O_3$
1440	M.A.T and $MgO.Al_2O_3$
1460	No pattern

The most important fact arising from the results of this work, is that the "approximate melting temperatures", derived indirectly for reduced slags, truly have the significance so far attached to them. This particular reduced derivative has an actual liquidus temperature between 1440° and 1460°C. There may be a temperature interval within this 20° range, over which either one of the two phases M.A.T. or $MgO.Al_2O_3$ exists as a single true primary phase. However, it appears to be more important that the presence of a phase not present at high temperature in the unreduced slag, was proved for the reduced slag beyond any doubt.

4.2.4.2 Slags with perovskite as the primary phase - B11

The sample of slag that had been reduced for 90 minutes at 1550°C, was treated in essentially the same way as the corresponding sample of B14.

The surface powders again contained what appeared to be a mixture of lower titanium oxides, in addition to perovskite.

The core powder quenched from a temperature of 1430° generally showed only the pattern of perovskite, although one of the samples showed signs of the presence of the spinel phase. Two later experiments employing different samples but the same quenching temperature, failed to confirm the existence of $MgO.Al_2O_3$.

The single X-ray sample prepared from the bulk on which viscosity and resistance measurements had been performed, and quenched from 1430°C, showed the presence of $CaO.TiO_2$ only.

The secondary phase of the unreduced slag was M.A.T.

From these findings it must be concluded that under the particular set of experimental conditions used, the primary phase of slag B11 (taken to represent all those compositions the primary phase of which is perovskite) is not altered by reduction. However, if the primary phase of the unreduced slag is M.A.T., then loss of oxygen from the system causes the appearance of the spinel phase $MgO.Al_2O_3$, which can be expected to give rise to an increase in the liquidus temperature of the slag.

Although the primary phase of unreduced A8 was not determined, its behaviour during reduction strongly suggests that the primary phase was M.A.T. Also, the series of slags with CaO/MgO = 1 and basicity ratios differing by 0,05 (B28-B29-B14-B30-B31-B32-B33-B34-B11) may be expected to go through a change in the primary crystallization product from M.A.T. on the acidic side to perovskite on the basic side, at a $(CaO+MgO)/SiO_2$ value of 1,50 to 1,55 (represented by slags B31 and B32). There can be no doubt about a change taking place between B14 (M.A.T.) and B11($CaO.TiO_2$) with basicity ratios 1,4 and 1,7 respectively, but the change in behaviour under reducing conditions as outlined in section 4.2.1.1 appears to indicate the point where the change actually occurs, more closely.

4.2.5 Degree of reduction of reduced slags

The technique employed for determining approximate degrees of reduction after the slags had been allowed to react with graphite for selected time intervals, and for determining the rate of reduction of titania to lower oxides in some slags, was described in section 3.9.

Not all compositions involved during the determination of properties such as viscosity and electrical resistivity that has been described, were tested in this study. Starting slags were again selected on the basis of the parameters $(CaO+MgO)/SiO_2$, CaO/MgO and mass % $(TiO_2 + Al_2O_3)$, but a single series comprising three slags, was used to demonstrate the influence of a given composition variable upon the extent of reduction with respect to titanium oxide. Generally, slags of a particular series are compared on the basis of the mass gain suffered during complete re-oxidation of the various members, after reduction for one specified time interval at 1550°C.

Comprehensive testing at increasing reduction time, in order to determine a rate of reduction, was performed for slags B11, B14 and B17 only. These are also the slags that were more fully reported on in the section dealing with variations in viscosity and melting temperature under reducing conditions. (4.1.1)

The effect of temperature on the rate of reduction was only determined

for these three slags as well, and once again, the emphasis was on slag B14, which was subjected to reduction at three different temperatures.

Miscellaneous reoxidation experiments were conducted on a plant slag and also on the reduced derivatives arising from slag-metal-graphite reaction where the initial slag contained iron and vanadium oxides in addition to the basic five components.

4.2.5.1 Preliminary work

(a) The plant slag HV

The composition of this slag was given in table 13. The results of viscosity measurements carried out upon it, were reported in section 4.2.1.4.

The aim of the experiment described here was to determine an approximate state of oxidation of titanium in a typical plant slag. The choice of the most emphasized reduction times, derived from a degree of reduction, that were to be used for synthetic slags during measurements of viscosity and electrical resistance, was partially based on the result of this work.

Apart from the analytical results reported in table 13, the slag HV was separated into magnetic and non-magnetic fractions. The former was further analysed for Fe and this figure was assumed to represent only metallic iron. The remainder of the figure reported as Fe_2O_3 in the table, was assumed to be in the form of FeO. The slag was also subjected to oxidation at 1100°C and the mass gain recorded.

It must further be borne in mind that the mass gain measured, cannot be ascribed entirely to oxidation of lower titanium oxides. This can reasonably be done in the case of a reduced synthetic slag. In the case of the plant slag, the following oxidation reactions had to be taken into account:

$$2Fe + 3/2O_2 = Fe_2O_3 \quad \ldots\ldots(1)$$

$$2FeO + \tfrac{1}{2}O_2 = Fe_2O_3 \quad \ldots\ldots(2)$$

$$V_2O_3 + O_2 = V_2O_5 \quad \ldots\ldots(3)$$

$$MnO + \tfrac{1}{2}O_2 = MnO_2 \quad \ldots\ldots(4)$$

$$2CrO + \tfrac{1}{2}O_2 = Cr_2O_3 \quad \ldots\ldots(5)$$

The states of oxidation shown on the left hand side above, were assumed to exist before reoxidation of the slag. Those on the right represent the highest state of oxidation, believed to exist after oxidation. If an oxidation state other than the lowest was reported in table 13, it was converted to the lowest form and the mass gain for its complete oxidation calculated. The total of such results had to be subtracted from the value obtained from thermogravimetric analysis, to find the mass gain due only to the oxidation of lower titanium oxides. The relevant results are summarized in table 35.

Table 35 Results of stoichiometry calculations for slag HV.

Metallic iron content of HV	= 1,922 %
FeO content	= 0,32 %
Mol Ti per 100 gm slag	= 0,3868
Mass gain per 100 gm slag during oxidation	= 2,2 gm
Mol oxygen gain per 100 gm slag	= 0,1375
Mol oxygen gain for (1)	= 0,052
(2)	= 0,003
(3)	= 0,008
(4)	= 0,009
(5)	= 0,002
Total (1) to (5)	= 0,074
Molar oxygen gain for Ti alone	= 0,063
Moles oxygen to satisfy TiO_2	= 0,774
Actual moles oxygen available for Ti	= 0,711
O/Ti ratio	= 1,839

Although this figure was useful in deciding upon the reduction times that were to be used for synthetic slags, direct comparison between HV and the synthetic slag B14 as an example, regarding viscosity as a function of reduction time, must be done with great care:

(i) The plant slag does contain other oxides, eg. MnO, FeO, CrO and V_2O_5, whose effects on viscosity in this system are mostly unknown, but which might reasonably be expected to increase the fluidity of the slag. The viscosity lowering effect of FeO was actually proved experimentally (section 4.2.1.4)

(ii) The compositions of B14 and HV differ, even with respect to the five components CaO, MgO, SiO_2, TiO_2 and Al_2O_3 eg. the basicity of HV is 1,53 , compared with 1,40 for B14.

(iii) The analytical figures in table 13 suffer from uncertain degrees of inaccuracy

(b) The synthetic slag M1/1

Primarily the aim of the set of experiments described below, was to follow the rate of reduction of a titaniferous slag with respect to all reducible oxides i.e. FeO, V_2O_5, TiO_2 and SiO_2, by using a dual system of slag in contact with carbon saturated iron. Secondarily, it would allow the determination of a reduction time (on laboratory scale under the particular set of experimental conditions and relative to the starting composition of the slag) which would be necessary for complete reduction of FeO and V_2O_5. The corresponding degree of reduction of TiO_2, when related to earlier experimental results, would give an indication of the state of fluidity of the slag at the time of satisfactory recovery of iron and vanadium. It was intended to follow the course of reduction by analysis of both slag and metal.

A comprehensive study was envisaged, involving mainly the starting slag composition and reduction temperature as variables.

Due to the high fluidity of titaniferous slags and their extremely corrosive action on refractory materials, the common problem of finding a high temperature container for a slag-metal system, was an even more acute one. Several unsuccessful attempts were made to construct a compound crucible to hold the system.

The final procedure was the following: a graphite crucible was charged with a mixture of iron and sufficient carbon to saturate the iron at 1550°C. This was heated in the furnace for 2 hours at 1550° in an argon atmosphere. An equal mass (25 gm) of slag containing both FeO and V_2O_5 was then added to the crucible contents and allowed to react for periods of 30, 60 and 120 minutes, after which the crucible was quenched to room temperature.

This experimental procedure suffered from several drawbacks, including the fact that the reaction was extremely violent. Difficulty was experienced in keeping the slag-metal system inside the crucible. Moreover, the products were difficult to separate, as they consisted of the parent iron layer at the bottom and globules of metal of varying sizes not coalescing with the bulk, in addition to the slag layer. For purposes of analysing the results, the reaction between slag and dissolved carbon and that between slag and free carbon would be impossible to separate.

For these reasons the single slag M1/1 was tested and all further work confined to slags reduced by carbon alone, as described before.

The composition of the starting slag was given in table 13. Results of chemical analyses performed on the reduced slags are shown in table 36.

Table 36 Analyses of reduced derivatives of slag M1/1

Product	Mass per cent concentration		
	MgO	FeO	V_2O_5
Original slag	16,40	5,88	2,75
Slag reduced 30 mins.	17,14	0,39	0,57
Slag reduced 60 mins.	18,33	0,30	0,18
Slag reduced 120 mins.	18,57	0,11	0,08

Assuming the MgO to be unaffected by the reduction process, the percentage reduction of FeO and V_2O_5 could be calculated. By further re-oxidizing the slag at 1100°C for two hours in an oxygen atmosphere, an approximate molar O/Ti ratio could be found.

The approximate degrees of reduction for Fe, V and Ti are given in table 37. The same results are presented graphically in figure 115.

On the basis of these very approximate results, it appears that titanium oxide is only appreciably reduced after the more readily reducible oxides have been virtually completely reduced. Satisfactory recovery of iron and vanadium corresponds to an O/Ti ratio representing only mild titanium oxide reduction. The time scale of these experiments and that applicable

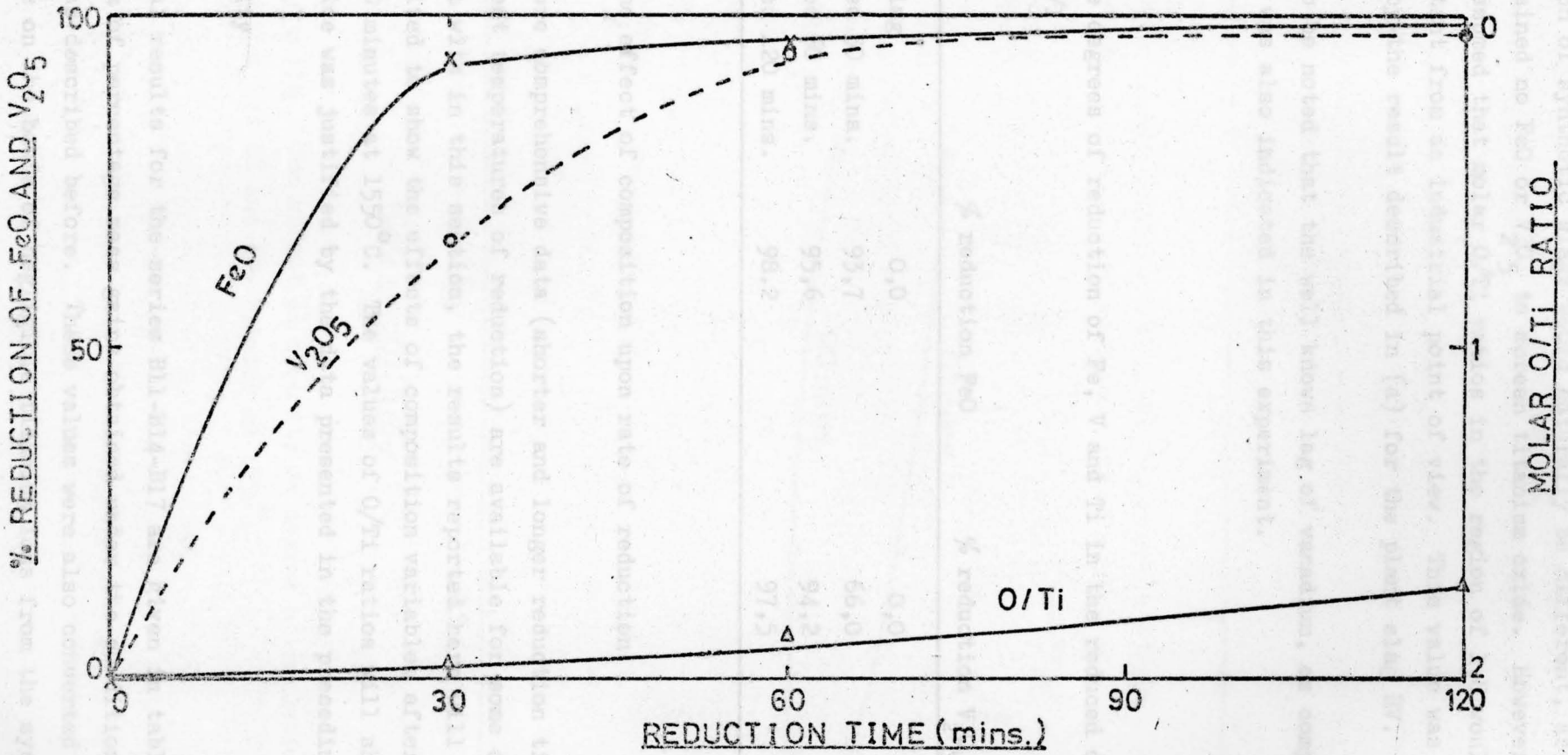


Figure 115 Approximate degrees of reduction of Fe, V and Ti in the reduced derivatives of M1/1

to reduction of synthetic slags would naturally be different, as the latter group contained no FeO or V_2O_5 to screen titanium oxide. However, it could be assumed that molar O/Ti ratios in the region of 1,8 would be most important from an industrial point of view. This value was also indicated by the result described in (a) for the plant slag HV.

It may also be noted that the well known lag of vanadium, as compared with iron, was also indicated in this experiment.

Table 37

Approximate degrees of reduction of Fe, V and Ti in the reduced derivatives of slag M1/1

Product	% reduction FeO	% reduction V_2O_5	O/Ti
Original slag	0,0	0,0	2,00
Slag reduced 30 mins.	93,7	66,0	1,95
Slag reduced 60 mins.	95,6	94,2	1,87
Slag reduced 120 mins.	98.2	97,5	1,72

4.2.5.2 The effect of composition upon rate of reduction.

Although more comprehensive data (shorter and longer reduction times, and different temperatures of reduction) are available for some of the slags dealt with in this section, the results reported here will be mainly limited to show the effects of composition variables after reduction for 60 minutes at 1550°C. The values of O/Ti ratios will show that such a choice was justified by the data presented in the preceding section.

(a) Basicity

Experimental results for the series B11-B14-B17 are given in table 38 in the form of percentage mass gains obtained under the conditions of re-oxidation as described before. These values were also converted to molar O/Ti ratios on the basis of negligible titanium loss from the system . The reduction parameters were plotted against basicity ratio in figure 116.

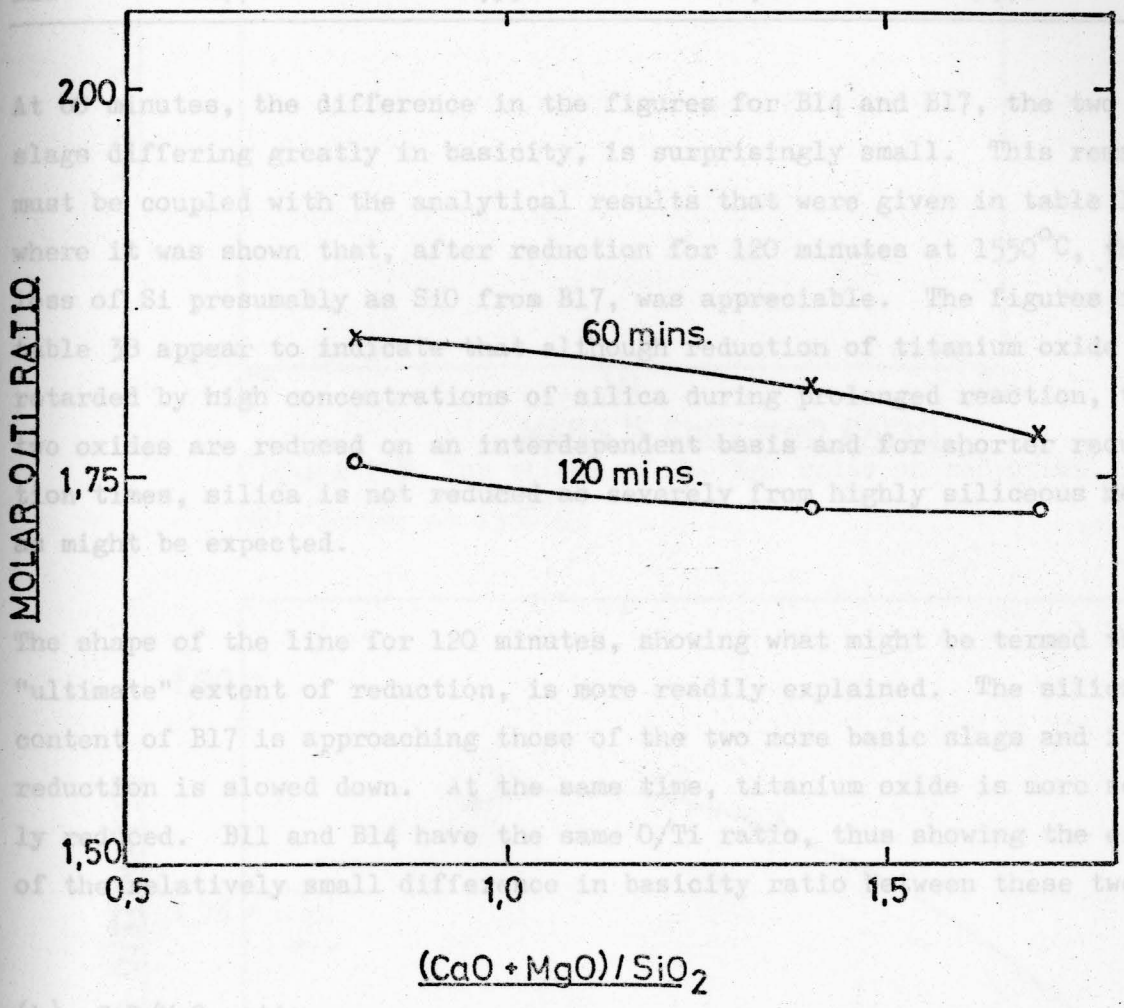


Figure 116 The effect of basicity on degree of reduction, after reduction for 60 and 120 minutes at 1550°C

Table 38 The effect of basicity on degree of reduction, after reduction for 60 and 120 minutes at 1550°C

Slag No.	$(CaO+MgO)/SiO_2$	% mass gain (60 mins.)	% mass gain (120 mins.)	O/Ti (60 mins.)	O/Ti (120 mins.)
B17	0,8	0,982	1,460	1,84	1,76
B14	1,4	1,125	1,628	1,81	1,73
B11	1,7	1,350	1,610	1,78	1,73

At 60 minutes, the difference in the figures for B14 and B17, the two slags differing greatly in basicity, is surprisingly small. This remark must be coupled with the analytical results that were given in table 13 where it was shown that, after reduction for 120 minutes at 1550°C, the loss of Si presumably as SiO from B17, was appreciable. The figures in table 38 appear to indicate that although reduction of titanium oxide is retarded by high concentrations of silica during prolonged reaction, the two oxides are reduced on an interdependent basis and for shorter reduction times, silica is not reduced as severely from highly siliceous melts as might be expected.

The shape of the line for 120 minutes, showing what might be termed the "ultimate" extent of reduction, is more readily explained. The silica content of B17 is approaching those of the two more basic slags and its reduction is slowed down. At the same time, titanium oxide is more severely reduced. B11 and B14 have the same O/Ti ratio, thus showing the effect of the relatively small difference in basicity ratio between these two slags.

(b) CaO/MgO ratio

The series B13-B14-B15 is used to illustrate the effect of the mass % ratio CaO/MgO upon the reduction behaviour of titanium oxide. Experimental results are shown in table 39 and figure 117.

Although the experimental figures are small and must necessarily involve relatively large errors, higher magnesia contents do give rise to slightly faster rates of reduction of titania. It must also be pointed out that the three slags B13, B14 and B15 possess molar $(CaO+MgO)/SiO_2$ ratios of

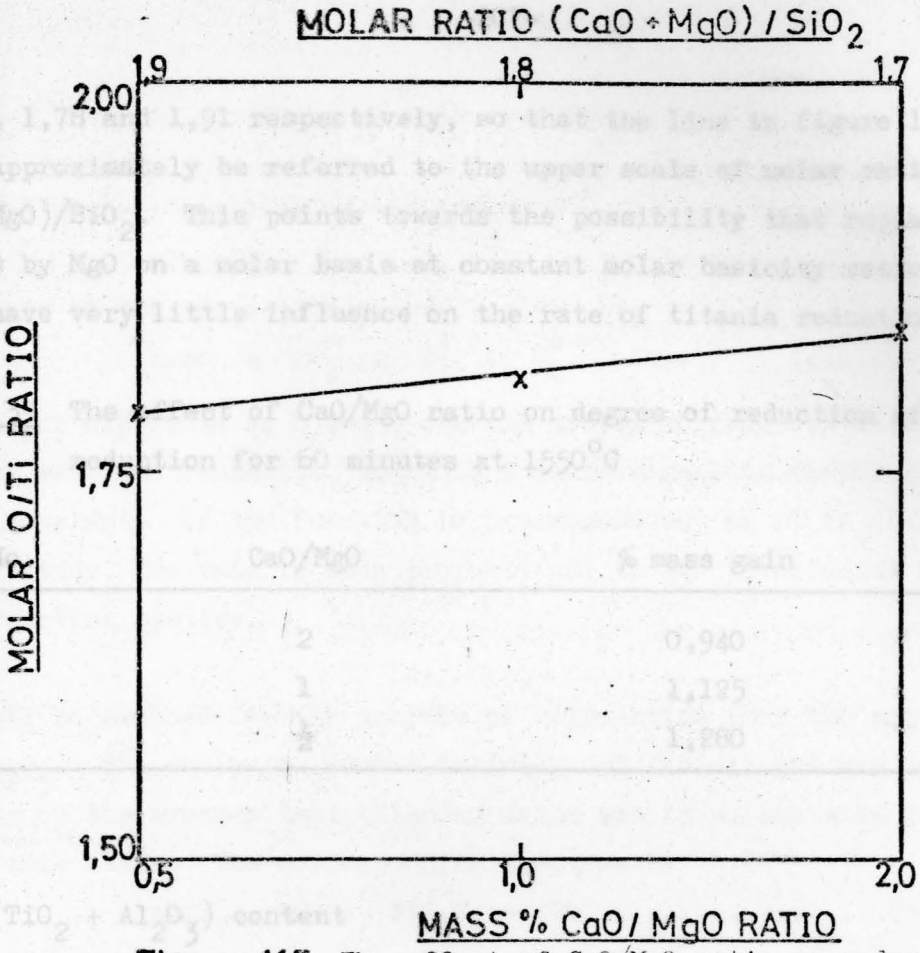


Figure 117 The effect of CaO/MgO ratio on reduction. (60 minutes at 1550°C)

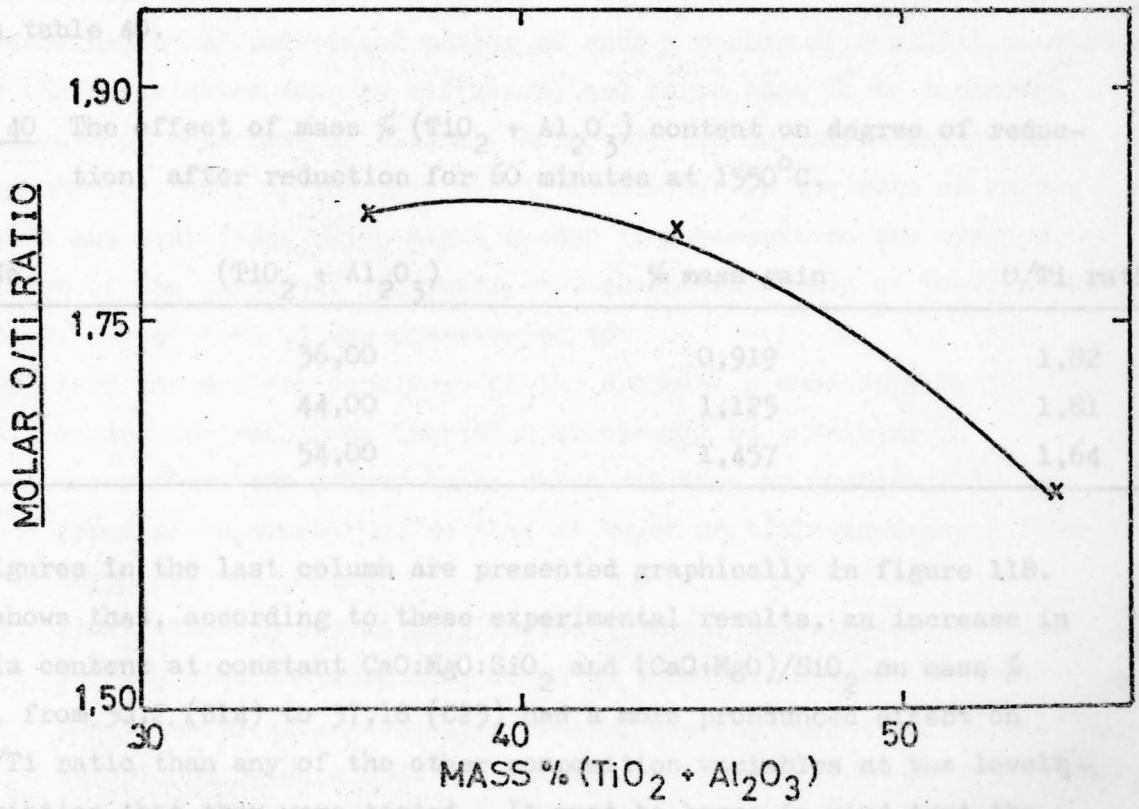


Figure 118 The effect of $(TiO_2 + Al_2O_3)$ on reduction. (60 minutes at 1550°C)

1,70 , 1,78 and 1,91 respectively, so that the line in figure 117 could also approximately be referred to the upper scale of molar ratio $(CaO+MgO)/SiO_2$. This points towards the possibility that replacement of CaO by MgO on a molar basis at constant molar basicity ratio, may in fact have very little influence on the rate of titania reduction.

Table 39 The effect of CaO/MgO ratio on degree of reduction after reduction for 60 minutes at 1550°C

Slag No.	CaO/MgO	% mass gain	O/Ti ratio
B13	2	0,940	1,84
B14	1	1,125	1,81
B15	½	1,280	1,79

(c) $(TiO_2 + Al_2O_3)$ content

The relevant reoxidation results for the three slags used for determining the importance of this parameter in the reduction of titania, are presented in table 40.

Table 40 The effect of mass % $(TiO_2 + Al_2O_3)$ content on degree of reduction, after reduction for 60 minutes at 1550°C.

Slag No.	$(TiO_2 + Al_2O_3)$	% mass gain	O/Ti ratio
A5	36,00	0,919	1,82
B14	44,00	1,125	1,81
C23	54,00	1,457	1,64

The figures in the last column are presented graphically in figure 118. This shows that, according to these experimental results, an increase in titania content at constant $CaO:MgO:SiO_2$ and $(CaO+MgO)/SiO_2$ on mass % basis, from 30,2 (B14) to 37,18 (C23) had a more pronounced effect on the O/Ti ratio than any of the other composition variables at the levels of variation that they were tested. It must be borne in mind that the increase in titania content was accompanied by a rise in the alumina level in such a way that the mass % TiO_2/Al_2O_3 ratio remained constant at 2,21.

4.2.5.3 General treatment of rate results

For the general reaction of the type:

$$aX + bY + cZ + \ldots\ldots\ldots = \text{Products} \ldots\ldots\ldots(1),$$

the rate of the forward reaction is given by:

$$\text{Rate} = kC_X^a \cdot C_Y^b \cdot C_Z^c \ldots\ldots \qquad \ldots\ldots(2),$$

where the exponents a, b and c are the orders of reaction with respect to the relevant reactants, and k is a proportionality factor called the rate constant. If the reaction is heterogeneous, as it is in this particular study, the rate is also proportional to the interfacial area between the reacting species.

It will be assumed for the purpose of calculation that the reaction product is Ti_2O_3. The choice is almost entirely artificial, and was decided upon solely on the grounds that titanium oxide was in no instance reduced beyond this state. The corresponding reaction is:

$$aTiO_2 + bC = dTi_2O_3 + fCO \ldots\ldots\ldots\ldots\ldots(3).$$

It is realized that even though equation (3) may represent the overall reaction, a step-wise mechanism involving mainly the lower oxides of titanium between $TiO_{1,67}$ and $TiO_{2,00}$ may be more feasible. The rate may be determined by an individual member of such a series of chemical reactions, or by other variables such as diffusion, and is certain to be dependent on the rate of reduction of silica. Moreover, the mechanism may be an electrochemical one, or the rate may be determined by the rate of carbon monoxide gas evolution, which might render it dependent on the surface condition of the graphite. Virtually no account was taken of these possibilities, except that it was endeavoured to:

(i) Keep the surface condition of the graphite a constant, by reproducing the machining operation as closely as possible;

(ii) Using reduction temperatures which represented considerable degrees of superheating, so that at least initial viscosity differences were minimized;

(iii) Limit stirring action only to that induced by gas evolution and

(iv) Using a constant slag mass of 70 gm in every instance so that the relative slag-reductant geometry was kept constant, if small variations in slag S.G. are ignored.

For the overall reaction represented by equation (3) the rate is expressed as:

$$-\frac{d M_{TiO_2}}{dt} = -S/100 \frac{d C_{TiO_2}}{dt} = kA (C_{TiO_2})^a . (C_C)^b \ldots\ldots(4)$$

where $-\frac{d M_{TiO_2}}{dt}$ = rate of consumption of TiO_2 (gm/min)

S = mass of slag (gm)

C_{TiO_2} = concentration of TiO_2 in the slag (mass %)

C_C = concentration of carbon

A = interfacial area (cm^2)

k = rate constant.

Since the concentration of carbon is constant (with the reaction taking place in a graphite crucible), it may be combined with the rate constant:

$$k' = k (C_C)^b \ldots\ldots(5)$$

Moreover, the slag mass and interfacial area were assumed constant and equation (4) simplifies to:

$$-\frac{d C_{TiO_2}}{dt} = k'' (C_{TiO_2})^a \ldots\ldots(6)$$

where $k'' = (100\ k'\ A)/S$

(a) The order of reaction

The value of a can be determined by using the logarithmic form of (6):

$$\log \left(-\frac{d C_{TiO_2}}{dt} \right) = \log k'' + a \log (C_{TiO_2}) \ldots\ldots(7)$$

A plot of $\log \left(-\frac{d C_{TiO_2}}{dt} \right)$ against $\log C_{TiO_2}$ should be a straight line of slope a, and the intercept of the straight line on the 1% TiO_2 ordinate should yield the value of k". Numerical values to be used in such plots may be obtained by fitting smooth curves to the experimental

points of ($\%TiO_2$) against time, and determining the slopes of the curves at selected titania cocentrations. These slopes give the values of $\frac{d\,C_{TiO_2}}{dt}$ at the corresponding values of C_{TiO_2}.

(b) Once the order of reaction is established, the value of k" obtained above, can be checked with the aid of a direct plot of experimental points without an intermediate graphical step. This is accomplished by substituting the appropriate value of a in equation (6) and integrating between the limits of concentration C_o at t = 0 and C at time t.

For a first order reaction:

$$\log_e C_o / C = k'' t \quad \ldots\ldots\ldots\ldots (8)$$

and a plot of $\log_e C_o / C$ against t should give a straight line through the origin and the slope of the line is equal to k".

For a second order reaction:

$$1/C - 1/C_o = k'' t \quad \ldots\ldots\ldots\ldots (9)$$

Then a plot of $(1/C - 1/C_o)$ against t should give a straight line passing through the origin, with a slope = k".

This procedure also should provide a check on the validity of the value of a inserted in equation (6).

From a knowledge of the interfacial area between reacting phases (A), and of slag mass (S), the value of k' can then be found.

(c) Activation energy

In order to determine the activation energy for the reduction reaction, the temperature dependence of the constant k' must be ascertained. These two parameters are related through the Arrhenius equation:

$$k' = A \exp (- E_A / RT) \quad \ldots\ldots\ldots\ldots (10),$$

where A is a frequency factor and E_A is the activation energy. In logarithmic form equation 10 becomes:

$$\log_e k' = \log_e A - E_A/RT \quad \ldots\ldots\ldots\ldots(11),$$

so that a plot of log k' against 1/T must be a straight line, the slope of which should give the value of E_A.

The treatment oulined above, was applied to the slag compositions B11, B14 and B17. B11 and B17 were tested at two temperatures each (1550° and 1600°C), while B14 was reduced at three different temperatures (1500°, 1550° and 1600°C), in order to determine the effect of temperature on the rate constant k'.

As indicated before, k' is obtained from k" through the relationship $k' = (S\ k")/100\ A$. An approximate value of the conversion factor S/100A of $1,83 \times 10^{-2}$ was used throughout. This figure is based on the assumed values:

Density of slag = 3,0 gm/cm^3

Slag mass (S) = 70 gm, from which

A (slag-graphite contact area) = 38,2 cm^2

4.2.5.4 The rate of reduction of slag B11 : $(CaO+MgO)/SiO_2 = 1,7$

(a) 1550°C

The relevant experimental results as obtained from reoxidation of the various reduced derivatives as well as the unreduced slag, are given in table 41.

Table 41 Rate results for slag B11 reduced at 1550°C

Reduction time (minutes)	% mass gain	O/Ti	$z(Ti_3O_5)$ (%)	$z(Ti_2O_3)$ (%)	z(TiO) (%)	C_{TiO_2} (mass%)
0	0,283	1,95	14,0	9,4	4,7	27,4
30	0,940	1,84	46,7	31,1	15,6	20,8
60	1,350	1,78	67,0	44,8	22,4	16,7
90	1,500	1,75	74,5	49,7	24,9	15,2
120	1,610	1,73	79,8	53,4	26,7	14,1

The table alsc includes the values of the molar O/Ti ratios of every reduced derivative, calculated on the basis of the assumptions that:

(i) the mass gain during oxidation is due only to the oxidation of the lower oxides of titanium and that the carbon content of the slag is negligible,

(ii) no titanium is lost from the system during reduction and

(iii) the decrease in mass during reduction is small enough to be ignored in determining the atom fraction of titanium in the reduced slag as compared with the unreduced one.

The value of z represents a percentage conversion of TiO_2 to the various lower oxides Ti_3O_5, Ti_2O_3 and TiO. The concentration of TiO_2 (C_{TiO_2}) was calculated from the value of $z(Ti_2O_3)$, which was assumed to be the overall reaction product. This concentration measure is shown as a function of reduction time in figure 119. It will be observed that zero reduction time does not correspond to 30,2 % TiO_2 which was the original titania content of the slag as prepared. The difference is due to the loss of oxygen from the slag in an inert atmosphere during premelting and determination of viscosity and electrical resistance. While every effort was made to reproduce the thermal histories of the three unreduced slags, oxygen losses from these are small and errors can be expected to be comparatively large.

Values of $\left(- \frac{d\, C_{TiO_2}}{dt} \right)$ corresponding to the various concentrations of TiO_2 were obtained from the data presented in figure 119. These are given in table 42. Rates were determined at intermediate reduction times that were not covered experimentally. However, the trends shown by the concentration-time curves were considered sufficiently well-defined to allow such a procedure.

The figures in the last two columns of the table are presented in figure 120.

Table 42 Logarithmic rate data for slag B11 reduced at 1550°C

Reduction time (minutes)	C_{TiO_2} (mass%)	$-\frac{dC_{TiO_2}}{dt}$	$\log C_{TiO_2}$	$\log -\frac{dC_{TiO_2}}{dt}$
10	24,8	0,20	1,395	- 0,699
20	22,7	0,19	1,356	- 0,727
30	20,8	0,17	1,318	- 0,770
40	19,3	0,15	1,286	- 0,824
50	17,9	0,13	1,253	- 0,886
60	16,8	0,11	1,225	- 0,959
70	15,9	0,09	1,201	- 1,046
80	15,1	0,07	1,179	- 1,155
90	14,5	0,05	1,161	- 1,301
100	14,2	0,04	1,152	- 1,398
110	13,9	0,03	1,143	- 1,523

(b) 1600°C

The experimental results were treated in exactly the same manner as those from the work at lower temperature in (a), and are listed in tables 43 and 44. Graphs representing the figures in these tables are given in figures 121 and 122.

Table 43 Rate results for slag B11 reduced at 1600°C

Reduction time (minutes)	% mass gain	O/Ti	$z(Ti_3O_5)$ (%)	$z(Ti_2O_3)$ (%)	z(TiO) (%)	C_{TiO_2} (mass%)
0	0,283	1,95	14,0	9,4	4,7	27,4
30	1,139	1,81	57,0	37,8	18,9	18,8
60	1,750	1,72	87,0	58,0	29,0	12,7
90	2,040	1,66	101,0	67,5	33,8	9,8
120	2,130	1,64	105,5	70,5	35,3	8,9

Table 44 Logarithmic rate data for slag B11 reduced at 1600°C

Reduction time (minutes)	C_{TiO_2} (mass%)	$-\frac{dC_{TiO_2}}{dt}$	$\log C_{TiO_2}$	$\log -\frac{dC_{TiO_2}}{dt}$
10	24,1	0,28	1,382	- 0,553
20	21,4	0,26	1,330	- 0,585
30	18,8	0,25	1,274	- 0,602
40	16,5	0,22	1,218	- 0,658
50	14,5	0,19	1,161	- 0,721
60	12,7	0,15	1,104	- 0,824
70	11,5	0,12	1,061	- 0,921
80	10,6	0,08	1,025	- 1,097
90	9,8	0,06	0,991	- 1,222
100	9,3	0,05	0,969	- 1,301
110	9,0	0,03	0,954	- 1,523

Figures 120 and 122 show that the logarithmic plots can be divided into two distinct sections, both of which can be approximated to by straight lines.

Based on these results, the ultimate kinetic parameters for reaction (3) were obtained. These are given in table 45.

Table 45 Order of reaction and rate constant for slag B11

Temperature (°C)	k"	k'	a
1550	$4,169 \times 10^{-3}$	$7,65 \times 10^{-5}$	1,2
1600	$1,698 \times 10^{-2}$	$3,11 \times 10^{-4}$	0,9

The values of the orders of reaction, a, given in the table, were obtained from the slopes of the lines drawn for the initial period of reduction. Over this period an average value of close to 1,0 is indicated. The existence of such a region appears to verify chemical reaction rate control. The transition to higher order (3 to 4) is not sharp. It may however be significant that it occurs, for the two temperatures of reduction, after rather similar reduction periods ($\pm$ 60 minutes for 1600° and $\pm$ 70 minutes for 1550°C). The possible implications of a higher order will be pointed out in a later section. The value of k'_{1600} is approximately five times as large as that of k'_{1550}.

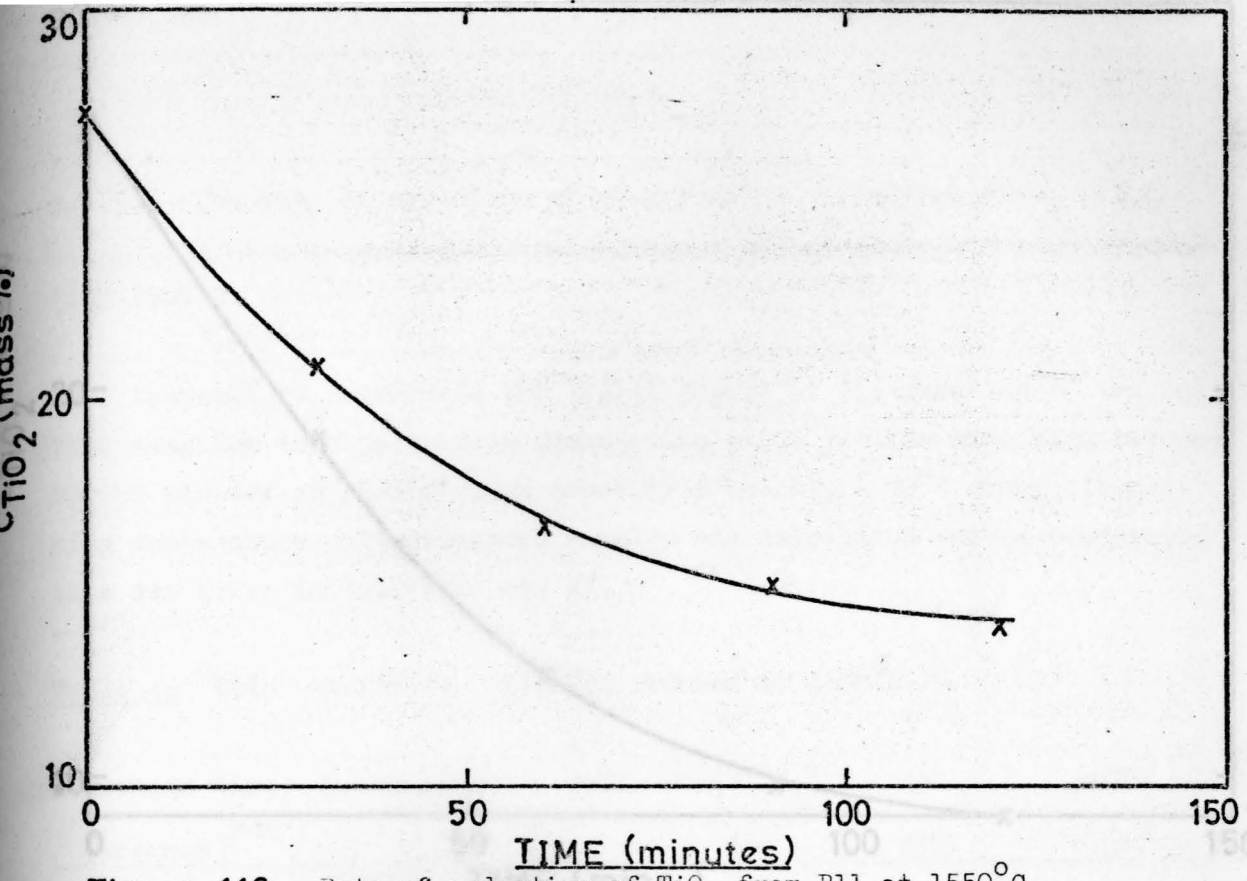


Figure 119 Rate of reduction of TiO_2 from B11 at 1550°C

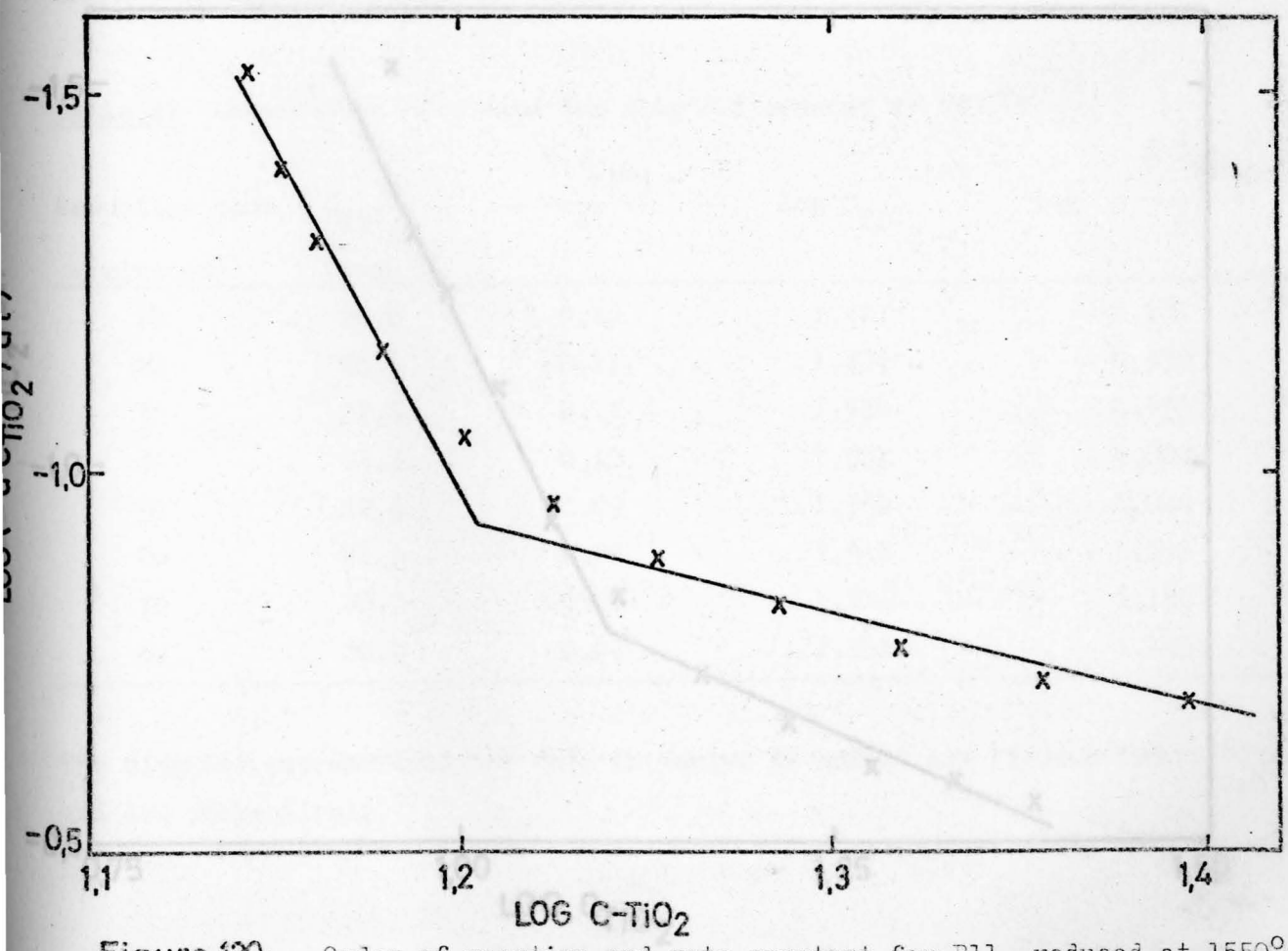


Figure 120 Order of reaction and rate constant for B11, reduced at 1550°C

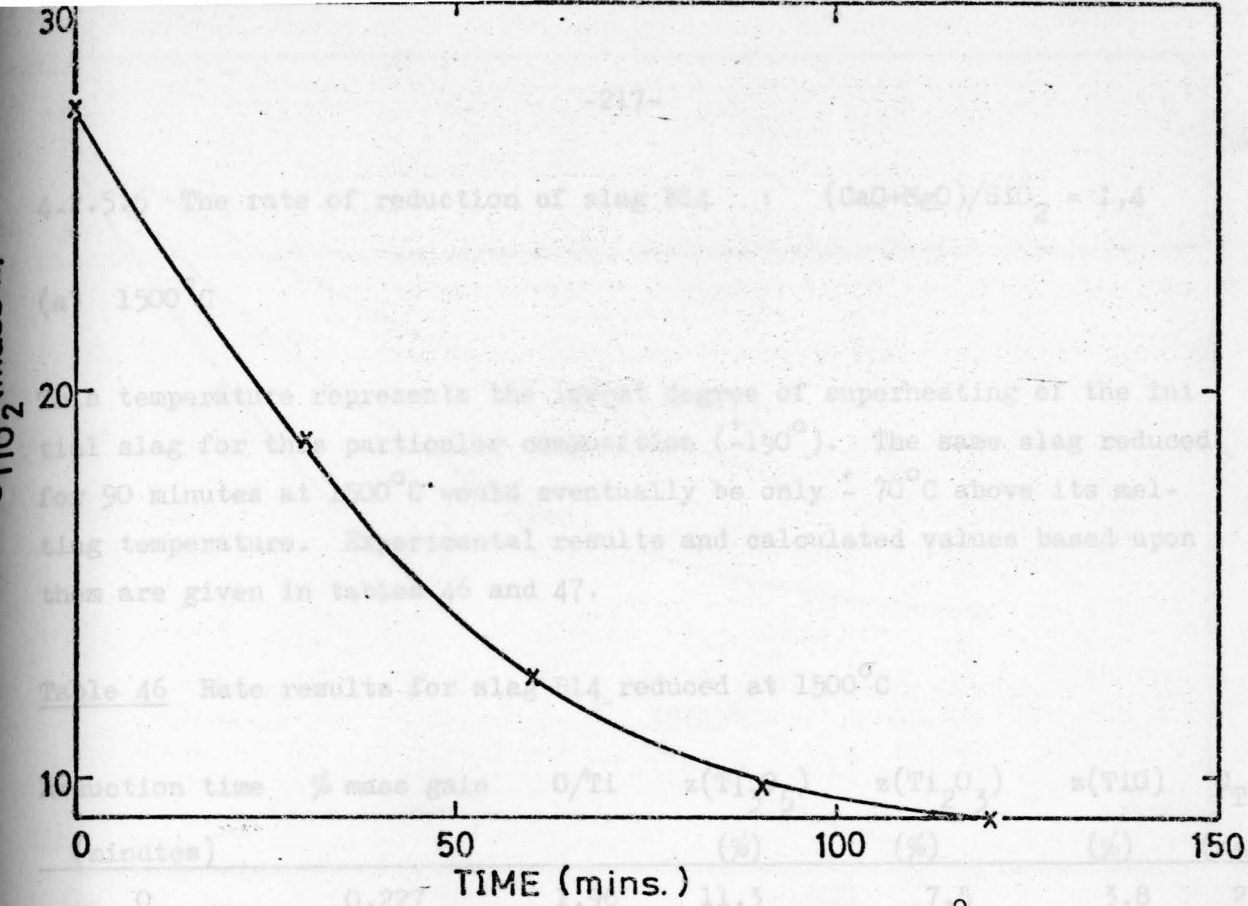


Figure 121 Rate of reduction of TiO_2 from B11 at 1600°C

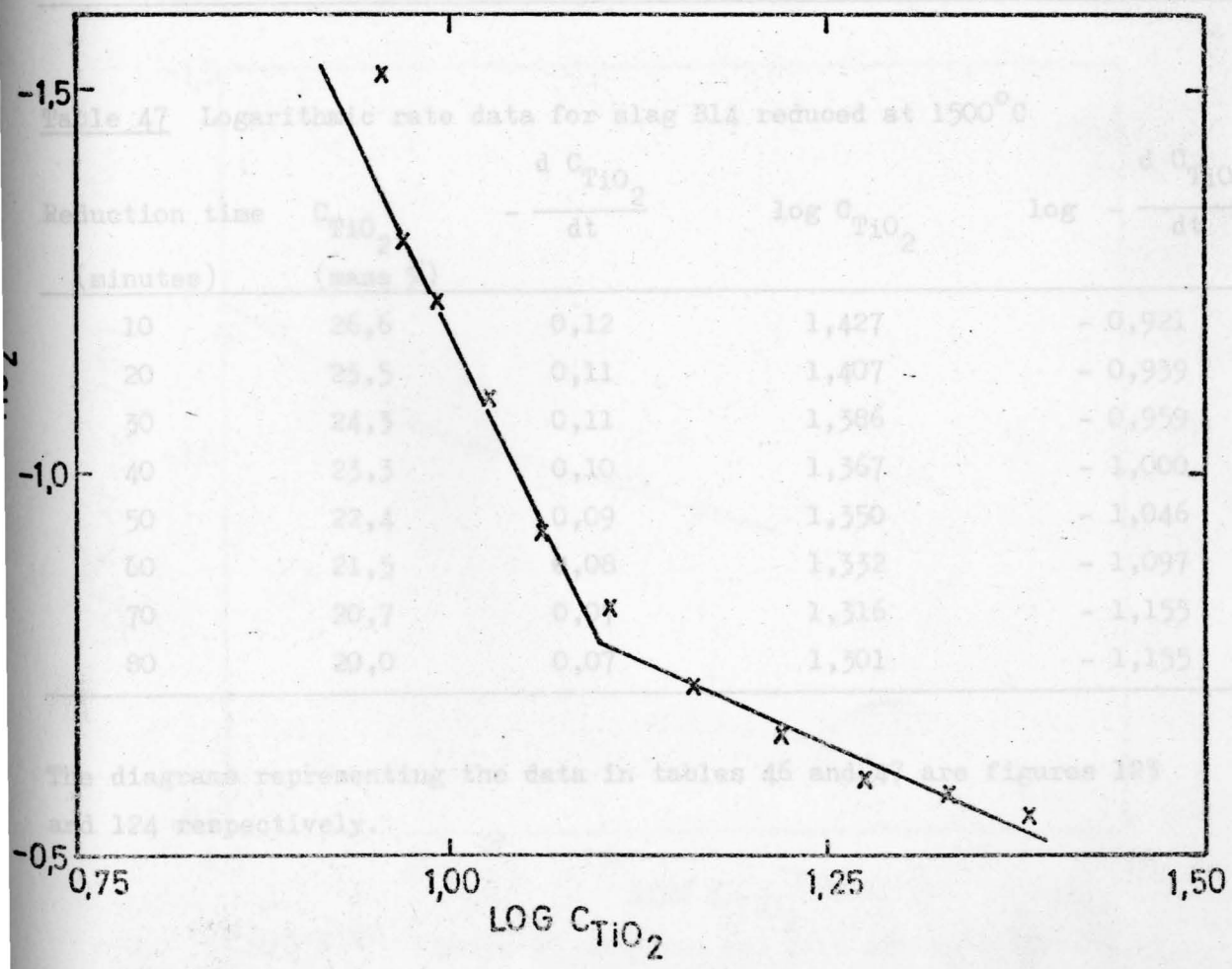


Figure 122 Order of reaction and rate constant for B11, reduced at 1600°C

4.2.5.5 The rate of reduction of slag B14 : $(CaO+MgO)/SiO_2 = 1,4$

(a) 1500°C

This temperature represents the lowest degree of superheating of the initial slag for this particular composition ($\pm$150°). The same slag reduced for 90 minutes at 1500°C would eventually be only $\pm$ 70°C above its melting temperature. Experimental results and calculated values based upon them are given in tables 46 and 47.

Table 46 Rate results for slag B14 reduced at 1500°C

Reduction time (minutes)	% mass gain	O/Ti	$z(Ti_3O_5)$ (%)	$z(Ti_2O_3)$ (%)	z(TiO) (%)	C_{TiO_2} (mass%)
0	0,227	1,96	11,3	7,5	3,8	27,9
30	0,500	1,92	24,8	16,6	8,3	25,2
60	0,880	1,85	43,7	29,2	14,6	21,4
90	1,070	1,82	53,2	35,5	17,8	19,5

Table 47 Logarithmic rate data for slag B14 reduced at 1500°C

Reduction time (minutes)	C_{TiO_2} (mass %)	$-\frac{d\,C_{TiO_2}}{dt}$	$\log C_{TiO_2}$	$\log -\frac{d\,C_{TiO_2}}{dt}$
10	26,6	0,12	1,427	- 0,921
20	25,5	0,11	1,407	- 0,959
30	24,3	0,11	1,386	- 0,959
40	23,3	0,10	1,367	- 1,000
50	22,4	0,09	1,350	- 1,046
60	21,5	0,08	1,332	- 1,097
70	20,7	0,07	1,316	- 1,155
80	20,0	0,07	1,301	- 1,155

The diagrams representing the data in tables 46 and 47 are figures 123 and 124 respectively.

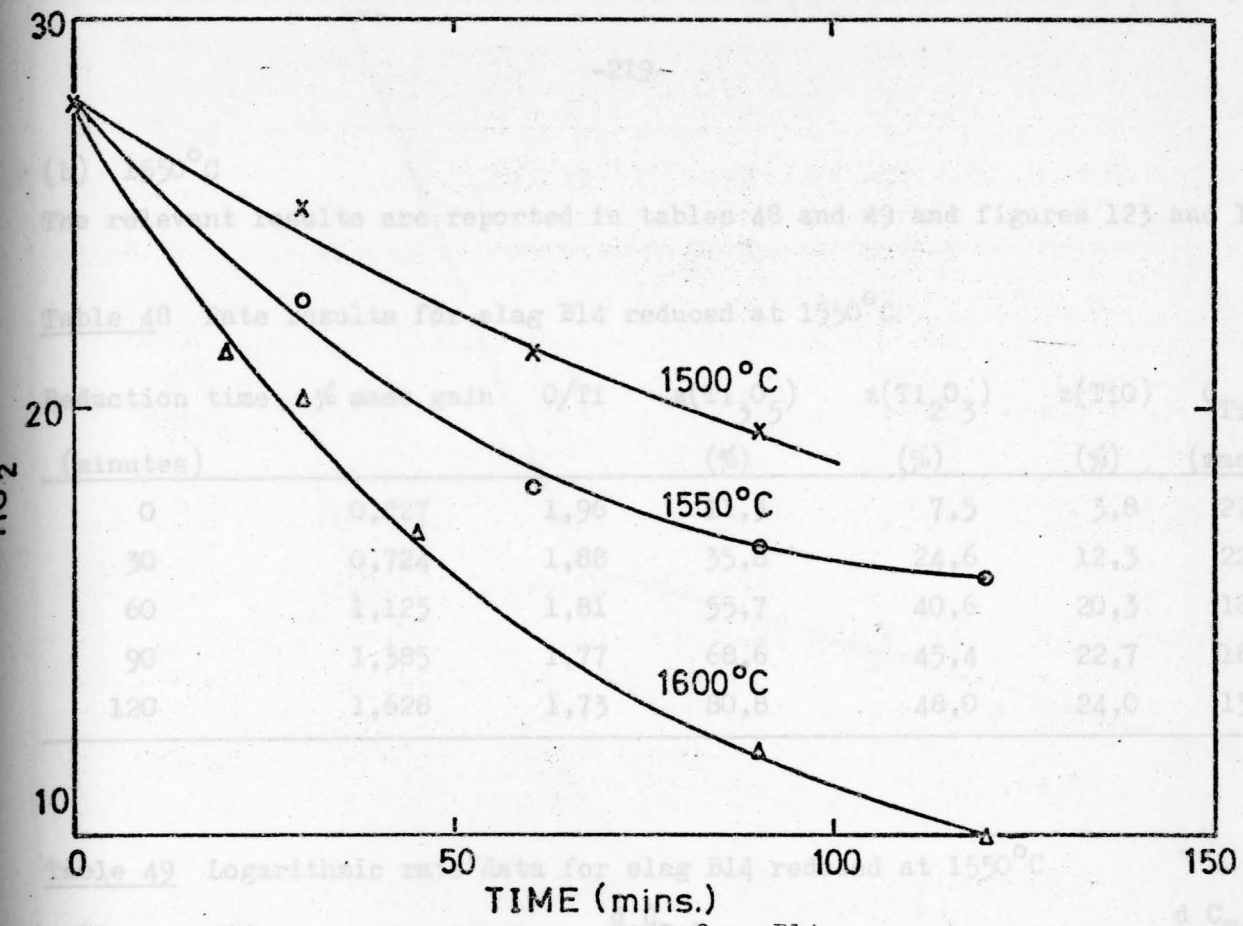


Figure 123 Rate of reduction of TiO_2 from B14

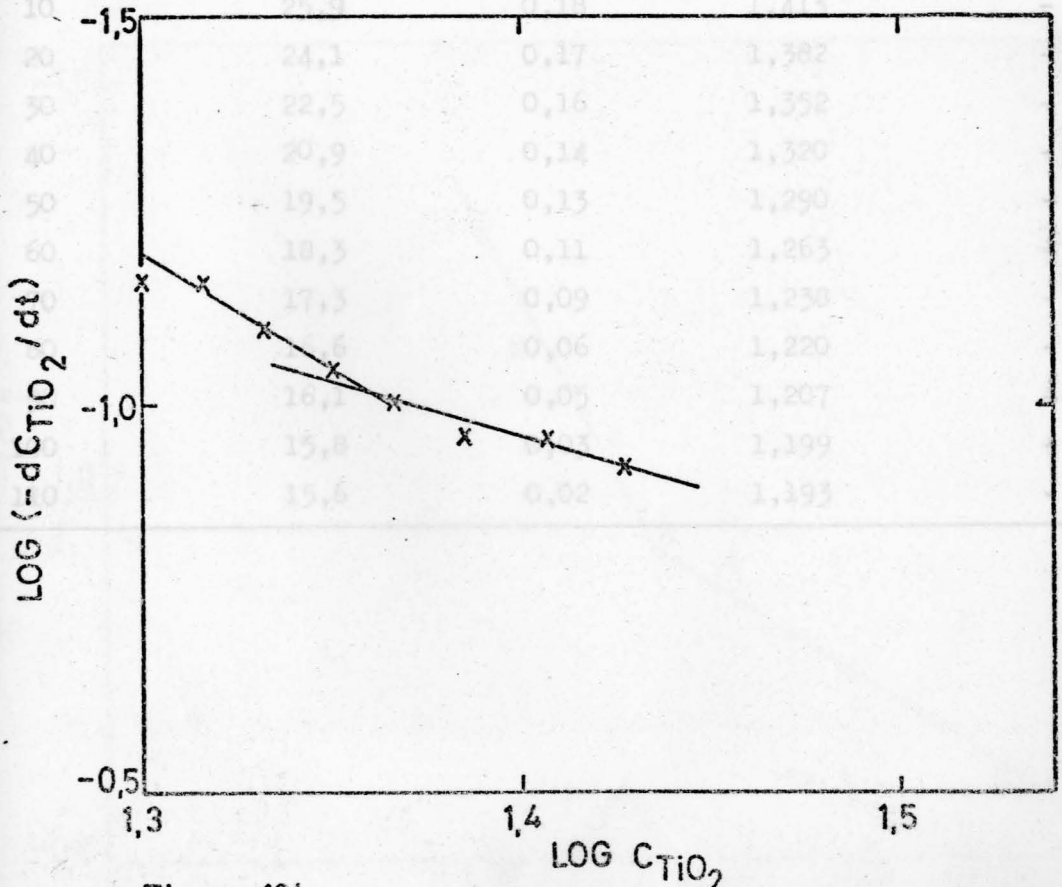


Figure 124 Order of reaction and rate constant for B14, reduced at 1500°C

(b) 1550°C

The relevant results are reported in tables 48 and 49 and figures 123 and 125.

Table 48 Rate results for slag B14 reduced at 1550°C

Reduction time (minutes)	% mass gain	O/Ti	$z(Ti_3O_5)$ (%)	$z(Ti_2O_3)$ (%)	z(TiO) (%)	C_{TiO_2} (mass%)
0	0,227	1,96	11,3	7,5	3,8	27,9
30	0,724	1,88	35,8	24,6	12,3	22,8
60	1,125	1,81	55,7	40,6	20,3	18,0
90	1,385	1,77	68,6	45,4	22,7	16,5
120	1,628	1,73	80,8	48,0	24,0	15,7

Table 49 Logarithmic rate data for slag B14 reduced at 1550°C

Reduction time (minutes)	C_{TiO_2} (mass %)	$-\frac{d\,C_{TiO_2}}{dt}$	$\log C_{TiO_2}$	$\log -\frac{d\,C_{TiO_2}}{dt}$
10	25,9	0,18	1,413	- 0,745
20	24,1	0,17	1,382	- 0,770
30	22,5	0,16	1,352	- 0,796
40	20,9	0,14	1,320	- 0,854
50	19,5	0,13	1,290	- 0,886
60	18,3	0,11	1,263	- 0,959
70	17,3	0,09	1,238	- 1,046
80	16,6	0,06	1,220	- 1,222
90	16,1	0,05	1,207	- 1,301
100	15,8	0,03	1,199	- 1,523
110	15,6	0,02	1,193	- 1,699

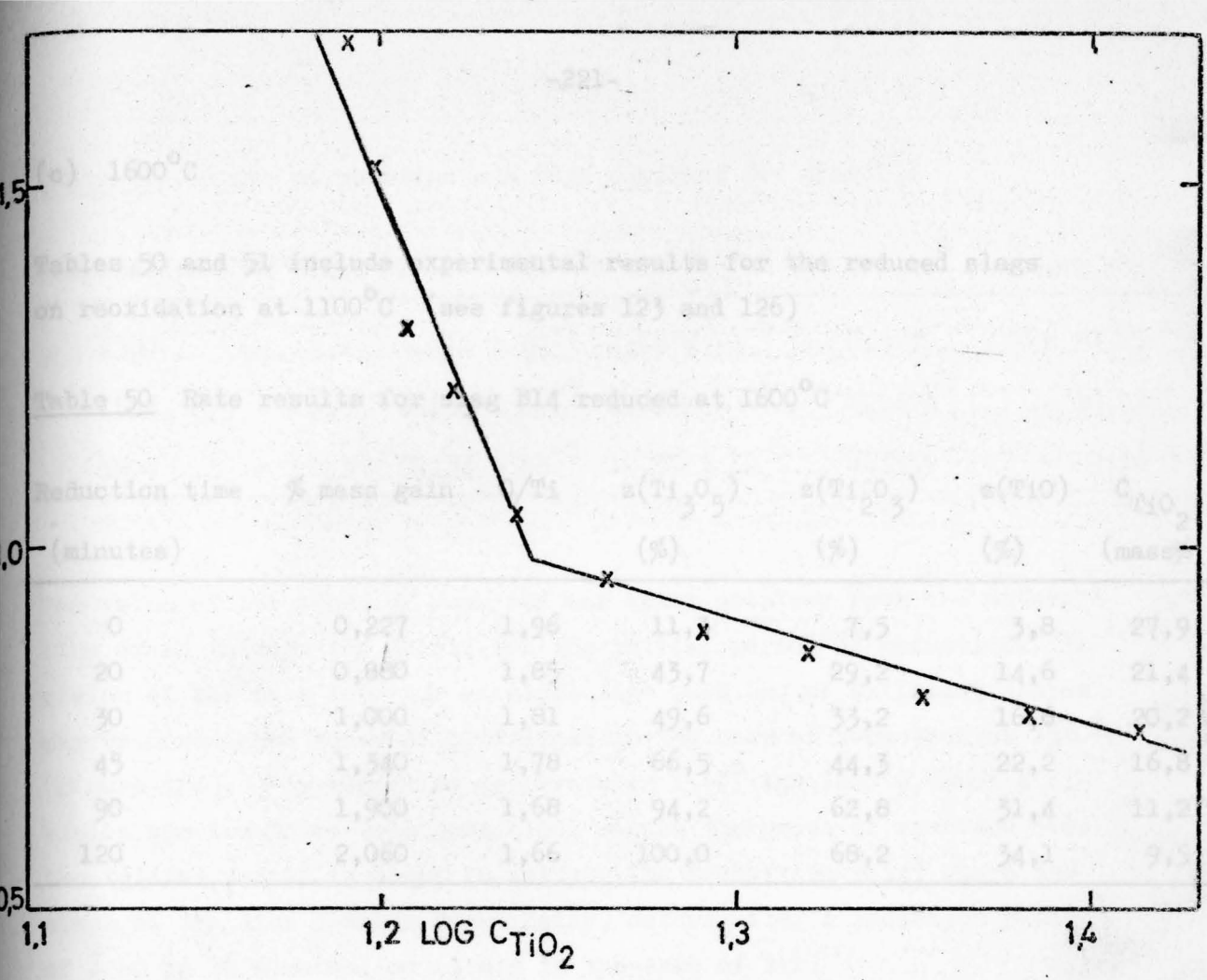


Figure 125 Order of reaction and rate constant for B14 reduced at 1550°C

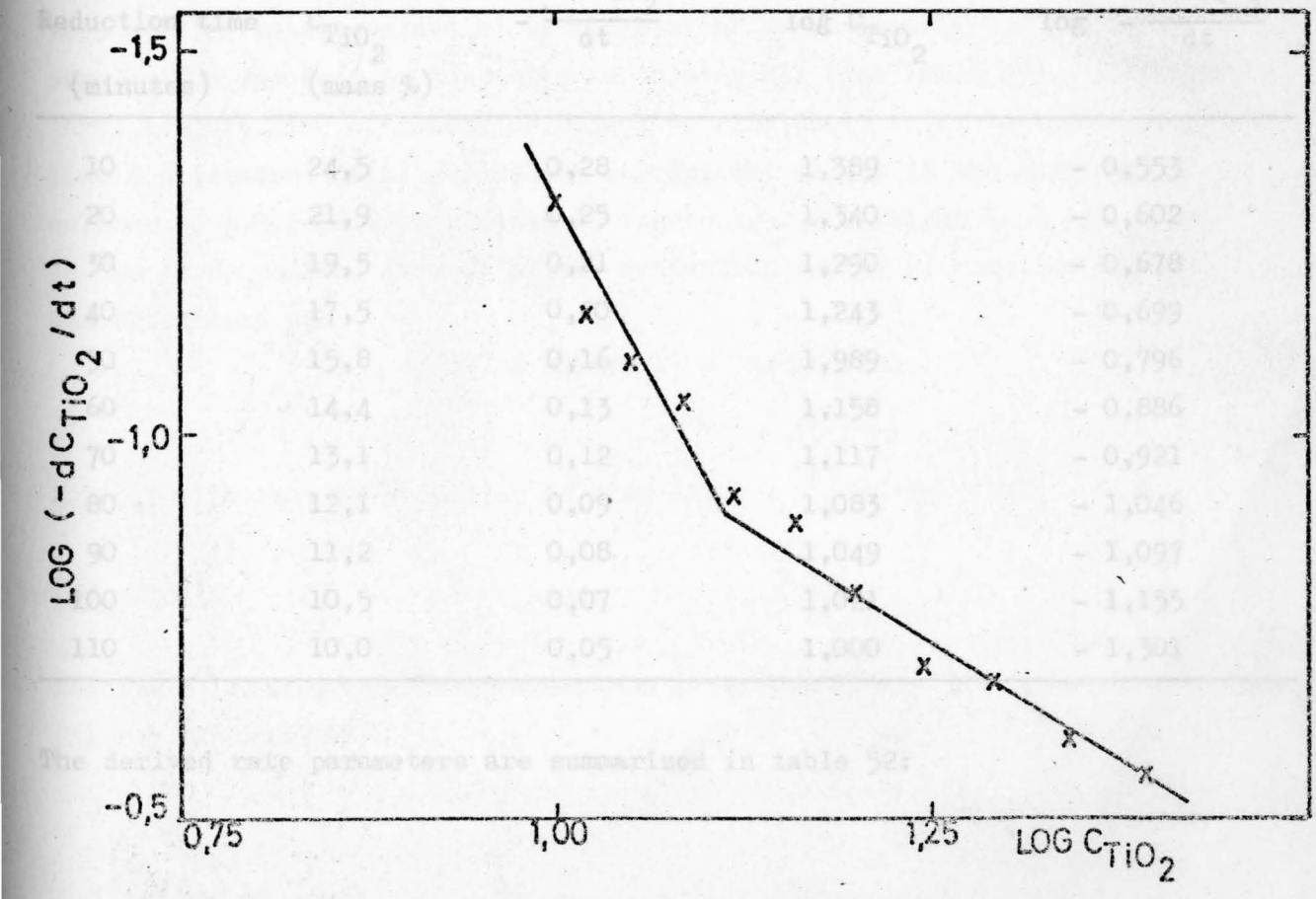


Figure 126 Order of reaction and rate constant for B14 reduced at 1600°C

(c) 1600°C

Tables 50 and 51 include experimental results for the reduced slags on reoxidation at 1100°C (see figures 123 and 126)

Table 50 Rate results for slag B14 reduced at 1600°C

Reduction time (minutes)	% mass gain	O/Ti	$z(Ti_3O_5)$ (%)	$z(Ti_2O_3)$ (%)	z(TiO) (%)	C_{TiO_2} (mass%)
0	0,227	1,96	11,3	7,5	3,8	27,9
20	0,880	1,85	43,7	29,2	14,6	21,4
30	1,000	1,81	49,6	33,2	16,6	20,2
45	1,340	1,78	66,5	44,3	22,2	16,8
90	1,900	1,68	94,2	62,8	31,4	11,2
120	2,060	1,66	100,0	68,2	34,1	9,5

Table 51 Logarithmic rate data for slag B14 reduced at 1600°C

Reduction time (minutes)	C_{TiO_2} (mass %)	$-\frac{d\,C_{TiO_2}}{dt}$	$\log C_{TiO_2}$	$\log -\frac{d\,C_{TiO_2}}{dt}$
10	24,5	0,28	1,389	- 0,553
20	21,9	0,25	1,340	- 0,602
30	19,5	0,21	1,290	- 0,678
40	17,5	0,20	1,243	- 0,699
50	15,8	0,16	1,989	- 0,796
60	14,4	0,13	1,158	- 0,886
70	13,1	0,12	1,117	- 0,921
80	12,1	0,09	1,083	- 1,046
90	11,2	0,08	1,049	- 1,097
100	10,5	0,07	1,021	- 1,155
110	10,0	0,05	1,000	- 1,301

The derived rate parameters are summarized in table 52:

Table 52 Order of reaction and rate constant for slag B14

Temperature (^{o}C)	a	k"	k'	$1/T \times 10^{3}$	$\log_e k'$
1500	1,4	$1,175 \times 10^{-3}$	$2,15 \times 10^{-5}$	0,5640	- 10,75
1550	1,3	$2,239 \times 10^{-3}$	$4,09 \times 10^{-5}$	0,5486	- 10,12
1600	1,3	$5,754 \times 10^{-3}$	$10,53 \times 10^{-5}$	0,5339	- 9,16

The value of the order of reaction was again obtained from the straight line drawn through the points for the initial period of reduction. Division of the data into two straight line portions of different slopes may be considered somewhat artificial in the case of reduction at 1500^{o}C (figure 124). For reduction temperatures 1550^{o} and 1600^{o}C, such a division appears to be well justified. Again the order of reaction over the initial period is close to unity. The transition point where the slope of the line changes drastically, occurs after a reduction period of $\pm$ 60 to 70 minutes, as it did in the case of B11.

Also, table 52 shows that a temperature increment of 50^{o} increases the value of the rate constant k' by a factor of approximately 5. The same observation was made in connection with slag B11 (see table 45). Although three temperatures of reduction cannot be considered sufficient for reliable determination of activation energy, the values in the last two columns of table 52 were plotted in figure 129. A straight line was fitted to the three points, from which the activation energy of reaction (3) was determined as:

$$E_A = 107 \text{ K cals/mol} = 448 \text{ KJ/mol.}$$

4.2.5.6 The rate of reduction of slag B17 : $(CaO+MgO)/SiO_2 = 0,8$

(a) 1550^{o}C

Results of reoxidation tests are given in tables 53 and 54. (see also figures 127 and 128).

Table 53 Rate results for slag B17 reduced at 1550°C

Reduction time (minutes)	% mass gain	O/Ti	$z(Ti_3O_5)$ (%)	$z(Ti_2O_3)$ (%)	z(TiO) (%)	C_{TiO_2} (mass%)
0	0,255	1,96	12,6	7,1	3,5	28,2
30	0,600	1,90	29,8	19,9	9,9	24,2
60	0,982	1,84	48,7	32,5	16,3	20,4
90	1,238	1,79	61,4	41,1	20,5	17,8
120	1,460	1,76	72,3	48,3	24,2	15,6

Table 54 Logarithmic rate data for slag B17 reduced at 1550°C

Reduction time (minutes)	C_{TiO_2} (mass %)	$-\frac{d\,C_{TiO_2}}{dt}$	$\log C_{TiO_2}$	$\log -\frac{d\,C_{TiO_2}}{dt}$
10	26,6	0,14	1,425	- 0,854
20	25,3	0,13	1,403	- 0,886
30	24,0	0,12	1,380	- 0,921
40	22,8	0,12	1,358	- 0,921
50	21,7	0,12	1,337	- 0,921
60	20,6	0,11	1,314	- 0,959
70	19,6	$0,09_5$	1,292	- 1,022
80	18,7	0,09	1,272	- 1,046
90	17,9	0,08	1,253	- 1,097
100	17,1	$0,07_5$	1,233	- 1,125
110	16,4	0,07	1,215	- 1,155

(b) 1600°C

Experimental results for reduction times up to 90 minutes are given in tables 55 and 56. These are shown graphically in figures 127 and 128 as well.

Table 55 Rate results for slag B17 reduced at 1600°C

Reduction time (minutes)	% mass gain	O/Ti	$z(Ti_3O_5)$ (%)	$z(Ti_2O_3)$ (%)	z(TiO) (%)	C_{TiO_2} (mass%)
0	0,255	1,96	12,6	7,1	3,5	28,1
20	0,610	1,90	30,3	20,2	10,1	24,2
40	0,920	1,85	45,7	30,5	15,3	21,0
60	1,218	1,80	60,2	40,3	20,2	18,1
90	1,608	1,73	79,8	53,3	26,7	14,1

Table 56 Logarithmic rate data for slag B17 reduced at 1600°C

Reduction time (minutes)	C_{TiO_2} (mass %)	$-\frac{d\,C_{TiO_2}}{dt}$	$\log C_{TiO_2}$	$\log -\frac{d\,C_{TiO_2}}{dt}$
10	26,2	0,18	1,418	- 0,745
20	24,4	0,17	1,387	- 0,770
30	22,7	0,17	1,356	- 0,770
40	21,0	0,16	1,322	- 0,796
50	19,4	0,14	1,288	- 0,854
60	18,0	$0,13_5$	1,255	- 0,870
70	16,6	$0,12_5$	1,220	- 0,903
80	15,3	0,12	1,185	- 0,921

The kinetic parameters derived from these, are presented in table 57.

Table 57 Order of reaction and rate constant for slag B17

Temperature (°C)	a	k"	k'
1550	1,4	$1,413 \times 10^{-3}$	$2,59 \times 10^{-5}$
1600	1,1	$5,495 \times 10^{-3}$	$10,05 \times 10^{-5}$

Figures 127 and 128 show that there is very little evidence of a severe change in the value of the order of reaction for this particular slag composition, as compared with the more basic members of the series. Consequently 'a' in table 57 represents the slope of the single straight line drawn through the points in figure 128.

In conclusion, the effect of basicity (as the mass % ratio $\frac{CaO + MgO}{SiO_2}$) may be condensed to the values of k' for the various slags. At the same time, the ultimate degree of reduction attained by every slag should be an important parameter.

Table 58 Effect of basicity upon rate and extent of reduction of TiO_2

Slag No.	$(CaO+MgO)/SiO_2$	Temperature (^{o}C)	k'	O/Ti *
B11	1,7	1550	$7,65 \times 10^{-5}$	1,73 (120)
		1600	$3,11 \times 10^{-4}$	1,64 (120)
B14	1,4	1550	$4,09 \times 10^{-5}$	1,73 (120)
		1600	$1,05 \times 10^{-4}$	1,66 (120)
B17	0,8	1550	$2,59 \times 10^{-5}$	1,76 (120)
		1600	$1,01 \times 10^{-4}$	1,73 (90)

*The figures in brackets are the reduction times in minutes.

At any given reduction temperature used, an increase in basicity ratio leads to an increase in the value of k'. The large effect of an increase from 1,4 to 1,7 as compared with the relatively small effect of the increase from 0,8 to 1,4 was already pointed out in section 4.2.5.2 (a).

It is significant that only one of the slags in the table suffered reduction with respect to titanium oxide, beyond that represented by the compound Ti_3O_5 (B11 reduced for 120 minutes at 1600°C). Even here the value of O/Ti is so slightly below 1,67 , that it may be due to experimental error.

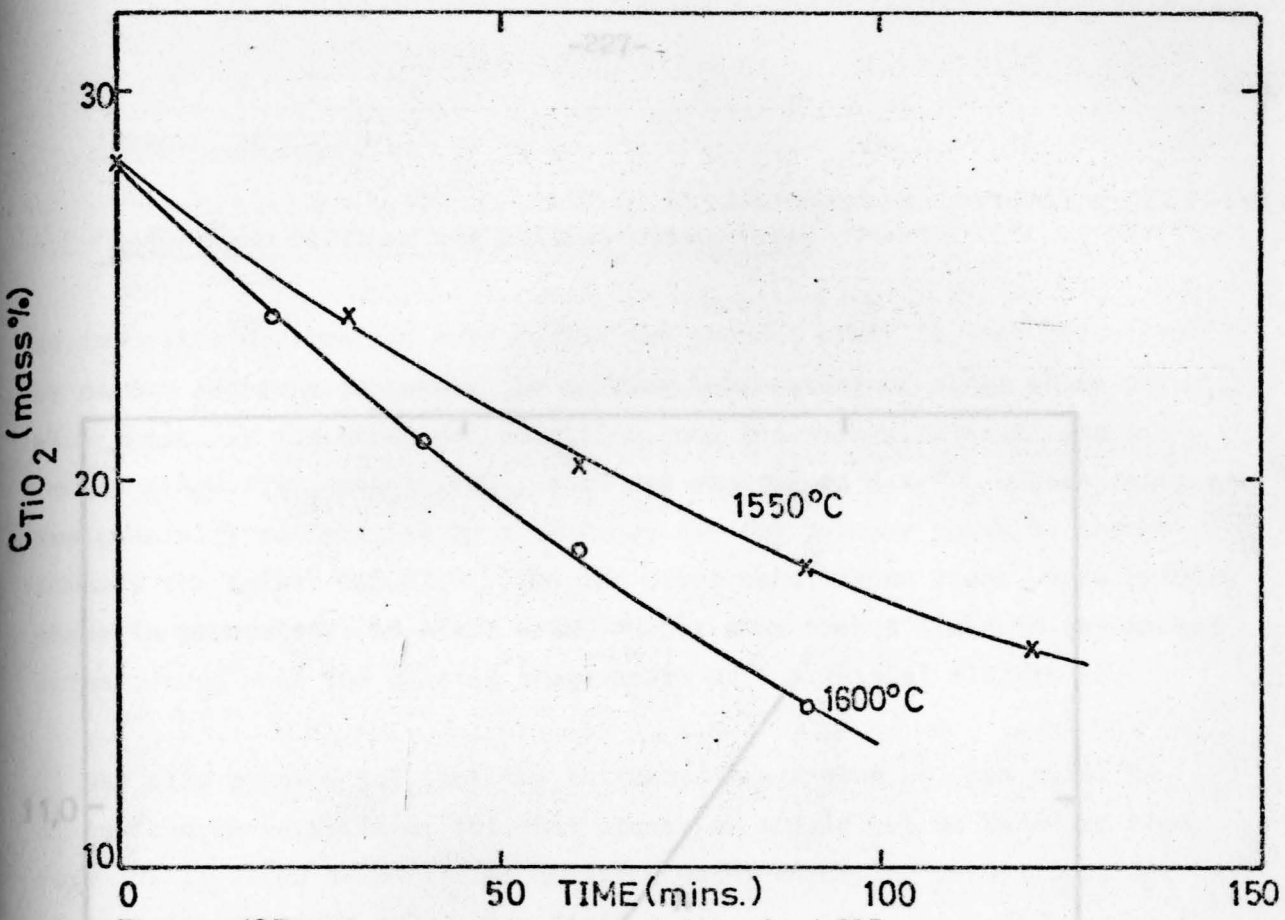


Figure 127 Rate of reduction of TiO_2 from B17

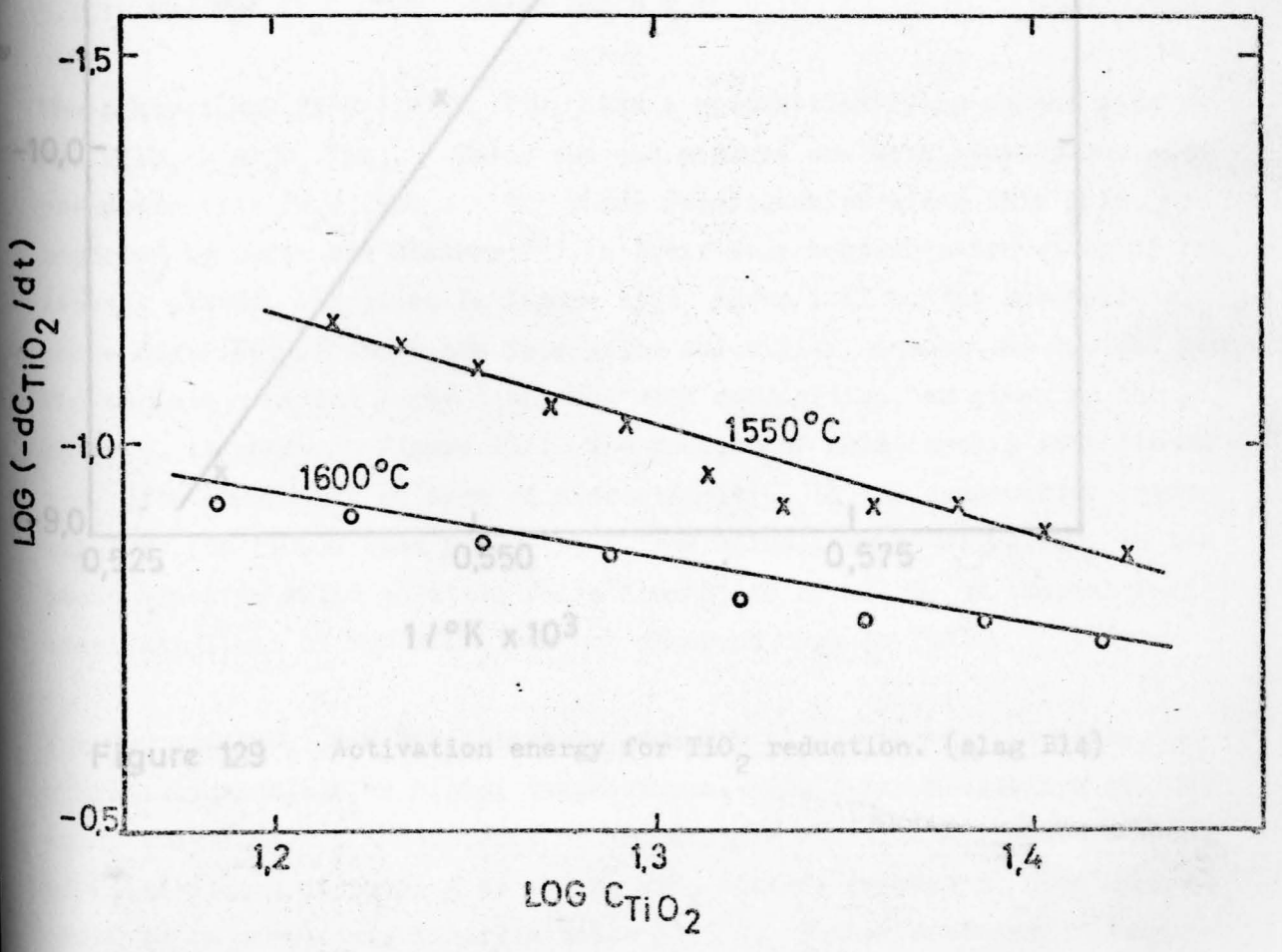


Figure 128 Order of reaction and rate constant for B17

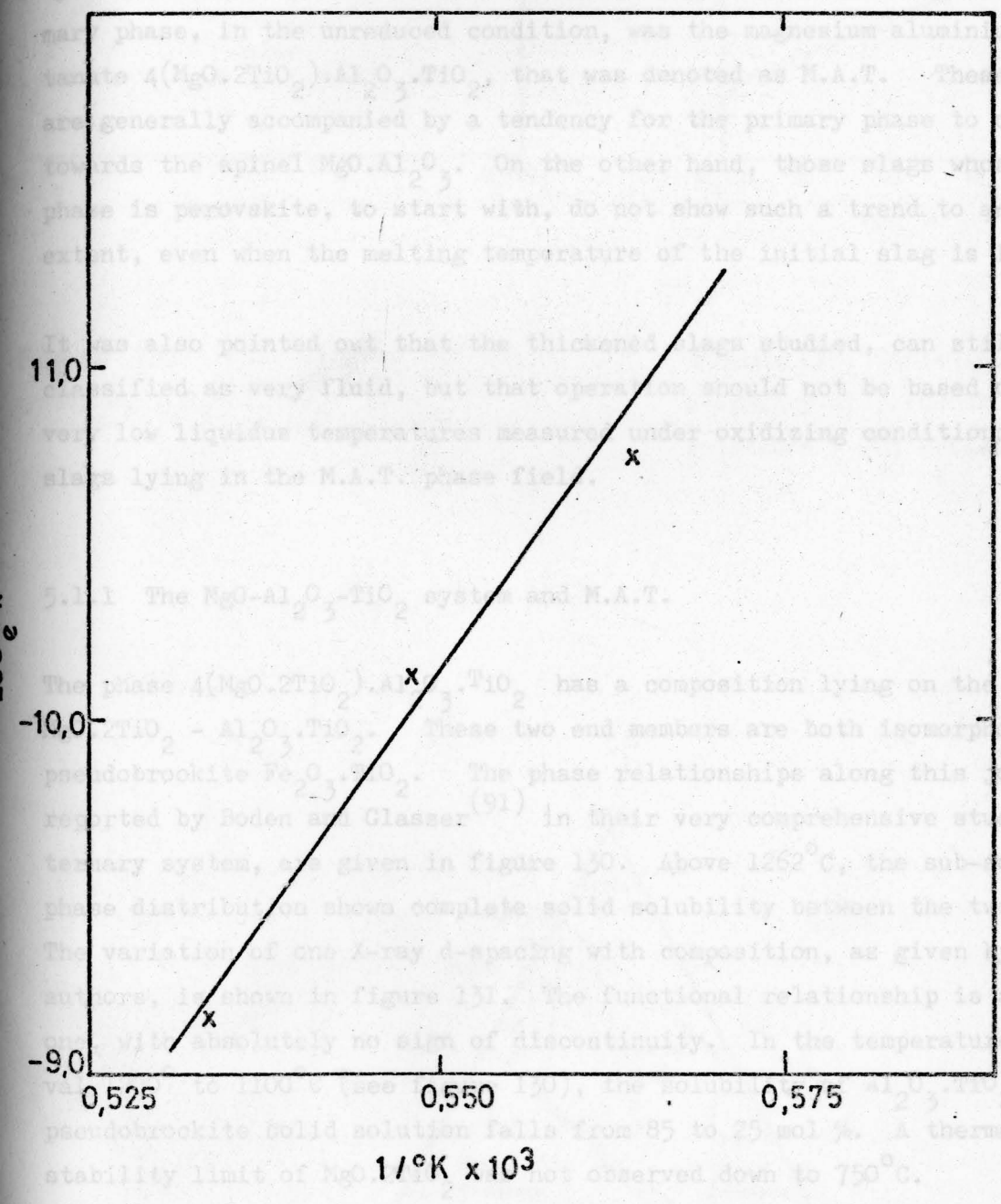


Figure 129 Activation energy for TiO_2 reduction. (slag B14)

5. GENERAL DISCUSSION

5.1 Reducing conditions and melting temperatures

An important observation made during the present study is that reduction by carbon severely increases the melting temperature of slags whose primary phase, in the unreduced condition, was the magnesium aluminium titanate $4(MgO.2TiO_2).Al_2O_3.TiO_2$, that was denoted as M.A.T. These changes are generally accompanied by a tendency for the primary phase to change towards the spinel $MgO.Al_2O_3$. On the other hand, those slags whose primary phase is perovskite, to start with, do not show such a trend to any marked extent, even when the melting temperature of the initial slag is low.

It was also pointed out that the thickened slags studied, can still be classified as very fluid, but that operation should not be based on some very low liquidus temperatures measured under oxidizing conditions, for slags lying in the M.A.T. phase field.

5.1.1 The $MgO-Al_2O_3-TiO_2$ system and M.A.T.

The phase $4(MgO.2TiO_2).Al_2O_3.TiO_2$ has a composition lying on the join $MgO.2TiO_2$ - $Al_2O_3.TiO_2$. These two end members are both isomorphous with pseudobrookite $Fe_2O_3.TiO_2$. The phase relationships along this join, as reported by Boden and Glasser[91] in their very comprehensive study of the ternary system, are given in figure 130. Above 1262°C, the sub-solidus phase distribution shows complete solid solubility between the two end members. The variation of one X-ray d-spacing with composition, as given by the authors, is shown in figure 131. The functional relationship is a linear one, with absolutely no sign of discontinuity. In the temperature interval 1200° to 1100°C (see figure 130), the solubility of $Al_2O_3.TiO_2$ in the pseudobrookite solid solution falls from 85 to 25 mol %. A thermal instability limit of $MgO.2TiO_2$ was not observed down to 750°C.

The two spinels, $2MgO.TiO_2$ (inverse) and $MgO.Al_2O_3$ (normal), are also completely miscible at higher temperatures. The X-ray d-spacings of the solid solutions are independent of temperature and also a linear function of composition, increasing as the Mg_2TiO_4 content increases. The spinels cease to be completely miscible below 1375°C. Futher decrease in temperature leads to the formation of assemblages containing two spinel phases.

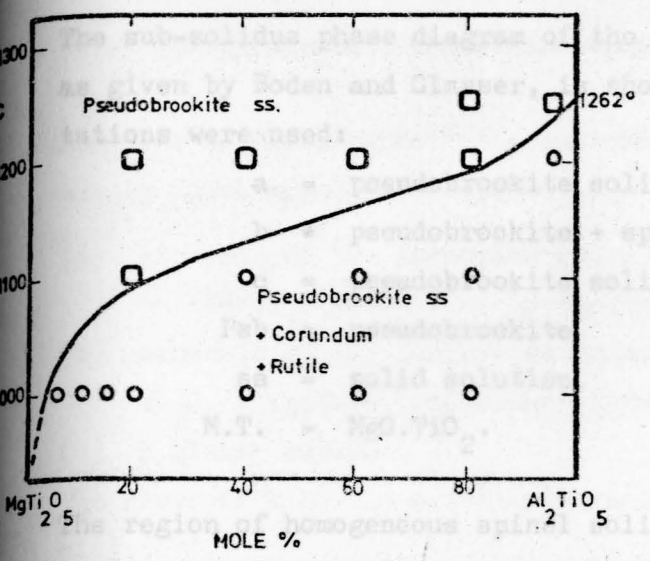


Figure 130 Phase diagram for the system $MgTi_2O_5$-Al_2TiO_5 (91)

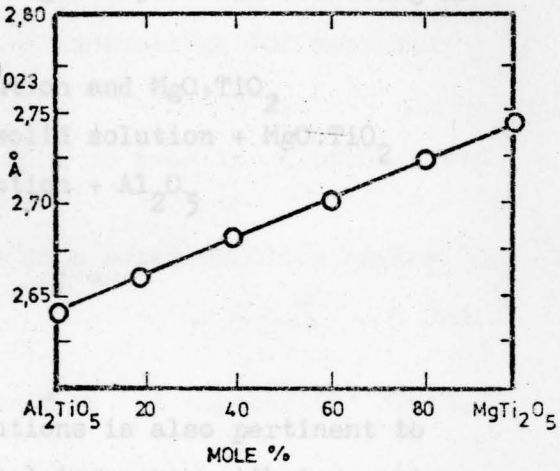


Figure 131 Variation in X-ray d-spacing of pseudobrookite solid solutions - 023 reflection. (91)

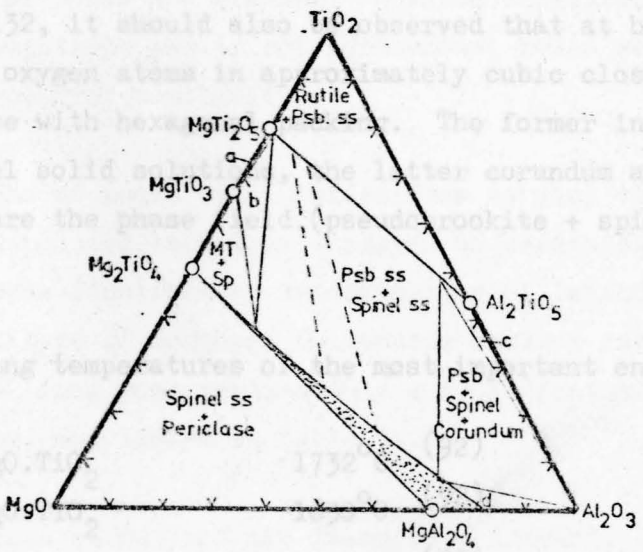


Figure 132 Subsolidus diagram of the MgO-Al_2O_3-TiO_2 system at 1550°C. (91)

The sub-solidus phase diagram of the system $MgO-Al_2O_3-TiO_2$ at 1550°C, as given by Boden and Glasser, is shown in figure 132. The following notations were used:

a = pseudobrookite solid solution and $MgO.TiO_2$
b = pseudobrookite + spinel solid solution + $MgO.TiO_2$
c = pseudobrookite solid solution + Al_2O_3
Psb = pseudobrookite
ss = solid solution
M.T. = $MgO.TiO_2$.

The region of homogeneous spinel solid solutions is also pertinent to this work. The solubility of Al_2O_3 in spinel increases with temperature, reaching $\pm$ 80 % at 1550°C. (The alumina content of $MgO.Al_2O_3$ is 71,66 %). The stoichiometry of Mg_2TiO_4 varies little at temperatures up to 1550°C, and substitution of Ti^{4+} into the aluminate spinel decreases the solubility of excess Al_2O_3. The wedge-like shape of the homogeneous spinel field is caused by the changing solubility of Al_2O_3.

It is very significant that the X-ray d-spacings of the ternary spinel solid solutions go through the "wedge" almost parallel to the iso-magnesia contours. These lines, as determined by Boden and Glasser, show for example that a spinel containing as mass % concentrations 32 % MgO, 44 % Al_2O_3 and 19 % TiO_2, has the same unit cell size as stoichiometric $MgO.Al_2O_3$.

Regarding figure 132, it should also be observed that at high temperature, phases containing oxygen atoms in approximately cubic close packing are favoured over those with hexagonal packing. The former include pseudobrookite and spinel solid solutions, the latter corundum and $MgO.TiO_2$. At lower temperature the phase field (pseudobrookite + spinel solid solutions) contract.

The proposed melting temperatures of the most important end members in the system are:

$2MgO.TiO_2$	1732°C	(92)
$MgO.TiO_2$	1630°C	(92)
$MgO.2TiO_2$	1652°C	(92)
$MgO.Al_2O_3$	2135°C	(93)
$Al_2O_3.TiO_2$	1860°C	(93)

5.1.2 Mineralogical composition of some titaniferous slags

According to Reznichenko[35] industrial high titania slags (of approximately Sorel type) are composed of:

(a) minerals of the anosovite group consisting of a solid solution based on the Ti_3O_5 structure (orthorhombic),
(b) minerals of the tagirovite group based on a solid solution having the Ti_2O_3 structure (rhombohedral) and
(c) a glassy matrix.

The group of minerals actually formed, depends on the composition of the slag.

The author proposed the following general formula for the anosovite group:

$$m\,[(Ti,Mg,Mn,Fe)O.\,2TiO_2]\;.\;n\,[(Ti,Fe,Al,Cr,V)_2O_3.\,TiO_2]$$

The possibility of complete mutual dissolution is strongly suggested by the variable valence of Ti in Ti_3O_5:

$$TiO.2TiO_2 \longleftarrow Ti_3O_5 \longrightarrow Ti_2O_3.TiO_2$$

The formula proposed for the tagirovite type minerals is:

$$a\,[(Ti,Mg,Mn,Fe)O.TiO_2]\;.\;b\,[(Ti,Al,Cr,V,Fe)_2O_3]$$

The existence of such a solid solution series appears doubtful in the light of the work of Boden and Glasser[91] which indicated that $MgO.TiO_2$ and Al_2O_3 are incompatible and do not form mutual solid solutions, in spite of their structural similarity.

The available values of ionic radii suffer from varying degrees of uncertainty, depending upon the technique employed to determine them (eg. calculation from wave functions or determination of lattice spacings of crystals where the type of compound introduces another variable). The radii of those ions most pertinent to a consideration of the above solid solution types, are listed in table 59.

Even when the obvious variations are taken into account, it appears that the ionic radii for di- and trivalent ions are sufficiently similar, as groups, to allow mutual substitution.

Table 59 Ionic radii of selected metal ions

Ion	Radius (Å)	Ion	Radius (Å)
Ti^{2+}	0,94	Ti^{3+}	0,76
Mg^{2+}	0,66	Fe^{3+}	0,64
Mn^{2+}	0,80	Al^{3+}	0,51
Fe^{2+}	0,74	Cr^{3+}	0,63
		V^{3+}	0,74

Forman, Prince and Bright, as quoted by Handfield and Charette[10], concluded from their work on Sorel type slags, that the main constituents of these slags have one of the two basic formulae:

(a) $RO.2TiO_2$ $(R = Mg^{2+}, Fe^{2+}, Ti^{2+})$

(b) $R_2O_3.TiO_2$ $(R = Fe^{3+}, Al^{3+}, Ti^{3+})$

These findings agree well with those of Reznichenko mentioned above.

The work on very high titania slags oulined in this section, is important in this context insofar as the results can be expected to represent extreme conditions in the present study.

Jochens[8] also mentioned that phase studies carried out on pilot plant slags of approximate compositions: 20 - 22% CaO, 8 - 10% MgO, 15 - 18% SiO_2, 10 - 12% Al_2O_3, 31 - 34% TiO_2, 1% FeO, 0,3% V_2O_5 and 0,25% Cr_2O_3, revealed that the primary phase was $CaO.TiO_2$. This was followed by (M.A.T. + $MgO.Al_2O_3$). This sequence applies to an operation when a mixture of limestone and dolomite was used as a flux. The order was reversed in slags produced when using dolomite as a flux. These slags arose from pilot plant testing prior to the commissioning of the Highveld iron plant.

In fact, Jochens[86] during his work on synthetic slags, showed that the M.A.T. phase was in many cases accompanied by "traces" of $MgO.Al_2O_3$. The latter phase could not be resolved microscopically.

5.1.3 The perovskite and ilmenite structures.

$CaO.TiO_2$ is known to be a very stable phase. It has a melting temperature of approximately 2000°C, compared with eg. $FeO.TiO_2$ (1470°), $MgO.TiO_2$(1630°)

and $MgO.Al_2O_3$ (2100°).

The perovskite structure is only ideally cubic, in which case the large Ca^{2+} ions occupy the centres of the cubes in the close packed arrangement with oxygen, while the smaller Ti^{4+} ions fill the corner interstices. Ti^{4+} is 6-coordinated, while Ca^{2+} has a coordination number of 12.

In the ideal structure there is a definite relation between the radii of A, B and O, if the general structure is represented by ABO_3:

$$r_A + r_O = \sqrt{2}\,(r_B + r_O).$$

Comparatively few compounds have the ideal cubic structure. Many, including $CaO.TiO_2$ itself, have distorted variants of lower symmetry, so that a more representative formula is:

$$r_A + r_O = t\sqrt{2}\,(r_B + r_O).$$

All compounds of perovskite structure have t = 0,8 to 1,0. Lower values of t lead to the formation of the ilmenite structure. For an ideal cubic structure, t = 0,89 and in the range t = 0,8 to 0,89 (in which perovskite falls), the tendency is towards monoclinic or orthorhombic structures.

Ilmenite, exemplifying the ilmenite structure, is isomorphous with α-Al_2O_3 and Fe_2O_3. $MgO.TiO_2$ has the same hexagonal structure. The metal ions are each surrounded by six oxygen ions.

It is also significant that, while solid state reduction of ilmenite is possible at comparatively high temperature, reduction is facilitated by pre-oxidation to a pseudobrookite type structure.

5.1.4 Consideration of the reduced condition of slags in this study

It was repeatedly indicated in section 4.2.5 that the oxygen content of the reduced slags apparently tended to a level corresponding to the stoichiometry of Ti_3O_5, as the reduction time was extended. It was also indicated, although not proved conclusively, that the reduction product at the slag-graphite interface appeared to contain a high concentration of the same compound.

It was pointed out in section 5.1.2 that the disproportionation

$TiO.2TiO_2 \longleftarrow Ti_3O_5 \longrightarrow Ti_2O_3.TiO_2$

in a system reduced to a level where the oxygen content is suitable, is a feasible one. The two extremes are isomorphous with the end members $MgO.2TiO_2$ and $Al_2O_3.TiO_2$ in the $MgO-Al_2O_3-TiO_2$ system, so that Ti^{2+} can replace Mg^{2+}, and Ti^{3+} can replace Al^{3+} in the magnesium aluminium titanate $4(MgO.2TiO_2).Al_2O_3.TiO_2$.

Extreme replacement under severe non-equilibrium conditions as do exist at the reaction phase boundary, must lead to the separation of a lower titanium oxide. It has been shown that even in the oxidized state, the spinel phase $MgO.Al_2O_3$ accompanies M.A.T. when the latter is the primary crystallization product. Replacement of Mg^{2+} by Ti^{2+}, and of Al^{3+} by Ti^{3+} must necessarily lead towards at least a change favouring the spinel phase in the bulk of the slag. The spinel in its pure form, is a stable high temperature phase. Lower titanium oxides at the molar O/Ti ratios at which they are present in this system, are not believed to be congruently melting, but the general temperature where a true liquid is expected to exist, is high ($+1800^{o}C$).

This mechanism appears to be in accord with the observations made in this study when the slag with the original primary phase M.A.T. was investigated in the as-reduced condition. The primary crystallization product $MgO.Al_2O_3$ reported as being present in the core powders of such reduced slags, is not expected to conform stoichiometrically to the pure spinel, but rather to be a member of the solid solution series containing MgO, Al_2O_3 and TiO_2. The results of Boden and Glasser appear to confirm such a possibility, when only X-ray diffraction results are used for the identification of the crystalline phase.

However, the increased melting temperatures reported in sections 4.2.1 and 4.2.2 referred to homogenized melts in which lower oxides of titanium were not identified. The primary crystallization product consisted of M.A.T. and spinel and the experimental evidence for the latter was very conclusive. It is suggested that the lower oxides of titanium, containing Ti^{2+} and Ti^{3+}, were redistributed, a pseudobrookite solid solution phase of composition similar to the one suggested by Reznichenko (section 5.2.1) was reconstructed, and because of the mutual substitution the spinel phase persisted. The effect of the substitutions on the melting behaviour of the pseudobrookite solid solution is virtually impossible to predict, but

the appearance of the spinel phase may reasonably be expected to give rise to an increase in the liquidus temperature of the slag.

Those slags initially having perovskite as the primary phase, showed little, if any significant rise in melting temperature upon reduction.

It was indicated that $CaO.TiO_2$ is a very stable phase. Moreover, replacement of CaO by TiO, although configurationally feasible, would imply a non-equilibrium oxidation state of titanium under the conditions obtaining during viscosity measurement. While it is believed that $CaO.TiO_2$ may eventually be replaced by a spinel phase as the primary crystallization product, reducing conditions employed during this study were not severe enough to bring about such a change.

In conclusion, it is suggested that changes in liquidus temperature occurring during reduction by carbon, are not simply related to slag basicity. Such an explanation seems to be implied by eg. Gruzdev et al[58] (section 2.4.8). Instead, the solution must be sought in the nature of the primary phase of the initial slag which in this study, was not determined by basicity only, but also by the CaO/MgO ratio and the titania content of the slag. It is however significant that the three highly acidic members of the B series (B16, B17 and B18) had M.A.T. as a primary phase, regardless of the CaO/MgO ratio.

5.2 Reducing conditions and viscosity

5.2.1 A possible relationship between the rate of titania reduction and viscosity

It was illutrated in section 4.2.5 that although first order kinetics, believed to be associated with chemical reaction rate control, was followed by the system over the initial reduction period, such a model could not be used to interpret the rate data over the entire period of reduction. This statement appeared to be particularly valid for more basic slags. For more acidic slags (represented by B17) and possibly even for slag B14 (basicity ratio 1,4) when reduced at the lowest temperature (1500°C), the linear logarithmic relationship between rate of titania reduction and the apparent concentration of TiO_2 in the melt, was maintained for

even prolonged reaction.

It was also shown in section 4.1.1 that viscosity is a function of the time of reduction. During reduction at temperatures up to 1550°C the viscosity of the three slags B11, B14 and B17, with the basicity decreasing in this order, showed an initial tendency to decrease. This was followed for the two more basic slags, by "thickening". The viscosity of B17 did not increase. When the reaction temperature was raised to 1600°C, the viscosity minimum disappeared in the case of B11, became less pronounced in the case of B14, while B17 now became less fluid during prolonged reduction.

If a slag "thickens" appreciably relative to its initial viscosity, it is reasonable to expect that the apparent rate of titania reduction will become dependent on transfer of oxygen from the bulk of the slag to the reaction interface. Such a transition may be accompanied by a change in the order of reaction from unity to higher orders. If diffusion is to become the rate limiting step, a treatment of the rate data as outlined below, suggests itself.

Still referring to the reaction:

$$aTiO_2 + bC = dTi_2O_3 + fCO \quad \ldots\ldots\ldots(3),$$

the rate of reaction is given by:

$$-\frac{d\,C_{TiO_2}}{dt} = \frac{D_{TiO_2}.A}{\delta}\left[C_{TiO_2}(i) - C_{TiO_2}(b)\right] \quad \ldots\ldots(12)$$

where D_{TiO_2} = diffusivity of TiO_2 in the slag,

A = interfacial area,

δ = effective boundary layer thickness at the slag-graphite interface,

$C_{TiO_2}(i)$ = concentration of TiO_2 at the interface,

$C_{TiO_2}(b)$ = bulk concentration of TiO_2.

If $C_{TiO_2}(i)$ is assumed to be negligible, equation (12) becomes:

$$\frac{d\,C_{TiO_2}}{dt} = \frac{D_{TiO_2}.A}{\delta}\left(C_{TiO_2}\right) \quad \ldots\ldots\ldots(13)$$

The diffusion boundary layer will only be of constant thickness (δ) if there is no gas evolution. In the present system, this condition is not

fulfilled. On the contrary, the rate of agitation of the melt by bubbles of carbon monoxide and possibly silicon monoxide will be a function of both silica and titania reduction rates. If it were possible to assume that δ was a function only of $\frac{d\,C_{TiO_2}}{dt}$, Wagner's [94] proposed empirical relation might have been useful:

$$\delta = j\left[\frac{d\,C_{TiO_2}}{A\,dt}\right]^{-\beta} \qquad \ldots\ldots\ldots(14)$$

where j and β are constants.

Substitution of equation (14) into (13) leads to:

$$\frac{d\,C_{TiO_2}}{dt} = A^{1-\beta}\left[\frac{D_{TiO_2}\cdot C_{TiO_2}}{j}\right]^{1/(1-\beta)} \qquad \ldots\ldots\ldots(15)$$

An approximate value of the order of reaction might be obtained from the kinetic data presented before. Substitution into equation 15 would give a value of β and the apparent rate constant would be expressed in terms of A, D_{TiO_2} and j. However, D_{TiO_2} is not a constant either, but is related to viscosity through the relationship:

$$D_{TiO_2} = \text{const.}/\eta \qquad \ldots\ldots\ldots(16),$$

according to Yavoyskiy[95].

Accordingly, a relationship was sought between the apparent rate of titanium oxide reduction and the viscosity at the reduction temperature. The relevant results are presented graphically in figures 133 to 137. For those slags showing a well-defined "thickening" period, there exists a linear relationship between viscosity and reduction rate - B11 reduced at 1550°C (figure 133) and B14 reduced at 1550° and 1600°C (figures 135 and 136 respectively). The illustrations for B14 (1500°) in figure 134 and for B17 (1550°C) in figure 137 were included merely to show the lack of any obvious relationship between the two variables. As was expected, this linear correllation existed approximately over the region where a first order rate law was shown previously not to apply. Similarly, it was absent over the time intervals where first order rate control was suggested by the experimental data.

These results therefore strongly suggest that the reduction of titanium oxide from titaniferous slags is initially chemical reaction rate controlled.

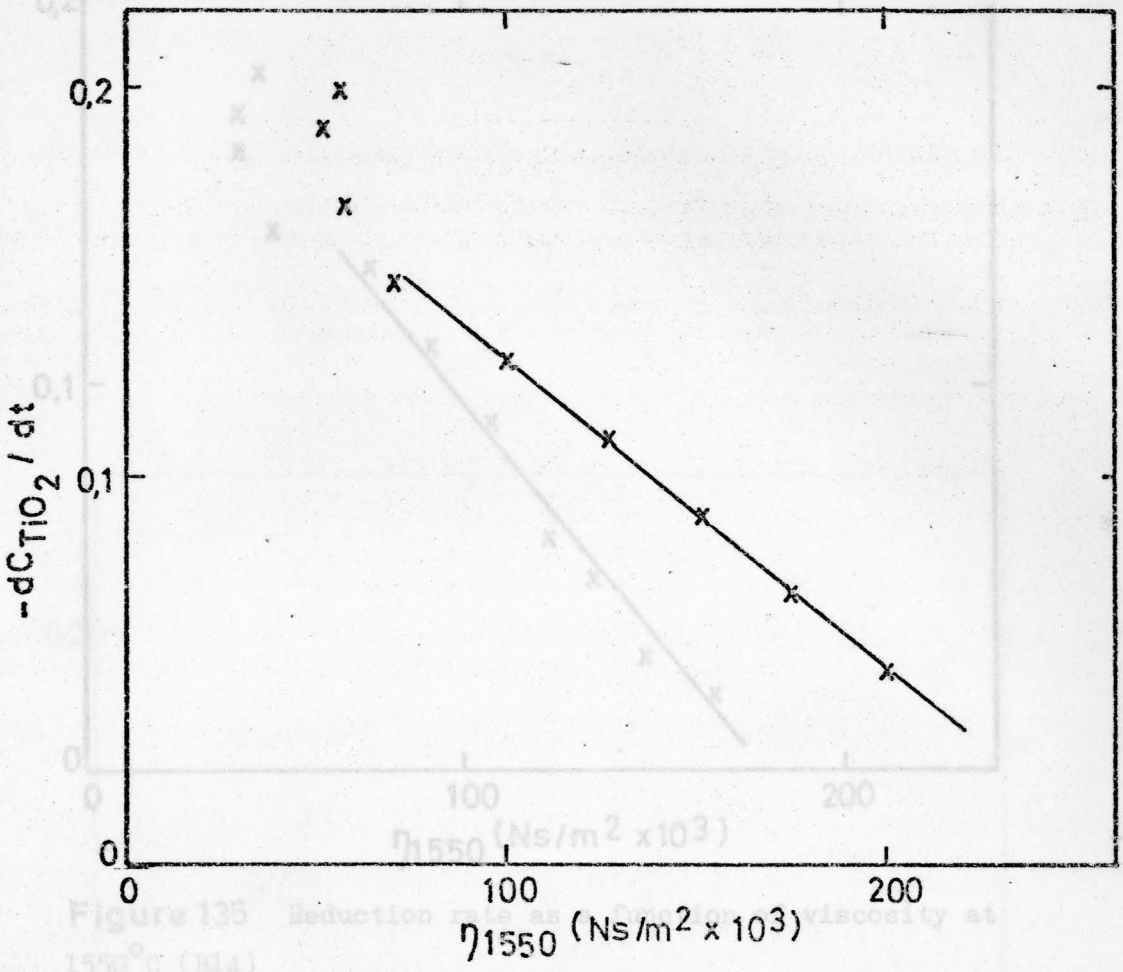


Figure 133 Reduction rate as a function of viscosity at 1550°C (B11)

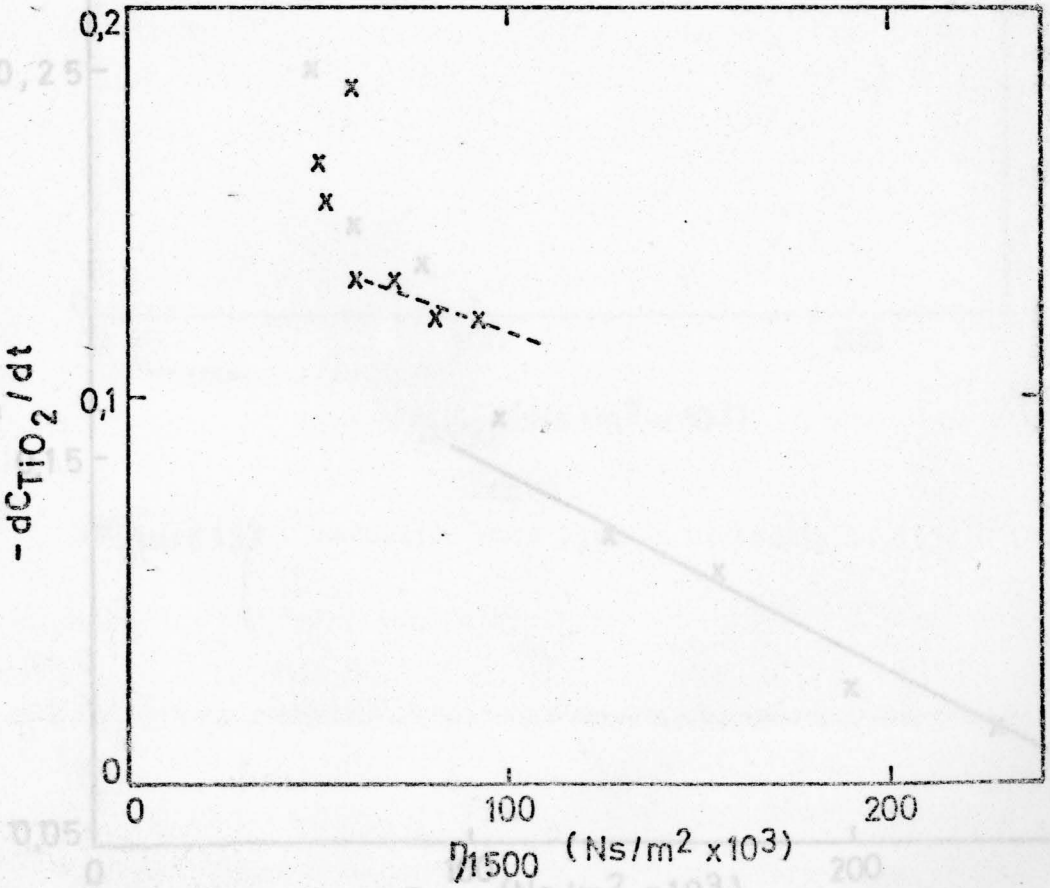


Figure 134 Reduction rate as a function of viscosity at 1500°C (B14)

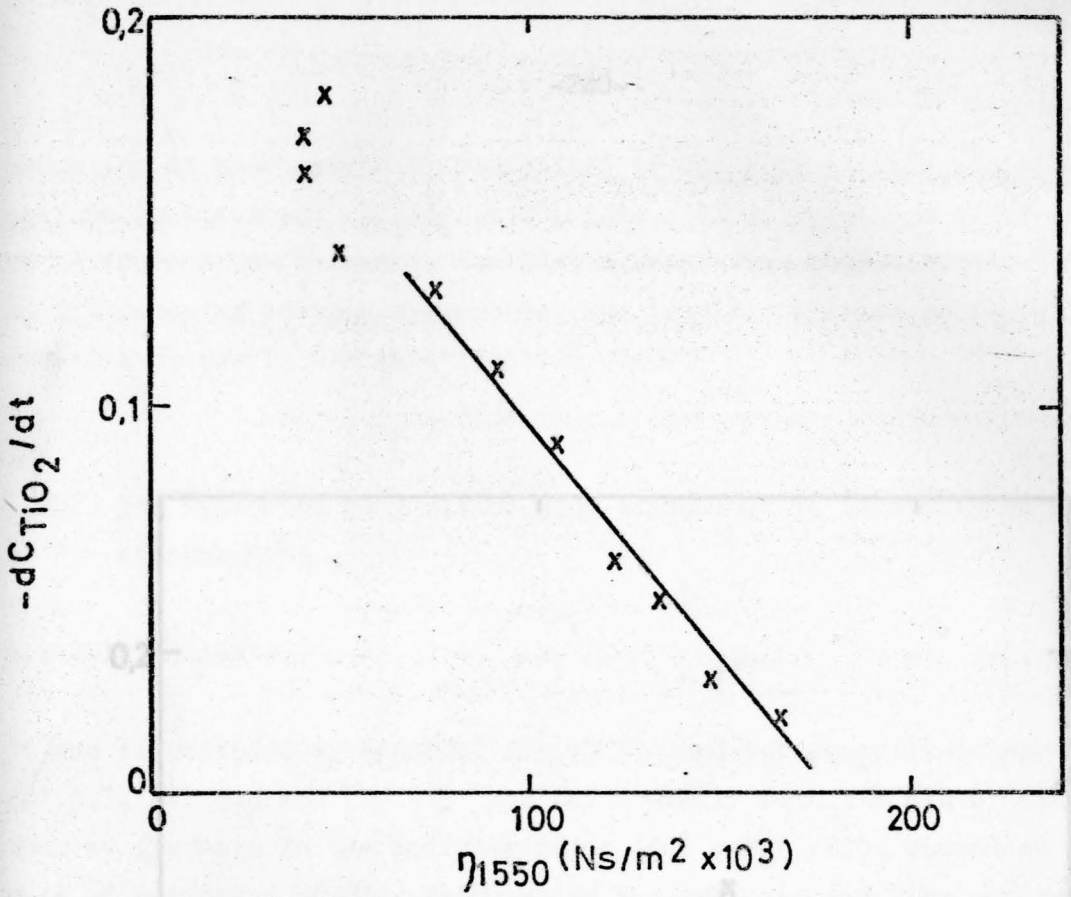


Figure 135 Reduction rate as a function of viscosity at 1550°C (B14)

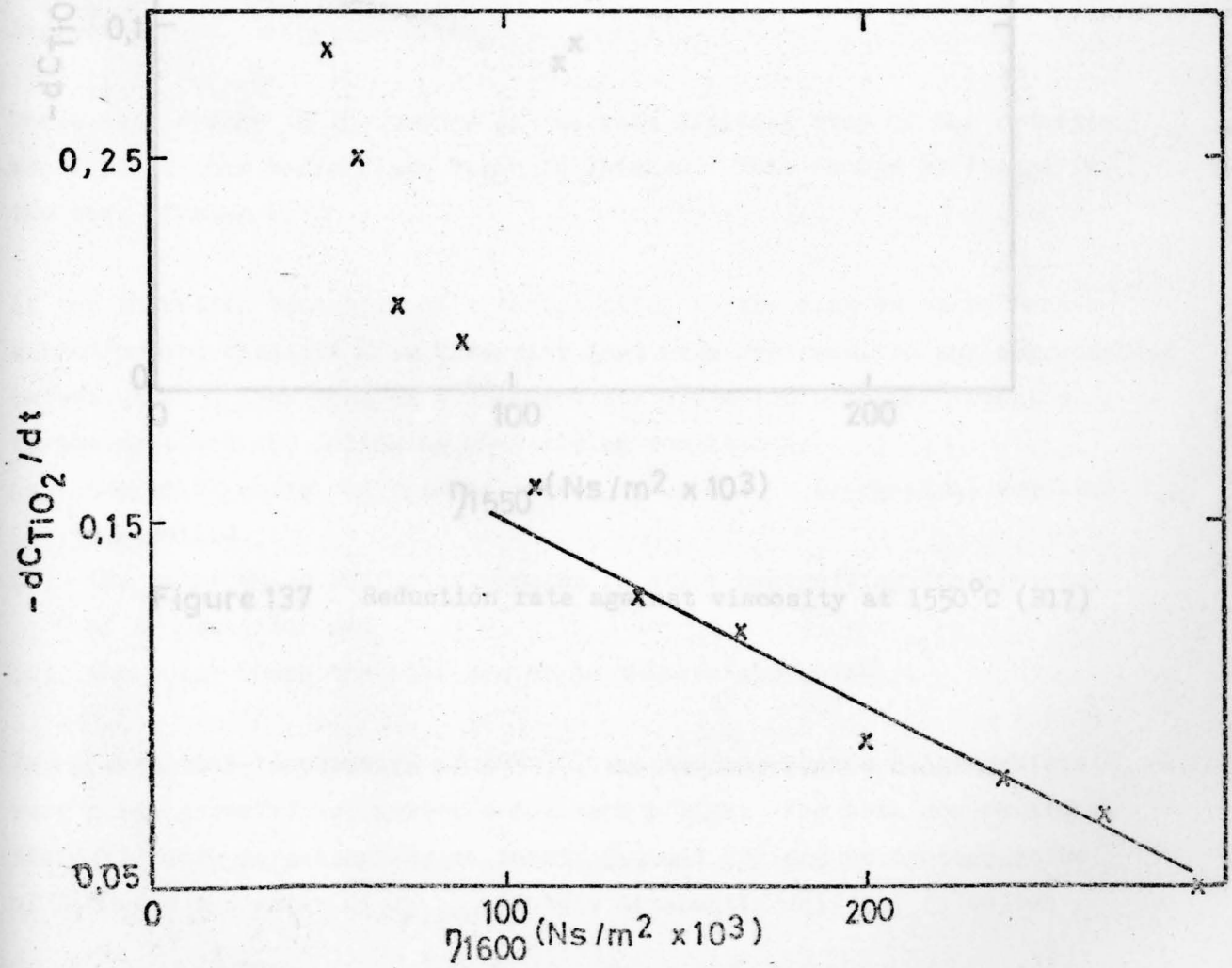


Figure 136 Reduction rate as a function of viscosity at 1600°C (B14)

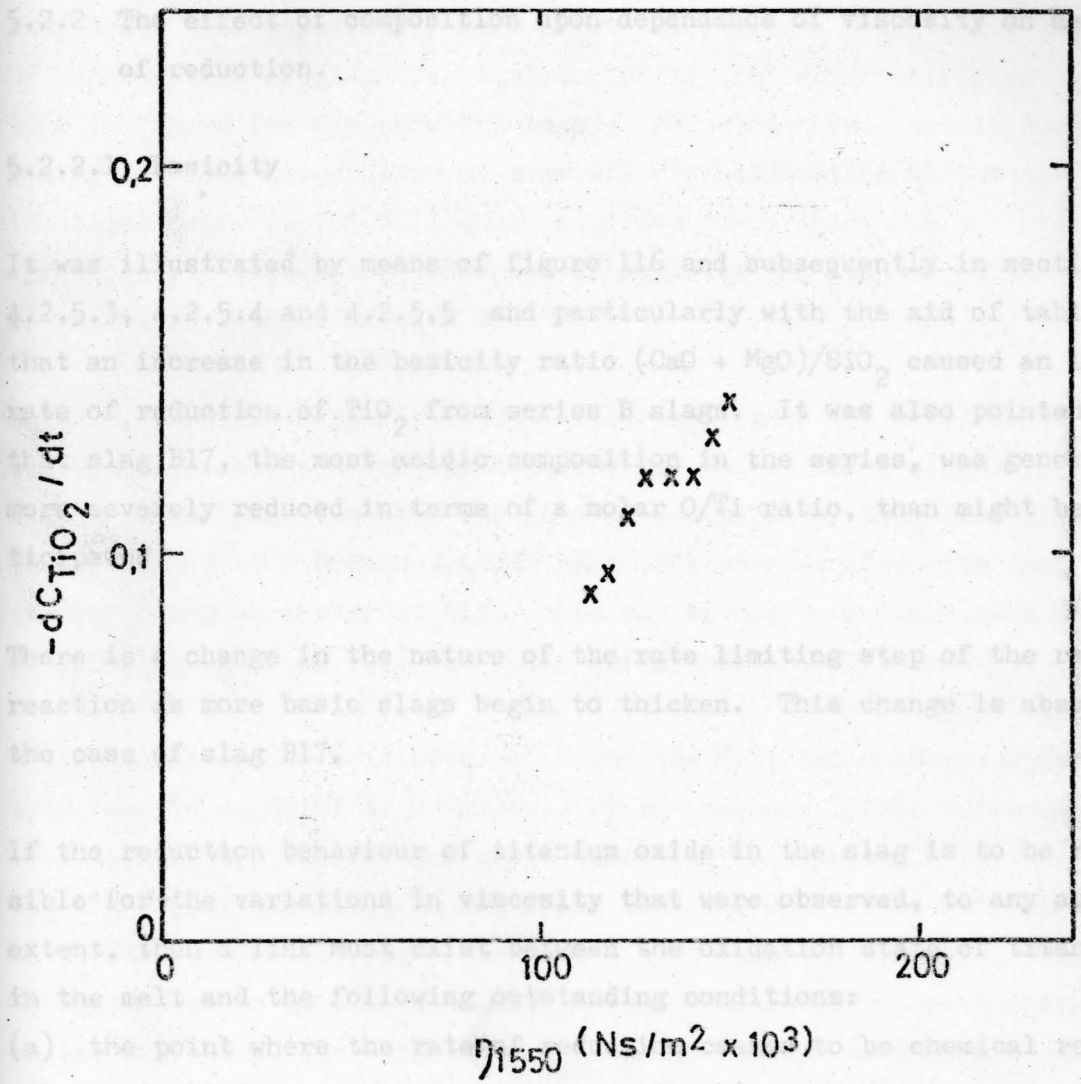


Figure 137 Reduction rate against viscosity at 1550°C (B17)

Reduction is accompanied by "thinning" of the slag until a fluidity maximum is attained. Beyond this point, further reduction gives rise to an increase in viscosity for highly basic slag compositions. When such thickening becomes appreciable, the reaction becomes self-inhibiting due to a change in the rate limiting step.

5.2.2 The effect of composition upon dependence of viscosity on degree of reduction.

5.2.2.1 Basicity

It was illustrated by means of figure 116 and subsequently in sections 4.2.5.3, 4.2.5.4 and 4.2.5.5 and particularly with the aid of table 58, that an increase in the basicity ratio $(CaO + MgO)/SiO_2$ caused an increased rate of reduction of TiO_2 from series B slags. It was also pointed out that slag B17, the most acidic composition in the series, was generally more severely reduced in terms of a molar O/Ti ratio, than might be anticipated.

There is a change in the nature of the rate limiting step of the reduction reaction as more basic slags begin to thicken. This change is absent in the case of slag B17.

If the reduction behaviour of titanium oxide in the slag is to be responsible for the variations in viscosity that were observed, to any appreciable extent, then a link must exist between the oxidation state of titanium in the melt and the following outstanding conditions:

(a) the point where the rate of reduction ceases to be chemical reaction controlled,

(b) the point where diffusion appears to start controlling the kinetics of the reaction and

(c) the point where the slag begins to thicken appreciably.

For a reduction temperature of 1550°C, the two more basic slags exhibit very clear experimental evidence for such a link. For both compositions, the O/Ti ratio corresponding to points (a) and (b) has an average value of 1,80 and the value of η_{1550} at this apparently critical oxidation

state has a value of approximately two times that of the unreduced slag at the same temperature. Point (c) cannot be expected to coincide with (a) and (b), as the existence of an initial viscosity minimum was proved for both slags.

The effect of a rising liquidus temperature was taken into account when the viscosities of reduced slags were reported (see eg. figure 89 b for slag B14). The possibility does exist that, with a diminishing degree of superheating of slag B14, a plot such as that shown in figure 135 and that in figure 136 may show the trends indicated there, solely due to rising liquidus temperature of slag B14. Consideration of the almost identical behaviour of B11, whose liquidus temperature was not greatly influenced by reduction, rules out effectively the argument that might be raised in connection with B14.

However, comparison of figure 133 (B11) and figure 135 (B14) shows that the reaction rate - viscosity line for the latter has a slightly greater slope. This indicates that the rate of reduction of TiO_2 from slag B14 is influenced to a greater extent by an increase in viscosity than the corresponding parameter of B11. This may be due to an increased degree of ordering for slag B14, not fully reflected in its viscosity.

The critical points mentioned above and the O/Ti ratio corresponding to them, can be expected to be altered by an increase in the temperature of reduction or the temperature where viscosity is measured. For the same two slags (B11 and B14), it was found that the O/Ti ratio corresponding to points (a) and (b) was reduced to $\pm$ 1,73 when the reduction temperature was increased to 1600°C, viscosity being reported at the same temperature. At the same time, the value of η_{1600} corresponding to such a degree of reduction, increased to three times the value of η_{1600} of the unreduced slag. Such a temperature dependence is to be expected, as the rate constants of reactions controlled by both chemical reaction and diffusion should be related to temperature by Arrhenius type equations. The extent to which temperature influences the rate is largely a function of the particular system. Investigation of figures 135 and 136 (slag B14 reduced at 1550° and 1600°C respectively) reveals that the slope of the rate-viscosity line is decreased by an increase in the temperature. This signifies that viscosity becomes relatively less important in the determination of the reaction rate, as the temperature is raised. On industrial

scale it means that "thickening" is less likely to retard the reaction when the temperature is high.

Little mention has so far been made of the acidic slag B17 with $(CaO + MgO)/SiO_2 = 0,8$. It does not conform to the general rules proposed above, but the significance of the O/Ti ratios 1,80 and 1,73 does not entirely disappear. These two values correspond to a reduction time of 90 minutes at both temperatures of reduction used (1550° and 1600°C). Figures 104 and 106 show that the viscosity of the slag in such a state is either levelling out or beginning to increase.

It is suggested that the behaviour of B17 involves an aspect which was not covered in this work - that of silica reduction to mainly SiO. In this connection, reference must be made to table 13 where it was shown that very significant losses of silicon occurred during reduction of B17. This does not apply to slags B11 and B14.

Figure 127 illustrates the fact that titanium oxide is reduced from B17 at a rate that decreases little as time goes on. This gives rise to the unexpectedly high degree of ultimate reduction and must in part be attributed to the continuously decreasing viscosity, because although slag behaviour was generally divided into regions of chemical reaction and diffusion rate control, neither of these mechanisms can be considered pure. A reaction of the former type may be influenced by the fluidity of the liquid medium. The increase in fluidity is partly due to the removal of SiO_2 from the system. A decrease in silica content of the magnitude shown in table 13, for this system, gives rise to marked decreases in viscosity.. This is borne out by the results reported in section 4.1.2.1. At the same time, the concentration of TiO_2 is raised, which was also shown to improve the fluidity of slags at least under oxidizing conditions.

Silica reduction also affects the rate of titania reduction by means other than the two consequences above, both causing greater fluidity. More severe bubble agitation must necessarily aid the reduction of titania in a relatively viscous slag. Moreover, the resultant increase in titania level should have a similar effect, judging from the curve in figure 118.

Slags B11 and B14, when reduced at 1550°, pass through a fluidity maximum

at an O/Ti ratio of approximately 1,88. Tables 3 and 59 give the values of the radii of titanium in its various valency states. During the reduction sequence $Ti^{4+} \longrightarrow Ti^{3+} \longrightarrow Ti^{2+}$ there is evidently a marked decrease in the cationic field strength I. If a high cationic field strength is accepted to be associated with a low coordination number and a pronounced network forming tendency, progressive removal of oxygen from these titaniferous melts must give rise to enhanced fluidity.

In section 2.2.5, an attempt was made to offer an explanation for the high fluidity of titaniferous slags under oxidizing conditions. The possible effects of oxygen contents, that in the solid state would correspond to non-stoichiometric rutile, was also indicated. It was further suggested that even tetrahedrally coordinated titanium could not possibly give rise to a viscous slag by a mechanism comparable to that which controls the action of Al^{3+}.

As was indicated above, small decreases in silica content of these slags cause measurable reductions in viscosity. While appreciable silica losses were reported only for the most acidic slag, such losses cannot disappear entirely when more basic slags are reduced by carbon.

Furthermore the manner which a metal oxide affects the viscosity of a siliceous melt, is a function of two very important parameters:
(a) the oxygen contribution made and
(b) the nature of the other metal ions present.

On a molar basis, the titanium oxides TiO_2, $TiO_{1,5}$ and TiO contribute oxygen anions as shown by their stoichiometries, if the availability of oxygen towards network modification is assumed to be the same in all cases.

Removal of oxygen from the system in this case not only affects the behaviour of titanium ions, but also that of other ions whose coordination may be much more critically affected by such a change. A good example of these in the slags examined, is Al^{3+}. It is now well known that in the system $CaO-Al_2O_3-SiO_2$, the CaO/Al_2O_3 ratio markedly affects the viscosity of the melt.

In the light of these comments, it is suggested the viscosity minimum

so frequently reported in this work, is associated with:

(a) The disappearance of any trace of tetrahedrally coordinated titanium. The viscosity lowering effect of this is not great (the trough is a shallow one), because of the mixed and predominantly higher coordination already existing and because of the mild change brought about by a change in the coordination number of titanium.

(b) Small losses of silicon as SiO from the system.

The overridingly important "thickening" effect is due to the loss of oxygen from the melt. Not only does this lead to more extensive sharing of oxygen between silicate tetrahedra, but also possibly to a change in the role of alumina. The lowered field strength of titanium ions in the melt is almost entirely cancelled out by these effects. The role of Ti^{2+} eventually formed to a considerable degree, should then be seen as one of network distortion with very pronounced "bridging".

The effect of a high initial silica concentration is:

(a) to retard the rate of reduction of titanium oxide and

(b) to actually cause a decrease in viscosity during reduction due to the removal of SiO. The overall effect is to delay the start of the thickening process down to O/Ti ratios as low as 1,7.

Finally, while every effort was made to avoid the formation of titanium carbide during this investigation, it is very logical that it will be formed eventually, more readily in a basic slag.

5.2.2.2 CaO/MgO ratio

It was illustrated in figure 117 that reduction for 60 minutes at 1550°C had a more pronounced effect on the O/Ti ratio of the slag as the mass % CaO/MgO ratio was lowered.

Slag B13 had an O/Ti ratio of 1,84. Figure 85 shows that the viscosity minimum has been passed, but the fluidity at 60 minutes is very close to that of the unreduced slag. If in this range of slag compositions, the viscosity minimum is still taken as corresponding to O/Ti = 1,88, while "thickening" to the extent where it can begin to influence the rate limiting step of the reaction, corresponds to O/Ti = 1,80, then $1,80 < 1,84 < 1,88$.

Slag B14 is reduced to a level where O/Ti = 1,81 i.e. $1,80 < 1,81 \ll 1,88$ and its viscosity after 60 minutes is unmistakably above that of the unreduced slag. (see figure 89 b)

In the case of B15, O/Ti = 1,79. Its viscosity after reduction for 60 minutes was not measured, but if the values for 30 and 45 minutes (figure 100) are taken into account, the value of η_{L+50} (60 minutes) will be very considerably above the corresponding parameter of the unreduced slag.

Reoxidation experiments were not carried out on slags B10, B12, B16 and B18, so that it is not possible to provide correllations for the series B12-B11-B10 and B18-B17-B16, similar to the one for B15-B14-B13 given above. However, for B12-B11-B10, figures 83, 81 b and 78 a again show the deleterious effect of high magnesia contents. As the CaO/MgO ratio is reduced, (B10 to B12) the fluidity maximum eventually completely disappears, which probably means that it occurs at a reduction time shorter than 15 minutes for B12. In general, the trough is very shallow for all three slags, due to the high basicity.

The general trend for the series B16-B17-B18 is similar, if the very acidic nature of the slag is taken into account. Again B18 ($CaO/MgO = \frac{1}{2}$) is the only slag which shows any sign of an increased viscosity, although even here, η_{L+50} has not attained, after 45 minutes, the value of η_{L+50} of the unreduced slag.

The comments above are based on metal oxide concentrations expressed as mass per cent. This is desirable from an industrial viewpoint. However, it was pointed out in section 4.2.5.2 that the composition variable in the case of B13-B14-B15 could equally well be altered to a molar basicity ratio $(CaO + MgO)/SiO_2$, as far as degree of reduction is concerned. The same argument could be used to explain the effect of MgO in increasing the fluidity of unreduced slags. Consequently, the deleterious effect of magnesia in connection with thickening may be partially or entirely explained by the fact that a decrease in CaO/MgO ratio as used in this investigation, simultaneously meant an actual increase in basicity of the slag, a factor that is known to increase oxygen activity, rate of reduction and consequently thickening rate.

Another factor that may have to be taken into account is the fact that

Mg^{2+} has a greater field strength than Ca^{2+}. In the unreduced slag this would tend to cancel out the effect of the increased basicity which accompanies a decrease in the CaO/MgO ratio, and explain the small effect of such variation on viscosity. In the reduced slag, Mg^{2+} may be expected to have a greater "bridging" effect than Ca^{2+} and hence to aid the thickening process in the system of diminished oxygen concentration.

5.2.2.3 Mass per cent (TiO_2 + Al_2O_3) content

Table 40, when compared with the graphical data in figures 74, 89 b and 109 for slags A5, B14 and C23, again shows that there is good correllation between degree of reduction and viscosity. However, the O/Ti ratio of C23 (1,64) appears very low after reduction for 60 minutes at 1550°C, and the increase in viscosity illustrated in figure 109 appears particularly drastic. This apparently magnified version of the expected trends is thought to be due to two factors:

(a) The increased concentration of TiO_2 from 30,2 % to 37,18 % (B14 to C23) is bound to have a pronounced effect on oxygen activity and consequently rate of reduction.

(b) The change in titania concentration is accompanied by an increase in alumina content from 13,80 to 16,82. In an oxygen ion deficient liquid structure, Al^{3+} may be forced to enter into 4-fold coordination to a greater extent as the Al_2O_3 concentration is raised.

5.2.2.4 Oxides more readily reduced than TiO_2

The graphically presented results in figure 110 and the numerical data reported in section 4.2.5.1 are now readily interpreted.

The O/Ti ratio of the plant slag was calculated as 1,84 (1,80 < 1,84 < 1,88). Such a slag is not expected to be thickened. This was confirmed by viscosity measurement.

FeO is suggested to act mainly in two ways during the reduction of a titaniferous slag:

(a) It screens TiO_2 from reduction by carbon, much more effectively than SiO_2. This is borne out by the results given in table 37.

(b) Residual FeO provides oxygen ions to the melt which must serve to lower the viscosity. This was shown in figure 110.

5.2.3 Comparison of results with those reported in the literature

Many of the conclusions reached by earlier investigators, that were reported in section 2.4, although generally in agreement with the results of this investigation, are incomplete. This is due to the failure to distinguish between true thickening and an increase in the melting temperature of the slag. Moreover, it was not always clear whether or not titanium carbide was present in the melt.

Mikhailov and Belyakova[52] (section 2.4.2) found that addition of TiO or Ti_2O_3 increased the viscosity of both acidic and basic slags. No mention was made of the melting temperatures of the slags.

Semik[57] (section 2.4.3) found that reduction by carbon initially lowered the viscosity of blast furnace type titaniferous slags, but that the viscosity was raised subsequently. The thickening effect became pronounced only when the titania content approached 30 %. TiC was found present in the reduced melts.

The author agrees with the conclusions reached by Delve, Meyer and Lander[51], section 2.4.4. Blast furnace slags of low CaO/SiO_2 ratios and high oxygen potentials as do exist in the bosh region of the furnace, should not cause operational difficulty. Even the increased viscosity eventually attained, can cause no such difficulty. Problems in blast furnace operation are almost entirely due to formation of TiC and TiN.

As pointed out in section 2.4.5, the work of Ohno and Ross[18] did not clearly show the relative effects of a change in viscosity and of a possible increase in liquidus temperature or precipitation of such high temperature phases as TiC or TiN. The fact that basic slags were reduced faster and yet "thickened" at a slower rate, seems to indicate that the "thickening" that they observed, was mainly due to an increase in the liquidus temperature or to the precipitation of carbides and nitrides.

Even so, increased temperature, increased titania concentration and a

higher alumina concentration all served to increase the thickening rate.

McRae[23] section 2.4.7) reduced slags at relatively low temperature to illustrate there was an increase in the melting temperature. The viscosity was found to be slightly lower than that of the slag under oxidizing conditions. A maximum mass gain of 1,28 % was reported when reduced slags were reoxidized. As the author did not detect TiC in his reduced slags either, a calculation by methods similar to those used in this work, indicates an O/Ti ratio of 1,83 corresponding to the figure above. Slightly reduced values of viscosity are therefore not impossible.

The research work carried out by Gruzdev et al[58] (section 2.4.8) revealed that both acidic and basic slags were thickened after reduction for 5 hours at 1600°C. They also reported changes in liquidus temperature. Such severe reducing conditions were not used in this work and the formation of TiC might have been considerable. However, the same authors also reported that addition of TiO_2 and Ti_2O_3 to a parent slag both caused increases in fluidity, the effect of the former being more pronounced. As they found Ti_2O_3 to increase the liquidus temperature of acid slags, but to reduce the liquidus temperature of basic slags, consideration of particularly the former in conjunction with the effect of Ti_2O_3 on viscosity, appears to indicate a phenomenon similar to what was found during this work.

Handfield, Charette and Lee[59] (section 2.4.9) added similar quantities of the various titanium oxides to a base slag. They concluded that the capacity for network modification was raised when TiO_2 was replaced by Ti_2O_3 and that Ti_2O_3 appeared to be a better network modifier than TiO. Recalculation of the composition of the slag containing 20 % titanium oxide reveals that it would contain approximately 30 % SiO_2, 28 % CaO, 14,5 % MgO with very little Al_2O_3. Taking into account the relative effects of these oxides as suggested on the basis of this investigation, the results obtained by Handfield et al are not surprising.

5.3 Reducing conditions and electrical conductivity

The conclusions derived from earlier experimental data, as summarized in sections 2.5.1 and 2.5.2, present a confusing picture. Russian research work was concentrated on high titania slags containing both titanium and

iron oxides. More fundamental data resulting from attempts to separate the effects of the two semiconductors are seriously lacking.

Reznichenko and Balikhin[64] reported that FeO additions to high titania slags lowered the conductivity of the melts. This agrees with the results of Denisov, Degtyarev and Reznichenko[67,68] (section 2.5.2). There is no clear explanation of whether the higher conductivity of low-FeO slags is associated with the greater degree of reduction of titanium oxide which necessarily follows and whether the two oxides exhibit similar mechanisms of semiconduction at least in slags. Iron oxide is known to owe its semiconducting properties to electron exchange between Fe^{2+} and Fe^{3+}. A similar mechanism seems to be indicated for titanium by the work of Musikhin et al[65].

Nikitin et al[96] however showed that addition of TiO_2 to FeO lowered the conductivity at 1400°C. The effect is less marked than those of SiO_2, Al_2O_3 and CaO.

As might be expected from the mechanism of semiconduction, Fe^{2+} and Fe^{3+} represent limiting conditions in slags containing iron oxides. At either x = 0 or x = 1 where x = Fe^{3+}/Fe, ionic conduction is the unique mode of charge transfer. It was shown in section 2.6.1 that the value of x = 0,5 frequently corresponds to a conductivity maximum associated with electronic conduction. This is to be expected. Other results reported in the same section[76,77] revealed dependence of such properties as viscosity, liquidus temperature and electrical conductivity upon the ratio x, but generally the effects were the reverse of what was found for titaniferous slags in this work, at least as far as the first two properties are concerned.

Molten oxide systems containing titanium oxides in different states of reduction lack the simplicity of iron oxide containing systems due to the absence of a well defined boundary condition. This is best appreciated if the electrical properties of the solid titanium oxides are considered.

5.3.1 Electrical properties of TiO_2, Ti_2O_3 and TiO[97]

The electronic conductivity of these oxides is closely connected with the

contraction of 3 d metal ions (eg. Sc^{3+}, Ti^{3+}, V^{3+}, Cr^{3+}, Mn^{3+}, and Fe^{3+}) in conjunction with the decreasing feasibility of a 3 d band due to overlapping. In the above series, Cr_2O_3 and Fe_2O_3 are normally insulators.

(a) TiO_2 (configuration d^0)

If a 3 d band exists, one would expect it to be normally empty. Electrons may be supplied to the 3 d band by excitation from imperfections or from the filled 2 p band. The Hall mobility of rutile is approximately 1,0 $cm^2/V.sec.$, and it decreases in the normal manner with increasing temperature. There are also indications that the forbidden energy gap is increased beyond 1200°K.

(b) TiO (configuration d^2)

Apart from TiO_2 the only oxide with very clear evidence of a 3 d band is TiO. It behaves like a metal, indicating the existence of a partially filled 3 d band. Room temperature conductivity is high ($\pm$ 3 500 $ohm^{-1}cm^{-1}$). The mobility is comparable to that of TiO_2 and it increases slowly with decreasing temperature. Conductivity also decreases in the ratio 7/12 as the oxygen content is increased from $TiO_{0,7}$ to $TiO_{1,2}$. This is to be expected if the change in stoichiometry is accepted to cause an equal change in the number of 3 d electrons in the 3 d band.

(c) Ti_2O_3 (configuration d^1)

The conductivity increases as the temperature rises and mobilities are considerably lower than for the other two oxides.

From this brief review, it is at least clear that the Ti - O system does not have the relative simplicity of Fe-O, regarding the nature of the current carrying mechanism. Observed conduction appears to be the combined expression of three mechanisms instead of two.

5.3.2 Relation between degree of reduction and resistivity

Electrical resistivity measurements were carried out on the full range of reduced derivatives of slag B14 only. Table 60 gives the values of the molar O/Ti ratios of the slags that were reduced at 1550°C, together with

resistivities at the same temperature.

Table 60 Electrical resistivity as a function of degree of reduction - slag B14 reduced at 1550°C

Reduction time (minutes)	Molar O/Ti	ρ_{1550} (ohm cm)
0	1,96	0,535
30	1,88	0,452
60	1,81	0,405
90	1,77	0,350
120	1,73	0,360

The same information is presented graphically in figure 138. The abscissa was modified to the quantity $x = (2 - O/Ti)$.

The curve that was fitted to the experimental points is well represented by the quadratic:

$$\rho = 2,32\ x^2 - 1,54\ x + 0,59$$

There exists little experimental evidence for a parabolic relationship. The function is merely one good representation of observed data over the region tested. The approach is based on that of Engell and Vygen[74] as outlined in section 2.6.1. They based their assumption that the contribution of electronic conduction in the iron oxide containing slags must be given by $bx\ (1 - x)$ where $x = Fe^{3+}/Fe$, on the fact that the number of nearest neighbours of Fe^{3+} to an Fe^{2+} ion is proportional to $x(1 - x)$. Such a function has a maximum where $x = \frac{1}{2}$, which appears correct in the light of the accepted mechanism of electronic conduction for the system considered. The value of the maximum of the overall conductivity - x relation will be unaltered only if the influence of x on ionic conductivity is negligible.

The above equation has a projected minimum at $x = 0,33$. This is remarkable as this corresponds to the stoichiometry of Ti_3O_5 or $TiO.Ti_2O_3$ or $TiO.2TiO_2$. If any significance is to be attached to such a result, it would appear that an electronic conductivity optimum is moved to between Ti^{4+} and Ti^{3+}, rather than being in the range Ti^{3+} to Ti^{2+}. As was pointed out before,

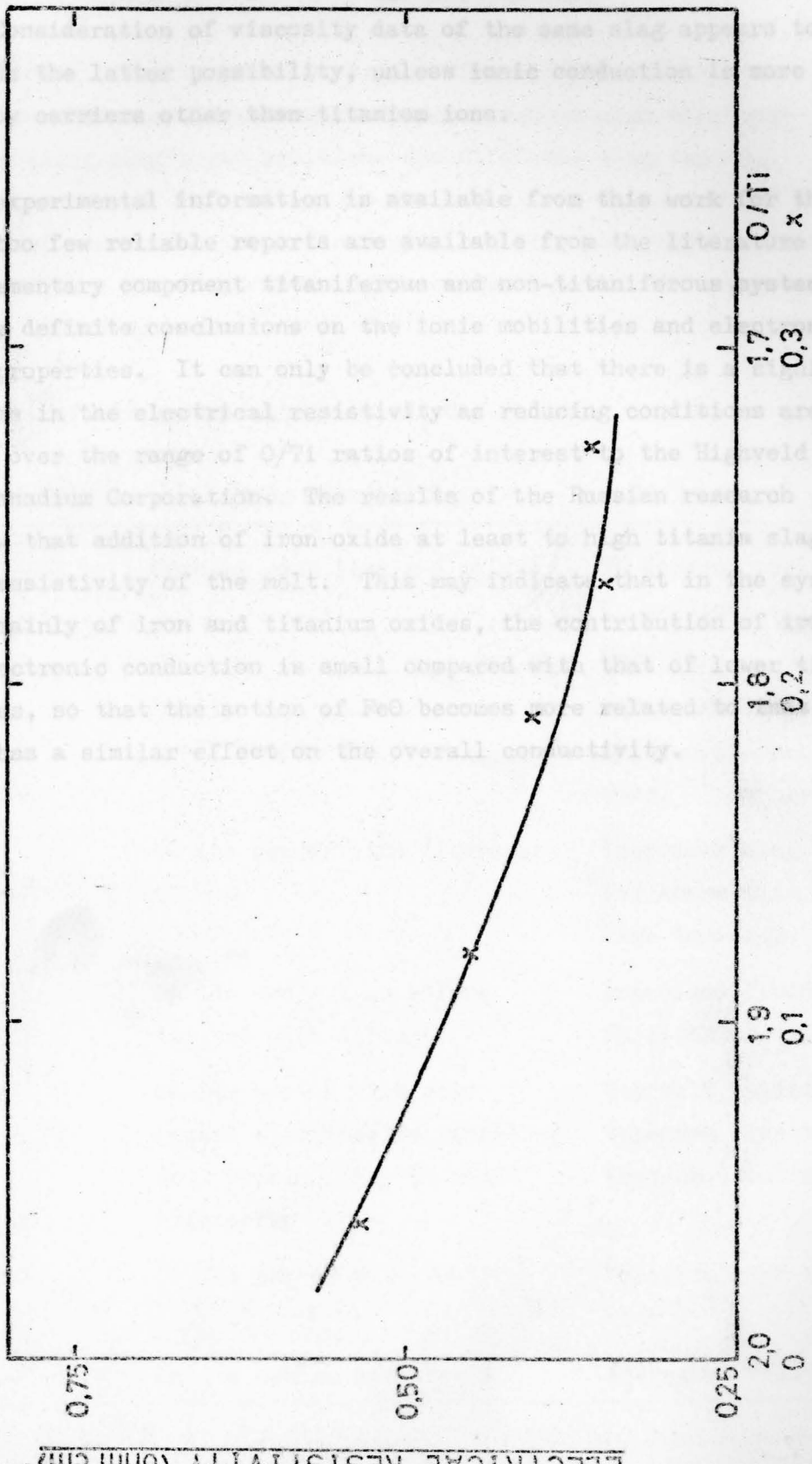


Figure 138 Relation between degree of reduction and resistivity for slag B14 (1550°C)

this apparent minimum will only be truly important in connection with electronic conduction if ionic conduction is independent of x. The condition will deteriorate through the stages of linear to non-linear dependence. Consideration of viscosity data of the same slag appears to point towards the latter possibility, unless ionic conduction is more severely influenced by carriers other than titanium ions.

Too little experimental information is available from this work for this system and too few reliable reports are available from the literature on the more elementary component titaniferous and non-titaniferous systems, to allow any definite conclusions on the ionic mobilities and electronic conduction properties. It can only be concluded that there is a significant decrease in the electrical resistivity as reducing conditions are intensified over the range of O/Ti ratios of interest to the Highveld Steel and Vanadium Corporation. The results of the Russian research workers show that addition of iron oxide at least to high titania slags, raises the resistivity of the melt. This may indicate that in the system consisting mainly of iron and titanium oxides, the contribution of iron oxide to electronic conduction is small compared with that of lower titanium oxides, so that the action of FeO becomes more related to that of CaO, which has a similar effect on the overall conductivity.

6. INDUSTRIAL SIGNIFICANCE

6.1 Operational problems and some corrective measures

The symptoms of difficult operation at the Highveld iron plant were outlined in chapter 1. These could possibly be summarized as high electrode position, "boiling slag", gas eruptions and difficult slag tapping.

The addition of corrective materials during smelting is a regular feature of operation. Standing orders will change, but the following was taken from a report by Hejja[98]:

Table 61 List of corrective materials added

Dressing material	Mode of addition	Purpose
Ore	Usually with lime and silica	To correct resistivity. It oxidizes excess C in burden.
Lime	Mostly with iron ore	maintains target basicity, increases slag temperature.
Silica	On its own or with fluorspar	Increases slag fluidity, for correction of too high basicity.
Fluorspar	On its own ± 1 hr before tap, or with silica	Increases fluidity, facilitates tapping.
Ferrosilicon	On its own or with coke (under electrode for smelting down burden). May be added with scrap	Corrects resistivity - improves electrode penetration. Controls "boiling"
Scrap	On its own or with Fe-Si	Corrects high resistivity.
Coke	On its own or with Fe-Si	Increases resistivity.

A general decrease in burden resistivity takes place 1 - 1½ hours before tapping. The electrodes tend to rise as consequence. This appears

natural in view of the increase in the thickness of the slag layer. If corrective materials are added in this instance, these are ore and lime.

Due to breakage, all electrodes may not be of equal length. The control system tries to maintain balanced operation and corrective measures must be taken according to electrode position.

When all electrodes are high, a condition that may arise when a furnace is severely "overcarboned", little appears to be achieved by material additions and in the extreme case the feed would have to be stopped, the furnace blanked off and the contents smelted down. Coke could then be added at the exposed electrode tips before recharging.

Severe slag "boiling" was thought to call for addition of fluorspar for greater fluidity, iron to react with some of the oxygen that is thought to be evolved in abnormal quantity and ferrosilicon to provide extra heat.

A no-slag tap is not immediately followed by blanking off the furnace. A combination of silica and fluorspar is added as corrective measure. These materials are also used later when a blank-off proves necessary.

When the taphole becomes blocked during tapping, oxygen lancing and the shooting of lead bullets into the taphole are used as remedies.

6.2 Some research ventures conducted specifically in connection with the iron plant at Highveld

6.2.1 Laboratory investigations

The work conducted by Jochens[8,86] and by McRae[23] was described in chapter 2. The former author determined liquidus temperatures and primary phases of slags whose compositions were based on the indications from pilot plant work. Dolomite was shown to be desirable as a flux, judging from the liquidus temperatures measured under oxidizing conditions. McRae determined the viscosities of slags of similar composition, mainly under oxidizing conditions and showed that these slags possessed extraordinarily high fluidity. His test work also indicated that the melting

temperature of the slag might be increased under reducing conditions.

It has already been pointed out that the sulphur capacities of slags of compositions similar to those used by Jochens and McRae, as determined by Pothas,[60] might have been influenced by the fact that the sulphurizing atmosphere consisted of CO, CO_2 and SO_2. In this respect, changes in liquidus temperature may be considered the more important modifying influence. Although a CO-containing atmosphere is not likely to cause marked slag thickening, it may well cause thinning. If the sulphur capacity is considered to be a function of basicity in terms of oxygen availability, bearing in mind the desirability of Ca^{2+}, some of the trends indicated by Pothas may now be more readily explained.

When tests were conducted at 50°C above the initial slag liquidus, a decrease in CaO/MgO ratio caused an initial increase in sulphur solubility, followed by a substantial decrease. Slags of high CaO/MgO ratio are less likely to undergo an increase in liquidus temperature. This may account for the initial rise in sulphur capacity, as a decreasing CaO/MgO ratio effectively means an increase in molar basicity ratio. Greater fluidity over this initial range (up to CaO/MgO~1) may have a similar effect. The drop in sulphur capacity can only be due to an increase in liquidus temperature of high-magnesia slags. This could be aided by the fact that the test temperature would be higher for these slags of higher initial liquidus temperature so that reduction of TiO_2 was promoted.

When the tests were carried out at 1550°C, the initial rise in sulphur solubility became less pronounced. This is suggested to be due to a higher degree of reduction of titania and reduced oxygen activity.

The same author also found that replacement of TiO_2 by SiO_2 decreased the sulphur capacity very drastically when the ratio $SiO_2/TiO_2 \sim 1{,}5$. On either side of this, the changes are more gradual. The tests were conducted at 1550°C. The general trend is understandable. Again, there may be changes in primary phase involved, the slags of higher SiO_2 content being more likely to undergo an increase in liquidus temperature during reduction. Levelling out of the curve when approaching a ratio of 2/1 may also be associated with SiO_2 shielding TiO_2 to such an extent that the role of titanium oxide is restored to what it would be in a truly unreduced slag.

The initial virtually constant sulphur capacity would then be explained by exactly the opposite effect operative in low-SiO_2 slags.

The work carried out by Rennie[99] is very pertinent to any attempt at assessing the industrial significance of the results of the present investigation. The author measured the electrical resistance of synthetic prereduced burdens and of burden components used in the arc furnaces at Highveld. The measuring cell consisted of a graphite crucible with a central graphite electrode of 25,4 mm diameter and constant conducting surface area. A line frequency impressed current - voltage measuring circuit was used. All measurements were made under argon. The majority of the tests were done on material in the size range $\frac{1}{2}$" to $\frac{1}{4}$".

The composition of the synthetic discharge material was:

Ore	:	4,584 Kg
Reductant	:	0,690 Kg
Dolomite	:	0,534 Kg
Silica	:	0,192 Kg

These proportions are almost identical to those given in chapter 1, as representing plant practice.

The characteristic variation of the resistance of such a charge, with temperature, is shown by the solid curve in figure 139. (The reductant was charred coal). There is a rapid initial decrease in resistance, thought to be associated with semiconduction. In the range 1100° to 1400°C the resistance is relatively high. This was attributed to (a) chemical reaction with accompanying breakdown of conduction lattices and (b) sintering, which causes the charge to draw away from the electrode. This is followed by ionic conduction in a liquid medium, which is modified by the presence of metal. The curve obtained for prereduced ore alone was very similar to the one for the synthetic burden, except for the "hump" that was absent, so that the general shape for the latter type of charge must be determined primarily by the characteristics of the ore.

Various reductants were used in conjunction with the remaining charge components. Replacement of charred coal by coke did not bring about any major change in the general shape of the curve in figure 139. The "reaction hump" disappeared however, indicating that coke may be less reactive. Anthracite gave higher resistance above 500°C, suggesting a greater volatile

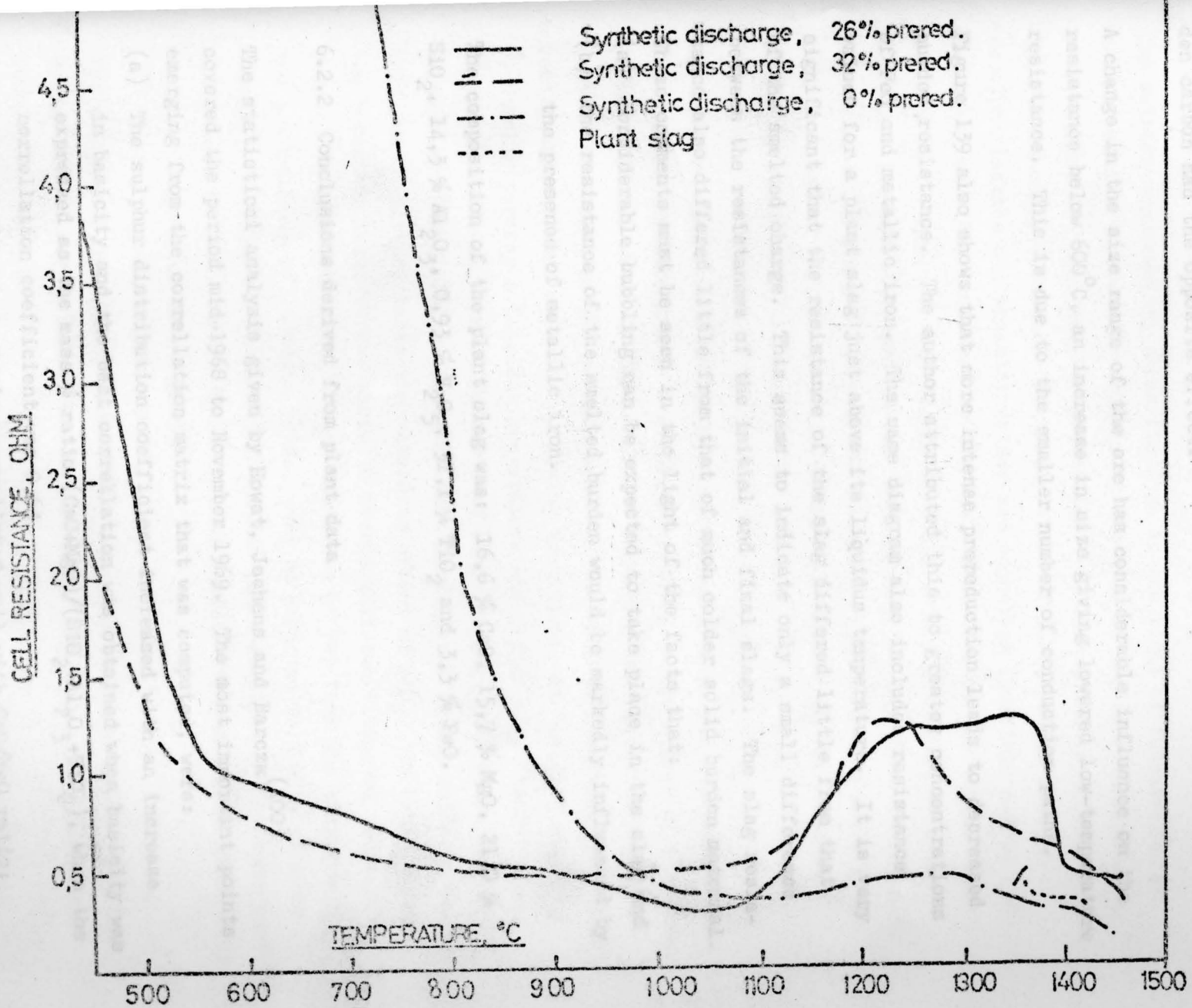


Figure 160. Changes in burden resistance characteristics with degree of prereduction of the ore (99)

content.

An increase in the carbon content of the burden lowered its resistance over the entire temperature interval investigated. A decrease in burden carbon had the opposite effect.

A change in the size range of the ore has considerable influence on the resistance below 600°C, an increase in size giving lowered low-temperature resistance. This is due to the smaller number of conduction paths.

Figure 139 also shows that more intense prereduction leads to decreased burden resistance. The author attributed this to greater concentrations of FeO and metallic iron. The same diagram also includes resistance values for a plant slag just above its liquidus temperature. It is very significant that the resistance of the slag differed little from that of the smelted charge. This seems to indicate only a small difference between the resistances of the initial and final slags. The slag resistance also differed little from that of much colder solid burden material. These comments must be seen in the light of the facts that:

(a) considerable bubbling can be expected to take place in the slag and
(b) the resistance of the smelted burden would be markedly influenced by the presence of metallic iron.

The composition of the plant slag was: 16,6 % CaO, 15,7 % MgO, 21,0 % SiO_2, 14,3 % Al_2O_3, 0,93 % V_2O_5, 31,1 % TiO_2 and 3,3 % FeO.

6.2.2 Conclusions derived from plant data

The statistical analysis given by Howat, Jochens and Barcza[100] covered the period mid-1968 to November 1969. The most important points emerging from the correllation matrix that was computed, were:

(a) The sulphur distribution coefficient increased with an increase in basicity and the best correllation was obtained when basicity was expressed as the mass % ratio $(CaO+MgO)/(SiO_2+Al_2O_3+TiO_2)$, when the correllation coefficient was 0,64.
(b) Slag sulphur content also correllated well with CaO/MgO ratio:

$$(\%S) = 0,124\ CaO/MgO - 0,38$$

(c) There was also an inverse relationship between vanadium in the metal

and basicity:

$$[\%V] = -0,255\ (CaO+MgO)/SiO_2 + 1,50$$

(d) Finally, it was found that there was strong positive correllation between the FeO content of the slag and the various basicity ratios.

The authors commented on these findings in the light of fundamental research results that were available at the time on liquidus temperatures,[8,86] viscosities,[23] and sulphur capacities.[60] Such comments included the apparent anomaly indicated by the behaviour of the titanium ion, where desulphurization and basicity ratios are concerned (possible 4-fold coordination) and that indicated by the low viscosities of the slags. The authors also suggested that higher basicity ratios gave rise to slags of higher liquidus temperature and that thereby the superheat in the slag in the vicinity of the electrode was decreased. This in turn would give rise to melts of higher viscosity which would hinder direct reduction of FeO by carbon.

Generalizations of this nature have little value when the results of the present work are taken into account. Depending on the degree of reduction of the titanium oxide in the melt, the anomalous low viscosities may not exist. Depending on the primary phase of the slag as predicted from investigations conducted under oxidizing conditions, an "acidic" slag may eventually possess a liquidus temperature above that of a "basic" slag. FeO is known to be reduced faster from basic slags. This means faster removal of the shielding effect of this oxide for titanium oxide in the melt, which already lacks the retarding effect of SiO_2. In basic slags the reduction reaction was shown to become self-inhibiting at least with respect to titanium oxide. Final reduction of FeO from the slag phase and particularly of vanadium oxide, must be expected to follow similar trends. Finally, the increased reduction rates associated with more basic slags lead to lower values of electrical resistivity and indeed eventually to lower degrees of slag superheat.

For the period end-1969 to June 1971, a similar analysis was carried out by members of the research team at Highveld.[101] The most important conclusions were:

(a) Increased slag basicity resulted in increased carbon and silicon contents of the pig iron, but the vanadium content of the latter was not materially influenced.

(b) An increase in the coal/ore ratio in the kiln feed material increased the carbon and silicon contents of the metal. It appeared that the slag basicity probably exerted greater influence on the carbon content of the metal than did the coal content of the feed:

$[\%C] = 0{,}003\ \text{Coal} + 2{,}635\ B - 3{,}088$, where Coal = lb/ton of ore and $B = (CaO+MgO)/SiO_2$.

(c) It appeared that high carbon and silicon contents in the metal were associated with high power consumption.

(d) Skull iron losses depended on carbon and silicon contents of the hot metal:

$$\frac{\%\ \text{Skull iron losses}}{\text{ton produced}} = -6{,}9095\ [\%C] - 3{,}2965\ [\%Si] + 49{,}4807$$

Further plant tests were also described by Hejja.[98] A possibility that was investigated was the addition of hematite instead of magnetite as electrode dressing material. It appeared[102] that under good furnace conditions, hematite by itself was sufficient to maintain good operation. Under conditions of difficult operation this did not apply and limestone had to be added to secure better metal chemistry even when the electrodes were short. The conventional magnetite additions were later retuned to, as it was suggested that hematite would cause faster electrode consumption due to its greater reactivity.

It was also suggested that a portion of the coal added to the kiln should be replaced by coke added at the discharge end of the kiln. The suggestion was based on the possibility that many of the operational problems might be due to small carbon particles floating in the melt. These would by their mere physical presence, reduce the resistivity of the burden and cause high electrode position. It is now known that the electrical properties of an overcarboned slag will differ from those of a normal slag much more markedly than might be anticipated on the basis of extra carbon only.

It is obvious that the fixed carbon in the furnace feed should constitute a major factor determining the process in the furnace. Carbon enters the kiln both as pulverized coal and as actual charged coal reductant. Hejja pointed out that the prereduction of the ore at a given coal input to the kiln depends on the feed rate and quoted an example based on a statistical survey for a particular kiln:

Tons/hour kiln feed	Prereduction (%)
40	31
45	28
50	25

In this connection, the author pointed out that the process was designed for 45 - 50 % prereduction and that the furnace might be overloaded at times, especially at high kiln throughput rates.

Hejja also indicated that pile-up of contaminants in the furnace, particularly in the form of electrode carbon might be the main trouble source in furnace operation.

6.3 The importance of slag melting temperature

The liquidus temperature of the slag must necessarily be highly significant on its own. This was pointed out in chapter 1. However, in work of the present type, its influence on the properties viscosity and electrical resistivity with respect to temperature profiles existing in the furnace, is of equal importance. For this reason, the possible importance of slag liquidus temperature will frequently recur in sections 6.4 and 6.5 dealing with resistivity and viscosity respectively.

Hejja[103] made an attempt to estimate the radial temperature profile around an electrode of a rectangular six-in-line matte smelting electric furnace. Assuming that under the electrode in the slag layer, there exists a "disc" of material of definite thickness, over which no vertical temperature gradient exists, that steady state radial heat transfer takes place and that there is no turbulence, he derived the following differential equation:

$$\frac{d^2T}{dr^2} + 1/r \frac{dT}{dr} - \frac{h(T - Ta)}{k} = 0 \quad \ldots\ldots(1),$$

where T = temperature at a distance r from the centre of the disc and thus from the axis of the electrode,

Ta = the minimum allowable temperature towards the periphery of the disc,

h = convective heat transfer coefficient and

k = thermal conductivity of the slag.

Apart from the doubtful validity of such a model even for the system in connection with which it was derived, it is realized that its application to a pig iron producing furnace can have even less claim on validity. It will simply be endeavoured to show the possible effect of a varying slag liquidus temperature on furnace operation, on the basis of one idealized model, with little regard for absolute numerical values.

If $T - Ta = y$ and $h/k = \sigma$, equation (1) becomes:

$$r^2 \frac{d^2y}{dr^2} + r \frac{dy}{dr} - \sigma r^2 y = 0 \quad \ldots\ldots(2)$$

This represents a form of the modified Bessel function:

$$z^2 w'' + zw' - mz^2 w = 0 \quad \ldots\ldots\ldots(3),$$

the solution of which is:

$$y = C_1 I_o (r\sqrt{\sigma}) + C_2 k_o (r\sqrt{\sigma}) \quad \ldots\ldots(4)$$

The first term on the right hand side can be eliminated as I_o increases with increasing value of the variable, while the temperature should decrease more or less asymptotically with increasing r. The final form of the solution is then:

$$T - Ta = C_2 k_o (r\sqrt{\sigma}) \quad \ldots\ldots\ldots\ldots(5)$$

The value of the constant C_2 was evaluated for every selected value of Ta, assuming the ratio $\sigma = 0{,}67$ and

the temperature at the periphery of the 1,6 m diameter hot zone below the electrode = 1900°C in all cases.

Different values of Ta were chosen on the basis of slag liquidus temperature (as 50°C below this temperature). The values of slag liquidus temperature that were selected, were:

(a) 1350°C - the average liquidus temperature of "low melting" slags in this investigation (measured under oxidizing conditions);

(b) 1450°C - the average liquidus temperature of "high melting" slags (measured under oxidizing conditions) and also the ultimate liquidus temperature of slags reduced by carbon at 1550°C, if their melting temperatures were influenced by reduction and the initial values were close to 1350°C.

(c) 1550°C - the melting temperature of slags reduced at 1600° for comparatively long times, even when their initial liquidus temperatures were "low". This again presupposes dependence of melting temperature upon degree of reduction.

The values of C_2 corresponding to these different levels of Ta are 880, 735 and 590 respectively. Table 62 shows the radial temperature distribution from the electrode axis for the different values of Ta.

Table 62 Radial temperature profile in an imaginary slag "disc" below the electrode.

r (m)	T for Ta=1300° (°C)	T for Ta= 1400° (°C)	T for Ta=1500° (°C)
0,8	1900	1900	1900
1,0	1775	1797	1818
1,5	1564	1660	1677
2,0	1454	1529	1603
2,5	1392	1477	1562
3,0	1348	1444	1535
3,5	1334	1429	1523
4,0	1321	1418	1514

The same information is presented in figure 140.

If the radius of the reaction zone is to be determined by the maximum radial distance over which the slag will be above its liquidus temperature, R_r can be seen to decrease through the values 3,0 m , 2,9 m and 2,7 m as the value of Ta increases from 1300° through 1400° to 1500°C. A furnace should be designed according to the lowest melting point slag for satisfactory lining protection. If a slag of uniformly higher liquidus temperature is used, the reaction zone must shrink. Such thinking is based on the assumption that the slags have uniform liquidus temperatures. It cannot be stated that eg. slag B14 which has an initial liquidus temperature of $\pm$ 1350°C, will finally only be completely molten at 1550° or 1450°C, depending on the equivalent reduction temperature, and that this will reduce the value of R_r. However, the rapid solidification of non-equilibrium high melting slag from the region between the electrodes on

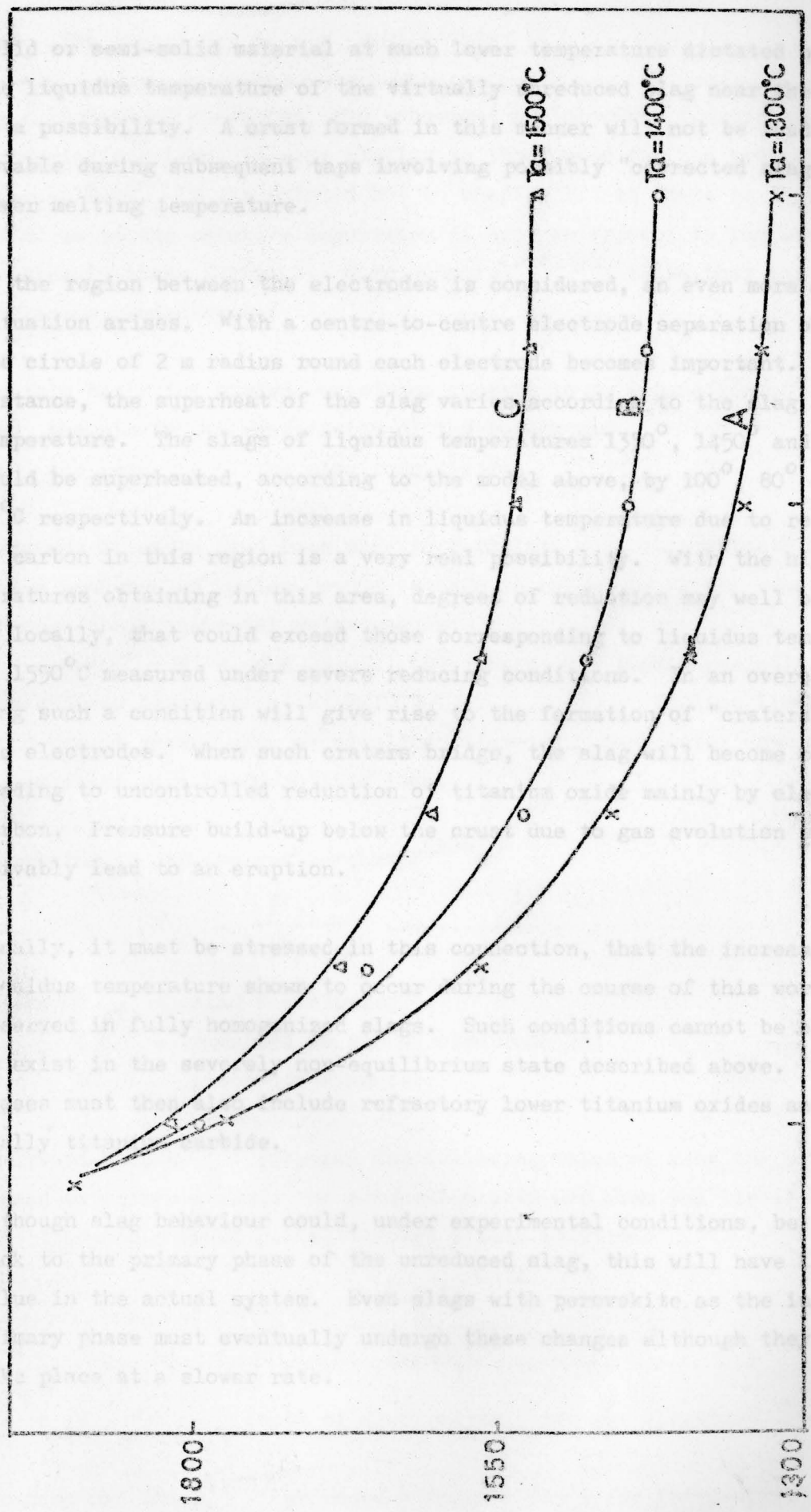


Figure 140 A not impossible temperature profile around an electrode.

solid or semi-solid material at much lower temperature dictated by the liquidus temperature of the virtually unreduced slag near the lining, is a possibility. A crust formed in this manner will not be readily removable during subsequent taps involving possibly "corrected slags" of lower melting temperature.

If the region between the electrodes is considered, an even more alarming situation arises. With a centre-to-centre electrode separation of 4 m, the circle of 2 m radius round each electrode becomes important. At this distance, the superheat of the slag varies according to the slag liquidus temperature. The slags of liquidus temperatures 1350°, 1450° and 1550°C would be superheated, according to the model above, by 100°, 80° and 50°C respectively. An increase in liquidus temperature due to reduction by carbon in this region is a very real possibility. With the high temperatures obtaining in this area, degrees of reduction may well be attained locally, that could exceed those corresponding to liquidus temperatures of 1550°C measured under severe reducing conditions. In an overcarboned slag such a condition will give rise to the formation of "craters" around the electrodes. When such craters bridge, the slag will become confined, leading to uncontrolled reduction of titanium oxide mainly by electrode carbon. Pressure build-up below the crust due to gas evolution may conceivably lead to an eruption.

Finally, it must be stressed in this connection, that the increases in liquidus temperature shown to occur during the course of this work, were observed in fully homogenized slags. Such conditions cannot be expected to exist in the severely non-equilibrium state described above. Solid phases must then also include refractory lower titanium oxides and eventually titanium carbide.

Although slag behaviour could, under experimental conditions, be traced back to the primary phase of the unreduced slag, this will have limited value in the actual system. Even slags with perovskite as the initial primary phase must eventually undergo these changes although they possibly take place at a slower rate.

6.4 The importance of slag resistivity

In principle of operation, the submerged arc electric furnace used for producing pig iron, is very similar to those used for the production of ferro-alloys. It was pointed out in chapter 1 that there is no absolute guide as to the relative importance of arc- as opposed to resistance heating in these furnaces. Some authors[104,105] claim that the latter mechanism predominates.

On this basis the burden resistance appears to be a function of:

(a) the electrical resistivity of the burden and

(b) the geometry of the electrode system.

Numerous attempts have been made to formulate a "cell constant" k, which, for a homogeneous system, could be used to calculate burden resistance through the fundamental relationship:

$$R = \rho k \quad \ldots\ldots\ldots (6),$$ where ρ = burden resistivity.

The Andreae concept: $k = E/I\pi D$ ..... (7) implies linear dependence of resistivity on electrode diameter. Many later approaches to the problem were based on this idea.

According to Schwarz von Bergkampf[106]

$$R = \frac{\rho_{sl} \cdot L}{D^2/4} \quad \ldots\ldots\ldots (8),$$

where ρ_{sl} = slag resistivity,

L = immersed length of electrode and

D = electrode diameter.

Hallvard-Nilsen[107] proposed the following value of k on the basis of single phase experiments where the conduction path was from the tip of a brass electrode to a brass plate, through a salt solution:

$$k = \frac{0,1517}{D} \cdot \frac{\left(\frac{H - P}{D}\right)^{0,24}}{(P/D)^{0,45}} \quad \ldots\ldots\ldots (9)$$

where (H - P) = depth of electrolyte below the electrode tip.

Downing and Urban[108] proposed a formula for k for ferro-chromium producing furnaces:

$$= 1/\pi \left\{ \frac{1}{\frac{H}{\ln\left(S/D + \sqrt{(S/D)^2 - 1}\right)} + D/2 \left\{1 + D/2S + (D/2S)^2 + \ldots\right\}} \right\} \quad \ldots\ldots(10)$$

where H = electrode immersion,

S = centre-to-centre electrode separation,

D = electrode diameter.

In general, too little significance has been attached to

(a) the heterogeneity of the burden material in the furnace and

(b) the different conduction paths between the electrodes.

In this context, the work carried out by Urquhart[109] is particularly significant. According to this author, the upper region of the furnace would tend to behave as a delta connection, whilst the lower region would conduct electricity as a mixture of star and delta connections.

In order to define the possible conduction paths, the values of k were measured for three phase - three electrode systems. In the experimental arrangement, the electrolyte was a standard solution of sodium chloride of known resistivity, and brass electrodes were used. Balaced line frequency three phase power was maintained across the electrodes by three single phase variable transformers. The cell resistances were determined from line voltages and currents. A star point was provided by a mercury pool at the bottom of the glass beaker containing the electrolyte. The conduction surface could be limited by blanking off either the sides or the tips of the electrodes. The ratio of pitch circle diameter to electrode diameter was kept constant at a value of 3,0.

When only delta conduction was possible, the cell constant was a function mainly of the solution depth. When conduction could only take place from the electrode tips, the cell constant was found to be related to the electrode diameter (D) through:

$$k = 2{,}46\ D^{-0{,}8} \quad \ldots\ldots\ldots\ldots(11)$$

By dividing the submerged depth of electrode into 25 mm sections and using the corresponding value of k for delta conduction above the electrode tips (knowing the variation of burden resistivity with temperature), the

pattern of power dissipation in this region could be calculated. This was done by assuming an overall depth of electrode immersion in the ferro-chromium furnace and evaluating the currents carried by all the 25 mm thick resistors in parallel, assuming a constant inter-electrode voltage.

For the region below the electrode tips, a cell constant was also known, burden resistivity here was assumed constant and a similar calculation of the delta/star conduction could be performed.

The author found that just over 50 % of the power was dissipated below the electrode tips and that about 75 % was dissipated over the lower 300 mm of electrode (overall immersion 1500 mm). The total values of power and current agreed well with those measured for furnaces in operation.

A similar approach could be employed to form an idea of the pattern of power dissipation in a pig iron producing furnace. The burden resistance as determined by Rennie[99], together with slag resistivity values as determined in this work could be used for the purpose if the following obstacles could be overcome:

(a) The actual depth of immersion of the electrodes under conditions of optimum operation must be known.

(b) The temperature profile in the burden along the immersed part of the electrode is another unknown.

(c) The resistance values of Rennie must be converted to resistivities.

The temperature variation from the burden surface was adapted from the suggestions of Bezobrazov[110] et al and Urquhart[109] in such a way as to have a burden surface temperature of 700°C. At the level of the electrode tips the temperature was assumed to be 1550°C. This suggested an immersion depth for steady near-tap operation of 1250 mm. The proposed temperature profile is shown in figure 141.

Rennie determined the resistance of one slag just above its liquidus temperature. This is shown in figure 139 together with the resistance of the rest of the burden. The composition of this particular slag was fairly close to that of slag B14 of this study. As it was decided to use the unreduced condition of slag B14 as a datum point in this exercise, a value

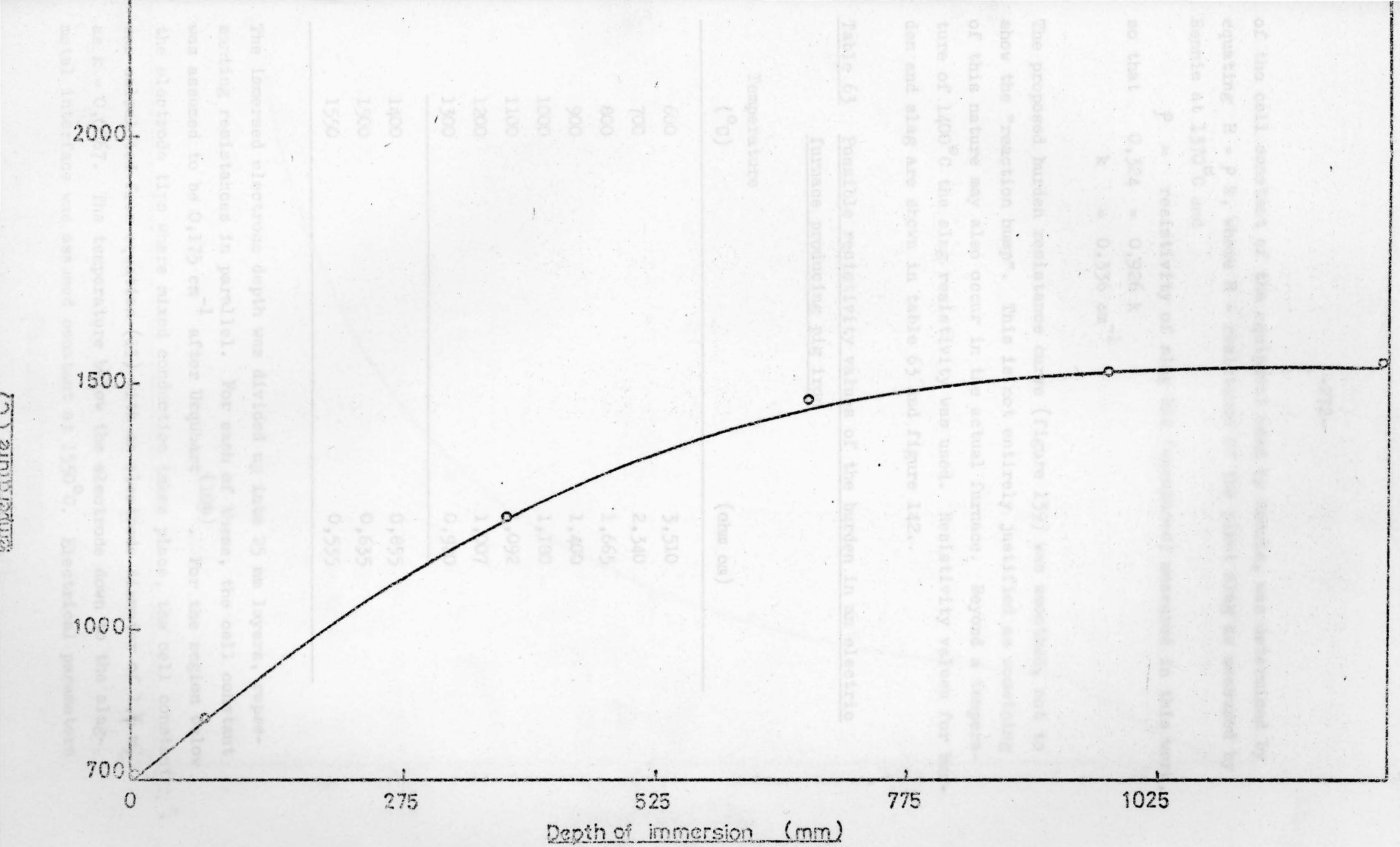


Figure 141 Suggested temperature profile for immersed electrode

of the cell constant of the equipment used by Rennie, was determined by equating $R = \rho k$, where R = resistance of the plant slag as measured by Rennie at 1370°C and

ρ = resistivity of slag B14 (unreduced) measured in this work,

so that $0,324 = 0,926\ k$

$k = 0,336\ cm^{-1}$

The proposed burden resistance curve (figure 139) was smoothed, not to show the "reaction hump". This is not entirely justified as something of this nature may also occur in the actual furnace. Beyond a temperature of 1400°C the slag resistivity was used. Resistivity values for burden and slag are shown in table 63 and figure 142.

Table 63 Possible resistivity values of the burden in an electric furnace producing pig iron

Temperature (°C)	(ohm cm)
600	3,510
700	2,340
800	1,665
900	1,400
1000	1,180
1100	1,092
1200	1,007
1300	0,920
1400	0,855
1500	0,635
1550	0,535

The immersed electrode depth was divided up into 25 mm layers, representing resistances in parallel. For each of these, the cell constant was assumed to be $0,175\ cm^{-1}$ after Urquhart[109]. For the region below the electrode tips where mixed conduction takes place, the cell constant was calculated from equation (11) with an electrode diameter of 1,6 m, as $k = 0,0067$. The temperature below the electrode down to the slag-metal interface was assumed constant at 1550°C. Electrical parameters

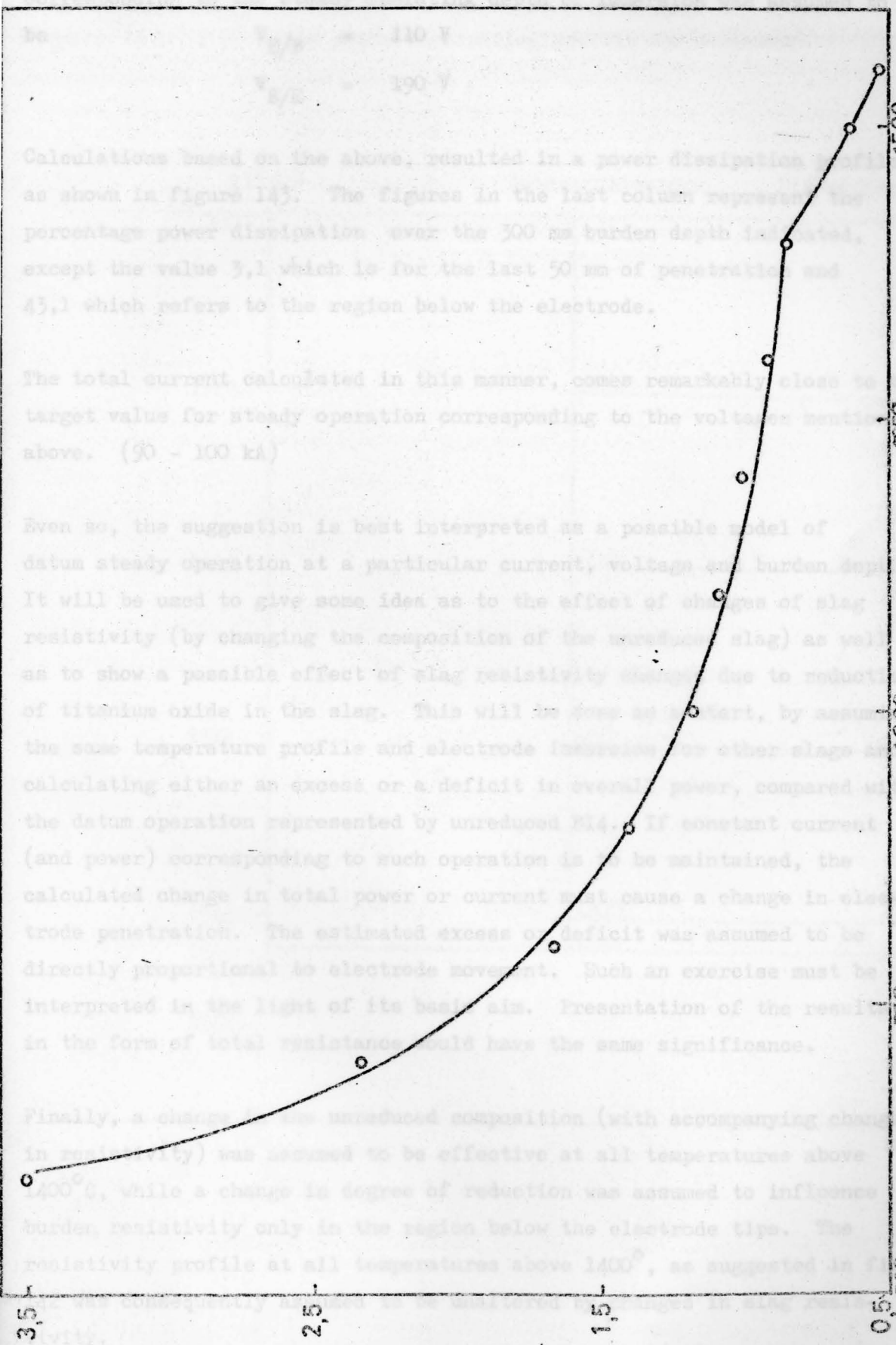


Figure 142 Suggested resistivity of burden materials

corresponding to the steady operating depth of immersion was assumed to be

$V_{E/B}$ = 110 V

$V_{E/E}$ = 190 V

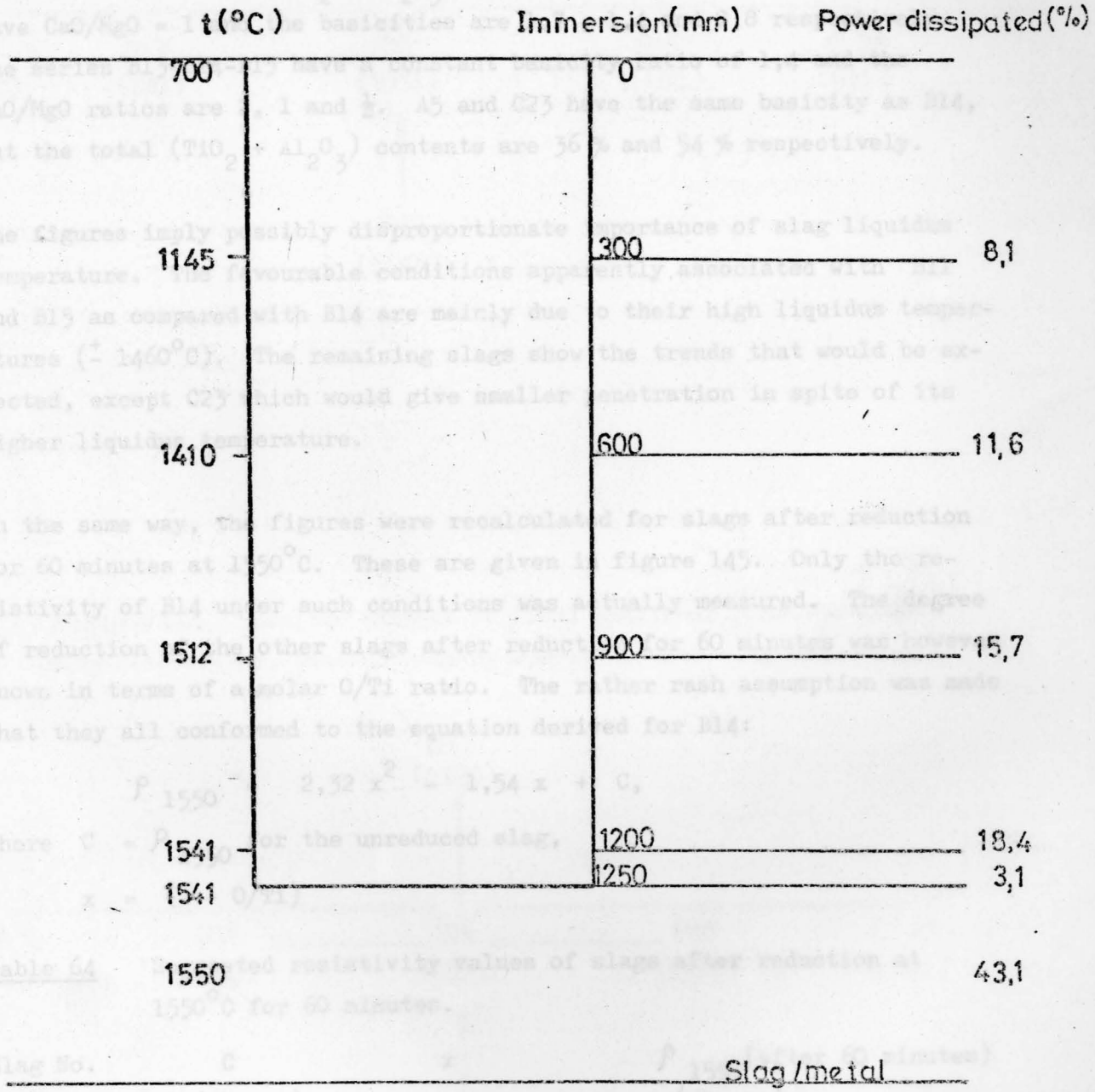
Calculations based on the above, resulted in a power dissipation profile as shown in figure 143. The figures in the last column represent the percentage power dissipation over the 300 mm burden depth indicated, except the value 3,1 which is for the last 50 mm of penetration and 43,1 which refers to the region below the electrode.

The total current calculated in this manner, comes remarkably close to the target value for steady operation corresponding to the voltages mentioned above. (90 - 100 kA)

Even so, the suggestion is best interpreted as a possible model of datum steady operation at a particular current, voltage and burden depth. It will be used to give some idea as to the effect of changes of slag resistivity (by changing the composition of the unreduced slag) as well as to show a possible effect of slag resistivity changes due to reduction of titanium oxide in the slag. This will be done as a start, by assuming the same temperature profile and electrode immersion for other slags and calculating either an excess or a deficit in overall power, compared with the datum operation represented by unreduced B14. If constant current (and power) corresponding to such operation is to be maintained, the calculated change in total power or current must cause a change in electrode penetration. The estimated excess or deficit was assumed to be directly proportional to electrode movement. Such an exercise must be interpreted in the light of its basic aim. Presentation of the results in the form of total resistance would have the same significance.

Finally, a change in the unreduced composition (with accompanying change in resistivity) was assumed to be effective at all temperatures above 1400°C, while a change in degree of reduction was assumed to influence burden resistivity only in the region below the electrode tips. The resistivity profile at all temperatures above 1400°, as suggested in figure 142 was consequently assumed to be unaltered by changes in slag resistivity.

Figure 143 A possible power dissipation profile for a burden corresponding to unreduced slag B14 (steady operation)



On this basis, figure 144 shows the expected changes in electrode immersion for changes in slag composition, the slags being in the unreduced state. The figures in brackets represent the electrode penetration in mm. The arrows show the trends in slag composition. The slags B11, B13, B14, B15 and B17 all have (TiO_2 + Al_2O_3) = 44 mass %. The series B11-B14-B17 have CaO/MgO = 1 and the basicities are 1,7 , 1,4 and 0,8 respectively. The series B13-B14-B15 have a constant basicity ratio of 1,4 and the CaO/MgO ratios are 2, 1 and $\frac{1}{2}$. A5 and C23 have the same basicity as B14, but the total (TiO_2 + Al_2O_3) contents are 36 % and 54 % respectively.

The figures imply possibly disproportionate importance of slag liquidus temperature. The favourable conditions apparently associated with B11 and B15 as compared with B14 are mainly due to their high liquidus temperatures ($\pm$ 1460°C). The remaining slags show the trends that would be expected, except C23 which would give smaller penetration in spite of its higher liquidus temperature.

In the same way, the figures were recalculated for slags after reduction for 60 minutes at 1550°C. These are given in figure 145. Only the resistivity of B14 under such conditions was actually measured. The degree of reduction of the other slags after reduction for 60 minutes was however known in terms of a molar O/Ti ratio. The rather rash assumption was made that they all conformed to the equation derived for B14:

$$\rho_{1550} = 2{,}32\ x^2 - 1{,}54\ x + C,$$

where $C = \rho_{1550}$ for the unreduced slag,

$x = (2 - O/Ti)$

Table 64 Suggested resistivity values of slags after reduction at 1550°C for 60 minutes.

Slag No.	C (ohm cm)	x	ρ_{1550} (after 60 minutes) (ohm cm)
A5	0,750	0,18	0,578
B13	0,570	0,16	0,413
B11	0,578	0,22	0,382
B17	0,725	0,16	0,568
B15	0,800	0,21	0,609
C23	0,475	0,36	0,253

Figure 145 Possible changes in final electrode penetration with slag composition, based on steady operation with B14. (all slags reduced by carbon at 1550°C for 60 minutes)

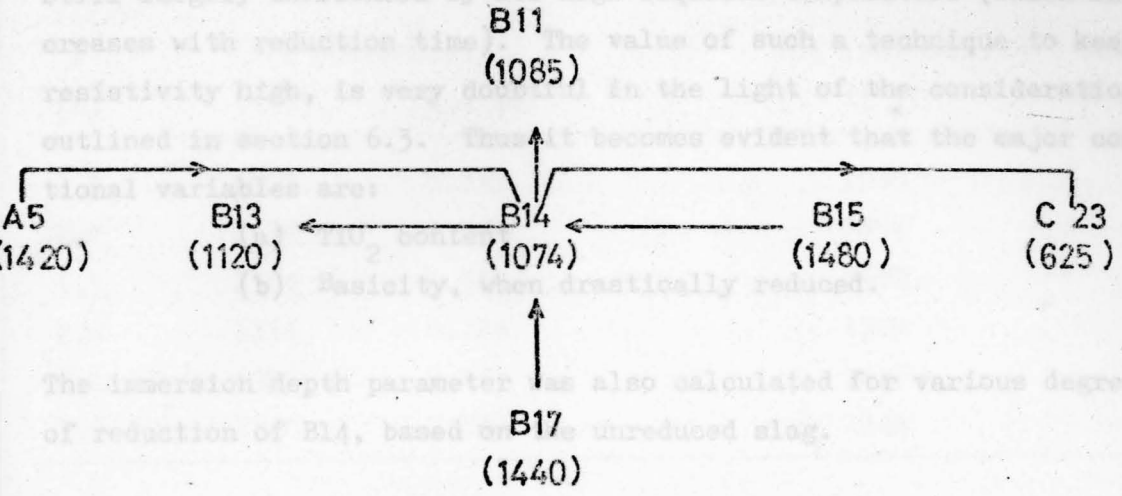


Figure 144 Possible changes in final electrode position with slag composition, based on steady operation with slag B14.

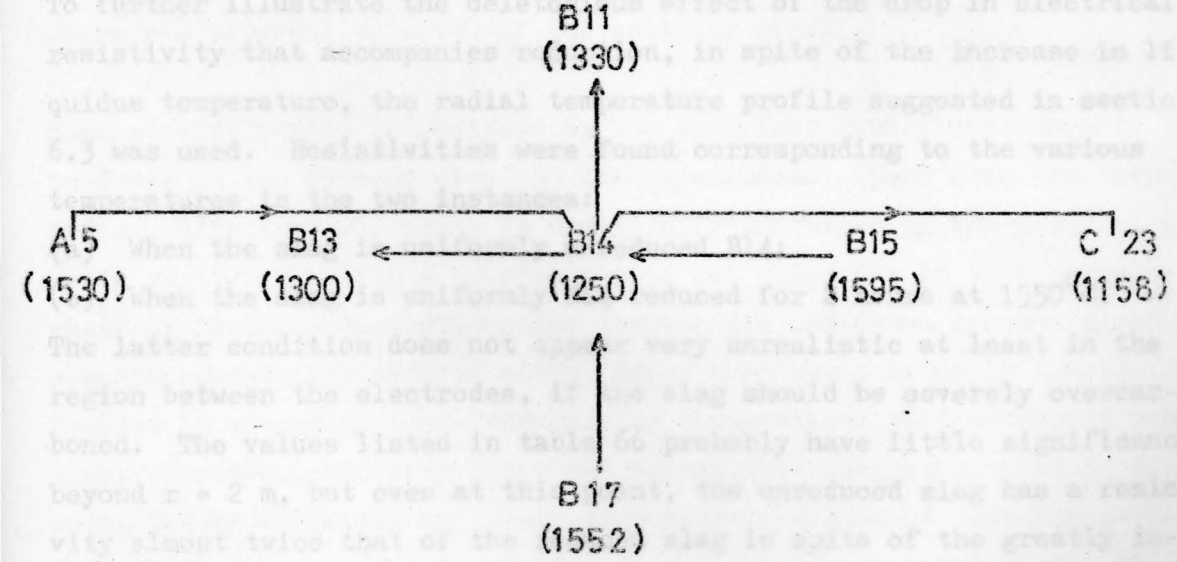


Figure 145 appears to indicate that the suggested value for B15 is still largely inflienced by its high liquidus temperature (which increases with reduction time). The value of such a technique to keep resistivity high, is very doubtful in the light of the considerations outlined in section 6.3. Thus it becomes evident that the major compositional variables are:

(a) TiO_2 content

(b) Basicity, when drastically reduced.

The immersion depth parameter was also calculated for various degrees of reduction of B14, based on the unreduced slag.

Table 65 Penetration depths for the reduced derivatives of B14

Reduction time at 1550°C (minutes)	Penetration depth (mm)
0	1250
30	1198
60	1074
90	1000
120	1016

To further illustrate the deleterious effect of the drop in electrical resistivity that accompanies reduction, in spite of the increase in liquidus temperature, the radial temperature profile suggested in section 6.3 was used. Resistivities were found corresponding to the various temperatures in the two instances:

(a) When the slag is uniformly unreduced B14;

(b) When the slag is uniformly B14 reduced for 2 hours at 1550°C.

The latter condition does not appear very unrealistic at least in the region between the electrodes, if the slag should be severely overcarboned. The values listed in table 66 probably have little significance beyond r = 2 m, but even at this point, the unreduced slag has a resistivity almost twice that of the reduced slag in spite of the greatly increased melting temperature of the latter.

Table 66 Radial resistivity profile round the electrode

r (m)	B14 (unreduced) t(°C)	B14 (unreduced) ρ (ohm cm)	B14 (reduced for 2 hrs at 1550°C) t(°C)	B14 (reduced for 2 hrs at 1550°C) ρ (ohm cm)
0,8	1900	0,230	1900	0,202
1,0	1775	0,301	1797	0,247
1,5	1564	0,538	1660	0,303
2,0	1454	0,725	1529	0,390
2,5	1392	0,870	1477	0,495
3,0	1348	1,060	1444	0,525

6.5 The importance of viscosity

The manner in which slag viscosity influences furnace operation and eventually production was briefly outlined in chapter 1.

Stokes' law gives the basis for determining the rate of settling of metal droplets through a slag medium:

$$v = \frac{2 R^2 \rho g}{9 \eta} \quad \text{.....(12)}$$

where v = terminal velocity of the settling reguli.

Such a relationship is modified by the turbulent conditions thought to exist in the furnace close to the electrodes. Apart from the turbulence factor, effective viscosity is drastically increased by the presence of solid particles. Such a possibility is not ruled out in this system where an increase in the liquidus temperature was shown to take place even in homogenized reduced slags, apart from the relatively drastic increases in viscosity above the melting temperature, that accompany reduction. Moreover, the very important aspect that was not covered in this work, is the formation of finely dispersed particles of titanium carbide in the slag phase. Qualitatively, it may still be assumed on the basis of rates of reduction to lower oxides, that the formation of carbide will start sooner in slags of high basicity, high MgO/CaO ratio and high titanium oxide content. According to the Einstein equation already given in section 2.4.6: $\eta = \eta_o (1 - 2{,}5\,\phi)$ .....(13), where

η_o = viscosity of the homoheneous medium,
η = effective viscosity of the heterogeneous system and
ϕ = degree of heterogeneity.

Such heterogeneity also influences the overall process through viscosity in a different sense. It was mentioned in section 2.4.6 that Freidenzon[22] calculated, from the analyses of the slag and metal fractions of "buckshot slag" formed during production of vanadium bearing pig iron in a blast furnace, the modified viscosities of both the pig iron and the slag in such particles. He suggested values of 0,4 poise and 28 poise for the two products respectively. With diffusion being a function of viscosity, refining of the buckshot metal becomes virtually a physical impossibility. This does not even take into account the possibility that coated metal droplets will coalesce with the metal bath only with the greatest difficulty. It was mentioned in section 4.2.5.1 that evidence of this problem was found during this research programme as well.

The rate at which recoverable oxides dissolve in a slag phase can be described by the Nernst equation:

$$Q = \frac{D(C_s - C_o)S}{\delta} \quad \text{.....(14),}$$

where Q = amount of material dissolved per unit time,
S = surface area,
C_s, C_o = concentrations at the surface and in the bulk,
D = diffusivity,
δ = thickness of the diffusion layer.

It was suggested by Johnston[81] that:

$$\delta \propto \eta^n, \text{ where } n = \tfrac{1}{2} - 1.$$

It is also known that D is a function of the viscosity.

It must however be pointed out that the viscosity value that is important in this sense, is probably that of the primary slag formed in the reaction zone.

Finally, it was indicated in section 5.2 that, under reducing conditions, the reduction of titanium oxide eventually became a function of viscosity. For slag B14 reduced at 1550°C, the relationship might be expressed as:

$$\frac{d\,C_{TiO_2}}{dt} = 0{,}20 - 0{,}10\,\eta \quad \ldots\ldots(15), \text{ where}$$

$\frac{d\,C_{TiO_2}}{dt}$ = rate of TiO_2 reduction in mass % /min

and η = viscosity (poise).

Such a correllation cannot be expected to be unique to the reduction of titanium oxide. Similar considerations must apply to the final reduction of iron and vanadium oxides from the slag by solid carbon and by carbon dissolved in the metal. Desulphurization of the metal by the slag either when the two layers are finally in contact or when metal droplets are settling through the slag layer, must also be influenced by the slag viscosity.

Even though the final viscosities attained after severe reduction in this work are by no means large, such figures must be evaluated relative to the viscosities of unreduced slags. This clearly shows the inhibiting action that slag thickening might have, relative to operation under "easy" conditions.

Again using slag B14 as an example and basing calculations on the radial temperature profile of section 6.3, viscosities corresponding to the various conditions were calculated:

Table 67 Radial viscosity profiles around the electrode

r	B14 (unreduced)		B14 (reduced 2 hrs at 1550°C)	
(m)	t(°C)	η (cp)	t(°C)	η (cp)
0,8	1900	17	1900	29
1,0	1775	26	1797	47
1,5	1564	58	1660	96
2,0	1454	87	1529	204
2,5	1392	117	1477	230
3,0	1348	158	1444	-
3,5	1334	183	1429	-
4,0	1321	226	1418	-

6.6 Conclusion

Although the remarks in connection with liquidus temperature, viscosity and electrical resistivity in this chapter are largely speculative, they do serve, through comparison, to stress the effects of major changes in slag composition.

The melting temperatures of these slags are of paramount importance, particularly as the tapped slag will rarely possess the liquidus temperature predicted by a phase diagram. Moreover, laboratory determinations of viscosity and resistivity performed for a particular slag composition, have little industrial significance if the slag in the furnace is below its liquidus temperature.

The combined effect of the changes in the various properties, under reducing conditions, can certainly assert itself when slag becomes confined under conditions of high temperature in the presence of excess reductant. Such a possibility, leading to crater formation, has already been discussed in section 6.3 in conjunction with possible increases in melting temperature. When such a condition arises and titanium oxide is reduced uncontrollably, viscosity and electrical conductivity will also increase. "Boiling" will be promoted locally due to the lower fluidity and the lower degree of slag superheat and eventually due to solid particles consisting of titanium carbide. The condition will deteriorate due to high electrode position and the consequent cooling of the slag. The more violent turbulence near the electrode tip will deposit more and more high melting material on the "walls of the crater".

An attempt to suggest corrective measures according to bad operation symptoms on the basis of laboratory findings, would be futile. Moreover, the author believes that little can be added to what has already been established at the plant. If the system is known to be overcarboned and titanium oxide to be in severely reduced condition, the most logical step is the removal of the trouble source - addition of oxygen in its most readily available form eg. hematite. If the composition of the boiling slag is known, particularly with respect to basicity, limestone might be a great aid to lower the melting temperature of the slag by increasing the CaO/MgO ratio. However, if the basicity is already high, little will be gained. In such an instance, silica in conjunction with limestone might

be more feasible, restoring target basicity and holding the possibility of local fluxing in the low temperature sphene composition range.

However, troublesome operation is not the rule and it appears far more logical to avoid operational possibilities calling for "instant correction". Heat is used in the furnace mainly for reduction reactions and for actually heating the contents of the furnace. With a constant feed rate, it appears feasible that the ratio of these requirements must be disturbed as little as possible. This means that the feed must also be a constant with respect to the degree of prereduction and fixed carbon content.

Electrode erosion and continual carbon addition from this source is unavoidable. More severe electrode breakages occur. Extra carbon added in this manner is not a controllable parameter. Some of it will dissolve in the metal, but accumulation that also appears unavoidable, not only interferes with tapping, but may eventually contribute substantially to the condition of "overcarboning". Periodic cleaning of the furnaces should be accepted as an absolute necessity in a process where slag properties are influenced by the presence of excess reductant.

If these requirements so broadly repeated here, are implemented, the author firmly believes that the process will tolerate variation in slag composition over a very wide region without serious effect on metal chemistry.

The object of this research work was to clarify some of the peculiarities of titaniferous slags when they are subjected to reducing conditions. With the amount of care exercised during the experimental work, it is believed that this goal was achieved.

The aim was <u>not</u> to find an optimum slag composition. The programme did not involve a search of any nature, but was confined to slag compositions in or adjacent to the region that is familiar to the plant. It is evident however, that optimization would have to be based on the degree of reduction of titanium oxide in the slag. In this connection one is confronted with the old problem - that of <u>which</u> slag is to be considered important. For primary slag formation the slag is probably close to some of the highly siliceous slags tested in this work, in their unreduced state. The final slag is probably represented fairly well by the synthetic slags in

the basicity range 1,4 to 1,5 , reduced for the equivalent of 60 minutes at 1550°C. Under conditions of severe overcarboning, the state of the slag is likely to be outside the range tested. For such extreme conditions the optimizing parameter would be best defined as the rate of reduction of titania to lower oxides and eventually to carbide.

Finally, four parameters were determined experimentally - liquidus temperature, viscosity, electrical resistivity and apparent rate of titanium oxide reduction. The first three are differently affected by the last. Although it was attempted in previous sections to point out the importance of each of these, it is not possible to assess their relative significance to furnace operation.

The exercise that follows, must be interpreted in the light of the above comments. Not even all the basic slag compositions investigated, will be included. The aim is primarily to show that, if optimization is attempted, the following facts must be borne in mind:

(a) The parameters viscosity, liquidus temperature and electrical resistivity are all significant in the process.

(b) The slags must be compared under the conditions that are pertinent to the problem.

For the purpose of the exercise, the following parameters were defined:

(a) $C_L = R_{sl}/R_{B14}$. The values of R represent "radii of reaction zones" calculated by the technique outlined in section 6.3. R_{sl} is the radius evaluated for any slag composition, as the radial distance from the electrode centre, where the temperature drops to below the liquidus temperature of the slag. R_{B14} which was previously given as 3,0 m, is the corresponding value for the unreduced state of slag B14 that is taken as representative of average plant operation.

(b) $C_\rho = \rho_{sl}/\rho_{B14}$. Here ρ_{sl} is the resistivity of a given slag at the temperature predicted to exist at a radius of 2 m from the electrode axis. The temperature is found from the radial profile used in (a). Again, ρ_{B14} is the same parameter for unreduced B14 (0,71 ohm cm)

(c) $C\eta = \eta_{B14}/\eta_{sl}$. The symbols have the same meanings as in (b) except that viscosity (η) replaces resistivity (ρ). The reference value for B14 is 0,85 poise.

(d) $C' = C_L + C_\rho + C\eta$

The value of C' for unreduced B14 would then be 3,0.

Although equal importance is assigned to the three parameters, they are dimensionless, take account of liquidus temperature and refer to values of resistivity and viscosity at comparatively realistic temperatures which also take into account the liquidus temperature of the slag.

For the purpose of the calculation, only the slags used in section 6.4 were considered to show the main trends when composition deviates from that of B14 with respect to $(CaO + MgO)/SiO_2$, CaO/MgO and $(TiO_2 + Al_2O_3)$.

The calculations were performed for the unreduced slags as well as for the slags reduced by carbon for 60 minutes at 1550°C. The choice of these conditions is again based on the behaviour of B14, as it was indicated previously that such a state of this slag appeared to represent approximately conditions in the furnace when operation is normal. The calculated values are given in table 68.

The table shows in compact form, the trends that might be expected from a detailed examination of the experimental results:

(a) For the variables $(TiO_2 + Al_2O_3)$ and (MgO/CaO), the trend shown by the unreduced slags is enhanced for the reduced slags.

(b) For variation in basicity, the trend is reversed.

A rather sweeping conclusion on the basis of these values would be:

(a) If the basicity is to be maintained at 1,4 to 1,5 , improved operation compared with the present, should be obtained from either greater dilution or from addition of limestone (and silica to keep the basicity constant). The first alternative is unattractive for obvious reasons.

(b) Based purely on this exercise and the parameters used in it, a decrease in basicity to values closer to 1,0 can only be beneficial. However, bearing in mind the deleterious effect of such a change on desulphurization, it is less advisable than an increase in the CaO/MgO ratio.

Table 68 Values of C' for major changes in composition

Slag No.	Increasing variable	Unreduced slags					Slags reduced for 60 minutes at 1550°C				
		Ref.temp. (η and ρ)	C_L	$C\eta$	$C\rho$	C'	Ref.temp. (η and ρ)	C_L	$C\eta$	$C\rho$	C'
A5		1480	1,00	0,87	1,30	3,17	1460	1,00	1,00	1,00	3,00
B14	$(TiO_2+Al_2O_3)$	1460	1,00	1,00	1,00	3,00	1536	0,95	0,79	0,59	2,33
C23		1536	0,95	1,15	0,70	2,80	1580	0,91	0,83	0,33	2,07
B13		1460	1,00	1,02	1,08	3,10	1460	1,00	0,83	0,86	2,69
B14	(MgO/CaO)	1460	1,00	1,00	1,00	3,00	1536	0,95	0,79	0,59	2,33
B15		1560	0,92	1,00	1,08	3,00	1600	0,91	0,53	0,77	2,21
B11		1536	0,95	1,15	0,85	2,95	1548	0,93	0,65	0,55	2.13
B14	$SiO_2/(CaO+MgO)$	1460	1,00	1,00	1,00	3,00	1536	0,95	0,79	0,59	2,33
B17		1495	0,99	0,42	1,43	2,84	1560	0,92	0,65	0,86	2,43

7. References

1. Agamawi, Y.M. and White, J., Trans. Brit. Ceram. Soc., 51, 1952, 293-325
2. Agamawi, Y.M. and White, J., Trans. Brit. Ceram. Soc., 53, 1954, 1-38
3. Ohno, A. and Ross, H.U., Can. Met. Quart., 2, No.3, 1963, 243-258
4. DeVries, R.C., Roy, R. and Osborn, E.F., J. Amer. Ceram. Soc., 38, 1955, 158-171
5. Holmes, W.T., Banning, L.H. and Brown, L.L., U.S. Bur. Mines Rep. Invest. No. 7081, 1968
6. Zhilo, N.L., Gruzdev, Yu.A., Gorokh, A.V. and Pershina, A.F., Izv. Akad. Nauk. SSSR. Metally., 6, 1969, 3-8
7. Handfield, G. et al, Light Metals 1971, AIME, 1971, New York
8. Jochens, P.R., Sommer, G., and Howat, D.D., J.I.S.I., Feb.1969, 187-192
9. Hejja, A.A., University of the Witwatersrand, Johannesburg. Unpublished work 1972.
10. Handfield, G. and Charette, G.G., Can. Met. Quart., 10, No.3, 1971, 235-243
11. Tuset, J., Kr. Tidsskr. Kjemi. Bergv. Metallugi., 28, 1968, 232
12. Frohberg, M.G. and Weber, R., Arch. Eisenhuettenw., 7, 1965, 477-480
13. Pliner, Yu.L., Shtengelmeier, S.V., Ignatenko, G.F. and Rubinshtein, E.A., Stal' in English, 4, 1966, 284-286.
14. Schenk, H. and Frohberg, M.G., Arch. Eisenhuettenw., 7, 1962, 421-425
15. Thakur, R.L. as quoted by Marboe, E.C. and Weyl, W.A., J. Soc. Glass Tech., 37, 1955, 16-36
16. Endell, K. and Brinkmann, G., Stahl u Eisen, 59, 1939, 1319-1321
17. Mikhailov, V. and Belyakova, E., Ural Met., No.6, 1939, 7-9
18. Ohno, A. and Ross, H.U., Can. Met. Quart., 2, No.3, 1963, 259-279
19. Behrendt, G. and Kootz, T., Stahl u Eisen, 69, 1949, 399-403
20. Shavrin, S. and Sakharov, I., Izv. Akad. Nauk. SSSR. Metal., 2, 1967, 14-21
21. Zhilo, N.L., Gruzdev, Yu.A., Gorokh, A.V. and Pershina, R.F., Izv. Akad. Nauk. SSSR. Metal., No.1, 1970, 65-69
22. Freidenzon, E.Z., Pushkash, I.I., Lazarev, B.L. and Gladyshev, V.I., Stal' in English, 6, 1965, 433-437
23. McRae, L.B., M.Sc. dissertation, University of the Witwatersrand, Johannesburg, 1968
24. Gordy, W. and Thomas, W.J.O., J. Chem. Phys., 24, 1956, 439-444
25. Wells, A.F., Structural Inorganic Chemistry, Clarendon Press, Oxford, 1950
26. Pauling, L., The nature of the chemical bond, Cornell University Press, Ithaca, 1960
27. Bockris, J.O'M., Ignatowicz, S., Kitchener, J.A. and Tomlinson, J.W., Trans, Farad. Soc., 48, 1952, 75-91
28. Bockris, J.O'M. and Lowe, D.C., Proc. Roy. Soc. A., 226, 1954, 423-435
29. Bockris, J.O'M., Mackenzie, J.D. and Kitchener, J.A., Trans. Farad. Soc., 51, 1955, 1734-1748

30. Bockris, J.O'M., Kitchener, J.A. and Davies, A.E., Ibid., 48, 1952, 536-548

31. Richardson, F.D., The vitreous state, Glass delegacy of the University of Sheffield, 1955, p 63

32. Toop, G.W. and Samis, C.S., Trans. Met. Soc. A.I.M.E., 224, 1962, 878-887

33. Masson, C.R., Proc. Roy. Soc. Lond., 278A, 1965, 201-220

34. Kozakevitch, P., Met. Soc. Conf., Vol.7, Physical chemistry of process metallurgy, Part 1. Interscience, New York. 1961, 97-116

35. Reznichenko, V.A., Izv. Akad. Nauk. SSSR. Metal., 5, 1967, 43

36. DeVries, R.C. and Roy, R., J. Amer. Ceram. Soc., 33, 1954, 370-372

37. Andersson, S., Collen, B., Kuylenstierna, U. and Magneli, A., Acta Chem. Scand., 11, 1957, 1641-1652

38. Bright, F.H., Ninth annual conference on application of X-ray analysis, 1960

39. Rusakov, A.A. and Zhdanov, G.S., Dokl. Akad. Nauk. SSSR., 77, 1951, 411

40. Åsbrink, S and Magneli, A., Acta Cryst., 12, 1959, 575-581

41. Assayag, P., Dode, M.and Faivre, R., Compt. Rend., 240, 1955, 1212-1214

42. Nishimura, H. and Kimura, K., Bull. Eng. Research Inst. Kyoto Univ., 6, 1954, 19-25

43. Mikhailov, V and Belyakova, E.P., Ural Met., No.4-5, 1939, 14-19

44. Ohno, A. and Ross, H.U., Can. Met. Quart., 3, 1964, 257-267

45. Belyakova, E.P., Komar, A. and Mikhailov, V., Ural Met., No.4-5, 1939, 23-25

46. Kubo, K. and Shurniki, K., Kogyo Kagaku Zasshi, 63, 1960, 64-70

47. Osann, B., Stahl u Eisen, 41, 1921, 1487

48. Jansson, S., Jernkontorets Analer, 124, 1940, 274-276

49. Wentrup, H., Maetz,H. and Heller, P., Arch. Eisenhuettenw., 20, 1949, 139

50. Shavrin, S., Frolov, F., Sakharov, I. et al, Stal', 26, 1966, 392-397

51. Delve, F.D., Meyer, H.W. and Lander, H.N., Met. Soc. Conf., 8, 1961, 1111-1159

52. Mikhailov, V. and Belyakova, E., Ural Met., No.6, 1939, 7-9

53. Chukukere, E.U. and Ross, H.U., Can. Met. Quart., 6, 137-152

54. Darken, L.S. and Gurry, R.W., Physical chemistry of metals, McGraw-Hill, 1953

55. Faust, E., Arch. Eisenhuettenw., 12, 1939, 361

56. Mori, K., Tetsu to Hagane, 46, 1960, 548-555

57. Semik, I.P., Bull. Akad. Sci. U.S.S.R., 4, 1941, 55

58. Gruzdev, Yu.A. et al, Izv. Akad. Nauk. SSSR, No.6, 1971, 38-41

59. Handfield, G., Charette, G.G. and Lee, H.Y., Jour. of Metals, Sept,1972, 37-40

60. Pothas, E., M.Sc. dissertation, University of the Witwatersrand, Johannesburg, 1968

61. Wyatt, J.L., Trans. A.I.M.E., 188, 1950, 989

62. Denisov, S.I. and Moriz, Y.A., Proekt. Inst. Titana, 5, 1970, 14-22

63. Balikhin, V.S. and Reznichenko, V.A., Izv. Akad. Nauk. SSSR. Otdel. Tekh. Nauk. Met. i Toplevo, No.4, 1961, 24-28

64. Balikhin, V.S. and Reznichenko, V.A., Titan i ego Splavy Akad. Nauk. SSSR. Inst. Met., No.5, 1961, 95-101

65. Musikhin, V.I., Lepinskikh, V.M. and Fomichev, Yu.A., Trans. Inst. Met. Sverdlovsk, 18, 1969, 293-305

66. Degtyarev, V.S., Denisov, S.I., Denisova, N.V. and Gobov, A.P., Izv. Akad. Nauk. SSSR. Met., No.6, 1970, 27-29

67. Denisov, S.I., Degtyarev, V.S. and Reznichenko, V.A., Ibid., 1970, 80-82

68. Degtyarev, V.S., Reznichenko, V.A. and Denisov, S.I., Izv. Vyssh. Ucheb. Zaved. Tsvet. Met., No.1, 1970, 43-47

69. Reznichenko, V.A., Izv. Akad. Nauk. SSSR. Metal., 5, 1967, 43

70. Kato, M. and Minowa, S., Tetsu to Hagane, 51, 1965, 1849; 52, 1966, 582, 584, 586

71. Kato, M. and Minowa, S., Ibid., 52, 1966, 580; 52, 1966, 1436, 1438, 1441

72. Kato, M. and Minowa, S., Trans. Iron and Steel Inst. Jap., 9, 1969, 47-52

73. Hansen, K.W., J. Electrochem. Soc., 112, 1965, 994

74. Engell, H.-J. and Vygen, P., Zeitschr. Elektrochem. (Ber. Bunsengesellsch.), 72, 1968, 5-12

75. Higgins, R. and Jones, T.J.B., Trans. I.M.M., 72, 1962-3, 825-864

76. Hejja, A.A., Private Communication, 1974

77. Ossin, D.I., Private Communication, 1974

78. Munakata, M., Solid state electron, 1, 1960, 159

79. Liutikov, R.A. and Tsylev, L.M., Izv. Akad. Nauk. SSSR. O.T.N. Metal. i Gornoe Delo., No.2, 1963, 59-66

80. Van Wazer, J.R. et al, Viscosity and flow measurement - A laboratory handbook of Rheology, Interscience, N.Y., 1966

81. Johnston, G.H., Ph.D thesis, University of the Witwatersrand, Johannesburg, 1972

82. Shedlovsky, T., J. Amer. Chem. Soc., 54, No.4, 1411-1428

83. Chambers, J.F., Stokes, J.M. and Stokes, R.H., J. Phys. Chem., 60, 1956, 985.

84. Cavalier, G., Ceram. Bull., 39, 1960, 142-144

85. Welch, J.H., J. Sci. Instr., 31, 1954, 458-462

86. Jochens, P.R., Ph.D thesis, University of the Witwatersrand, Johannesburg, 1967

87. Turkdogan, E.T. and Bills, P.M., Amer. Ceram. Soc. Bull., 39, 1960, 682-687

88. Woollacott, L.C., University of the Witwatersrand, Johannesburg, Private Communication, 1973

89. Hejja, A.A., University of the Witwatersrand, Johannesburg, Private Communication, 1973

90. Machin, J.S., Tin Boo Yee and Hannah, D.L., J. Amer. Ceram. Soc., 35, 1952, 322-325

91. Boden, P. and Glasser, F.P., Trans. and Jour. Br. Ceram. Soc., 72, 1973, 215-220

92. Coughanour, L.W. and DeProsse, V.A., J. Research Natl. Bur. Standards, 51, 1953, 87

93. Berezhnoi, A.S. and Gul'ko, N.V., Ukrain Khim. Zhur., 21, 1955, 162

94. Wagner, C., The physical chemistry of steel making, M.I.T. symp. 1956, 237-251

95. Yaroyskiy, V.I., Theory of steel making reactions, Metallurgiya, 1967

96. Nikitin, Yu.P., Lopatin, V.M. and Barmin, L.N., Steel in the U.S.S.R., April 1973, 121

97. Morin, F.J. in "Semiconductors" ed. N.B. Hannay, Rheinhold Publ. Corp. 1959

98. Hejja, A.A., "Progress report on trial tests conducted on the No.1 submerged arc furnace at the Iron Plant of the Highveld Steel and Vanadium Corporation Ltd." October 1971

99. Rennie, M.S., N.I.M. report No. 1606, Feb.1974

100. Howat, D.D., Jochens, P.R. and Barcza, N.A., Preprint for Proc. Int. Conf. on Sci. and Tech. of Iron and Steel, Japan, 1971, (Not publ.)

101. Rohrmann, B. and Parkinson, R., "Investigation of factors influencing iron plant hot metal production." Internal report - Highveld Steel and Vanadium Corporation, Witbank, August 1971

102. Engelbrecht, G.J., "Interim report on results obtained in No.1 Elkem furnace trials to date" Period covered 16th March to 15th May 1971, Witbank, May 1971

103. Hejja, A.A., Private Communication, University of the Witwatersrand, May 1974

104. Riss, A. and Khodorovsky, Y., Production of ferro-alloys, Moscow, Foreign Languages Publ. House.

105. Pasckris, V. and Persson, J., Industrial electric furnaces and appliances, 2nd ed., N.Y., Interscience, 1960

106. Schwarz von Bergkampf, H., Modellbetrachtungen des Lichtbogenofens in Durrer-Volkert. Metallurgie des Ferrolegierungen 2, Aufl.1970, Kap.5

107. Hallvard-Nilsen, P., Tids. Kjemi. Berg. Metall., 24, 1964, 203-208

108. Downing, J.H. and Urban, L., J. Metals, N.Y., Mar.1966, 337-344

109. Urquhart, R.C., N.I.M. report No. 1521, Feb.1973

110. Bezobrazov, S.V. et al, Stal' in English, 10, 1961, 740-744